

Identification of bacterial post-translational modifications that regulate antimicrobial resistance



A thesis submitted to Cardiff University for the degree of
Doctor of Philosophy by:

Victoria Barlow

June 2022

Supervisors: Dr Yu-Hsuan Tsai, Dr Louis Luk, Dr Yi Jin



Acknowledgements

I would like to extend my greatest thanks to my supervisor, Dr Yu-Hsuan Tsai, without whom this work could not have been completed. Throughout my time under his supervision, he has not only provided me with valuable knowledge and expertise to help me complete this project but has also shown me continued support, encouragement and patience. I will always be grateful to have had the opportunity to complete my PhD in his research group. I would also like to thank Dr Louis Luk and Dr Yi Jin, both of whom provided wider supervision and gave insightful feedback and suggestions on this work.

I am grateful to Dr Thomas Williams for providing advice on my project and lab work, in addition to extensive help with mass spectrometry data collection and interpretation. I am also indebted to Dr Alexander Nödling for guidance both within the lab and in life. I thank Sanjay Patel who gave me important training, and whose previous works on these projects are a foundation on which this current work was built. I am deeply appreciative of Dr Emily Mills, Dr Patrick Baumann, Heather Hayes, Davide Zappala, Davide Cardella, Dr Adriana Coricello, Luke Spear, Alex Lander, Dr Nicolò Santi, Dr Simon Tang, Xiaoting Meng, Muge Ma, Mochen Dong, and all other current and previous members of the Tsai, Luk, and Jin groups. In addition to the help and advice in the lab, the camaraderie in the group has been a highlight of my time in Cardiff.

I am thankful to our collaborator Dr Shih-Hsiung Wu and his group at Academia Sinica for their initial and complementary works which helped guide the direction of the second chapter of this thesis. I would like to thank Cardiff University for allowing use of their facilities and I am particularly grateful to Analytical Services, and all the technical and administrative staff who keep the School of Chemistry running. This work could not have been completed without the generous funding of the Engineering and Physical Sciences Research Council, and I am most grateful for their support.

Finally, I would like to thank my family and friends for showing me continued support throughout the course of this PhD. Much has changed over the past four years, yet their enduring interest and encouragement has propelled me forwards. Particularly, my boyfriend Adam and both of our families have inspired me to continue and provided welcome respite in perfect measure. I am so appreciative of all who have helped me reach this point.

Abstract

Rapidly spreading antimicrobial resistance is one of the greatest threats to human health of our time. There exists many mechanisms by which bacteria evade destruction by antibiotics and various research is being conducted globally in an attempt to combat this alarming situation. A so far under-researched area is the hypothesised role of protein post-translational modifications in the regulation of antimicrobial resistance responses. This thesis identifies two proteins involved in antimicrobial resistance and known to undergo post-translational modification, then uses genetic code expansion and unnatural amino acid incorporation to characterise the effect of these modifications on protein function. The first protein is AdeT1, a component of a multi-drug efflux pump from the multidrug resistant pathogen *Acinetobacter baumannii*, which undergoes lysine propionylation at Lys280 *in vivo*. Here, such propionylation is shown to modulate function of the efflux pump in living cells, with the propionylated protein complex demonstrating increased ethidium bromide efflux. Further, cells producing propionylated AdeT1 required a 6-fold higher concentration of erythromycin to inhibit their growth compared to cells producing unmodified AdeT1. The second protein investigated is the DNA-binding protein HU from *Escherichia coli*, which undergoes acetylation at five lysine residues *in vivo*. The protein was characterised in DNA-binding assays *in vitro*, which revealed that protein acetylated at Lys86 has significantly lower affinity for DNA compared to its wildtype counterpart. The consequences of such altered binding on bacterial gene expression and antimicrobial resistance are contemplated. Together, the results presented here are in agreement with the known roles of post-translational modifications in modulating protein function and provide evidence toward a novel analysis of post-translational modifications as regulatory components in antimicrobial resistance responses.

Table of contents

Acknowledgements.....	i
Abstract	ii
Table of contents	iii
List of publications	vii
List of figures	viii
List of tables	xiv
List of abbreviations	xv
Chapter 1 – Introduction	1
1.1 Antimicrobial resistance	2
1.1.1 Antimicrobial resistance mechanisms	5
1.1.2 Spread of antimicrobial resistance	16
1.1.3 Fighting antimicrobial resistance.....	22
1.2 Bacterial post-translational modifications	28
1.2.1 Detecting PTMs	29
1.2.2 Types of PTMs	31
1.2.3 PTM crosstalk.....	48
1.3 PTMs and antimicrobial resistance.....	52
1.3.1 PTM of antimicrobial resistance proteins	52
1.3.2 Bacterial PTMs regulating antimicrobial resistance.....	54
1.3.3 PTMs as antimicrobial drug targets.....	58
1.4 Characterising PTMs	61
1.4.1 Unnatural amino acid incorporation	62
1.5 Aims and objectives of thesis	65
Chapter 2 – Investigating the effects of lysine propionylation on the <i>Acinetobacter baumannii</i> AdeT1 protein	66
2.1 Summary	67
2.2 Introduction	68
2.2.1 <i>Acinetobacter baumannii</i>	68
2.2.2 Multidrug efflux pumps.....	69
2.2.3 RND-type multidrug efflux pumps	70
2.2.4 Post-translational modifications of multidrug efflux pumps.....	72
2.2.5 AdeT1.....	73
2.2.6 Lysine propionylation of AdeT1.....	74
2.2.5 Characterising the effects of PTMs on efflux pump function	78
2.2.6 Assessing efflux pump activity	79

2.3 Aims and objectives	81
2.4 Results.....	82
2.4.1 Establishing an AdeT1 bioassay.....	82
2.4.2 Confirmation of AdeT1 expression.....	111
2.4.3 Confirmation of AdeT1 efflux pump activity.....	113
2.4.4 Producing AdeT1 ^{K280Pr}	116
2.2.5 Confirmation of AdeT1 ^{K280Pr} production.....	122
2.2.6 Confirmation of AdeT1 ^{K280Pr} efflux activity	124
2.4.7 Minimum inhibitory concentration testing with AdeT1 ^{K280Pr}	126
2.5 Discussion	132
2.5.1 Producing AdeT1 in <i>E. coli</i>	132
2.5.2 Functionality of AdeT1 in <i>E. coli</i>	135
2.5.3 Effect of AdeT1 on antimicrobial resistance in <i>E. coli</i>	136
2.5.2 Production of AdeT1 ^{K280Pr} through incorporation of propionyl-lysine.....	137
2.5.3 Functionality of AdeT1 ^{K280Pr} in <i>E. coli</i>	138
2.5.4 Effect AdeT1 ^{K280Pr} on antimicrobial resistance in <i>E. coli</i>	138
2.5.5 Propionylation of AdeT1 in <i>A. baumannii</i>	140
2.5.6 Post-translational modification to regulate efflux pump function.....	140
2.6. Conclusions	142
2.7 Materials and methods.....	144
2.7.1 Plasmid construction	144
2.7.2 Bacterial protein expression	151
2.7.3 Minimum Inhibitory Concentration testing	152
2.7.4 SDS-PAGE and Western blot	153
2.7.5 Fluorescence intensity measurements.....	153
2.7.6 Ethidium bromide efflux and accumulation assays.....	154
2.7.7 Protein purification.....	154
2.7.8 Mass spectrometry	155
Chapter 3 – Investigating the effects of lysine acetylation on the <i>Escherichia coli</i>	
DNA-binding HU protein	156
3.1 Summary	157
3.2 Introduction	158
3.2.1 <i>Escherichia coli</i>	158
3.2.2 Histone-like HU protein.....	159
3.2.3 DNA binding by HU protein.....	160
3.2.4 Physiological roles of HU.....	164
3.2.5 Role in antimicrobial resistance	166

3.2.6 Post-translational modifications of DNA-binding proteins.....	166
3.2.7 Lysine acetylation	167
3.3 Aims and objectives	170
3.4 Results.....	171
3.4.1 Expression and purification of wild-type HU protein	171
3.4.2 Expression and purification of acetylated HU proteins	175
3.4.3 Verifying dimer formation.....	181
3.4.4 Electrophoretic mobility shift assay	185
3.4.5 Circular dichroism.....	198
3.5 Discussion	201
3.5.1 Acetylation of Lys67 and Lys86	201
3.5.2 Effect of acetylation on interaction with 30-bp DNA	202
3.5.3 Acetylation in the HU β_2 homodimer vs the HU $\alpha\beta$ heterodimer	204
3.5.4 Effect of acetylation on interaction with longer DNA.....	208
3.5.5 Physiological effects of acetylation	211
3.6 Conclusions	213
3.7 Materials and methods.....	215
3.7.1 Genomic DNA extraction	215
3.7.2 Plasmid construction	215
3.7.3 Bacterial protein expression	216
3.7.4 Protein purification.....	217
3.7.5 Heterodimer formation.....	218
3.7.6 Native PAGE	218
3.7.7. Analytical size exclusion high-performance liquid chromatography.....	219
3.7.8 Electrophoretic mobility shift assay	220
3.7.9 Circular dichroism.....	222
Chapter 4 - Discussion, conclusions and future work.....	223
4.1 Discussion and conclusions	224
4.1.1 Insights into the role of PTMs in regulating antimicrobial resistance	224
4.1.2 Role of PTM crosstalk in regulating antimicrobial resistance	226
4.2 Future work and closing remarks	228
Chapter 5 - General materials and methods	229
5.1 Bacterial strains	230
5.2 Cloning	230
5.2.1 PCR Conditions	230
5.2.2 Site directed mutagenesis	230
5.2.3 Assembly of multiple fragments	231

5.2.4 Restriction enzyme digestion	231
5.2.5 Agarose gels	231
5.2.6 DNA purification from agarose gels	231
5.2.7 Plasmid minipreps	231
5.2.8 DNA sequencing.....	231
5.3 Protein expression and purification	232
5.3.1 Antibiotic selection.....	232
5.3.2 Media and buffers.....	232
5.3.3 Chemical transformation.....	233
5.4 Protein purification	234
5.4.1 Nickel affinity purification	234
5.4.2 SDS-PAGE.....	234
5.5 Mass spectrometry.....	235
5.6 Figures.....	235
References.....	236
Appendix	263

List of publications

Mills, E. M. *, **Barlow, V. L. ***, Luk, L. Y. P., and Tsai, Y.-H. Applying switchable Cas9 variants to *in vivo* gene editing for therapeutic applications. *Cell Biology and Toxicology*, **36**, 17-29 (2020).

Barlow, V. L., Lai, S.-J., Chen, C.-Y., Tsai, C.-H., Wu, S.-H., and Tsai, Y.-T. Effect of membrane fusion protein AdeT1 on the antimicrobial resistance of *Escherichia coli*. *Scientific Reports*, **10**, 20464 (2020).

Mills, E. M. *, **Barlow, V. L. ***, Jones, A. T., and Tsai, Y.-H. Development of mammalian cell logic gates controlled by unnatural amino acids. *Cell Reports Methods*, **1**, 100073 (2021).

Sayers, E. J., **Barlow, V. L.**, Tsai, Y.-H., and Jones, A. T. Quantitative subcellular analysis of cyclic cell-penetrating peptide EJP18 in non-adherent cells. In: Langel, Ü. ed. *Cell Penetrating Peptides: Methods and Protocols* (Methods in Molecular Biology, 2383). 3rd edition (2022).

Barlow, V. L. and Tsai, Y. H. Acetylation at lysine 86 of *Escherichia coli* HU β modulates the DNA-binding capability of the protein. *Frontiers in Microbiology*, 12:809030 (2022).

*denotes equal contribution

List of figures

Figure 1.1 The four major categories of antibiotic resistance mechanisms displayed by bacteria.....	6
Figure 1.2 Penicillin mechanism of action and resistance mechanisms	7
Figure 1.3 Fluoroquinolone mechanism of action and resistance mechanisms	10
Figure 1.4 Structure of MfpA, a Qnr protein from <i>M. tuberculosis</i> (PDB: 2BM6).....	11
Figure 1.5 Antimicrobial resistance <i>via</i> reduced antibiotic entry or accumulation ...	13
Figure 1.6 Antimicrobial resistance and persistence	16
Figure 1.7 Bacterial conjugation	19
Figure 1.8 Widespread antibiotic use contributes towards antimicrobial resistance	21
Figure 1.9 Schematic representation of Ser, Thr and Tyr phosphorylation.....	32
Figure 1.10 Schematic representation of lysine acetylation.....	35
Figure 1.11 Schematic of chemical (non-enzymatic) and enzymatic protein acetylation in bacteria.....	37
Figure 1.12 Schematic representation of lysine succinylation.	40
Figure 1.13 Schematic representation of lysine propionylation	42
Figure 1.14 Schematic representation of lysine malonylation.....	43
Figure 1.15 Schematic representation of lysine methylation	45
Figure 1.16 Factors contributing to antimicrobial resistance.....	58
Figure 1.17 Schematic of genetic code expansion.....	64
Figure 2.1 Classes of multidrug efflux pumps	70
Figure 2.2 Schematic of a resistance nodulation division (RND)-type multidrug efflux pump.....	71
Figure 2.3 Schematic representation of lysine (K) and propionyl-lysine (PrK)	74
Figure 2.4 Tandem mass spectrometry of AGIYDPKprMMNFLK peptide from <i>Acinetobacter baumannii</i> strain A) SK17-R and B) SK17-S.....	76
Figure 2.5 Alignment of AdeT1 with AcrA	77
Figure 2.6 Schematic depicting incorporation of propionyl-lysine into position 280 of <i>A. baumannii</i> AdeT1 protein <i>in vivo</i> in <i>E. coli</i>	79
Figure 2.7 Investigating the effect of propionylation at lysine 280 of AdeT1 on minimum inhibitory concentration (MIC).....	80
Figure 2.8 Cloning of pAdeT1 as described by Srinivasa <i>et al</i>	82
Figure 2.9 SDS-PAGE analysis of cell lysate from <i>E. coli</i> BL21(DE3) containing pAdeT1	83
Figure 2.10 Immunoblot analysis of AdeT1 production in <i>E. coli</i> KAM32 from three plasmids.....	84
Figure 2.11 A ₆₀₀ standard curve for <i>E. coli</i> KAM32 cells.....	85

Figure 2.12 Preliminary MIC test of KAM32 cells expressing pUC18, pAdeT1* or pAdeT1*-His6	87
Figure 2.13 Immunoblot analysis of AdeT1 production during preliminary MIC test with chloramphenicol of <i>E. coli</i> KAM32 cells with or without induction of pAdeT1*-His6	88
Figure 2.14 Immunoblot analysis of production of AdeT1 when diluted to two cellular densities	89
Figure 2.15 SDS-PAGE analysis of cell lysate from <i>E. coli</i> BL21(DE3) containing pET28a AdeT1-His6	90
Figure 2.16 Western blot analysis of pET28a AdeT1-His6 expression after dilution to low cellular density	91
Figure 2.17 Fluorescence intensity of <i>E. coli</i> BL21(DE3) cells expressing pET28a sfGFP-His6 when diluted to A ₆₀₀ 0.01 or 0.001 into fresh IPTG-containing media, 1 hour post-induction with IPTG	92
Figure 2.18 Immunoblot analysis of AdeT1 expression in liquid <i>E. coli</i> KAM32 pAdeT1*-His6 cultures to which varying concentrations of chloramphenicol have been added 2 hours post-induction with IPTG	93
Figure 2.19 SDS-PAGE analysis of AdeT1 expression in liquid <i>E. coli</i> BL21(DE3) pET28a AdeT1-His6 cultures to which varying concentrations of chloramphenicol have been added 2 hours post-induction with IPTG	94
Figure 2.20 A ₆₀₀ measurements of cultures of <i>E. coli</i> KAM32 cells containing expression plasmid pAdeT1*-His6 or control plasmid pUC18 after overnight incubation in the presence of varying concentrations of chloramphenicol	95
Figure 2.21 A ₆₀₀ measurements of cultures of <i>E. coli</i> BL21(DE3) cells containing expression plasmid pET28a AdeT1-His6 or control plasmid pET28a after overnight incubation in the presence of varying concentrations of chloramphenicol	96
Figure 2.22 Fluorescence intensity (FI) of cells containing sfGFP under the control of three constitutive promoters: the ampicillin resistance gene promoter (AmpR); the LacUV5 promoter (LacUV5); or the Lac repressor promoter (LacI)	98
Figure 2.23 Immunoblot analysis of AdeT1 expression under the control of constitutively active promoters: ampicillin resistance gene promoter (AmpR), LacUV5 promoter, and the lac repressor gene promoter (LacI)	99
Figure 2.24 Chloramphenicol MIC analysis of <i>E. coli</i> KAM32 carrying either pUC18 or pAdeT1*-His6	100
Figure 2.25 Immunoblot analysis of AdeT1 expression from <i>E. coli</i> KAM32 carrying pAdeT1*-His6 during MIC testing with chloramphenicol	101
Figure 2.26 Erythromycin MIC analysis of <i>E. coli</i> KAM32 carrying either pUC18 or pAdeT1*-His6	101
Figure 2.27 Immunoblot analysis of AdeT1 expression from <i>E. coli</i> KAM32 carrying pAdeT1*-His6 during MIC testing with erythromycin	102
Figure 2.28 Tetracycline MIC analysis of <i>E. coli</i> KAM32 carrying either pUC18 or pAdeT1*-His6	102

Figure 2.29 Immunoblot analysis of AdeT1 expression from <i>E. coli</i> KAM32 carrying pAdeT1*-His6 during MIC testing with tetracycline	103
Figure 2.30 Acridine orange MIC analysis of <i>E. coli</i> KAM32 carrying either pUC18 or pAdeT1*-His6.....	104
Figure 2.31 Chloramphenicol MIC analysis of <i>E. coli</i> BL21(DE3) carrying either pET28a or pET28a AdeT1-His6	106
Figure 2.32 Immunoblot analysis of AdeT1 expression from <i>E. coli</i> BL21(DE3) carrying pET28a AdeT1-His6 during MIC testing with chloramphenicol.....	107
Figure 2.33 Erythromycin MIC analysis of <i>E. coli</i> BL21(DE3) carrying either pET28a or pET28a AdeT1-His6.....	107
Figure 2.34 Immunoblot analysis of AdeT1 expression from <i>E. coli</i> BL21(DE3) carrying pET28a AdeT1-His6 during MIC testing with erythromycin	108
Figure 2.35 Tetracycline MIC analysis of <i>E. coli</i> BL21(DE3) carrying either pET28a or pET28a AdeT1-His6.....	108
Figure 2.36 Immunoblot analysis of AdeT1 expression from <i>E. coli</i> BL21(DE3) carrying pET28a AdeT1-His6 during MIC testing with tetracycline.....	109
Figure 2.37 Acridine orange MIC analysis of <i>E. coli</i> BL21(DE3) carrying either pET28a or pET28a AdeT1-His6	110
Figure 2.38 Nickel affinity chromatography of wildtype AdeT1 protein with a 6x Histidine tag on the protein C-terminus.....	111
Figure 2.39 Mass spectrometry analysis of purified wild-type <i>A. baumannii</i> AdeT1 protein	112
Figure 2.40 Peptide fragments of wild type AdeT1 digested with trypsin identified by mass spectrometry	112
Figure 2.41 Efflux of ethidium bromide from <i>E. coli</i> cells expressing pUC18 or pAdeT1*	114
Figure 2.42 Efflux of ethidium bromide from <i>E. coli</i> cells expressing pET28a or pET28a AdeT1*-His6.....	115
Figure 2.43 MS data of sfGFP(K150Pr) purified from cultures grown in the absence of nicotinamide	117
Figure 2.44 MS data of sfGFP(K150Pr) purified from cultures grown in the presence of nicotinamide	118
Figure 2.45 Immunoblot analysis of propionyl-lysine (PrK) incorporation into position 280 of AdeT1 protein in <i>E. coli</i> BL21(DE3)	119
Figure 2.46 Immunoblot of PrK incorporation into AdeT1 protein in <i>E. coli</i> KAM32 expressing plasmids pAdeT1*(K280TAG)-His6 and pAckST	120
Figure 2.47 Immunoblot of PrK incorporation into AdeT1 protein in <i>E. coli</i> BL21(DE3) expressing plasmids pET28a AdeT1(K280TAG)-His6 and pAckST ...	121
Figure 2.48 Nickel affinity chromatography of AdeT1 ^{K280Pr} with a 6x Histidine tag on the protein C-terminus	122
Figure 2.49 Mass spectrometry analysis of AdeT1 protein with propionyl-lysine incorporated into amino acid position 280.....	123

Figure 2.50 Peptide fragments of AdeT1 ^{K280Pr} digested with trypsin identified by mass spectrometry	123
Figure 2.51 Efflux of ethidium bromide from <i>E. coli</i> cells expressing pET28a AdeT1(K280TAG)-His6	124
Figure 2.52 Accumulation of ethidium bromide in <i>E. coli</i> cells expressing pET28a AdeT1(K280TAG)-His6	125
Figure 2.53 Chloramphenicol MIC analysis of <i>E. coli</i> BL21(DE3) expressing pET28a AdeT1(K280TAG)-His6 and pAckST	126
Figure 2.54 Immunoblot analysis of <i>E. coli</i> BL21(DE3) expressing pET28a AdeT1(K280TAG)-His6 and pAckST during MIC testing with chloramphenicol	127
Figure 2.55 Erythromycin MIC analysis of <i>E. coli</i> BL21(DE3) expressing pET28a AdeT1(K280TAG)-His6 and pAckST	128
Figure 2.56 Immunoblot analysis of <i>E. coli</i> BL21(DE3) expressing pET28a AdeT1(K280TAG)-His6 and pAckST during MIC testing with erythromycin.....	128
Figure 2.57 Tetracycline MIC analysis of <i>E. coli</i> BL21(DE3) expressing pET28a AdeT1(K280TAG)-His6 and pAckST	129
Figure 2.58 Immunoblot analysis of <i>E. coli</i> BL21(DE3) expressing pET28a AdeT1(K280TAG)-His6 and pAckST during MIC testing with tetracycline	130
Figure 2.59 Ampicillin MIC analysis of <i>E. coli</i> BL21(DE3) expressing pET28a AdeT1(K280TAG)-His6 and pAckST	130
Figure 2.60 Immunoblot analysis of <i>E. coli</i> BL21(DE3) expressing pET28a-AdeT1*(K280TAG)-His6 and pAckST during MIC testing with ampicillin	131
Figure 2.61 Ertapenem MIC analysis of <i>E. coli</i> BL21(DE3) expressing pET28a AdeT1(K280TAG)-His6 and pAckST	131
Figure 3.1. Crystal structures of the three dimeric forms of <i>E. coli</i> HU	160
Figure 3.2 Alternative DNA-binding modes of HU	162
Figure 3.3 Sequence alignment of <i>E. coli</i> HU α , <i>E. coli</i> HU β and <i>Anabaena</i> HU...163	
Figure 3.4 Schematic representation of lysine (K) and acetyl-lysine (Ack).....	168
Figure 3.5 Homology model of <i>Escherichia coli</i> HU β ₂ bound to DNA	169
Figure 3.6 SDS-PAGE analysis of pBAD hupA-His6 expression and subsequent nickel affinity chromatography purification	171
Figure 3.7 SDS-PAGE analysis of HU α cation exchange chromatography	172
Figure 3.8 Mass spectrometry analysis of purified wildtype HU α protein.....	172
Figure 3.9 SDS-PAGE analysis of pBAD hupB-His6 expression and subsequent nickel affinity chromatography purification	173
Figure 3.10 SDS-PAGE analysis of HU β cation exchange chromatography	174
Figure 3.11 Mass spectrometry analysis of purified wildtype HU β protein.....	174
Figure 3.12 SDS-PAGE analysis of pBAD hupB(K67TAG)-His6 expression and subsequent nickel affinity chromatography purification	176
Figure 3.13 SDS-PAGE analysis of HU β ^{K67ac} cation exchange chromatography ..	177

Figure 3.14 Mass spectrometry analysis of purified wildtype HU β^{K67ac} protein	177
Figure 3.15 SDS-PAGE analysis of pBAD hupB(K86TAG)-His6 expression and subsequent nickel affinity chromatography purification	179
Figure 3.16 SDS-PAGE analysis of HU β^{K86ac} cation exchange chromatography ..	180
Figure 3.17 SDS-PAGE analysis of HU β^{K86ac} cation exchange chromatography fractions 25-28.....	180
Figure 3.18 Mass spectrometry analysis of purified wildtype HU β^{K86ac} protein	181
Figure 3.19 SDS and native PAGE analysis of HU α_2 , HU $\alpha\beta$, and HU β_2 dimer formation	182
Figure 3.20 SDS and native PAGE analysis of all HU dimers	183
Figure 3.21 Analytical size exclusion high-performance liquid chromatography of HU protein samples.....	184
Figure 3.22 30 bp DNA fragments used in EMSAs	186
Figure 3.23 EMSA of HU β_2 with a 30 bp DNA fragment containing a 2-nt gap	187
Figure 3.24 EMSA of HU β_2 , HU β^{K67ac}_2 and HU β^{K86ac}_2 with a 30 bp DNA fragment containing a 2-nt gap	188
Figure 3.25 EMSA of HU $\alpha\beta$, HU $\alpha\beta^{K67ac}$ and HU $\alpha\beta^{K86ac}$ with a 30 bp DNA fragment containing a 2-nt gap	189
Figure 3.26 EMSA of HU $\alpha\beta$, HU $\alpha\beta^{K86ac}$, HU β_2 , and HU β^{K86ac}_2 with a 30 bp DNA fragment containing a 2-nt gap	191
Figure 3.27 EMSA of HU $\alpha\beta$, HU $\alpha\beta^{K86ac}$, HU β_2 , and HU β^{K86ac}_2 with a 30 bp DNA fragment containing a nicked backbone	192
Figure 3.28 EMSA of HU $\alpha\beta$, HU $\alpha\beta^{K86ac}$, HU β_2 , and HU β^{K86ac}_2 with a 30 bp DNA fragment with a complete duplex	193
Figure 3.29 Effect of HU acetylation on interaction with different types of DNA ...	194
Figure 3.30 EMSA of HU β_2 , HU β^{K67ac}_2 and HU β^{K86ac}_2 incubated with linearised 5500 bp plasmid DNA	196
Figure 3.31 EMSA of HU β_2 , HU β^{K67ac}_2 and HU β^{K86ac}_2 incubated with linearised 2700 bp plasmid DNA	197
Figure 3.32 EMSA of HU β_2 , HU β^{K67ac}_2 and HU β^{K86ac}_2 incubated with a 1300 bp PCR fragment.....	198
Figure 3.33 Effect of acetylation at Lys86 of <i>E. coli</i> HU β_2 homodimer on secondary structure	199
Figure 3.34 Effect of acetylation at Lys86 of <i>E. coli</i> HU β_2 homodimer on thermal stability analysed by circular dichroism.....	199
Figure 3.35 Schematic representation of possible effects of acetylation on binding to a 30 bp DNA fragment with a 2-nt gap by HU	205
Figure 3.36 Cocystal structure of <i>E. coli</i> HU $\alpha\beta$ with a native β -form 19 bp DNA duplex (PDB #4YEW)	206
Figure 3.37 Schematic representation of possible effects of acetylation on the interaction of HU with a 30 bp whole duplex DNA fragment.....	207

Figure 3.38 Example of the quantification of free DNA remaining in EMSAs.....	222
Figure A.1 Confirming 30 bp complex formation by combining smaller DNA fragments for use in EMSAs in Chapter 3	264
Figure A.2 Investigating the use of fluorescently labelled DNA for use in EMSAs in Chapter 3	265

List of tables

Table 1.1 Common antimicrobials and their mechanism of action. Adapted under license CC-BY-4.0 ¹	4
Table 1.2 Antibiotic resistance mechanisms against common antimicrobials. Adapted under license CC-BY-4.0 ¹	14
Table 2.1 Preliminary MIC results for <i>E. coli</i> KAM32 cells expressing pAdeT1*-His6	86
Table 2.2 Plasmids used in this study	147
Table 2.3 Primers used for PCR	149
Table 2.4 Primers used for sequencing.....	151
Table 3.1 Verifying the accuracy of a molecular weight (MW) calibration curve....	185
Table 3.2 Calculated molecular weights (MW) of HU proteins based on analytical size exclusion high-performance liquid chromatography.....	185
Table 3.3 Average melting temperatures of HU β_2 and HU β^{K86ac}_2 as determined by measuring circular dichroism at four different wavelengths.....	200
Table 3.4 Plasmids used in this study	215
Table 3.5 Primers for PCR	216
Table 3.6 Primers for sequencing.....	216
Table 3.7 Buffers for native PAGE.	218
Table 5.1 Bacterial strains used in this thesis.	230
Table 5.2 Media for bacterial protein expression	232
Table 5.3 Buffers used for protein purification and SDS-PAGE	233
Table 5.4 Protein LC-MS gradient parameters	235
Table A.1 FASTA sequences of the nucleotides of the primer through to the translated region and stop codon inclusive for all plasmids used in this thesis.	266

List of abbreviations

A	Absorbance
A₆₀₀	Absorbance at 600 nm
AA	Amino acid
AcK	N ^ε -acetyl-L-lysine
AcKRS	N ^ε -acetyl-L-lysine tRNA synthetase
ABC	ATP-binding cassette
AMP	Ampicillin
APS	Ammonium persulphate
ATP	Adenosine triphosphate
BCA	Bicinchoninic acid
bp	Base pair
BSA	Bovine serum albumin
CAM	Chloramphenicol
DNA	Deoxyribonucleic acid
dNTP	Deoxynucleoside triphosphate
DTT	Dithiothreitol
EDTA	Ethylenediaminetetraacetic acid
EMSA	Electrophoretic mobility shift assay
ERY	Erythromycin
FI	Fluorescence intensity
GFP	Green fluorescent protein
ICE	Integral and conjugative element
IPTG	Isopropyl β-D-1-thiogalactopyranoside
LB	Lysogeny broth
MATE	Multidrug and toxic efflux
MHB	Mueller-Hinton broth
MIC	Minimum inhibitory concentration
NAD⁺	Nicotinamide adenine dinucleotide
NAM	Nicotinamide
nt	Nucleotide
NTA	Nitrilotriacetic acid
ORF	Open reading frame
PAGE	Polyacrylamide gel electrophoresis
PASTA	Penicillin binding protein and Ser/Thr kinase-associated

PBS	Phosphate buffered saline
PBST	Phosphate buffered saline with 0.1% Tween20
PCR	Polymerase chain reaction
PES	Polyethersulfone
PrK	Propionyl-lysine
PrKRS	Propionyl-lysine tRNA synthetase
PTM	Post translational modification
RNA	Ribonucleic acid
RND	Resistance nodulation division
SDS	Sodium dodecyl sulfate
SDS-PAGE	Sodium dodecyl sulfate polyacrylamide gel electrophoresis
SMR	Small multidrug resistance
SOB	Super optimal broth
SOC	Super optimal broth with catabolite repression
TAE	Tris-acetate-EDTA
TB	Terrific broth
TBE	Tris-borate-EDTA
TCEP	Tris(2-carboxyethyl)phosphine
TET	Tetracycline
TEMED	Tetramethylethylenediamine
TFAcK	N ^ε -trifluoro-acetyl-L-lysine
UAA	Unnatural amino acid

Chapter 1 – Introduction

1.1 Antimicrobial resistance

The first commercially used antibiotic, penicillin, was discovered by Alexander Fleming in 1928.² Penicillin was successfully used to treat a patient in 1941³ and introduced as a therapeutic several years later. The discovery was the dawn of the antibiotic era, the first in a series of discoveries resulting in the easy treatment of bacterial infections of which we are accustomed today. However, even in Fleming's first report on penicillin, not all bacteria were susceptible to the compound. This was later revealed to be due to the production of a penicillin-degrading enzyme by these cells.⁴ In this regard, retrospectively, it appears the discovery of antibiotics occurred simultaneously with the discovery of antimicrobial resistance.

Penicillin is a natural product, produced by *Penicillium* mould. Throughout evolution every species has experienced selective pressures through interactions with other species, so it is not surprising that natural antimicrobial resistance mechanisms exist. Indeed, bacterial species which co-evolved with antibiotic-producing bacterial species developed resistance.⁵ Today, many of the commonly used antibiotics such as tetracycline, chloramphenicol, erythromycin and vancomycin are produced naturally by actinomycetes species.⁵ Bacterial species which produce antimicrobial products are necessarily resistant to the molecules they produce, and may be the origin of clinically relevant antimicrobial resistance genes.⁶ In fact, resistance genes pre-date the discovery of antibiotics by thousands of years,⁵ and have been found in microbial DNA isolated from 30,000 year old permafrost.⁷ These ancient genes conferring antimicrobial resistance are also involved in many other functions, contributing to basic cellular physiology in the natural ecosystem.⁸

Antimicrobial resistance is therefore a natural phenomenon in bacterial populations. However, the clinical use of antimicrobials, alongside the overuse and misuse in human medicine, veterinary practices and animal rearing, has greatly accelerated this process.^{9, 10} Over the past few decades, the introduction of novel antibiotics has initial success, before being closely followed by the emergence of bacteria with resistance to the new compounds. For example, resistance to methicillin, tetracycline and vancomycin were reported one, nine and twenty one years, respectively, after their introduction.^{8, 10} Antimicrobial resistance arises when the bacteria survive exposure to a medicine that would normally kill them or stop their growth.⁹ This allows strains that are capable of surviving exposure to a particular drug to grow and spread due to a lack of competition from other strains. The frequency and overuse of antibiotics

therefore imposes a selection pressure, which rapidly increases the evolution of resistance.

It is considerably difficult to treat infections caused by resistant bacteria and, as such, they can cause significant morbidity and mortality. In 2014, a report commissioned by the UK Government estimated there had been 700,000 deaths worldwide that year attributable to bacterial antimicrobial resistance.¹¹ The same report estimated that by 2050, antimicrobial resistance could result in 10 million deaths per year. This number has been both supported and criticised.¹² However, just 5 years later, another report estimated that in 2019 there were 1.27 million deaths directly attributed to antimicrobial resistance and a further 4.95 million where resistance was a contributing factor.¹² These reports demonstrate the rapid growth in casualties and suggest we may be closer than initially thought.

Particularly, six bacterial pathogens are increasingly responsible for hospital-acquired antibiotic-resistant infections.¹³ The pathogens, named ESKAPE, are *Enterococcus faecium*, *Staphylococcus aureus*, *Klebsiella pneumoniae*, *Acinetobacter baumannii*, *Pseudomonas aeruginosa*, and *Enterobacter species*. These pathogens, responsible for serious clinical diseases, have developed resistance to a broad range of antimicrobials and are leading causes of mortality.¹⁴ *Escherichia coli*, although not formally recognised as part of ESKAPE, is another pathogen of concern. Antimicrobial resistant *E. coli* is the leading cause of bloodstream infections and urinary tract infections globally and is one of the largest clinical burdens facing human and animal health.¹⁴ Also of concern is *Streptococcus pneumoniae*, the most common cause of community-acquired pneumonia. *S. pneumoniae* has high prevalence of drug resistance in some regions, particularly in the Asia-Pacific region where 49.8% of cases were multi-drug resistant.¹⁵ Together, infections caused by *E. coli*, *S. aureus*, *K. pneumoniae*, *S. pneumoniae*, *A. baumannii* and *P. aeruginosa* were accountable for 73.4% of deaths due to antimicrobial resistance in 2019.¹²

In our current era many routine medical procedures such as caesarean sections, joint surgery, and chemotherapy are made possible through the use of antibiotics to treat any resulting infections. It is difficult to imagine that this may not always be the case but, unfortunately, predictions suggest that without intervention this may be the future we are heading towards.¹¹ Gonorrhoea is one example of an infection which is no longer responsive to treatment with penicillin, the original antibiotic of choice, and has repeatedly developed resistance against subsequent antibiotics. It is currently successfully treated by cephalosporins, however, decreased susceptibility is being

reported and there is no alternative antibiotic to use if resistance develops.¹⁶ Bacterial antimicrobial resistance is a worldwide problem and is not confined to any one region.¹² Therefore, globally concerted, innovative methods are required to overcome what could be one of the biggest human health burdens of our time.¹¹

This section will explore bacterial antimicrobial resistance mechanisms, how resistance spreads and how we can fight it. For clarity, 'antimicrobials' refer to any compounds which kill microbes or prevent their growth and can include antibiotics, antivirals, antifungals and antimalarials. As this thesis is concerned only with the development of bacterial resistance to antimicrobials, the words 'antimicrobial', 'antibiotic', and 'drug' will be used interchangeably to refer to antimicrobial therapies targeted towards bacteria. A list of common antimicrobials and their mechanisms of action is provided in **Table 1.1**.

Table 1.1 Common antimicrobials and their mechanism of action. Adapted under license [CC-BY-4.0](#)¹

Mechanism of action	Antimicrobial group
Inhibit cell wall synthesis	β -Lactams <ul style="list-style-type: none"> - Penicillin - Carbapenem - Cephalosporins - Monobactam - Ertapenem Glycopeptides
Inhibit protein synthesis	Bind to 30S ribosomal subunit <ul style="list-style-type: none"> - Aminoglycosides - Tetracyclines Bind to 50S ribosomal subunit <ul style="list-style-type: none"> - Chloramphenicol - Macrolides - Lincosamides - Erythromycin - Streptogramins
Inhibit nucleic acid synthesis	Quinolones <ul style="list-style-type: none"> - Fluoroquinolones
Inhibit metabolic pathways	Sulphonamides Trimethoprim
Depolarise cell membrane	Lipopeptides

1.1.1 Antimicrobial resistance mechanisms

Antimicrobial resistance can manifest in three ways: intrinsic, acquired and adaptive resistance.^{10, 17} Intrinsic resistance is the result of mechanisms which are inherent to a species' physiology. For example, Gram-negative bacteria are intrinsically resistant to glycopeptides that are not able to pass through the outer membrane of these bacteria.¹⁰ Acquired resistance occurs when a species which was previously susceptible to an antibiotic displays resistance.¹⁸ Such resistance typically arises from chromosomal mutations or the receipt of new genetic material and is irreversible. Adaptive resistance describes when resistance is induced by specific environmental conditions, such as stress, growth state or pH.¹⁷ Crucially, adaptive resistance is transient, usually mediated through modulation of gene expression, and is reversed when the inducing factors are removed.¹⁸ However, adaptive resistance may allow for the development of more permanent resistance mechanisms.

These types of resistance are facilitated by a wide variety of mechanisms. Often, one mechanism can present as intrinsic, acquired or adaptive resistance depending on the bacterial species and the physiological background. For example, multi-drug efflux pumps facilitate the extrusion of toxic compounds, including antimicrobials, from the cell. In *A. baumannii*, the production of multi-drug efflux pumps is part of the normal cellular physiology, and provides the bacteria with broad intrinsic resistance. However, in other species of bacteria such as *P. aeruginosa*, the overexpression of multidrug efflux pumps in response to treatment with antibiotics facilitates acquired resistance.¹⁹ A single mechanism can facilitate resistance to multiple antimicrobials.¹⁸ For example, multi-drug efflux pumps often have a wide substrate range. Further, a bacterial species can possess multiple resistance mechanisms.¹⁸ For example, aminoglycoside resistance occurs through several mechanisms that can coexist simultaneously in the same cell.²⁰ Multidrug-resistant bacteria often have an arsenal of resistance mechanisms at their disposal. The specific resistance phenotype displayed by a bacterium depends on the interaction between its different mutations and resistance mechanisms.²¹ Such positive interactions between different resistance mechanisms can further increase the development of multi-drug resistance.

Although there are many mechanisms by which bacteria evade destruction by antimicrobials, they result in four main outcomes: inactivating the antibiotic *via* modification or degradation, modifying the target of the antibiotic, reducing antibiotic entry to the cell or decreasing the accumulation of the antibiotic in the cell (**Figure 1.1**). Additionally, the development of antimicrobial resistance mechanisms is heavily associated with bacterial biofilms and persister cells.

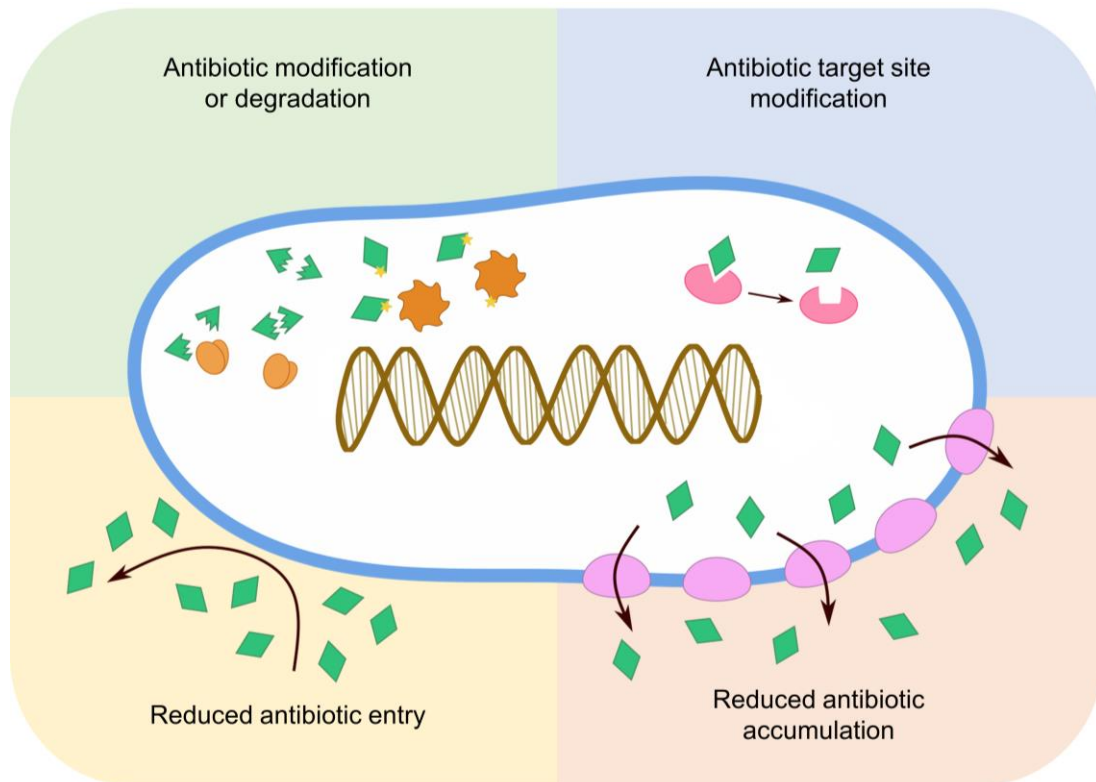


Figure 1.1 The four major categories of antibiotic resistance mechanisms displayed by bacteria. Generally, bacteria display resistance to antimicrobials *via* degradation or modification of the antibiotic molecule, modification of the antibiotic target site, reducing antibiotic entry, or reducing antibiotic accumulation.

Antibiotic modification or degradation

One of the most common antimicrobial resistance mechanisms employed is the production of enzymes which neutralise or degrade antibiotic molecules.¹⁴ β -lactams are a class of antibiotics characterised by the β -lactam ring and include penicillin and its derivatives, cephalosporins, carbapenems, clavams and monobactams. β -lactams work by binding to transpeptidases, known as penicillin-binding proteins, anchored in the cell wall.²² Transpeptidases are responsible for crosslinking the polysaccharide chains which compose the peptidoglycan *via* the small peptides which are attached to them. By mimicking the final two D-alanine residues, penicillin binds irreversibly to the active site of the penicillin-binding protein, preventing it from cross-linking peptidoglycan strands (**Figure 1.2**).^{22, 23} The bacterial cell is subsequently unable to build or maintain the cell membrane, resulting in cell lysis. β -lactam resistance is commonly observed, most often by the expression of β -lactamases, which cleave the amide bond of the β -lactam ring, rendering the antibiotic ineffective (**Figure 1.2**).²³

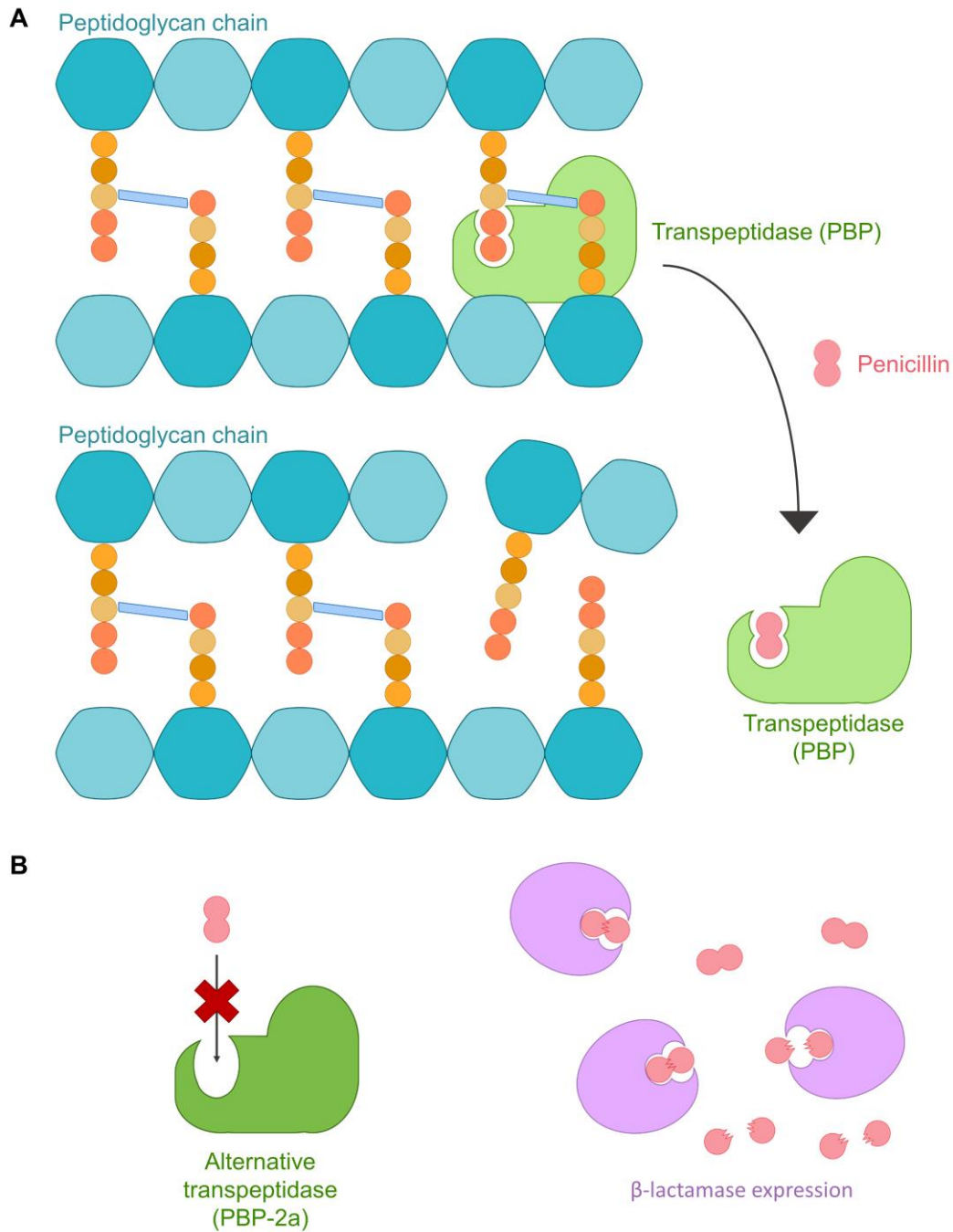


Figure 1.2 Penicillin mechanism of action and resistance mechanisms. **A** Penicillin and other β -lactams target the transpeptidase (penicillin binding protein, PBP) responsible for cross-linking the peptidoglycan subunits. By binding to the PBP active site, they prevent cell wall synthesis, resulting in cell lysis. **B** Penicillin resistance can be conferred by the expression of an alternative transpeptidase (PBP-2a) which is capable of cell wall synthesis but has low affinity for β -lactams or by the expression of β -lactamases, which cleave the β -lactam ring, rendering the antibiotic inactive.

Over 2600 β -lactamases have been described, constituting the most important resistance mechanism among Gram-negative ESKAPE pathogens.^{10, 24, 25} For example, in *S. aureus*, *blaZ*-encoded β -lactamases emerged before the use of penicillin and are now found in ~85% of clinical isolates.^{10, 14} Here, binding of β -lactam antibiotics to the membrane bound BlaR1 protein results in activation of the cytoplasmic domain of the protein, likely through conformational changes.²⁶ This cytoplasmic domain is a putative metalloprotease, which when activated degrades the gene repressor Blal.²⁷ Degradation of Blal prevents repression of the *bla* operon, which contains the genes *blaI*, *blaR1* and *blaZ*, encoding PC1 β -lactamase.²⁸⁻³⁰ Expression of the β -lactamase conveys antibiotic resistance to the cell, with these processes initiated within minutes of exposure.³¹ Once antibiotics are gone, the system is de-activated when no antibiotic is bound to BlaR1.³¹

Another family of antibiotics counteracted by modification are aminoglycosides, characterised by their aminocyclitol nucleus linked to amino sugars through glycosidic bonds.²⁰ Their exact mechanism of action differs, but commonly their binding leads to a change in conformation of the ribosomal A site. This change in conformation mimics the closed state induced when a cognate tRNA interacts with mRNA and eliminates ribosomal proofreading, encouraging mistranslation of proteins.²⁰ The most prolific method of aminoglycoside resistance in the clinical setting is the production of aminoglycoside modifying enzymes.^{14, 24} These enzymes catalyse the covalent transfer of an acetyl-, phospho-, or adenylyl-group to the amino or hydroxyl group of the molecule.²⁰ Such modification diminishes binding to the bacterial ribosomal subunit thereby reducing antimicrobial activity. Enzymatic modification is also the most common mechanism of chloramphenicol resistance.³²

Antibiotic target site modification

Bacteria may also obtain resistance through modification of the proteins or pathways which the antibiotic targets. Modification of target sites can range from a single point mutation in the corresponding gene, to replacement of an entire protein, to the addition of a novel protein which performs the function of the now inhibited protein.³³ For example, resistance to rifampicin is commonly obtained by point mutations in *rpoB*, the gene encoding a subunit of *E. coli* or *M. tuberculosis* RNA polymerase, the target of rifampicin.³⁴ A single point mutation changing Ser 450 to Leu was responsible for high rifampicin resistance (>128 mg/L) in almost half of *M. tuberculosis* isolates tested.³⁵ Replacement of penicillin binding protein is the mechanism underpinning both β -lactam resistance in *S. pneumoniae* and methicillin resistance in *S. aureus*.^{23, 36} Methicillin resistant *S. aureus* (MRSA) contain the

staphylococcal chromosomal cassette *mec*. One of the genes on this cassette is *mecA* which encodes penicillin binding protein 2a, a novel penicillin binding protein with low affinity for all β -lactams.^{23, 37} Expression of this protein enables effective cell wall synthesis in the presence of β -lactams, rendering them completely ineffective (**Figure 1.2**).

In Gram-positive ESKAPE pathogens, one of the most important resistance mechanisms is alterations to cell wall precursors.³⁸ Glycopeptides inhibit cell wall synthesis by targeting the D-Ala-D-Ala motif of peptidoglycan precursors. Such binding inhibits cell wall synthesis by preventing peptidoglycan crosslinking.²⁴ In Enterococci, acquisition of the *van* set of genes results in replacement of the precursor with D-Ala-D-Lactate or D-Ala-D-Ser.^{24, 38} Glycopeptides have reduced binding affinity to the modified precursor, enabling bacterial resistance as cell wall synthesis can continue. Specifically, the D-Ser residue provides low level resistance by reducing antibiotic binding affinity slightly while the lactate moiety results in high level resistance as it removes a hydrogen bond necessary for antibiotic binding.²⁴

Modification to antibiotic targets is also responsible for resistance to quinolones. Fluoroquinolones, such as ciprofloxacin and norfloxacin, work by targeting DNA gyrase and topoisomerase IV enzymes, which have essential roles in DNA repair and replication.³⁹ Both enzymes generate double-stranded breaks in the bacterial chromosome while carrying out their physiological functions. Fluoroquinolones increase the concentration of such enzyme-DNA cleavage complexes, resulting in lethal fragmentation of the genome (**Figure 1.3**).⁴⁰ Fluoroquinolones are synthetic molecules, not based on naturally-occurring compounds, and are some of the most commonly used antibiotics.⁴¹ Fluoroquinolone resistance still occurs, typically through chromosomal mutations in the genes encoding DNA gyrase subunit A or DNA topoisomerase IV subunit A (**Figure 1.3**).⁴⁰ The mutations result in amino acid substitutions in the site of the enzyme which is targeted by fluoroquinolones, preventing them from binding.

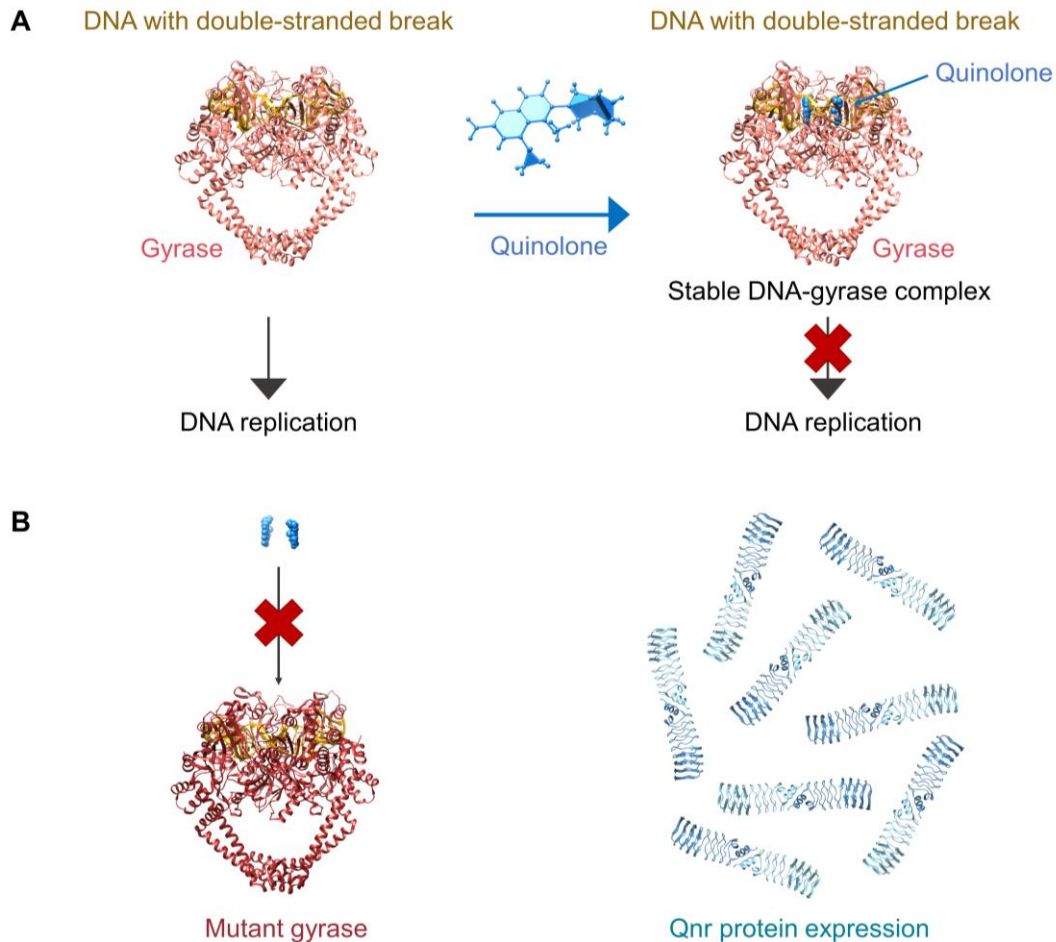


Figure 1.3 Fluoroquinolone mechanism of action and resistance mechanisms. **A** Fluoroquinolone mechanism of action. Fluoroquinolones target DNA gyrase and topoisomerase, enzymes which generate double-stranded breaks in the bacterial chromosome as part of DNA replication and repair processes. By stabilising the enzyme-DNA complexes (PDB #5BS8), fluoroquinolones prevent DNA replication and repair, leading to cell death. **B** Fluoroquinolone resistance is mediated by chromosomal mutations in the fluoroquinolone binding site of DNA gyrase or topoisomerase, resulting in decreased fluoroquinolone binding affinity, or *via* the expression of Qnr proteins (PDB: 2BM6), which are DNA analogues and are thought to reduce DNA-gyrase-fluoroquinolone toxic complexes by competing with DNA for enzyme binding.

Another method of quinolone resistance is the plasmid-acquired production of Qnr proteins, which act as DNA analogues (**Figure 1.3** and **Figure 1.4**).⁴¹ This is thought to provide resistance by binding to gyrase and topoisomerase and thereby reducing interactions with DNA, decreasing available quinolone binding sites, and preventing quinolone entry to DNA-bound complexes, although the exact manner remains controversial.^{40, 41} Nevertheless, bacteria producing Qnr proteins can effectively

replicate and repair their DNA in presence of fluoroquinolones. Another antibiotic targeting the transcriptional machinery is rifampicin, which inhibits transcription by binding to the RNA polymerase subunit B. Bacteria can develop resistance to rifampicin through mutations in the RNA polymerase B subunit gene, which modify the resulting protein.⁴²

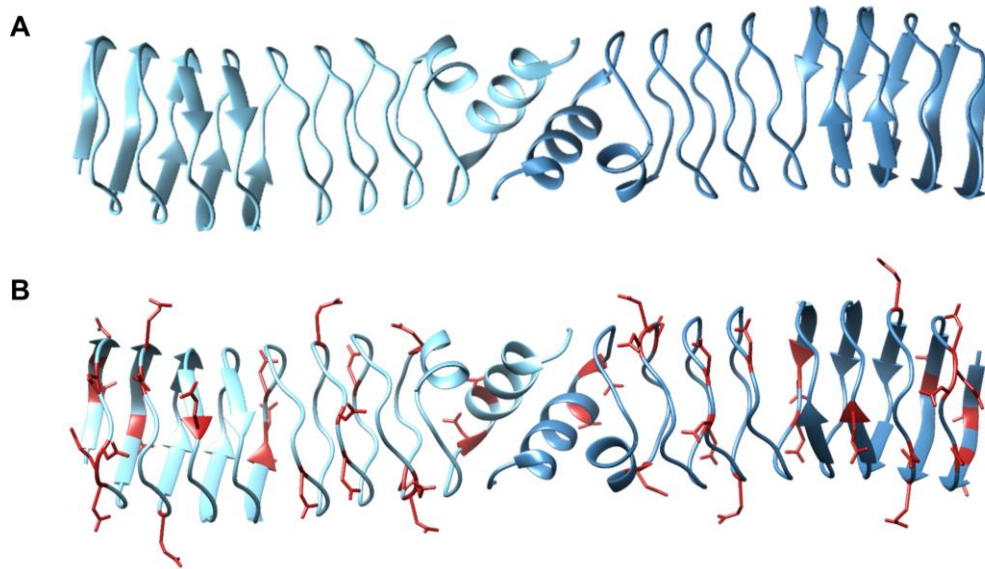


Figure 1.4 Structure of MfpA, a Qnr protein from *M. tuberculosis* (PDB: 2BM6). **A** The structure of Qnr protein mimics the double helix of B-form DNA. **B** Asp and Glu residues are indicated in red, these residues are negatively charged at physiological pH, mimicking the negatively charged DNA backbone.

Modification to the ribosomal RNA (rRNA) is a common resistance mechanism observed against antibiotics targeting the ribosome.¹⁴ Bacteria have three types of rRNA, the 5S and 23S rRNA, which are both located in the 50S ribosomal subunit, and the 16S rRNA, which is located in the 30S ribosomal subunit. An alternative mechanism of aminoglycoside resistance is mutation of the 16S rRNA to an altered sequence or methylation of the rRNA.²⁰ Linezolid inhibits bacterial growth by binding to the 23S rRNA and disrupting the docking of the charged tRNA to the A site of ribosome.²⁴ Methylation or mutation of the 23S rRNA provides resistance to linezolid and macrolide-lincosamide-streptogramin B antibiotics.¹⁴ Similarly, resistance to these antimicrobials can also arise through mutations in the 50S ribosomal subunit.¹⁴ Such modification of the rRNA prevents antibiotic binding, enabling translation to proceed.

Reduced antibiotic entry or accumulation

Gram-negative bacteria have an outer membrane, which acts as a permeability barrier and provides intrinsic resistance to certain antibiotics.⁴³ Porins are proteins located in the outer membrane, which allow substrates to pass in and out of the cell. Many hydrophilic antibiotics, such as β -lactams, fluoroquinolones, tetracyclines and chloramphenicol, rely on porins to enter the bacterial cell.¹⁴ Therefore, changes in the level or type of porins expressed can modulate bacterial susceptibility to these antimicrobials, providing acquired resistance.⁴⁴ Mutations leading to the downregulation or complete loss of porins are important multi-drug resistance mechanisms employed by Gram-negative ESKAPE pathogens.⁴⁴ For example, loss of the porin OprD in *P. aeruginosa* is linked to carbapenem resistance while loss of CarO in *A. baumannii* provides imipenem resistance.⁴⁵ Resistance provided by alterations in porins often co-exists and has a synergistic relationship with other antimicrobial resistance mechanisms such as the activity of antibiotic-degrading enzymes and efflux pumps.⁴⁴

Efflux pumps are complexes which sit in the bacterial membrane and extrude a variety of substrates, including toxins and antibiotics, from the bacterial cell.^{14, 44} Efflux pumps can be specific to certain antimicrobials, such as the plasmid-encoded tetracycline efflux pumps *tetK* and *tetL* in enterococci.²⁴ On the other hand, multidrug efflux pumps exist which have a wide substrate scope, providing broad antimicrobial resistance, and are a major contributor to antimicrobial multi-drug resistance.⁴⁶ A more detailed description of multi-drug efflux pumps is provided in **Chapter 2**. Multidrug efflux pumps are usually chromosomally-encoded and can provide intrinsic resistance in this manner in some species, such as *A. baumannii*.¹⁴ However, it is important to note that the majority of efflux pumps provide innate cellular functions and do not confer clinically relevant antimicrobial resistance.^{14, 47} Clinically-relevant resistance is often acquired as the result of mutations in efflux pump genes or promoter regions, resulting in increased pump function or expression, respectively.⁴⁶

Both reductions in porin expression and increases in efflux pump expression convey resistance by effectively decreasing the concentrations of antimicrobials in the cell (**Figure 1.5**). Although these are two separate resistance mechanisms, a bacterial cell may display both simultaneously. For example, aminoglycoside resistance is often the result of both reduced porin expression and increased efflux pump activity.²⁰ In turn, these mechanisms may also be complemented by the other antimicrobial resistance mechanisms described above. Resistance to a specific antibiotic can be

the result of various antimicrobial resistance mechanisms, which may be present in combination (**Table 1.2**).

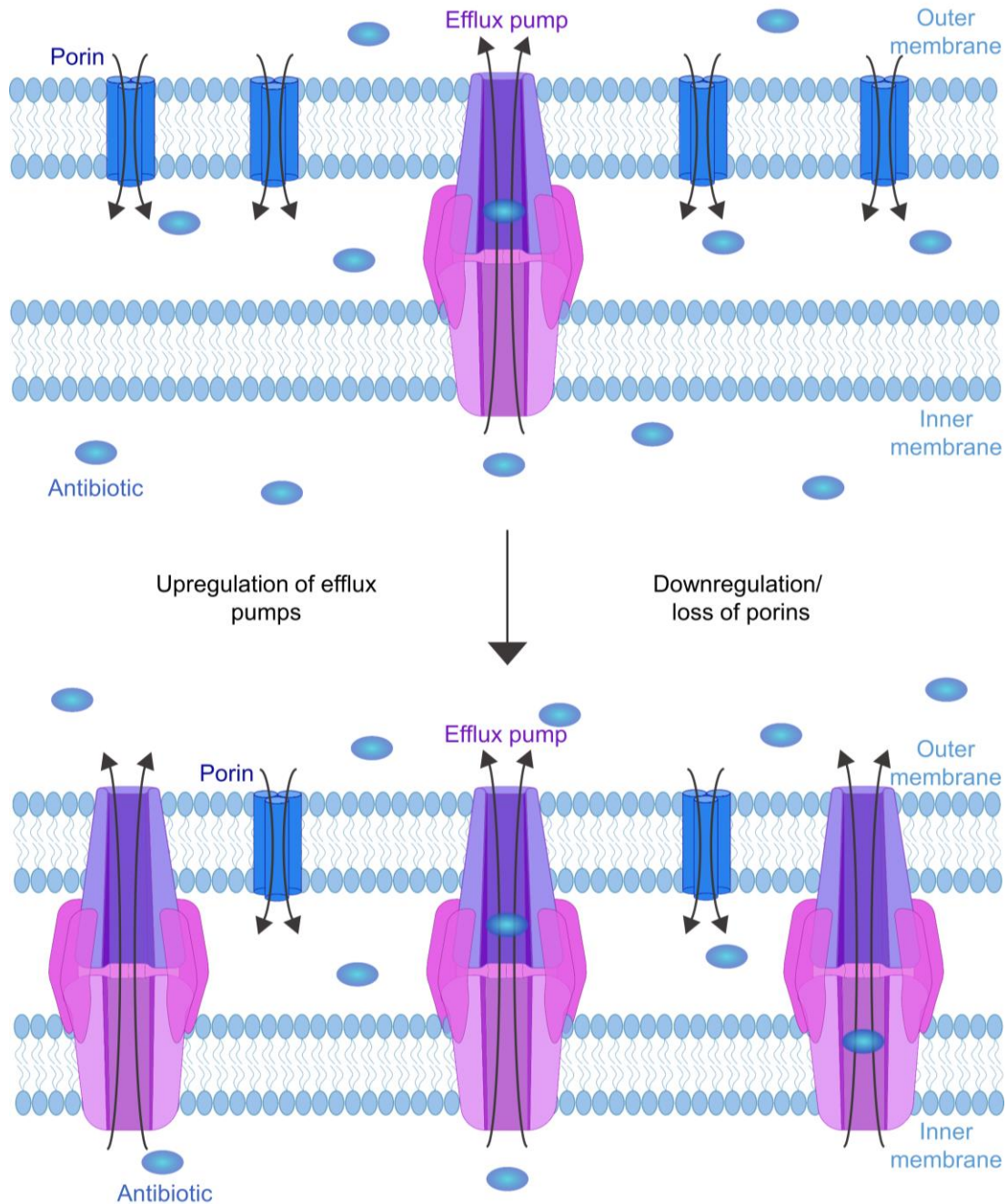


Figure 1.5 Antimicrobial resistance *via* reduced antibiotic entry or accumulation. Hydrophilic antimicrobials rely on porins to enter Gram-negative bacterial cells. A common antimicrobial resistance mechanism is a reduction or complete loss of porin expression to reduce antibiotic entry to the cell. Multi-drug efflux pumps are structures located in the bacterial membrane and extrude drugs and toxic compounds from the cell. The schematic shows an RND-type efflux pump. Another common resistance mechanism is the upregulation of multi-drug efflux pumps in response to an antibiotic to increase antibiotic extrusion from the cytoplasm. These two mechanisms may be present individually or simultaneously. Both mechanisms reduce the concentration of antimicrobials in the cytoplasm.

Table 1.2 Antibiotic resistance mechanisms against common antimicrobials. Adapted under license [CC-BY-4.0](#)¹

Antibiotic	Antibiotic modification	Antibiotic target modification	Reduced antibiotic entry	Reduced antibiotic uptake (efflux pumps)
β -Lactams	β -lactamases	Altered penicillin binding protein	Decreased porin expression	RND-type
Aminoglycosides	Aminoglycoside modifying enzymes, acetylation, phosphorylation, adenylation	Ribosomal mutation, methylation	Decreased porin expression, cell wall polarity	RND-type
Fluoroquinolones	Acetylation	DNA gyrase modification (Gram-negative), topoisomerase IV modification (Gram-positive)		MATE, MFS, RND-type
Tetracyclines	Oxidation	Ribosomal protection	Decreased porin expression	MFS, RND-type
Chloramphenicol	Acetylation	Ribosomal methylation		MFS, RND-type
Lincosamides		Ribosomal methylation (Gram-positive)		ABC, RND-type
Macrolides		Ribosomal mutation, methylation		ABC, MFS, RND-type
Glycopeptides		Modified peptidoglycan	Thickened cell wall, no outer cell wall	
Lipopeptides		Modified cell surface charge		

Biofilms and persistence

A bacterial biofilm describes a bacterial physiology where multiple cells are attached to a surface and are encased in an extracellular matrix.⁴⁸ Biofilms play an important role in the virulence of certain pathogens, for example, *S. aureus* biofilms can form on medical devices such as pacemakers while *P. aeruginosa* biofilms can colonise urinary catheters and cause chronic lung infections in cystic fibrosis patients.⁴⁹ Cells within a biofilm can require 100- to 1000-fold increased concentrations of antimicrobials to inhibit their growth compared to their planktonic counterparts.⁴⁸ In some cases, the extracellular matrix prevents or slows antibiotics reaching the bacterial cells, enabling resistance.⁴⁹ Cells in a biofilm may also secrete β -lactamases into the biofilm matrix, causing antibiotics to be degraded before they reach the cells.⁴⁹ Another element of a biofilm is the secretion of extracellular DNA. Extracellular DNA has been shown to influence antimicrobial susceptibility, this is thought to be facilitated by multiple mechanisms including antibiotic binding and/or sequestration by the DNA, induction of signalling cascades through a change in the extracellular environment and increased horizontal gene transfer.⁴⁹ The frequency of mutations and horizontal gene transfer is significantly increased in biofilms, enabling cells to easily display multiple resistance mechanisms and develop multidrug resistance.⁴⁸ Further, several enzymes are specifically produced or specifically provide resistance in a biofilm and not in planktonic cells.⁴⁹ Finally, biofilms often harbour persister cells.^{14, 49}

Persister cells are antibiotic-tolerant rather than resistant (**Figure 1.6**). Tolerance describes when a bacterial cell can survive but not grow in the presence of an antibiotic.⁴⁹ Antibiotic-tolerant cells often survive exposure to an antibiotic through entering an altered metabolic or dormant state. After the antibiotic challenge has been removed, the cells re-metabolise.¹⁴ Although slow at dividing, persister cells may support the development of antimicrobial resistance through an increased mutation rate.⁵⁰ Within a biofilm, cells near the surface of the biofilm use up oxygen and nutrients before they can reach the cells deeper in the biofilm. This leads to cells in deeper layers of the biofilm entering a reduced metabolic state, thought to confer tolerance to antimicrobials, as antibiotics target rapidly growing cells.⁴⁹ Persister cells are also observed as cells which can survive intracellularly within macrophages.¹⁴ These cells avoid exposure to the antibiotic, for example, MRSA sequestered in macrophages has a 100-fold increase in concentration of vancomycin required to inhibit growth compared to extracellular bacteria.⁵¹

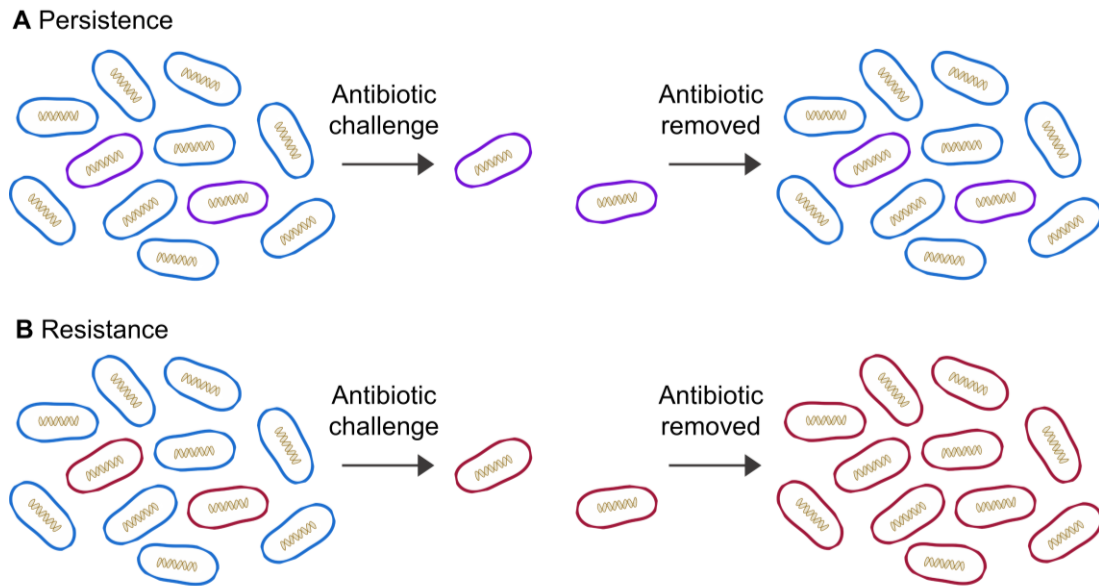


Figure 1.6 Antimicrobial resistance and persistence. **A** Persister cells (purple) may survive an antimicrobial challenge by entering a low metabolic or dormant state. Once the antimicrobial challenge is removed, the bacterial population will replenish and will still be sensitive to antibiotic treatment. **B** Antibiotic-resistant cells (red) survive an antimicrobial challenge. When the antimicrobial challenge is removed, the bacterial population will replenish and consist entirely of antimicrobial-resistant cells.

1.1.2 Spread of antimicrobial resistance

Unfortunately, as mentioned in **1.1 Antimicrobial resistance**, the resistance mechanisms described above have the capability to spread quickly through bacterial populations and between species. This is perhaps most evident in the rapid spread of multi-drug resistance in *A. baumannii*. Worldwide, 45% of *A. baumannii* isolates display multidrug resistance, but this is as high as 90% of isolates in some countries such as Turkey and Greece.^{52, 53} Further, global *A. baumannii* resistance to carbapenems and β -lactams increased 30% between 2011 and 2016 alone.⁵³ This section will discuss the ways in which resistance can be transferred between bacterial cells and species.

Mobile genetic elements and horizontal gene transfer

Mobile genetic elements are segments of DNA capable of moving within genomes or between bacterial cells. Mobile genetic elements include transposons, plasmids, integral and conjugative elements, and integrative and mobilizable elements. Transposons are genetic loci capable of intracellular transfer.⁵⁴ A common type of transposon are insertion sequences. Insertion sequences are small elements (less than 3 kb) capable of self-transposition within a genome.⁵⁵ The elements consist of

one or two genes necessary for mobility, flanked by short terminal repeats. Insertion sequences can also mobilise larger genes; when two copies of an insertion sequence are positioned on either side of the gene the whole loci moves as a single unit.⁵⁶ Examples of insertion sequences facilitating resistance are Tn9, containing the *catA1* gene encoding a chloramphenicol acetyltransferase and Tn10, containing *tet(B)* which encodes a tetracycline efflux pump.⁵⁶ Insertion sequences can disrupt expression of existing genes if their re-location interrupts a coding region.⁵⁵ This can provide resistance, e.g. by deactivating a porin-encoding gene.⁵⁵ Insertion sequences can also alter expression of genes by inserting promoter sequences in non-coding regions upstream of a gene.⁵⁵ For example, in *A. baumannii*, insertion of the insertion sequence *ISAbal* upstream of *bla_{OXA-51}* confers resistance to carbapenem through increased carbapenemase production.⁵⁷

Mobile genetic elements which can be transferred between cells include plasmids and ICEs.^{14, 58} Plasmids are circular, double stranded, self-replicating DNA molecules, distinct from chromosomal DNA.⁵⁴ Plasmids often contain other mobile genetic elements, such as insertion sequences, and antimicrobial resistance genes.¹⁴ Plasmids are particularly important for inter- and intra-species gene transfer.¹⁴ ICEs are sections of DNA (20-500 kb) typically carrying genes enabling excision of the element alongside those encoding the conserved conjugation machinery, enabling transfer of the element.⁵⁸ Additionally, ICEs often carry cargo genes which confer beneficial phenotypes to the host cell.⁵⁸ Genomic islands describe large regions (10-200 kb) of chromosomal DNA which have or previously had mobility and often contain resistance genes, usually resulting from insertion by mobile genetic elements.^{59, 60} For example, the above mentioned *Staphylococcus* chromosomal cassette *mec* is a genomic island responsible for the β -lactam resistance observed in MRSA.^{23, 37}

The movement of mobile genetic elements between cells is facilitated by horizontal gene transfer. Horizontal gene transfer can occur in three ways: transformation, transduction and conjugation. Transformation is the uptake of DNA from the environment and is mediated by chromosomally-encoded proteins, these are only found in some bacteria and there is little evidence that transformation is involved in resistance.^{10, 14} Transduction is another form of gene transfer mediated by bacteriophages, when bacteriophages accidentally pack segments of host DNA into their capsid and inject them into a new host cell. Transduction has been implicated in transfer of resistance genes in ESKAPE pathogens, but further verification is needed.¹⁴ Conjugation is the direct transfer of DNA between bacterial cells. To be

performed, conjugation requires close contact between cells, a 'sex pilus' to be formed between the bacteria, and specific genetic elements (**Figure 1.7**).

Conjugation is a natural bacterial mechanism which facilitates the transfer of many genes, not only those involved in antimicrobial resistance.⁶¹ However, it does frequently involve transfer of resistance genes and is thought to be the key mechanism facilitating the emergence and spread of antimicrobial resistance in pathogenic bacteria.¹⁴ Conjugation may be considered the most important mechanism of horizontal gene transfer as it allows transfer of plasmids. Multiple resistance genes can be present on one plasmid, which means that multi-drug resistance can be conferred to another cell in a single event.⁶² Perhaps the most pertinent example of resistance through horizontal gene transfer is aminoglycoside resistance. Genes encoding aminoglycoside modifying enzymes are most frequently located on mobile genetic elements, allowing their easy dissemination.²⁰ In fact, almost all clinically relevant bacteria have acquired aminoglycoside resistance through horizontal gene transfer.²⁰

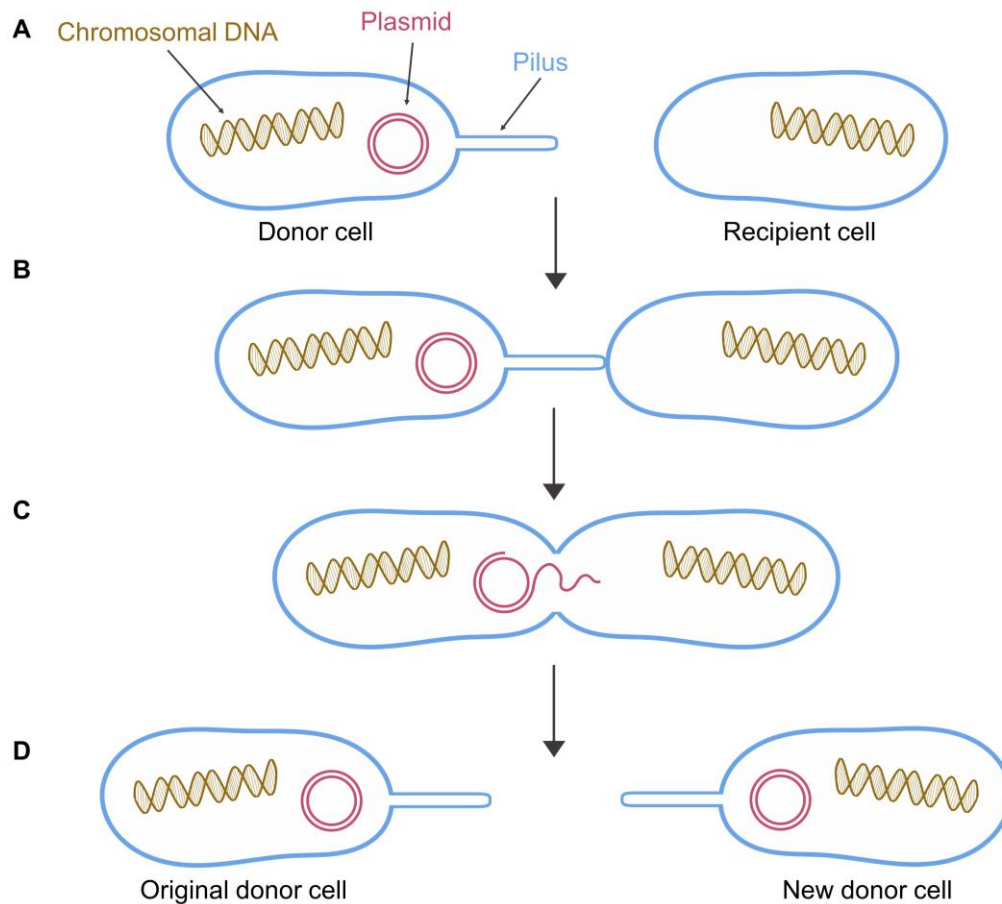


Figure 1.7 Bacterial conjugation. **A** A donor cell containing a conjugation-compatible plasmid produces a sex pilus. **B** The pilus attaches to a donor cell, which is brought into close contact. **C** The plasmid is nicked and a single strand of DNA transferred to the recipient cell. **D** Both cells transcribe the complementary plasmid DNA strand, resulting in a double stranded plasmid. Both the original donor cell and the new donor cell contain the plasmid and are capable of donating to new cells.⁶¹

Widespread use of antibiotics

As mentioned, the majority of antimicrobial drugs are compounds which are produced by microorganisms in nature, or synthetic derivatives of them, and antimicrobial-resistance is a naturally occurring phenomenon.⁵⁻⁸ However, these natural processes do not appear to account for the rapid spread of antimicrobial resistance which we observe today.⁶³ Indeed, there are increasing levels of resistance to synthetic antimicrobials not found in nature, for example, fluoroquinolone resistance is at 10-40% in *E. coli*.⁶⁴ There is strong evidence that the widespread use of antimicrobials has been the driving force behind the prolific spread of antimicrobial resistance genes.⁶⁵ Antibiotics act as a selective pressure, increasing the rate of chromosomal mutations and the likelihood of resistant populations appearing.^{63, 65, 66} Such selective

pressure has also been shown to induce horizontal gene transfer between cells. In both *E. coli* and *Vibrio cholerae*, induction of the SOS response as a direct response to ciprofloxacin increased transfer of a mobile genetic element which confers resistance to various antimicrobials.⁶⁷

Resistance has even been demonstrated to develop within a single patient during a treatment course. For example, sequential isolates of *K. pneumoniae* taken from a patient treated with ertapenem began as ertapenem-susceptible then developed ertapenem resistance.⁶⁸ Antimicrobials are the most commonly prescribed drugs in human medicine yet, unfortunately, unnecessary administration is rife, accounting for up to 50% of prescriptions in the US.⁶⁹⁻⁷¹ Such use of antimicrobials when a patient does not have a bacterial infection increases the likelihood of antimicrobial resistance occurring yet serves no beneficial purpose as it does not cure a disease. However, application in human medicine accounts for only a small part of global antibiotic usage, with more antimicrobials used in the production of food than for human diseases.⁷² Most worryingly, antimicrobial use in animal rearing is often preventative or to improve animal growth, and not for treatment. Often, the same antibiotics administered are used for treatment in humans.^{11, 73} This means that resistance can originate in agricultural setting and then spread to human pathogens.¹²

Antimicrobial resistance has also emerged through antimicrobial use in veterinary medicine, aquaculture, pest control, and waste from the pharmaceutical industry.⁷⁴ Such events result in antibiotics in the environment; in fact, antimicrobial resistant bacteria have been isolated from all environments examined to date.⁷⁴ This causes a constant selective pressure on bacteria to develop resistance to the antimicrobials.⁷³ Even relatively low concentrations of antimicrobials can have substantial effects on the rate of adaptive evolution.^{75, 76} Antimicrobial resistance genes can also be co-selected with resistance determinants to other toxins, e.g. the use of metals in agriculture has been demonstrated to select for antimicrobial resistance.⁷⁷ Together, the global widespread usage of antibiotics in human medicine, agriculture, aquaculture, and veterinary medicine imposes a constant selection pressure on bacteria from all environments to develop antimicrobial resistance (**Figure 1.8**).

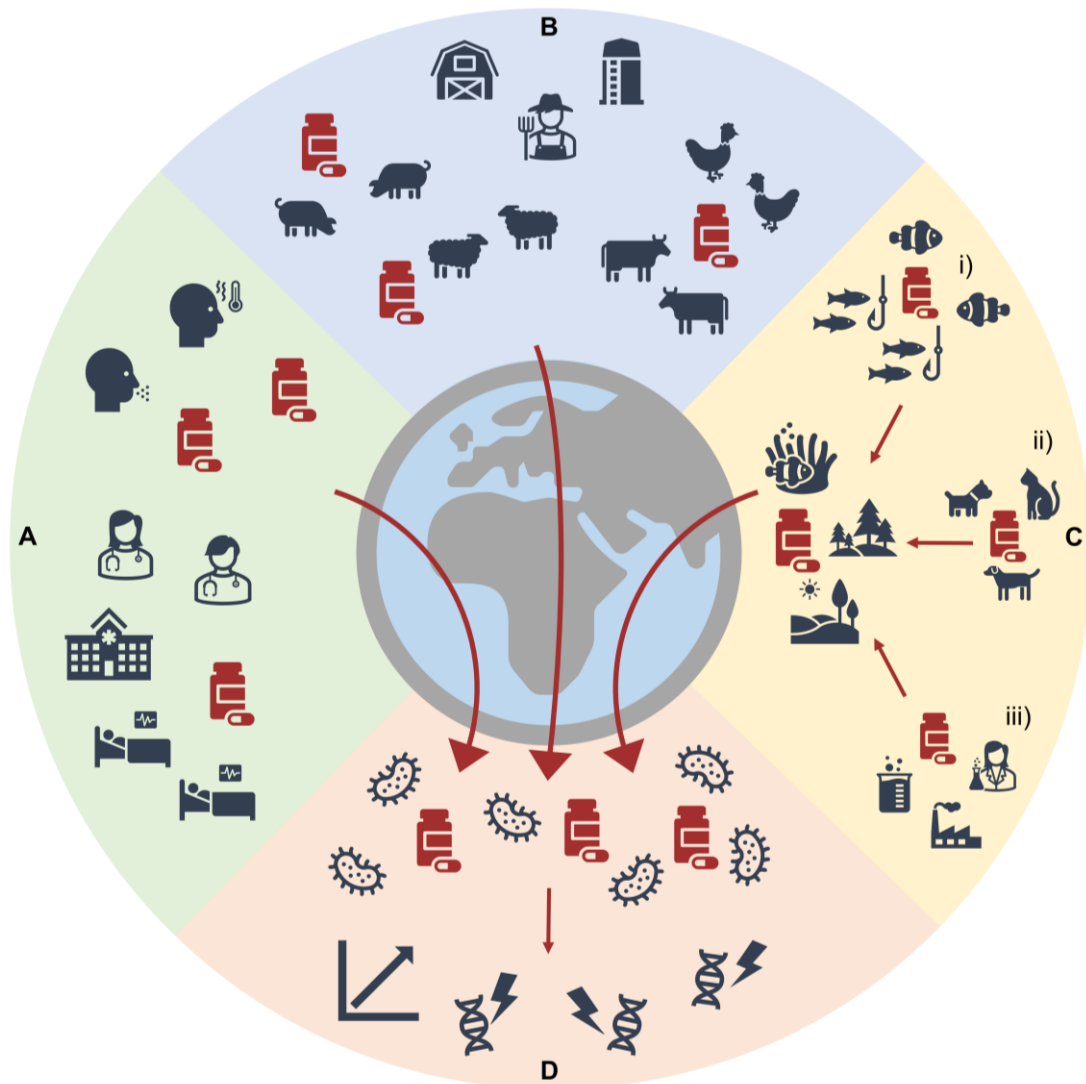


Figure 1.8 Widespread antibiotic use contributes towards antimicrobial resistance. **A** Antibiotics are the most prescribed drug in human medicine, and up to 50% of prescriptions in the US are unnecessary or inappropriate. **B** Antimicrobials are also widely used as growth promoters or as preventative treatment in animal rearing. **C** Further antibiotic use in i) aquaculture and ii) veterinary medicine alongside iii) pharmaceutical waste results in antibiotic accumulation in the environment. **D** This global widespread use of antibiotics applies a selective pressure to bacterial populations, resulting in bacterial antimicrobial resistance *via* increased chromosomal mutations and horizontal gene transfer.

1.1.3 Fighting antimicrobial resistance

The arsenal of resistance mechanisms possessed by bacteria and the ease of horizontal gene transfer has led to the rapid emergence of antimicrobial resistance observed since the implementation of antibiotics in human medicine. If left unchecked, humanity risks losing the public health gains enabled by the routine use of antimicrobials.^{11, 74} It is unquestionable that we must find ways to counter antimicrobial resistance, and many reports have been published with action.^{10-12, 14, 74, 78, 79} Key steps include reducing unnecessary antimicrobial use, increasing global awareness and surveillance, and improved research funding and incentives for new drugs.^{11, 12}

Reducing use of antimicrobials

Exposure to antimicrobials is central to resistance emergence and spread.⁷⁴ The easiest way to reduce use of antimicrobials is to prevent infection through improved clinical hygiene.¹¹ Indeed, preventing infection in hospitals also has more apparent benefits to the health of patients. Although it may be assumed that hospitals already have high standards of hygiene, this is not to be overlooked. Implementation of improved hygiene in hospitals in England as part of a nationwide infection control programme led to a 95% decline in MRSA bloodstream infections in ICU patients and a 78% decrease in bloodstream infections overall.⁸⁰ Another infection prevention strategy is the use of vaccines where available.¹¹ Vaccination has the added advantage of herd immunity if a high enough uptake is achieved.¹⁴ However, there are currently not enough vaccines available for antimicrobial resistant bacteria for this to be a viable strategy.¹⁴

Currently, many antibiotics are prescribed before, or in some cases without, bacterial infection being confirmed.⁸¹ This is because the tests used to identify bacterial infections are decades old, and require a sample to be taken and sent to a lab, where bacteria are cultured for 36 hours before the infection can be characterised.⁸¹ This means that clinicians are often forced to prescribe antibiotics based on their judgement of the likelihood of a bacterial infection, to avoid patient suffering or the infection developing while awaiting test results. However, this results in many antimicrobials being prescribed unnecessarily. For example, in the US between 2010 to 2011 approximately 30% of outpatient prescriptions were unnecessary.⁶⁹ To circumvent these unnecessary prescriptions, rapid diagnostic tests should be developed which allow clinicians to confirm bacterial infections on the spot and prescribe appropriately.⁸¹

Additionally, the general public has little understanding of when antibiotics are required and what antimicrobial resistance is; common misconceptions include that antibiotics are required when a patient feels very unwell, antimicrobial resistance is when the patient becomes resistant to antibiotics, and that doctors are reluctant to prescribe antibiotics for cost-cutting purposes.⁷⁹ Therefore, it is critical that the general public is educated about the use of antibiotics, the infections they are suitable for treating, and antimicrobial resistance. This will reduce patients demanding antibiotics from their clinician unnecessarily, e.g. to treat a viral infection.

Another major way to reduce antimicrobial use is to clamp down on the prolific use of antimicrobials in agriculture. The use of antimicrobials as growth promoters and infection prevention should be banned.^{11,73} The European Union has already banned the use of antibiotics for growth promoters in 2006.⁸² Further, when antimicrobials are used to treat infections in agriculture, different classes of antimicrobials should be used to those used in humans.⁸³ Antibiotics important for human medicine should not be used in agriculture, that way the use of antimicrobials in agriculture is less likely to lead to development of resistance in human bacterial infections.^{11,73}

While reducing the use of antimicrobials may prevent the emergence and spread of resistance, it is not guaranteed to eliminate resistance. There is a belief that microbes carrying resistance genes would be less fit compared to their antibiotic-susceptible counterparts in the absence of an antimicrobial challenge and would be outcompeted due to a fitness burden of carrying the genes.⁷⁴ Indeed, resistance genes sometimes have a cost, e.g. the acquisition of methicillin resistance reduces the growth rate of *S. aureus*.⁸⁴ In this case, it may be plausible that in the absence of antimicrobials bacteria would lose resistance genes. There is some evidence to back this up, for example, a 42% decrease in macrolide antibiotic use in Finland correlated to a decrease in erythromycin resistance in group A streptococcal isolates from 16.5% to 8.6% from 1992 to 1996.⁸⁵

Unfortunately, there appears to be more evidence in contrary to this assertion. Bacteria containing resistance genes have been shown to survive and proliferate in the absence of antibiotics.⁸⁶ For example, the UK introduced strict restrictions on sulphonamide prescriptions and from 1991 to 1999 prescriptions decreased from 320,000 to 7,000 per year. Despite this, the prevalence of resistance in *E. coli* clinical isolates only decreased from 46% to 40%.⁸⁷ The authors speculated that this may be due to compensatory mutations or co-selection with other resistance determinants.

However, they also noted that throughout this time period sulphonamides were still used in agriculture and aquaculture.

Resistance determinants can persist for years in the absence of antimicrobials.^{10, 88} Rather than evolve to revert to a pre-resistance phenotype, in the absence of antibiotics bacteria are more likely to have compensatory mutations in other genes which restore their fitness to the previous level.^{88, 89} In one striking example in *E. coli*, acquisition of a fourth resistance mutation resulted in dramatically decreased susceptibility to fluoroquinolones but a 5-10% increase in fitness per generation.⁸⁶ Indeed, some resistance genes do not carry a cost burden, depending on genetic background of bacteria.⁹⁰ Johnning *et al.* found no correlation between fluoroquinolone exposure and the presence of resistance mutations when analysing aquatic *Escherichia* samples from environments with varying levels of fluoroquinolone exposure, with the exception of extreme quinolone exposure having more mutations.⁹¹ Interestingly, in some genetic backgrounds, reversion to an antibiotic-susceptible phenotype may result in decreased fitness.⁸⁹ Additionally, multiple antibiotic resistance genes are often co-selected when located in close proximity. This means that reduction in the use of one antibiotic may not have any impact if another antimicrobial is still used, and resistance to this is encoded on a nearby gene.⁹² Therefore, while reduction in the use of antimicrobials is undoubtedly helpful, it is only part of the solution.

New drugs

After the discovery of antibiotics, development of new antimicrobials had initial success.⁹³ However, as mentioned above, resistance develops quickly. To combat resistance, new drugs to which there is little resistance are only used as a last line of defence when other treatments have failed. However, this greatly reduces incentives for pharmaceutical companies to develop drugs, as limited use means smaller profit margins.^{73, 83} Further, if resistance develops quickly to the novel drug, it can only be used for a short time period, again limiting potential profits.^{10, 73} There is therefore a need to increase incentives for pharmaceutical companies to develop new antimicrobials, e.g. by implementing delinking initiatives which give a financial reward for the development of innovative antibiotics independent of unit sales.^{11, 83} Heavy regulations are another obstacle preventing new drug development, it can take up to 12 years for approval.⁹³ In fact, there has been little progress in recent decades; since the 1960s there have only been 4 new classes of antibiotics. Instead, “new” drugs are often based on established antibiotics and the majority of drugs in clinical development today are derivatives of antibiotic classes to which there is already

resistance.^{10, 93} New drug discovery has repeatedly been described as essential.⁷⁴ However, the great challenges in our current drug discovery indicates that wider and more innovative approaches are needed.⁷³

New approaches

In addition to new antimicrobials in the traditional sense, novel treatments and new approaches are undoubtedly needed. For example, relatively simple changes to existing treatments, such as rapidly switching which antibiotic is being used, can reduce selective pressure on bacteria.¹⁴ Combinational drug therapy is such a strategy to address antimicrobial resistance.^{14, 73} It involves either using two antibiotics together or pairing an antimicrobial with an adjuvant to overcome resistance. The adjuvant could be an inhibitor of an antibiotic-degrading enzyme, a compound which generally reduces microbial health, or one that boosts the patient's immune system to allow antibiotics to work more effectively.¹⁴ One such example is the inhibition of aminoglycoside modifying enzymes through antisense oligonucleotides which reduce their expression.²⁰ Multi-drug efflux pump inhibitors have also been developed to increase antibiotic accumulation in the cell.⁹⁴

Bacteriophage therapy has not been in use for several decades, but carries promise for combating antimicrobial resistance.⁹⁵ For example, the Phagoburn project trialed the use of phage therapy to treat infected burns in European countries.⁹⁶ Patients received a cocktail of 12 natural lytic anti-*P. aeruginosa* bacteriophages or the current standard of care treatment, a topical cream. Unfortunately, the phase I/II clinical trial terminated early due to the insufficiency of the phage therapy. The authors concluded that the dosage used was too low and more investigations are needed with higher doses.⁹⁶ Despite these setbacks, phage therapy remains a promising area of future research.¹⁴ Particularly, a new area of research is the engineering of bacteriophages. Bacteriophages could be engineered to destroy bacterial DNA,¹⁴ to suppress bacterial survival responses, or to produce molecules which enhance antimicrobial therapy.⁹⁵ For example, Lu and Collins engineered an M13mp18 phage to overexpress *lexA3*, a repressor of the SOS response.⁹⁵ Addition of the phage to *E. coli* enhanced the bactericidal effect of ofloxacin by 4.5 orders of magnitude and also increased survival of mice infected with the bacteria.⁹⁵

Monoclonal antibody therapy represents another promising avenue to combat antimicrobial resistance.¹⁴ However, so far only 3 monoclonal antibodies have been approved for treatment in the US, and none of them are effective against ESKAPE pathogens. Two of the approved monoclonal antibodies, Raxibacumab and

Obiltoximab, both target the protective antigen secreted by *Bacillus anthracis*.^{97, 98} The other, bezlotoxumab, neutralises toxin B of *Clostridium difficile*.⁹⁹ The effectiveness of these therapies against their target species suggests that more research into this approach for ESKAPE pathogens is necessary.¹⁴ Another important area for further research are vaccines against bacterial infections.¹⁴ Vaccines have the potential to prevent both antibiotic-resistant and antibiotic-sensitive infections and have the further advantage of herd immunity if enough of the population are immunised. For example, successful implementation of the pneumococcal conjugate vaccine in US infants in 2000 led to a striking decrease in pneumococcal diseases, including antibiotic resistant infections.¹⁰⁰ Specifically, penicillin-resistant cases dropped by 81% in the vaccinated population.¹⁰⁰ Further, high vaccine uptake resulted in herd immunity, which led to a ~50% reduction in penicillin resistant cases overall.¹⁰⁰ However, there are currently no vaccines available for infections caused by ESKAPE pathogens, and these have been difficult to develop.¹⁴

There are even more new approaches worthy of further investigation. For example, an interesting area of research involves reprogramming bacterial cells to target antimicrobial-resistant infections. Hwang and colleagues successfully reprogrammed *E. coli* to specifically recognise, migrate towards and kill *P. aeruginosa* cells.¹⁰¹ The reprogrammed *E. coli* were effective against both planktonic cells and those in a biofilm. This was achieved by reprogramming the chemotaxis system to respond to and migrate towards a quorum-sensing molecule produced by *P. aeruginosa*. The *E. coli* cells were further modified to express and secrete an antimicrobial peptide and DNaseI upon detection of the quorum-sensing molecules.¹⁰¹ Another approach worthy of further consideration is to target horizontal gene transfer. As Graf and colleagues highlight, preventing the spread of antimicrobial genes may be an effective tactic to manage antimicrobial resistance.⁶² Specifically, the authors suggest targeting conjugation either through the use of CRISPR-Cas9 to degrade the donor plasmid, inhibit the mobile elements present on resistance plasmids, or inhibit the conjugation mechanisms themselves.

Overall, there is no straightforward solution to combat antimicrobial resistance. When new drugs and approaches are developed, it is inevitable that antimicrobial resistance will evolve, as we place a selection pressure on bacteria and they will adapt.^{10, 11} As such, it is essential that new approaches are continuously developed, with a more holistic understanding of bacterial adaptation and more antimicrobial targets.^{11, 74} There is unlikely to be a single answer and several overlapping and synergistic approaches are needed.⁷⁴ There is a need to understand wider mechanisms and

bacterial processes which facilitate bacterial adaptability and the emergence of resistance. One such area which is emerging as important are bacterial post-translational modifications. These highly versatile modifications allow bacteria to rapidly change the function of a protein or modulate its expression, allowing bacteria to quickly change their physiology.¹⁰² Recent data has implicated a role of post-translational modifications in resistance,¹⁰³⁻¹⁰⁷ and this novel area may represent an original avenue for combatting antimicrobial resistance.

1.2 Bacterial post-translational modifications

Post-translational modifications (PTMs) are covalent modifications to the protein polypeptide chain during or after translation.¹⁰⁸ Originally discovered in histones, PTMs revolutionised the central dogma of molecular biology which stipulated that one gene encodes one protein which serves one function.^{102, 109} PTMs can range from the addition of small chemical groups to large polypeptide chains.^{102, 108} Subsequently, this can alter the structure of proteins, modulate their function, impact protein complex formation or enzyme catalysis, and regulate gene expression.¹⁰² A key aspect of most PTMs is reversibility, with specific enzymes catalysing addition or removal of the functional group from the protein.¹⁰⁸ This allows precise control over the percentage of a specific protein in the cell containing the PTM. This reversibility also allows the rapid switching of protein function, permitting specific cellular processes to be switched on and off through a mechanism which is substantially faster than gene expression. In result, the cell can respond rapidly and dynamically to changes in the extracellular environment.

E. coli can adapt to environmental changes in seconds.^{110, 111} Modulating protein function *via* PTM in response to environmental changes allows the rapid enaction of cellular processes to survive or benefit from the extracellular conditions. Most proteins which are subjected to a PTM will be in a heterogenous pool in the cell, that is, not all proteins will be modified at any one time.¹¹² This provides an advantage as the cell can rapidly modify a pool of existing proteins to produce the required cellular response. On the other hand, responding to environmental conditions exclusively by regulating gene expression would take considerably longer and require the synthesis or degradation of proteins, while also being much more energetically costly. The expansion of protein function through PTM also helps to explain how bacteria can adapt to such a diverse range of environmental conditions with a relatively small genome.¹¹³ Further, bacteria are also capable of post-translationally modifying not only their own proteins, but eukaryotic proteins from a host cell.¹¹⁴

PTMs were first identified in eukaryotic histone proteins and many more types of PTMs were subsequently discovered. For some time, PTMs were assumed to be unique to eukaryotes, however, it is now clear that PTMs are just as prevalent in prokaryotes.^{102, 115, 116} To date, hundreds of different types of PTMs have been recorded.¹¹⁷ The development of MS-based proteomic studies has allowed the high-throughput assessment of PTMs of an entire organism's proteome. Such studies have

been performed on the proteomes of a diverse range of bacterial species including *E. coli*,¹¹⁸⁻¹²⁰ *B. subtilis*,¹²¹ *S. pneumoniae*,¹²² *M. tuberculosis*,¹²³ *S. enterica*,¹²⁴ *S. aureus*,¹²⁵ *T. thermophilus*,¹²⁶⁻¹²⁸ and *M. pneumoniae*.¹²⁹ These studies have revealed that PTMs are highly prevalent in bacteria, where numerous PTMs have been recorded and are still being uncovered.¹⁰² In bacteria, multiple reports have demonstrated that PTMs occur on proteins involved in almost all cellular functions including metabolism, cell cycle control, sporulation, dormancy, persistence and virulence.¹⁰⁸

1.2.1 Detecting PTMs

Before the advancement of mass spectrometry (MS) technologies, detection of PTMs was relatively limited. The main method of detection was western blotting of cell lysates with antibodies against the modification. While this method is still useful today to analyse changes in the global modification levels, for example during different growth stages or in response to different environmental conditions, it is not sensitive enough to identify modification of specific proteins in a mixture or to quantify the prevalence of the modification in a heterogeneous pool.¹³⁰ The limited sensitivity of western blotting may also prevent detection of all modified proteins if they do not have high enough abundance. Typically, modified proteins are not high in abundance relative to their unmodified counterparts.¹¹² This is particularly true of proteins in which the modification regulates protein function. Further, if a single protein is subjected to multiple PTMs the relative abundance of each modification may be small.

MS approaches have vastly increased capacity to study PTMs and provide the most reliable identification, characterisation and quantification.^{112, 131} MS is a highly sensitive technique involving the ionisation of a protein or peptide sample, and subsequent separation of the sample based on the mass-to-charge ratio of the components.¹³¹ The presence of a PTM can be inferred from the observance of a higher mass than the predicted mass of a peptide or protein. The mass difference corresponds to the expected mass of the modification, e.g. 14 Da for the addition of a methyl group, or 42 Da for the addition of an acetyl group. MS can also allow the discovery of unknown PTMs if an unexpected mass shift is observed.¹¹² In addition, tandem MS allows the isolation of an ion with specific mass-to-charge ratio, and this ion is then subjected to further fragmentation and analysis.^{131, 132} As the most labile bonds in peptides are usually the backbone amide bonds, the fragmentation mostly occurs between amino acid residues. The amino acid sequence of the peptide fragment can be determined from the fragment ion signals, composed of b-ions, where the peptide retained the charge on the N-terminus, and y-ions, when the

charge was retained on the C-terminus. The mass differences between the two series allows the determination of the exact sequence of amino acids and the exact site of any modification.¹³²

Different approaches for identifying PTMs can be considered. Bottom-up approaches involve the proteolytic digest of proteins before analysis.¹³¹ This could be all the proteins from a cell lysate, known as shotgun proteomics,¹³³ as well as an isolated group or single protein. Generally, few PTMs are detected by these approaches as the relative frequency in the proteome is low. Top-down approaches involve the ionisation of intact proteins before fragmentation and analysis.¹³⁴ An advantage of such approaches is that they permit relative quantification of the prevalence of the modification. Additionally, middle-down approaches are similar to top-down approaches but with mild proteolysis of samples before analysis.¹³¹ For all approaches, the techniques used to fragment the protein sample may affect the results. For example, collision-induced dissociation is frequently used but may lead to loss of PTMs during fragmentation, particularly those which are labile such as phosphorylation, ubiquitination, or acetylation.¹³⁵

As PTMs are relatively scarce, techniques to first enrich the sample are often employed to increase identification of PTMs.¹³² However, enrichment techniques do not yet exist for all PTMs. There are two main approaches for enrichment: enrichment at the protein level or enrichment at the peptide level after proteolytic digestion of protein lysate. Various enrichment strategies exist¹³⁶ with a common strategy being the use of immobilised metal ion affinity chromatography (IMAC) beads. For example, ferric ions can be used to isolate phosphorylated proteins, as phosphoproteins and phosphoamino acids will bind and can be eluted using a buffer with a high pH.^{137, 138} Enrichment approaches based on immunoaffinity purification are also used, such as the isolation of acetylated proteins using anti-acetyl-Lys antibodies.^{139, 140} It is also important to note that, as mentioned above, PTMs are dynamic and the frequency, relative abundance, and distribution of PTMs changes in response to external stimuli. Consequently, any analysis of PTMs is a snapshot from a certain point in time and will vary with, amongst other variables, cell growth stage and culture conditions.¹¹²

1.2.2 Types of PTMs

Across all species, the main PTMs are phosphorylation, acetylation and ubiquitylation which account for more than 90% of all reported PTMs.¹⁴¹ In bacteria, the primary PTMs are phosphorylation, acetylation, succinylation and pupylation, occurring on reactive side chains.¹⁰² In particular, lysine undergoes many different types of PTM. The following subsections will explore some of the most common PTMs in bacteria and their effects on cellular physiology.

Proteolysis

There are two classes of PTMs, modification to the peptide backbone and modification to the amino acid side chains. This thesis will discuss only the latter class of PTMs. However, it is worthwhile mentioning that proteolysis, the hydrolysis of peptide bonds, is the most ubiquitous PTM.¹⁰² Proteolysis facilitates breakdown of misfolded proteins, providing recycling of amino acids for translation. Proteolysis can have great effect on protein function and is irreversible.¹⁰² A prominent example in humans is the proteolysis of an insulin precursor by prohormone convertase 1/3, resulting in active insulin.¹⁴²

Phosphorylation

Phosphorylation in prokaryotes was a subject of debate for many years,^{115, 116} but is now known to be a ubiquitous PTM involving the attachment of phosphate onto the functional groups of amino acid side chains. This 80 Da modification most frequently occurs in both eukaryotes and prokaryotes on Ser, Thr and Tyr residues, with regulatory roles in a broad range of cellular processes.^{102, 115, 143} Phosphorylation of His occurs less frequently, in bacteria it is involved in bacterial two-component regulation.^{144, 145} Lys, Arg, Asp and Cys also undergo phosphorylation albeit less frequently.¹⁰² Phosphorylation is a reversible enzymatic reaction carried out by kinases, which add the phosphate group to the target residue, and phosphatases, which remove the phosphate group. Bacteria have a much greater diversity of catalytic protein kinases than eukaryotes and these are classified into five types based on the amino acid residue which they modify.^{115, 146} This higher variation may be related to the diversity of niches bacteria occupy, particularly, the number of Ser/Thr kinases reflects the complexity of the environment which the bacteria inhabits.¹⁴⁷ Phosphorylation is not a uniform modification and most bacterial protein kinases and phosphatases act exclusively on a specific residue.¹³⁵ The chemical stability of a phosphorylated side chain varies based on the amino acid modified, as does the effect on the target protein. Phosphorylation can rapidly modulate function

of proteins *via* allostery or occupation of interaction domains.¹⁴⁸ Phosphorylation has regulatory effects on a vast range of bacterial cell processes including production of toxins and adhesion molecules, motility, biofilm formation and drug resistance.¹⁴⁹

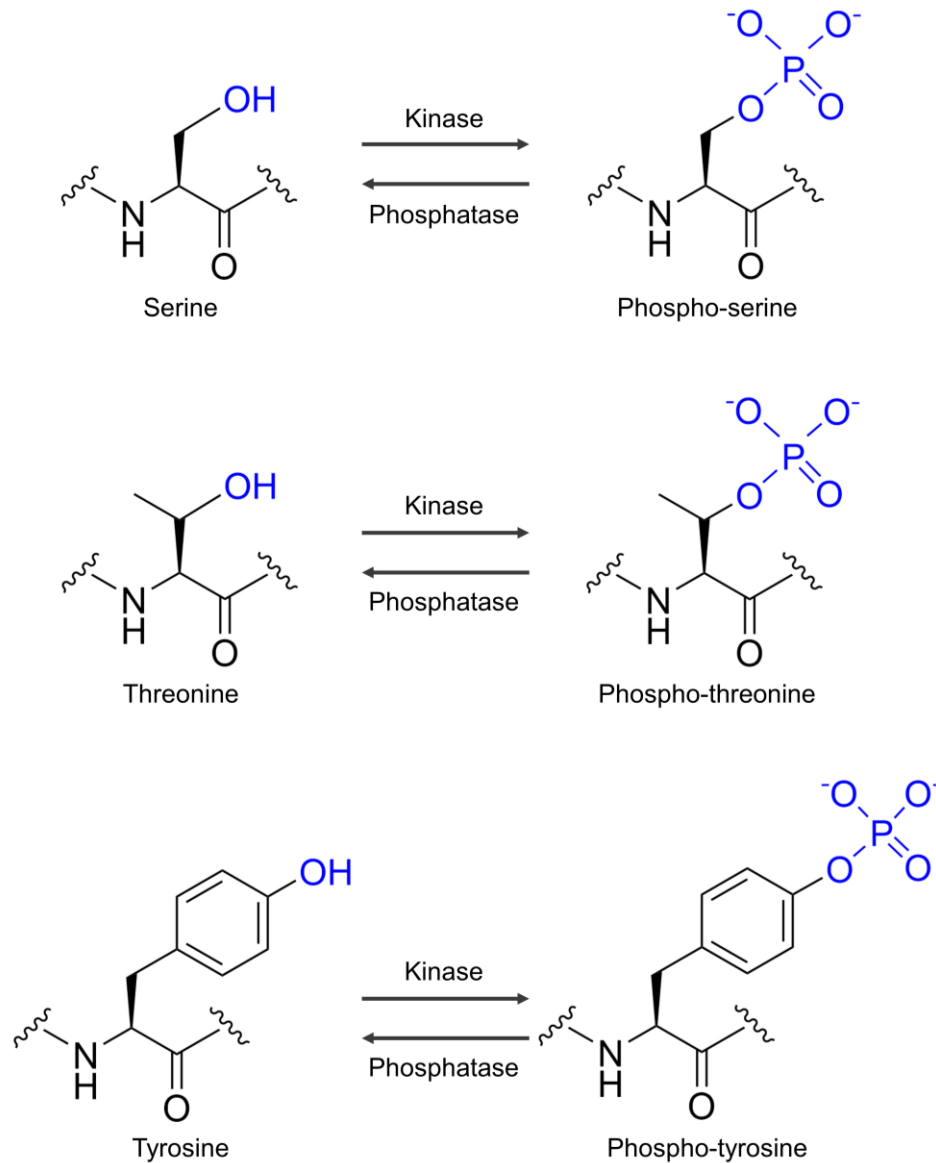


Figure 1.9 Schematic representation of Ser, Thr and Tyr phosphorylation. Phosphorylation is the addition of a phosphate group to a reactive side chain and is a reversible modification facilitated *via* kinases and removed by phosphatases.

In prokaryotes, Ser/Thr/Tyr phosphorylation have received disproportionate attention, as other types of phosphor-bonds are more chemically labile, making them difficult to be detected with typical mass spectrometry protocols.¹⁰⁶ Ser and Thr residues are mostly phosphorylated by Hanks-type Ser/Thr kinases, which are similar to eukaryotic kinases and likely evolved from the same ancestral genes.¹⁴⁷ Ser/Thr kinases and

phosphatases mediate gene expression through reversible PTM of two component system response regulators and transcriptional and translational machineries.¹⁵⁰ Such regulation allows modulation of gene expression in response to changing external signals and participates in multiple metabolic pathways including glycolysis, the tricarboxylic acid cycle, nucleotide metabolism, and synthesis and secretion of some virulence factors.¹⁵¹ In various species, phosphorylation is essential for cellular processes such as growth, cell division and morphology, sporulation, iron transport, symbiotic interactions with host plants, motility, oxidative stress response, virulence and antibiotic resistance.¹⁵⁰ The number of Ser/Thr kinases and their effects on cellular physiology varies by bacterial species. For example, *M. tuberculosis* has 11 Ser/Thr kinases involved in regulation of growth, development, biofilm formation, metabolism, stress responses, virulence and antibiotic resistance.¹⁵⁰ In contrast, only one Ser/Thr kinase and phosphatase pair has been identified in *S. aureus*, which is responsible for the phosphorylation of a large set of proteins including two global regulatory proteins.^{152, 153} These regulatory proteins are involved in quorum sensing and multidrug efflux pump expression, among others.

Most Tyr phosphorylation is carried out by bacterial tyrosine kinases, which have a cell-surface exposed feature permitting direct integration of extracellular signals into cytoplasmic kinase activity and diverse physiological responses such as capsule and lipopolysaccharide biogenesis, transcriptional regulation, stress responses and cell cycle regulation.¹⁵⁴ Some physiological responses are mediated through changes in gene expression. Multiple DNA binding proteins undergo Tyr phosphorylation, however, the effects of Tyr phosphorylation on DNA binding capacity can vary. For example, Tyr phosphorylation of the *B. subtilis* transcriptional repressor SalA enhances ATP binding. As ATP is necessary for DNA binding, phosphorylation enhances DNA binding capability.¹⁵⁵ Similarly, phosphorylation of Tyr on the *B. subtilis* single-stranded DNA binding protein increases the DNA binding capacity 200-fold.¹⁵⁶ It is likely that dephosphorylation during the DNA damage response allows DNA repair by other proteins to occur. In contrast, Tyr phosphorylation of the enterohemorrhagic *E. coli* transcriptional regulator Cra sterically hinders the protein and reduces its binding capacity.¹⁵⁷ Cra modulates the expression of *ler*, which encodes a major activator of type 3 secretion system gene.

Other physiological responses can result from direct modulation of protein function. For example, in the *B. subtilis* stress response to heat shock, the chaperone protein DnaK is phosphorylated on two Tyr residues. When one such residue, Tyr601, was mutated to non-phosphorylatable Phe, *B. subtilis* had diminished survival after heat

shock.¹⁵⁸ In another example, cell cycle regulation of *S. pneumoniae* appears to be regulated by Tyr phosphorylation as bacteria expressing non-phosphorylatable CpsD variants were deficient for capsule production and presented elongated cells with putative cell division defects.¹⁵⁹

Although phosphorylation events on other residues may be harder to identify, the available data suggests their physiological effects are not any less important. In two-component systems, His and Asp-based phosphorylation relay events are a classic mode of signal transduction, leading to a change in gene expression.^{144, 160} Arg phosphorylation and dephosphorylation is a critical component for spore germination in *B. subtilis*.¹⁶¹ Cys phosphorylation has long been regarded as a rare PTM, although this is likely due to lack of detection rather than prevalence.¹⁶² However, Cys phosphorylation may have a major role in cell physiology. In *S. aureus*, Cys phosphorylation is facilitated by the Syr/Thr kinase and phosphatase pair. Several global regulatory proteins undergo Cys phosphorylation, but three in particular, SarA, MgrA and SarZ are phosphorylated on a sole conserved Cys residue, resulting in reduced DNA binding affinity.¹⁶² Removal of phosphatase activity rendered the cells deficient in haemolysis and more resistant to cell-wall targeting antibiotics. Further, prevention of de-phosphorylation left the cells unable to establish infection in a mouse model.¹⁶²

Acetylation

Acetylation is the post- or co-translational addition of a 42 Da acetyl group to the ϵ -amines of lysine side chains (N^ϵ -acetylation), the α -amines of protein N-termini (N^α -acetylation) (**Figure 1.10**), or the hydroxyl group of Ser and Thr residues (O-acetylation). N^ϵ -acetylation is considered a rare modification in prokaryotes, with only about 1% of the *E. coli* proteome known to undergo N^ϵ -acetylation.^{102, 163} This contrasts with the high rates observed in eukaryotic cells, for instance 80-90% of human proteins are N^ϵ -acetylated, where this PTM is used as a signal for protein degradation.¹⁶⁴⁻¹⁶⁶ However, there may currently be insufficient data to draw conclusions on the wider prevalence or function of this modification in prokaryotes.¹⁶⁷ O-acetylation has, to date, only been reported in *M. tuberculosis* and *Streptomyces lividans*.^{168, 169} In *S. lividans*, O-acetylation of acetyl-CoA regulates protein activity, while the biological effects of O-acetylation in *M. tuberculosis* or the occurrence in other bacterial species remain unknown. Notably, *Yersinia pestis* acetyltransferase YopJ has been demonstrated to acetylate Ser of human proteins, suggesting O-acetylation may also take place in this species.¹⁷⁰ In bacteria, N^ϵ -acetylation is

widespread and thought to be biologically significant.¹⁷¹ Such modification increases the size of the lysine side chain and alters the chemistry of the affected amine. The charge of the affected group is converted from a net positive charge to neutral at physiological pH, resulting in a reduction of side chain reactivity, increased protein hydrophobicity, and possibly altered biological activity. As such, this thesis will only discuss *N*^ε-acetylation, which will be referred to as 'acetylation' from here.

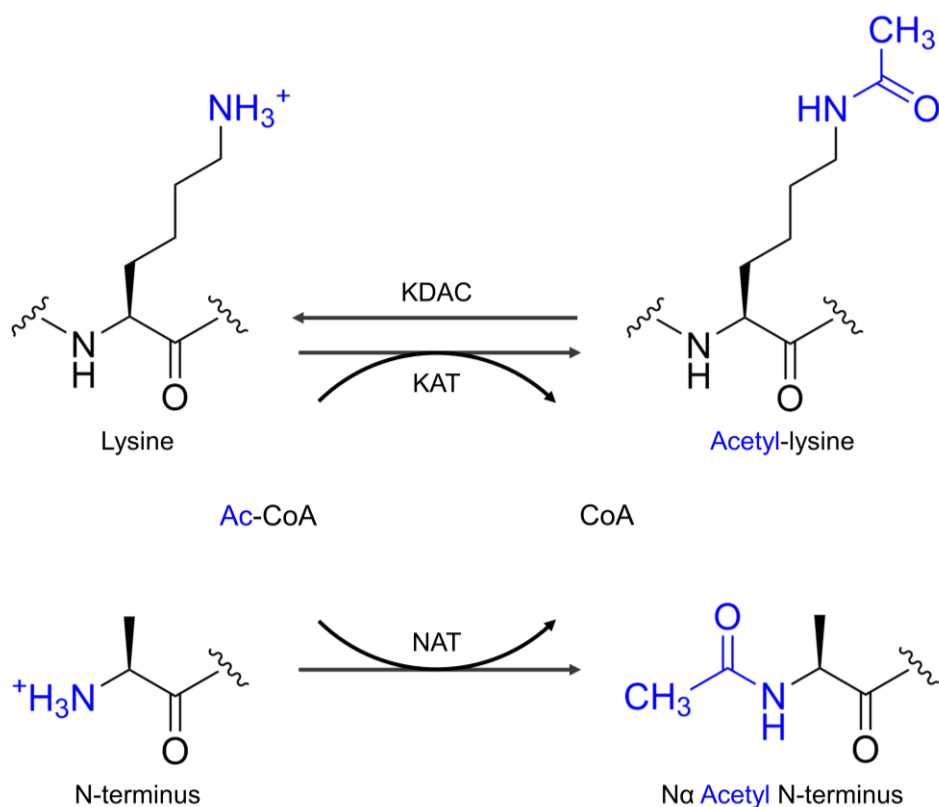


Figure 1.10 Schematic representation of lysine acetylation. Acetylation is the addition of an acetyl group to the ϵ -amine of the lysine side chain (top) or the α -amine of the N-terminus (bottom). Acetylation is facilitated by lysine acetyl-transferases (KATs) or N-terminal acetyl-transferases (NATs), using acetyl-coenzyme A (Ac-CoA) as a donor. *N*^ε-acetylation can be removed by lysine deacetyl-transferases (KDACs) and is reversible. So far, no enzyme capable of removing *N*^α-acetylation has been discovered.

Acetylation is a prominent PTM in bacteria, occurring at least as frequently as phosphorylation.^{119, 129, 172} Two types of acetylation exist. The first, and perhaps the most studied, is enzymatic acetylation, catalysed by lysine acetyl-transferase enzymes.¹⁷³ Several classes of acetyl-transferases exist, however, prokaryotes possess homologs of only one class, the Gen5 histone *N*-acetyltransferases, though they may express multiple versions.¹⁷³ Currently, the best studied is YfiQ (also known

as Pat), a conserved acetyl-transferase with homologs in many species including *E. coli* and *S. enterica*.¹⁷⁴ Lysine acetyl-transferases use acetyl-coenzyme A (CoA) as a cofactor to add an acetyl group to the ϵ -amino group of lysine side chains. The mechanism differs between acetyl-transferases, but generally the target lysine is deprotonated, followed by nucleophilic attack of the lysine on the carbonyl carbon of the acetyl group of acetyl-CoA, before protonation and dissociation of CoA.¹⁷⁴ The reaction is reversible, with deacetylases able to subsequently remove the acetyl group. There are four classes of lysine deacetylases; class III deacetylases, known as sirtuins, are the most prominent in bacteria and require NAD⁺ as a cofactor.¹⁷³ In *E. coli* and *S. enterica* the only known deacetylase is CobB, a sirtuin, which accounts for almost all deacetylase activity.¹⁷⁵ On removing the acetyl moiety from lysine, the acetyl group forms an intermediate with NAD⁺ which causes the release of nicotinamide, an inhibitor of sirtuin activity.¹⁷⁶ The outcome is the de-acetylation of lysine and the formation of O-acetyl-ADP-ribose.

The second type of acetylation is non-enzymatic acetylation by acetyl-CoA or acetyl-phosphate (**Figure 1.11**). Acetyl-phosphate is a high-energy molecule generated under high-acetate conditions. Acetyl-phosphate can non-enzymatically acetylate proteins and is the predominant acetyl donor in many species of bacteria.¹⁷⁷⁻¹⁷⁹ To allow such acetylation, the lysine must be deprotonated, e.g. by nearby negatively charged amino acids, and acetyl-phosphate must be able to position itself to attack lysine, e.g. via coordination by positively charged amino acids.¹⁷⁷ In *E. coli*, most proteins acetylated via chemical acetylation are not de-acetylated,^{175, 177, 178} however, a few can be deacetylated by CobB.¹⁶⁷ In eukaryotic mitochondria, acetyl-CoA can non-enzymatically acetylate proteins.¹⁸⁰ It is thought that this may too occur in prokaryotes, however, obtaining *in vivo* proof is difficult as acetyl-CoA is essential for cell growth and cannot be removed.¹⁶⁷

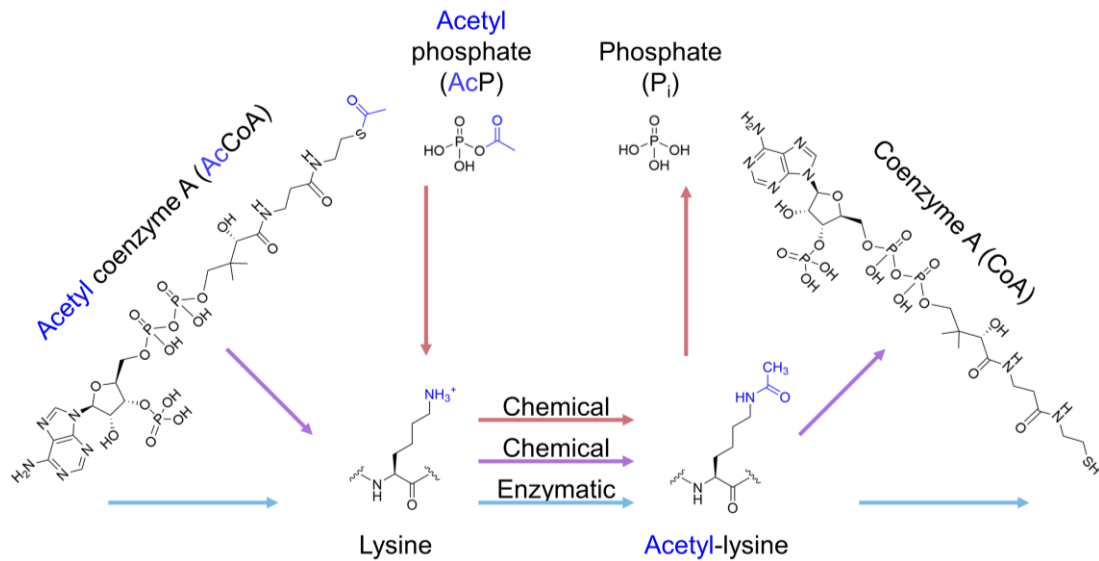


Figure 1.11 Schematic of chemical (non-enzymatic) and enzymatic protein acetylation in bacteria. Chemical acetylation of the ϵ -amine of the lysine side chain of a protein can occur with acetyl phosphate or acetyl coenzyme A. Enzymatic acetylation is facilitated by a lysine acetyl-transferase enzyme, using acetyl coenzyme A as a donor. Adapted from Christensen *et al.*¹⁶⁷ under licence [CC BY 4.0](#).

Regulation of acetylation appears to be finely tuned and is influenced by metabolic state and available carbon sources.^{124, 171, 176} Generation of acetyl-CoA by acetyl-CoA synthetase requires conversion of ATP to AMP. High acetyl-CoA activity results in the accumulation of AMP and depletion of ATP and can perturb other cellular processes requiring ATP, leading to growth arrest.¹⁸¹ Acetyl-CoA synthetase activity is regulated by reversible acetylation, with acetylation inactivating the enzyme.¹⁷³ Deacetylation by sirtuins is dependent on the availability of NAD⁺, which fluctuates with metabolism with high levels of NAD⁺ indicative of high cellular energy levels.¹⁸² Changes in the amount of free NAD⁺ will affect the amount of deacetylation, thereby tying sirtuin activity to the metabolic state of the cell.¹⁷⁶ In *S. enterica*, proteins involved in central metabolism are extensively acetylated and these acetylation profiles change depending on the available carbon source.¹²⁴ When glucose consumption is high in *E. coli*, such as in the stationary phase, the cell depletes free CoA faster than it can be recycled.¹⁷¹ To produce CoA, the cell ferments acetate from acetyl-CoA, however the process leaves behind a pool of the intermediate, acetyl-phosphate. The high amount of acetyl-phosphate combined with reduced protein synthesis in the stationary phase results in increased global acetylation.¹⁷¹

Advancements in mass spectrometry techniques have permitted investigations into the acetylome of various species. Acetylated proteins are responsible for a broad range of functions including motility and chemotaxis, transcription, metabolism, and stress responses.^{173, 183} Many proteomic analysis suggest that a large proportion of acetylated bacterial proteins are involved in metabolism,^{129, 184} for example, almost half of acetylated proteins in *E. coli* were reported to be involved in carbohydrate metabolism.¹⁸⁵ However, others have highlighted that such proteins may be over-represented due to their solubility and abundance in culture conditions and methods used.^{182, 186} There have been fewer investigations verifying the effects of acetylation on protein function. Acetylation of RcsB, an *E. coli* response regulator, results in diminished DNA binding capacity.¹⁸⁷ Acetylation has also been shown to alter protein stability, for example, acetylation of Lys544 of *E. coli* RNase R in the exponential phase greatly decreases the protein's half-life.¹⁸⁸ This is likely due to disruption of interactions between Lys and negatively charged amino acids in the C-terminus, which allows transfer-messenger RNA and its associated protein SmpB to bind and facilitate protein degradation.¹⁸⁸ Acetylation has also been shown to alter enzymatic activity, as already mentioned with acetyl-CoA synthetase and also the activity of *M. tuberculosis* isocitrate lyase is regulated by acetylation.¹⁸⁹ Acetylation can also interfere with protein-protein interactions.¹⁷¹

Such molecular effects are thought to have various implications for cell physiology. Many, if not all, acetyl-transferases in *E. coli* are found to be upregulated in biofilms or during the stationary phase.¹⁹⁰ Inhibition of protein acetylation interferes with biofilm formation in *M. tuberculosis* and *B. subtilis*.^{191, 192} Acetylation is necessary to maintain cellular homeostasis and influences the metabolic flux of the cell, channelling carbon through different pathways depending on the available energy source.¹²⁴ In various species, acetylation also regulates the response to environmental stressors.^{171, 173} For example, in *E. coli*, removal of acetylation by deleting *yfiQ* resulted in an increased susceptibility to heat and oxidative stress, while encouraging acetylation through deletion of *cobB* resulted in an increased resistance to the same stressors.¹⁹³ The authors found various stress related genes including those involved in heat shock, cold shock, osmotic stress, and acid resistance were repressed by deacetylation.¹⁹³

As others have noted, in cases where functional implications of acetylation have not been verified, consequences of acetylation on protein activity should not be assumed.^{167, 182} It is possible that some acetylation of lysine residues may be insignificant to protein function. For example, VanDrisse and Escalante-Semerena have suggested that such benign modifications may reflect an acetate storage

strategy to avoid loss of carbon.¹⁷³ While Christensen *et al.* have also hypothesised that many detected acetylation events may be neutral to protein function and exist as a result of evolutionary selective pressures caused by high production of acetyl-CoA in the last universal common ancestor.¹⁶⁷ This would provide an explanation as to why many acetyl-lysines are not subjected to deacetylation in *E. coli* and further highlights the importance of verifying any effects of acetylation on protein function rather than assuming a role based on proteomic data.

Lysine acylation

In addition to acetylation, lysine may also be subjected to a variety of other acylations including succinylation, propionylation and malonylation, among others.¹⁸² This is the addition of a succinyl, propionyl or malonyl group, respectively, to the ϵ -amino of the lysine side chain. Discovery of such modifications are relatively new, and while various proteomic analyses identifying modified proteins have been performed,^{119, 126, 194-203} there is little research characterising the effects on protein function. Comparably to acetylation, propionylation, succinylation and malonylation have been shown to be regulated by enzymes of the Gen5 histone *N*-acetyltransferases superfamily.^{102, 204} Here, they catalyse the transfer of the appropriate chemical group from propionyl-CoA, succinyl-CoA or malonyl-CoA. Similarly, some sirtuins are reported to have de-propionylase, de-succinylase, and de-malonylase activity.^{195, 205, 206} However, the exact mechanisms regulating these modifications remain uncertain, and may vary between prokaryotic species. The following sub-sections will describe the current knowledge of the regulation and functional implications of lysine succinylation, propionylation and malonylation. Often, the same lysine residues can be subjected to any combination of these modifications. Such flexibility in lysine acylation is thought to provide the cell with a greater versatility of modifications and allow response to particular changes in physiological or environmental conditions to maintain homeostasis.^{182, 195, 207}

Succinylation

Succinylation is the addition of a 100-Da group, which converts the positive charge of the lysine side chain to a negative charge (**Figure 1.12**).²⁰⁸ Succinylation appears to be as prevalent as acetylation, although the larger size and complete conversion of charge may mean it has a more profound impact on protein structure and/or function.²⁰⁹ The key mechanisms regulating succinylation remain largely unknown in bacteria,^{195, 209} however, it can occur non-enzymatically, with succinyl-CoA as a donor.¹⁹⁴ Global succinylation has been shown to be altered in response to the availability of succinate and pyruvate and, in particular, glucose.¹⁹⁵ The *E. coli* sirtuin

CobB also showed de-succinylase activity *in vitro*,¹⁹⁵ however *in vivo* its role remains unclear with one report of a *cobB* knockout strain showing elevated succinylation¹⁹⁵ and another showing no effect.¹⁹⁴

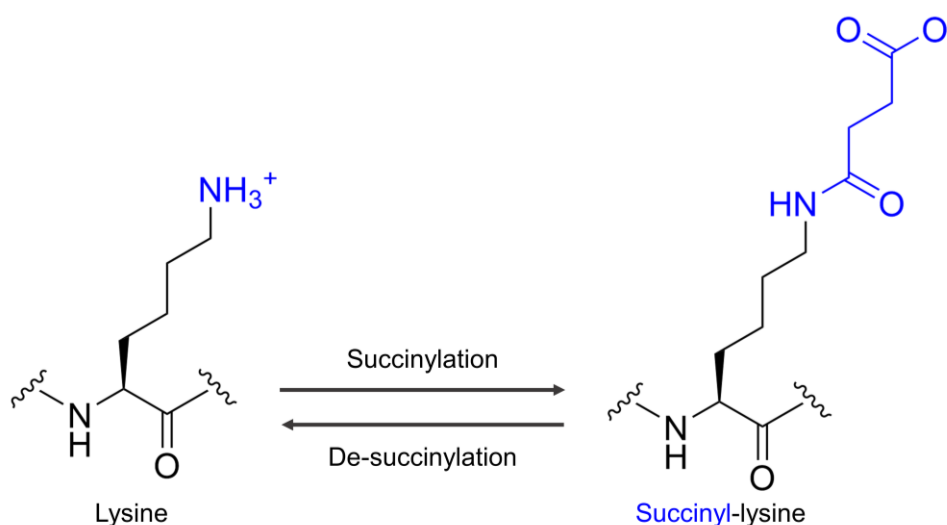


Figure 1.12 Schematic representation of lysine succinylation. Succinylation is the addition of a succinyl group to the lysine side chain. The exact mechanisms resulting in succinylation of the lysine side chain remain unclear. In bacteria, lysine succinylation is thought to occur both enzymatically and non-enzymatically with succinyl-coenzyme A as a donor. Succinylation is reversible, likely through enzymatic removal of the succinyl group.

Succinylation appears to be widespread in bacteria, with high prevalence in *E. coli*,¹⁹⁴,¹⁹⁵ *M. tuberculosis*,¹⁹⁶ and *Vibrio parahaemolyticus*,¹⁹⁷ suggesting it may be an important mechanism for regulating physiological changes. Overlap between succinylation and acetylation appears to be high in all investigated species,¹⁹⁴⁻¹⁹⁷ for example, in *E. coli* between 59-66% of sites that were succinylated were also subjected to acetylation.^{194, 195} The high frequency of sites which are subjected to both modifications suggests that these proteins could be regulated by crosstalk between these PTMs, although it remains unclear whether the two modifications have opposing functions or allow fine-tuning of protein activity.^{194, 195}

The biological effects of succinylation have not yet been characterised. Succinylation was first identified on *E. coli* isocitrate dehydrogenase,²⁰⁸ where mutation of residues which undergo succinylation to a succinyl mimic, glutamate, resulted in decreased enzymatic activity. Succinylation occurs on diverse proteins involved in nearly all aspects of cellular functions.¹⁹⁴ Particularly, succinylation is involved in multiple metabolic pathways and important for regulation of central metabolism such as glycolysis, TCA cycle, and fatty acid metabolism.¹⁹⁴⁻¹⁹⁷ In *M. tuberculosis*, 44% of

succinylated proteins are involved in metabolism.¹⁹⁶ It also appears to have a key role in aspects of gene and protein expression.^{195, 197}

Propionylation

Propionylation is the addition of a 56 Da propionyl group to the lysine side chain (**Figure 1.13**). Despite its discovery in 2007,²⁰⁴ the regulatory mechanisms behind propionylation remain unclear, although a few insights have been gained. For example, in *S. enterica* propionylation is regulated by the same enzymes as acetylation, YfiQ and CobB.²⁰⁵ While in *E. coli* both *patZ* overexpression and *cobB* knockdown resulted in increased global lysine propionylation.¹⁹⁸ CobB was also able to de-propionylate a propionylated peptide *in vitro*.¹⁹⁸ It has been suggested that propionylation may be regulated by growth phase dependent mechanisms. For example, in *T. thermophilus* the number of propionylated proteins increased 3-fold in the late stationary phase compared to the exponential phase.¹²⁶ In *E. coli* propionylation predominantly existed under low glucose conditions, exemplary of the stationary phase.¹⁹⁸ Propionylation appears to be regulated under distinct mechanisms to acetylation. In *T. thermophilus*, only a limited degree (20%) of overlap was found between propionylation and acetylation sites.¹²⁶ In addition, in *E. coli* growth in high glucose conditions results in decreased global propionylation but increased acetylation and succinylation.^{195, 198} Propionylation also increases in response to treatment with propionate¹⁹⁸ and is thought to also occur non-enzymatically.^{126, 198} In parallel with acetylation, activity of the *S. enterica* propionyl-CoA synthetase is regulated by propionylation, with propionylation inactivating the protein.²⁰⁵ Further, it was found that *E. coli* propionyl-CoA synthetase was propionylated in response to propionate treatment.¹⁹⁸ The effects of propionyl-CoA on the cell remain unclear, but cells avoid accumulating it.²⁰⁵ Propionyl-CoA-mediated propionylation of propionyl-CoA synthetase thereby allows a rapid modulation of enzyme activity to avoid the deleterious effects of its product.

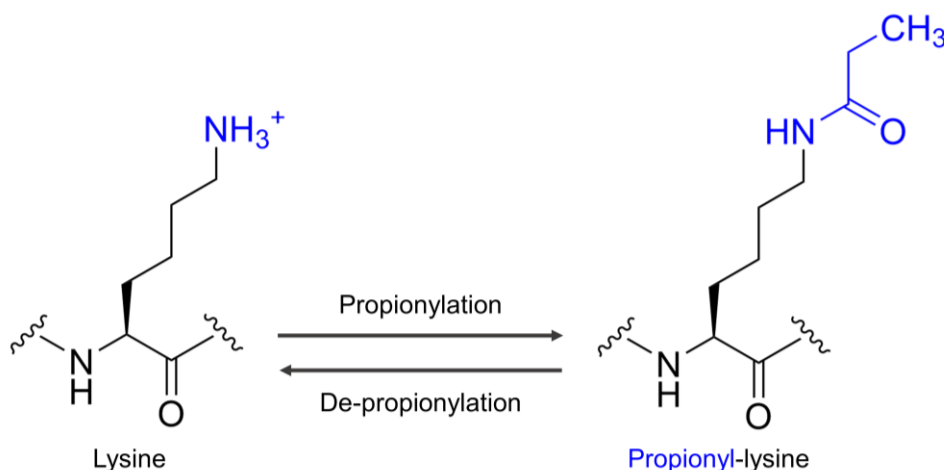


Figure 1.13 Schematic representation of lysine propionylation. Propionylation is the addition of a propionyl group to the lysine side chain. The exact mechanisms facilitating propionylation remain unclear, but it is a reversible modification likely regulated *via* enzymes similar to those which regulate acetylation.

The propionylome of various bacteria have been reported.^{126, 198-200} In *E. coli*, most propionylated proteins are associated with energy metabolism and protein-processing pathways e.g. translation and amino acid metabolism.¹⁹⁸ Similarly, in *T. thermophilus*, where propionylation is one of, if not the most, prevalent PTMs in this species, the largest group of propionylated proteins (59%) are those involved in metabolism.¹²⁶ The same study indicated that propionylation may play a role in propionate metabolism and propionyl-CoA degradation.¹²⁶ An investigation into propionylation in the model cyanobacteria *Synechocystis* sp. PCC 6803, a photosynthetic bacteria, found that the majority of propionylated proteins are involved in photosynthesis and metabolism, two processes that are heavily interrelated in cyanobacteria.¹⁹⁹ Further, the same study reported that the propionylation levels of several proteins involved in photosynthesis were increased after high light treatment, suggesting propionylation may be involved in high light adaptation or have regulatory roles in adaptation to environmental stimuli.

Malonylation

Malonylation is an 86 Da addition to lysine, converting the side chain to a net negative charge (**Figure 1.14**).²⁰⁶ Malonylation utilises malonyl-CoA as a cofactor, although little is known about the mechanisms of malonylation and de-malonylation. In eukaryotic cells, the sirtuin SIRT5 has been shown to have de-malonylation activity *in vivo*.²⁰⁶ Regulation of malonylation appears to be tied to fatty acid synthesis, in *E. coli* inhibition of fatty acid synthesis significantly increased global malonylation, as did

overexpression of a protein involved in fatty acid synthesis.²⁰¹ Malonylation is also thought to be involved in the stress response, as significant increases in global malonylation were observed in response to high light conditions in the cyanobacterium *Synechocystis*.²⁰² As malonyl-CoA is more reactive than acetyl-CoA, it likely leads to non-enzymatic malonylation.^{201, 202}

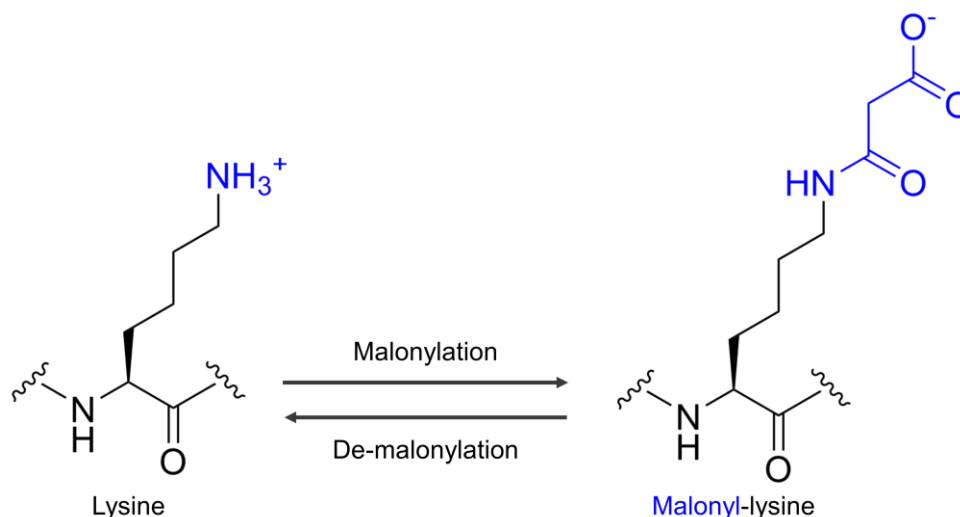


Figure 1.14 Schematic representation of lysine malonylation. Malonylation is the addition of a malonyl group to the lysine side chain. In bacteria, little is known about the regulation of lysine malonylation, although malonyl-coenzyme A is used as a donor.

Although malonylation has only been studied in a few prokaryotic species to date, it appears to be widespread and relatively conserved, suggesting this modification is likely prevalent among bacteria.^{202, 203} As with other lysine acylation, malonylation appears to have a role in cellular metabolism.²⁰¹⁻²⁰³ In *E. coli*, malonylation of 594 proteins has been reported, with malonylated proteins having roles in translation, the TCA cycle, glycolysis, and particularly, fatty acid metabolism.²⁰¹ In *S. aureus* 281 malonylated proteins were reported, again highly enriched in metabolic processes such as glycolysis, the TCA cycle and amino acid synthesis and degradation.²⁰³ In *Synechocystis*, 38% of malonylated proteins were involved in metabolic processes and 34% in cellular processes. Specifically, malonylated proteins were significantly enriched in ribosomes, photosynthesis and carbon metabolism. This infers a potential role of malonylation in protein translation, carbon metabolism and photosynthesis in *Synechocystis*.²⁰² Additionally, in *S. aureus*, malonylation has been implicated in gene expression as malonylation of several ribosomal subunits was reported.²⁰³ Overall, the available data suggests malonylation may have regulatory roles in metabolism

and protein synthesis. Direct evidence of the functional implications of malonylation is currently very limited but early data suggests roles in regulating protein function or activity. For example, malonylated sites were found at or near the active sites of several proteins in *S. aureus*.²⁰³ Further, *E. coli* citrate synthase, a rate limiting enzyme in the TCA cycle, is malonylated at five sites.²⁰¹ When two of these sites were independently mutated to glutamate, a malonylation mimic, enzymatic activity was significantly decreased.²⁰¹

In *E. coli*, 48% and 45% of malonylation sites can also be succinylated and acetylated, respectively.²⁰¹ In fact, 30% of malonylation sites can undergo all three types of modification, and these sites are mostly found on proteins involved in translation and glucose metabolic processes. However, 41% of sites are subjected exclusively to malonylation, suggesting that malonylation could have a distinct physiological roles from other two modifications.²⁰¹ In *Synechocystis*, 59% of malonylated proteins were also acetylated and these overlapping proteins were mainly those involved in photosynthesis and carbon metabolism.²⁰² However, when analysing specific sites of malonylation there was only a small overlap.²⁰² In addition, although *E. coli* malonylation levels were drastically altered by fatty acid synthesis inhibitors, acetylation and succinylation levels were unchanged.²⁰¹ Similarly, both acetylation and succinylation are increased by glucose or pyruvate treatment¹⁹⁵ while these conditions had no effect on malonylation.²⁰¹ Together, this suggests that the different lysine acylations may be modified by distinct enzymes and may be reactions to different metabolic environments.

Methylation

Methylation is the addition of a relatively small, 14 Da methyl group, and can occur on a variety of amino acid side chains including lysine (**Figure 1.15**), arginine, glutamine, cysteine, histidine, aspartic acid, asparagine, and glutamic acid, in addition to protein N-termini.²¹⁰ As this modification can occur on a range of amino acids, the chemical changes enacted can vary but may result in altered charge state, increased hydrophobicity and enlarged size of side chain. Correspondingly, this has the potential to affect molecular interactions through disruption of salt bridges, hydrogen bonds and Van der Waals interactions, which can in turn affect biological functions.²¹⁰
²¹¹ In prokaryotes, little is known about the regulatory mechanisms behind methylation. Several methyltransferases and demethylases have been identified²¹¹⁻²¹⁴ and in *E. coli* some methyltransferases themselves are subjected to methylation.²¹⁰ Overall, much remains unknown about the regulatory mechanisms behind methylation, including whether it can occur non-enzymatically.

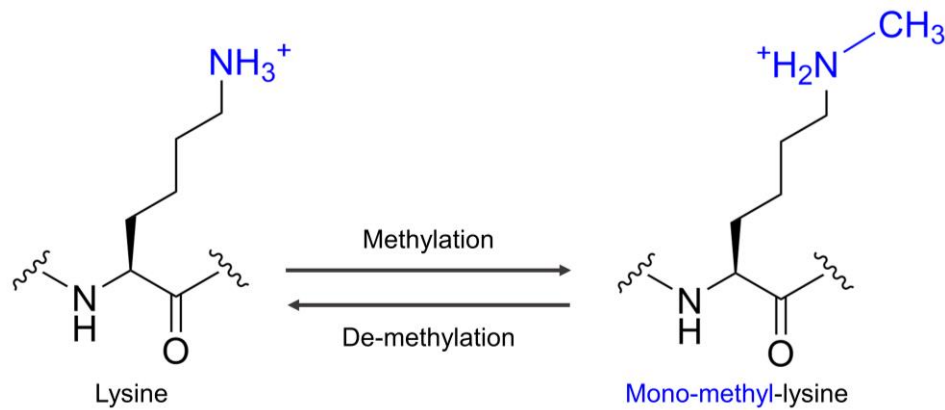


Figure 1.15 Schematic representation of lysine methylation. Methylation is the addition of a methyl group to a reactive side chain. Here, mono-methylation of lysine is shown. Methylation is a reversible reaction, facilitated by methyltransferase and demethylase enzymes.

Compared to other PTMs, there have been few analyses of protein methylomes of prokaryotic species. An analysis of the *E. coli* methylome revealed that proteins undergoing methylation are enriched in pathways related to central metabolism, including glycolysis, purine metabolism and the pentose phosphate pathway, as well as pyruvate metabolism, ribosome, riboflavin metabolism, and chemotaxis.²¹⁰ Particularly, enzymes in almost every step of the glycolysis pathway undergo methylation. In addition, extensive methylation of ribosomal proteins indicates a possible role in translation, as has been reported by others.²¹¹ In the pathogenic *Leptospira interrogans*, methylated proteins were found across a variety of functional classes but particularly in cell motility and chemotaxis.²¹⁵ The same study reported methylation of proteins involved in translation, such as ribosomal proteins, a translation initiation factor and an elongation factor. From these insights, it appears proteins related to central metabolism experience high levels of modification by methylation, as also observed with lysine acylation. In contrast to Lys acylation, methylation is a smaller modification and maintains the positive charge of the lysine side chain. It has been suggested that some methylation may serve as a protective group on lysine to prevent acylation.²¹⁰

Lysine methylation was first shown in the flagella of *Salmonella typhimurium* in 1959.²¹⁶ However, despite the early discovery of this modification, subsequent characterisation and determination of physiological implications has been slow.²¹⁷ Methylation of proteins involved in chemotaxis is frequently observed,^{210, 215, 216} and is necessary for a sensory response to chemotactic stimuli.²¹⁸ Methylation of flagella was recently shown to have a role in virulence in *S. enterica*.²¹⁹ Flagella are

composed of up to 20,000 copies of a small subunit protein called flagellin. Horstmann and colleagues demonstrated that Lys-methylation of flagellin by the methylase FliB increases the hydrophobicity of the flagella, thereby allowing a more intimate interaction with epithelial cells.²¹⁹ Correspondingly, an increase in methylation resulted in increased invasion of epithelial cells *in vitro* while a methylation deficient *S. enterica* mutant had diminished colonisation of a mouse model *in vivo*.²¹⁹

As mentioned, methylation is often observed on proteins involved in translation. In bacteria, translation release factors are essential for recognising stop codons and termination of translation.²²⁰ *E. coli* produces two release factors and both of these undergo methylation, which has been shown to increase protein activity.²²¹ Methylation of these release factors is important for cell physiology, as eradication of this modification leads to very poor growth.²¹² Similarly, in *Yersinia pseudotuberculosis*, the two release factors produced by this species both undergo modification *via* the methyltransferase, VagH.²¹⁴ A *vagH* knockout was 500-fold less virulent than the wild-type, more susceptible to killing by macrophages, and could not colonise mice.²¹⁴ The authors uncovered that the decrease in virulence was due to a deficient type III secretion system in the mutant strain. Overall, although considerably more research is needed to uncover the molecular and physiological effects of methylation on protein function, the available data indicates methylation may have a key role in various aspects of cellular physiology.

Pupylation

Pupylation is the covalent attachment of a prokaryotic, ubiquitin-like protein (Pup) of 64 amino acid residues onto the lysine side chain of target proteins.²²²⁻²²⁴ Pupylation is functionally analogous to eukaryotic ubiquitylation, although the two proteins do not have sequence or structural homology.^{223, 225, 226} As such, pupylation is thought to have likely evolved as a method of targeting protein substrates to the bacterial proteasome complex, a theory supported by its presence on an operon with proteasomal subunit genes. Unlike eukaryotic ubiquitylation, which is regulated by a plethora of E3 ligases, pupylation is dependent on only two enzymes, PafA and Dop.^{223, 227} Dop prepares Pup for ligation by deamidating the C-terminal glutamine to glutamate.²²³ Then, PafA catalyses the formation of an isopeptide bond between Pup's C-terminal glutamate and the amino side chain of lysine on the target protein. Dop is also responsible for depupylation, where it removes Pup from the target protein *via* specific cleavage of the isopeptide bond.²²⁷ Interestingly, PafA and Dop display high structural and sequence similarity and are likely both descended from an ancient glutamine synthetase.^{224, 228, 229}

Pupylation is only present in *Actinobacteria*, a large phylum of bacteria of which many species live in close association with eukaryotic hosts as either pathogens or symbionts, such as nitrogen-fixing or gastrointestinal species.²³⁰ In 20S proteasome-containing *Actinobacteria*, pupylated proteins are recruited to the 20S proteasome by the associated ring-shaped ATP-dependent regulator. On binding to the regulator, Pup adopts a helical structure to form a three-stranded coil and engages its N-terminus into the regulator pore. Pupylated substrates are threaded through the central pore, facilitating unfolding, and translocated into the 20S chamber for degradation.²³¹ Intriguingly, about half of *Actinobacteria* have lost the 20S proteasome but retain pupylation. This suggests that pupylation also has roles in non-proteasomal pathways and a broader role in regulation and cellular signalling.

The effects of pupylation are still under investigation although initial reports suggest they are wide ranging.²²⁴ Pupylation was first identified in *M. tuberculosis*, where loss of Pup severely diminishes colonisation of the lungs of mice.²²⁸ The exact cause of such reduced pathogenicity is yet to be determined. However, pupylation is not essential for growth nor does it affect growth under laboratory conditions of *Mycobacterium smegmatis*, *M. tuberculosis*, *Streptomyces coelicolor* or *Streptomyces lividans*, suggesting that pupylation may provide advantages under specific environmental conditions encountered by bacteria *in vivo*, or during the switch to a different life cycle stage.²²⁴ For example, loss of pupylation renders *M. tuberculosis* more sensitive to NO₂.²²⁸ In *M. smegmatis* when pupylation is disrupted survival under nitrogen starvation is impaired due to defects in amino acid recycling and regulation of nitrogen assimilation.²³² Pupylation may also protect against oxidative stress, as the 20S proteasome is thought to be involved in the removal of aberrant proteins modified by reactive oxygen species.²³² This PTM is also involved in the DNA damage response in *Mycobacteria*, where it removes upregulated DNA repair proteins.²³³ In *Corynebacteria*, pupylation has been linked to survival under iron starvation.²³⁴ Evidently, pupylation may have wide ranging effects on cellular physiology and it is likely that more roles may yet be uncovered. For example, proteomic studies of *M. tuberculosis* and *M. smegmatis* have identified ca. 700 pupylation targets associated with a wide range of cellular functions, including the regulation of bacterial metabolism.²²⁴

1.2.3 PTM crosstalk

As described above, cells are capable of using a variety of PTMs to modulate protein function and activity in various ways. However, an extra level of complexity arises when multiple PTMs occur simultaneously. This could be within a single protein, on proteins which interact, or on proteins at different stages of a signalling cascade. PTM crosstalk describes the interaction and interplay between multiple PTMs on protein function and on wider cellular processes.²³⁵ If a single residue is subjected to multiple PTMs, each could modulate protein function in a different way and the modifications may 'compete' with each other. For example, as mentioned above, lysine methylation has been proposed as a protective PTM to prevent further acylation.²¹⁰ Proteins may also undergo multiple PTMs at multiple residues and the effects of a combination of modifications on protein function could be synergistic, antagonistic or cumulative. The presence of one PTM may influence the likelihood of the protein to be modified by additional PTMs e.g. by changing the tertiary structure or interaction with other proteins to expose new sites for modification.¹⁰² Additionally, the effect of various PTMs on individual proteins in a protein complex or signalling cascade could all interplay and affect the physiological outcome. Together, the cumulative effects of numerous PTMs could lead to an intricate web of modifications which defines the specific cellular physiology. In eukaryotes, there have been significant advances in understanding and characterising some of the cross-talk between PTMs.²³⁵ In prokaryotes, cross-talk between PTMs is so far much less explored.^{146, 236} However, it is becoming increasingly evident that bacterial PTMs form a dynamic regulatory network too.^{129, 236}

As described in **Lysine acylation** there is significant overlap between lysine acetylation and other lysine modifications such as succinylation, propionylation and malonylation on both the same protein and the same sites. However, this is not limited to lysine, individual proteins are frequently reported to be subjected to multiple PTMs. For example, a number of studies have observed interplay between acetylation and phosphorylation in bacteria.^{113, 129, 236} Many *E. coli* proteins carry both acetylation and phosphorylation, mainly those involved in carbohydrate metabolism and protein biosynthesis.²³⁶ Another study encompassing a large range of human-colonising bacterial species found that some PTMs occur together, for example 52% of succinylated proteins and 34% of phosphorylated proteins were also acetylated.¹¹³ Such multiple modifications often occur in close sequence proximity. For instance, in *E. coli*, six acetylation and succinylation events of the fructose-bisphosphate aldolase

were found to be localised at the same positions, reflecting possible competition between PTMs.¹⁸⁵

Perhaps the most striking evidence for cross talk between bacterial PTMs comes from a study by van Noort and colleagues.¹²⁹ Here, the interplay between phosphorylation and acetylation was assessed in the human pathogen *Mycoplasma pneumoniae*. Overall, they reported a significant correlation between proteins which are phosphorylated and those which are acetylated. In fact, 72% of proteins which were phosphorylated were also subjected to acetylation. The sites of such modification were often located on interfaces of interactions with other proteins and the proteins undergoing modification were often those which are capable of forming parts of multiple protein complexes. As this bacterium only has two kinases and one phosphatase, the authors could relatively easily disrupt protein phosphorylation. Deletion of all three genes resulted in perturbation of the phosphorylome but also surprisingly resulted in modulation of lysine acetylation patterns. Further investigation revealed that deletion of just one kinase resulted in increased acetylation while deletion of the other kinase resulted in decreased acetylation, possibly indicating an antagonist effect between the two. Similarly, deletion of the two putative lysine acetyltransferases affected the level of phosphorylation. These results show that in this species phosphorylation and acetylation are intertwined with bi-directional interplay and strong cross-talk between the modifications.

An example of how both phosphorylation and acetylation can regulate activity comes from the global response regulator GlnR of *Streptomyces coelicolor*. GlnR controls the transcription of genes related to *N*-assimilation and was found to be regulated by both Ser/Thr phosphorylation and by lysine acetylation.²³⁷ The amount of phosphorylation correlated with the concentration of nitrogen in the environment, with more nitrogen resulting in increased phosphorylation. Conversely, acetylation levels did not show any relation to nitrogen concentration. Although not tested, the authors noted the acetylation state might reflect available carbon sources, as in other bacterial species. Phosphorylation of GlnR completely inhibited the protein from binding to its target DNA, while acetylation also appeared to change DNA binding affinity to a lesser extent. As GlnR regulates the expression of target genes, the data suggests that both modifications, each responding to different stimuli, together regulate gene expression.

Another protein likely controlled by PTM cross-talk is isocitrate dehydrogenase, which has a vital role in regulating partitioning between the TCA cycle and the glyoxylate bypass.²³⁸ In *E. coli*, isocitrate dehydrogenase is regulated by phosphorylation, which inactivates the enzyme and is essential for its function.²³⁹ Isocitrate dehydrogenase also undergoes acetylation at a lysine residue in the protein's active site.²⁴⁰ Although such acetylation has not been characterised, mutation of the residue to methionine resulted in decreased enzymatic activity to 1% of wildtype and a 500-fold decrease in substrate affinity.²⁴¹ This indicates that it is an important residue for protein function and that acetylation may influence protein function in addition to phosphorylation.^{186, 236} Isocitrate dehydrogenase is also acetylated on other lysine residues, which may have regulatory roles.^{119, 240} Further, isocitrate dehydrogenase also undergoes succinylation, although the potential functional impact remains unclear.²⁰⁸ In *S. enterica*, the enzyme responsible for the phosphorylation, isocitrate dehydrogenase phosphatase/kinase, is itself regulated by acetylation.¹²⁴ Acetylation appears to activate the phosphatase activity of the enzyme, resulting in an overall diminished capacity to phosphorylate, and inactivate, isocitrate dehydrogenase. Together, this suggests that both phosphorylation and acetylation have regulatory roles in determining isocitrate dehydrogenase activity.

The interdependence and crosstalk between bacterial kinase systems has been reported for decades^{242, 243} and evidence is still emerging on the crosstalk between these systems. Kinases are used in signalling cascades to coordinate cellular processes. Until recently, it was believed that in prokaryotes such signal transduction is mostly linear. However, evidence has emerged that kinases from both *M. tuberculosis* and *B. subtilis* are capable of cross-phosphorylation of other kinases and demonstrate network signalling.^{244, 245} In *M. tuberculosis*, it was demonstrated that alongside autophosphorylation, Ser/Thr kinases can undergo phosphorylation by other kinases and are capable of downstream phosphorylation of kinases.²⁴⁴ This results in horizontal as well as linear signalling, forming a branched regulatory network. In *B. subtilis*, all known kinases were found to interact with widespread cross-phosphorylation.²⁴⁵ Most cross-phosphorylation occurred at residues in or near protein and DNA interaction surfaces, activating loops or the active site, suggesting that cross-phosphorylation was likely to influence downstream phosphorylation by affected kinases. Such interconnectivity between kinases allows the integration of multiple signals, permitting a coordinated cellular response and is consistent with the role of kinases in complicated activities such as cell cycle control and the development of biofilms.²⁴⁵

The most comprehensive example of interplay between different PTMs in bacteria is the modification of proteins involved in chemotaxis. Chemotaxis is the observed changes in cell motility under a chemical stimulus, allowing a cell to travel toward chemical attractants and away from chemical repellents.²⁴⁶ These responses to external chemicals result from combinatorial effects of methylation and phosphorylation. Chemical attractants stimulate methylation of chemotaxis proteins in the outer membrane. These methylated proteins then interact with a sensor kinase, CheA, stimulating autophosphorylation and phosphorylation of a response regulator, CheY. Phosphorylated CheY localises to the flagella, where it binds to the FliM proteins and causes a change to motor output, either directionality or stasis, depending on bacterial species.²⁴⁷ CheY can also be acetylated by acetyl-CoA,²⁴⁸ which prevents CheY from binding to its protein targets.²⁴⁹ Therefore, CheY is active in its phosphorylated form and inactive in its acetylated form. As both phosphorylation and acetylation regulate the binding capabilities of CheY, this provides two levels of regulation of protein activity and cell motility.²⁴⁹ In addition, the protein responsible for methylation of chemotaxis proteins, CheR, is itself regulated by methylation¹⁰² while the protein responsible for removal of the methyl group, CheB, is activated by phosphorylation by histidine kinase CheA.^{250, 251} This intricate system provides multiple levels of regulation, giving insight into the complex web of PTMs regulating a biological output.

Cross-talk between PTMs give multiple levels of regulation within a pathway and such complex interconnectivity allows fine tuning of biological function. Frankly, we are still far from understanding all the delicate levels of control in biological systems. However, it is becoming increasingly evident that some bacterial cell processes are co-regulated by multiple PTMs and that global regulatory networks exist.¹²⁹ While we have much to uncover, it may be impossible to ever completely characterise the physiological output of such cross-talk, as it involves the integration of countless signals and a fine-tuned response to varying stimuli. Regardless, it is important to take PTM cross-talk into account when characterising even a single PTM, and consider how the modification could be influenced by other PTMs on the same protein, those it interacts with, or the effect it could have on the global regulatory scale.

1.3 PTMs and antimicrobial resistance

More recently, PTMs have been associated with the regulation of antimicrobial resistance.¹⁰³⁻¹⁰⁷ Many bacterial proteins directly involved in antimicrobial resistance have been reported to undergo post-translational modification, but there has so far been less research characterising any interactions. Establishing resistance through PTM may also be achieved with the modification of global regulatory proteins or transcription factors which regulate the expression of resistance proteins. Drug-resistant strains may further utilise PTMs to regulate metabolism and other proteins which influence bacterial susceptibility to drugs.¹⁰³ As such, PTMs may constitute a target for antimicrobial drugs or for a complementary therapy to be used alongside antibiotics, and targeting them may represent a new avenue in drug discovery. This section will assess the current knowledge and progress of the role of PTMs in resistance and as drug targets.

1.3.1 PTM of antimicrobial resistance proteins

With the advent of mass spectrometry techniques for identifying post-translational modifications, the repertoire of modifications which proteins are subjected to is being uncovered. Many proteomic studies report the PTM of proteins involved in antimicrobial resistance, however, the majority of these studies analyse the entire proteome of a particular species and, as such, do not characterise the effects of such modifications on protein function or cellular physiology. However, these investigations do provide insights into which modifications may have a role in regulating antimicrobial resistance and a basis for identifying PTMs for individual characterisation. For example, an investigation into histidine and aspartate phosphorylation in various bacterial species found that several proteins involved in antimicrobial resistance are subjected to these modifications.²⁵² As mentioned in **Reduced antibiotic entry or accumulation**, porins have been implicated in bacterial resistance with knockouts showing varying impacts of antimicrobial susceptibility.²⁵³ In *Corynebacterium*, porins in the cell envelope are mycoloylated and, as this is necessary for their pore-forming activity, it is likely to affect antimicrobial entry.²⁵⁴

Multiple multi-drug efflux pumps have been demonstrated to be subjected to PTM. For example, the multidrug and toxic compound extrusion efflux pump YeeO from *K. pneumoniae* is phosphorylated on a His residue.²⁵² The authors postulate that such phosphorylation may impact the conformational change required for pump function. The multidrug and toxic compound extrusion efflux pump AbeM is involved in

resistance to a variety of antimicrobials in *A. baumannii* and its components undergo acetylation.²⁵⁵ A component of an RND-type pump from *A. baumannii*, AdeT1, was shown to be propionylated *in vivo*.²⁵⁶

In *M. tuberculosis*, multiple links have been drawn between protein PTM and antimicrobial resistance.^{107, 168, 196} For example, Wag31, an *M. smegmatis* cell division protein involved in resistance to rifampicin, novobiocin, erythromycin and clofazimine²⁵⁷ is phosphorylated *in vivo*.²⁵⁸ An investigation into the acetylome discovered that multiple proteins involved in drug resistance undergo acetylation including: PpiA, involved in cationic antimicrobial peptide resistance; MurF, implicated in vancomycin resistance; DNA gyrase subunit B, involved in fluoroquinolone resistance; and Eis protein, an acetyltransferase which modifies and provides resistance to kanamycin.¹⁶⁸ When identifying the succinylome, Xie *et al.* uncovered 13 proteins involved in antibiotic resistance to be succinylated, 9 of which were associated with isoniazid resistance.¹⁹⁶ Both subunits of DNA gyrase, the target of fluoroquinolones, were succinylated while ribonucleic acid polymerase, the target of rifampicin, had 12 succinylation sites.

In a review on the association between post-translational modifications and *M. tuberculosis* resistance, Arora *et al.* collated numerous resistance proteins undergoing PTM.¹⁰⁷ To name a few examples, a protein responsible for linezolid resistance in *M. tuberculosis*, RplC, is pupylated in the sister and model strain *M. smegmatis*.^{259, 260} However, the role of pupylation in linezolid resistance is not known. Pupylation was also identified on RpoC, the beta subunit of RNA polymerase, which is associated with rifampicin resistance.^{259, 261} GroEL, a chaperone protein which maintains proper folding of proteins affected by antimicrobials, is acetylated on multiple residues.¹⁸⁹ Glycosylation may also be involved in resistance, as several antimicrobial resistance determinants and multidrug efflux pumps are subjected to this PTM.¹⁰⁷ A two component response regulator, MtrA, implicated in sensitising mycobacterial cells to multiple drugs, is subjected to multiple PTMs including His/Asp/Ser/Thr phosphorylation, acetylation and pupylation.¹⁰⁷ Several modifying enzymes such as the kinase PknG are involved in drug resistance in *M. tuberculosis* and undergo phosphorylation *in vivo*.¹⁰⁷ The effects of these modifications are unknown but are expected to have a role in regulating multi-drug resistance.¹⁰⁷

1.3.2 Bacterial PTMs regulating antimicrobial resistance

The association between PTM and antimicrobial resistance is still an emerging field, however, there are already several examples of PTM directly altering bacterial susceptibility to antimicrobials. In various species, antimicrobial resistance is achieved through PTM of antimicrobial targets or resistance proteins. Regulation of such resistance is mediated by the modifying enzymes which perform the PTM. In fact, several modifying enzymes have been demonstrated as essential for resistance to broad ranges of antimicrobials. The role of PTMs in broader cellular processes has also been shown to have roles in antimicrobial resistance and susceptibility to antibiotics.

PTM of antimicrobial targets/activators

Isoniazid, a prodrug used against *M. tuberculosis*, is activated inside the cells by a catalase-peroxidase, KatG.²⁶² Natural mutants of KatG with mutations at Ser315 and Arg463 have been reported. These mutants prevent enzyme function, resulting in an 100-fold increase in concentration of isoniazid required to inhibit growth, but also prevent the natural functions of the enzyme.²⁶³ On the other hand, succinylation at Lys310 reduces the peroxidase activity of the enzyme, preventing isoniazid activation, while retaining catalase activity.¹⁹⁶ Thereby, succinylation of KatG results in a 200-fold decrease in susceptibility to isoniazid. KatG also undergoes acetylation, but any effects of this have not yet been investigated.^{168, 189}

PTM of resistance proteins

In methicillin-resistant *S. aureus*, exposure to β -lactams induces the phosphorylation of an integral membrane protein, BlaR1, initiating a signal transduction event which results in the expression of β -lactamases.²⁶⁴ Inhibition of phosphorylation *via* small molecules reversed the methicillin-resistant phenotype, rendering the bacteria susceptible to β -lactams.²⁶⁴ Phosphorylation also regulates the three component signal transduction system, which responds to number of antibiotics which are active against the cell wall, including vancomycin. The response regulator of three component system, VraR, is phosphorylated by Ser/Thr kinase Stk1. Such phosphorylation negatively regulates the DNA binding of VraR, including to its promoter, and is likely to be involved in regulation of antibiotic resistance.²⁶⁵

Phosphorylation is also associated with regulating the expression of multidrug efflux pumps. MgrA, a global regulatory protein of *S. aureus* regulates the expression of two efflux pumps, NorA and NorB, which have different antimicrobial substrates.²⁶⁶ MgrA is phosphorylated *in vivo* and the phosphorylation state of MgrA regulates its affinity

for the *norA* and *norB* promoters.²⁶⁷ Specifically, compared to the wildtype, phosphorylated MgrA binds poorly to the *norA* promoter but strongly to the *norB* promoter. Correspondingly, expression of phosphatase-deficient or phosphatase-intact strains decreased the MIC of antibiotics which are substrates of NorA or NorB, respectively.²⁶⁷ Efflux pumps themselves may also be regulated by PTM, for example, prevention of glycosylation of the CmeABC multidrug efflux pump of *Campylobacter jejuni* reduces resistance to 4 antibiotic classes.²⁶⁸

In *M. tuberculosis*, the major DNA damage response regulator is LexA. LexA forms polymeric filaments on DNA with RecA, a DNA-dependent ATPase. During the DNA damage response, RecA gets phosphorylated on Ser207, which inactivates the protein and inhibits its binding to LexA.²⁶⁹ This inhibition causes enhanced DNA damage and the development of rifampicin resistant strains.²⁶⁹ *M. tuberculosis* EmbR, a transcription factor, is positively regulated by phosphorylation.²⁷⁰ Phosphorylation greatly increases DNA binding ability, leading to increased transcription of genes and resulting in altered resistance.²⁷⁰ Also in *M. tuberculosis*, DNA-binding protein HupB undergoes Lys-acetylation and Ser/Thr phosphorylation.^{271, 272} In the sister strain *M. smegmatis*, HupB undergoes both methylation and acetylation of lysine residues and is necessary for the development of drug-resistant subpopulations *in vitro*.¹⁰⁴ While the effect of post-translational modifications was not specifically tested, mutation of a Lys residue which is subjected to PTM to Arg resulted in reduced growth in presence of isoniazid.¹⁰⁴

Elongation factor P is a conserved bacterial protein which strikingly resembles a tRNA and interacts with translational machinery to regulate synthesis of certain proteins.^{273, 274} Elongation factor P is required for various stress-resistance phenotypes, including antibiotic resistance.²⁷⁵ In *S. enterica*, elongation factor P is modified by two enzymes, PoxA and YjeK, and deletion of either enzyme results in enhanced sensitivity to antibiotics.²⁷⁴ PoxA and YjeK facilitate the modification of a conserved Lys34 residue with R- β -Lys, generating lysyl- β -lysine, critical for elongation factor P function.^{274, 275} In *P. aeruginosa* elongation factor P has Arg at position 34, which undergoes glycosylation with a cyclic rhamnose, also critical to protein function.²⁷⁶ Mutants deficient in elongation factor P or rhamnosylation of elongation factor P displayed significantly increased sensitivity to antibiotics targeting cell wall synthesis.²⁷⁶

Modifying enzymes

Bacterial kinases appear to be heavily involved in several antibiotic resistance pathways. For example, numerous studies have demonstrated that transmembrane Hanks-type kinases with repeats of the penicillin binding protein and Ser/Thr kinase-associated (PASTA) domain confer resistance to cell wall-inhibiting β -lactam antibiotics.¹⁰⁶ For example in *M. tuberculosis*, deletion of kinase PknG resulted in increased sensitivity to multiple antibiotics.²⁷⁷ The same result was observed when PknG was knocked out of *M. smegmatis*.²⁷⁸ Here, it was found that PknG controls essential cellular functions, and its disruption results in pleiotropic defects which result in increased antimicrobial susceptibility. The authors concluded that PknG is involved in intrinsic drug resistance rather than a specific resistance pathway.²⁷⁸

In *S. aureus* deletion of the only Ser/Thr kinase and phosphatase pair, Stk1 and Stp1, resulted in changes to the cell wall structure including an almost doubled cell wall thickness.²⁷⁹ The mutants also had increased susceptibility to various β -lactam antibiotics, which act on the cell wall. Particularly, they showed a 50-fold increase in ertapenem susceptibility.²⁷⁹ Stk1 activity is inhibited by certain cell wall targeting antibiotics, such as vancomycin, and such inhibition of Stk1 activity reduces phosphorylation of various proteins, including SarA. SarA is a post-transcriptional regulatory protein, and when phosphorylated on Cys9 has reduced DNA binding affinity.¹⁶² Sun and colleagues demonstrated that both a *sarA* knockout and an *stp1* knockout displayed enhanced resistance to vancomycin.¹⁶² Susceptibility to vancomycin could be recovered by plasmid expression of *sarA* or expression of *sarA* with Cys9 replaced with Ser. However, susceptibility to vancomycin was not recovered by expression of *sarA* with Cys9 replaced with Glu, a phospo-Cys mimic. Overall, the data suggests that phosphorylation of SarA plays a critical role in its regulation of antimicrobial resistance.¹⁶²

In *S. pneumoniae* antibiotic-sensitive strains, exposure to sub-lethal concentrations of penicillin and cefotaxime induces the expression of a kinase and phosphatase pair. Deletion of the kinase increases phosphorylation levels and provides augmented resistance to the antibiotics.²⁸⁰ Modifying enzymes are also important for resistance mechanisms in *A. baumannii*, where acylation, phosphorylation and glycosylation of the lipid A components of lipopolysaccharide by modifying enzymes has been shown to confer resistance to colistin.²⁸¹

Role of PTMs in wider resistance mechanisms

There are also a couple of examples where PTMs have broader effects on cellular physiology which enable cells to have reduced susceptibility or resistance to antimicrobials. For example, DosRS is a two-component regulatory protein complex which helps *M. tuberculosis* maintain a low metabolic state that prevents antimicrobials from working.²⁸² Acetylation at Lys182 of the DosR transcription factor is essential for its DNA binding activity. Upon sensing the low metabolic state, Lys182 undergoes deacetylation and promotes gene regulation of hundreds of hypoxia-induced genes.²⁸³ In a different example, *S. aureus* strains deficient in prenylation exhibit various changes in cellular physiology, including altered antimicrobial resistance.²⁸⁴ Specifically, sensitivity to antibiotics targeting the cell wall is increased while sensitivity to antimicrobial peptides and aminoglycosides is decreased. This is thought to be due to changes in the structure of the cell envelope, as mutants displayed a thinner and more diffuse cell envelope.²⁸⁴

Overall, the number of antimicrobial resistance proteins which undergo PTM, alongside the more direct evidence of specific PTMs or modifying enzymes being implicated in antibiotic resistance phenotypes, suggests a possible role of PTMs in regulating antimicrobial resistance. In this way, alongside genetic mutations, horizontal gene transfer, changes in protein expression and cellular physiologies such as biofilms, PTMs may be one of the factors which contributes to the development or manifestation of antimicrobial resistance (**Figure 1.16**).

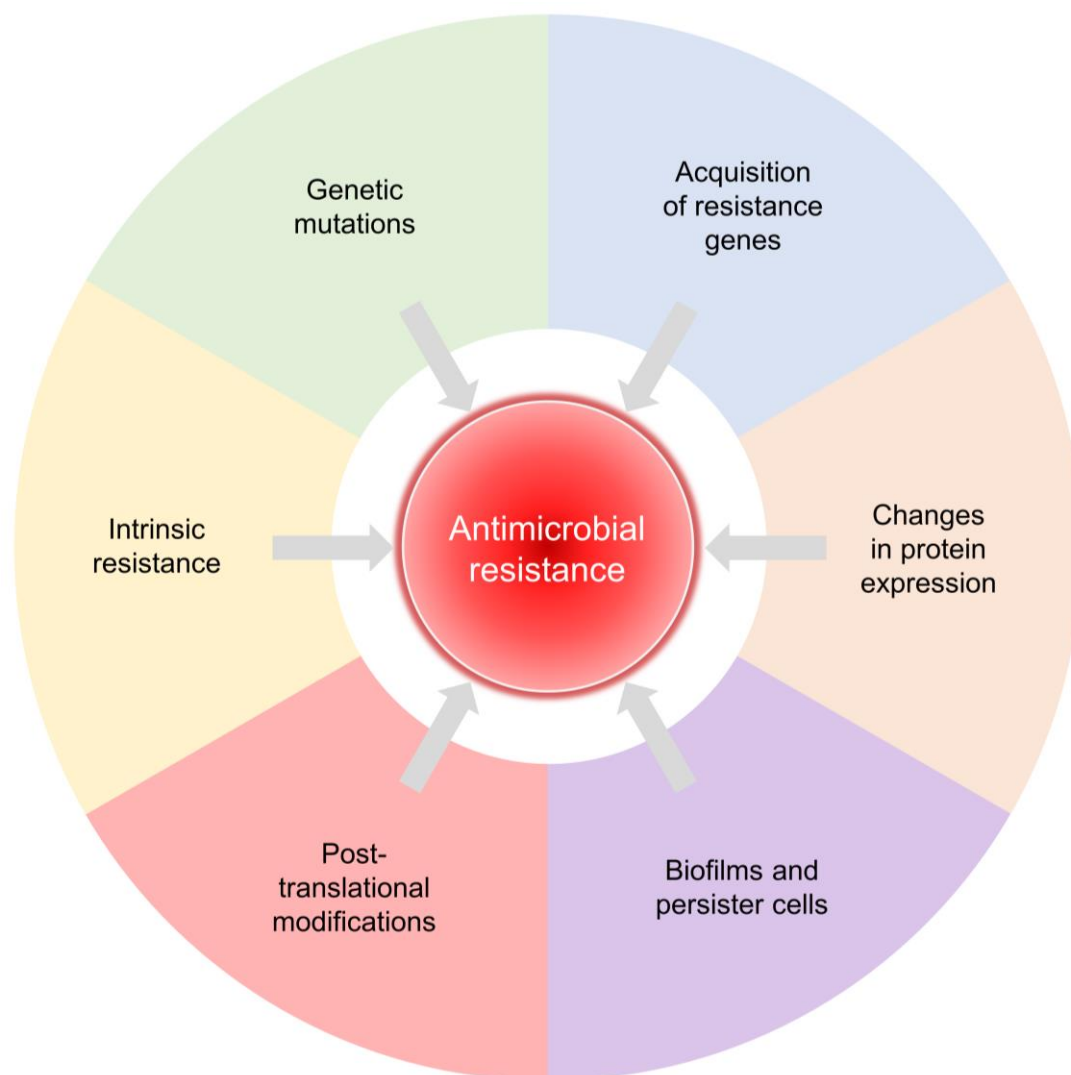


Figure 1.16 Factors contributing to antimicrobial resistance. Antimicrobial resistance can arise as a result of genetic changes such as genetic mutations or the acquisition of resistance genes through horizontal gene transfer. Resistance can also result from changes in the expression level of certain proteins. Some bacteria display intrinsic resistance, due to the composition of their cell membrane or the constitutive expression of efflux pumps. Further, cells that exist in a biofilm or which persist in the presence of an antibiotic can also encourage antimicrobial resistance to develop. Finally, recent evidence suggests a possible role of post-translational modifications in regulating antimicrobial resistance.

1.3.3 PTMs as antimicrobial drug targets

Many of the aforementioned studies reporting potential links between PTMs and antimicrobial resistance have suggested the possibility of PTMs as novel drug targets for antimicrobial therapy.^{105-107, 113, 224, 279} Perhaps the easiest way to inhibit a PTM is to target the enzyme which performs the modification. As modifying enzymes have been shown to be necessary for resistance to various antimicrobials, they appear to

be prime targets for new antimicrobial therapies. As mentioned, some kinases are directly implicated in antimicrobial resistance through activating resistance proteins such as global regulators or efflux pumps. In addition, as mentioned in **Antibiotic modification or degradation**, modification of antibiotics with small chemical groups is a commonly observed resistance mechanism in the clinical setting. While this is a separate process from PTM of proteins, it is often mediated by similar or the same modifying enzymes which modify bacterial proteins. For example, most of the aforementioned aminoglycoside modifying enzymes are from the GNAT superfamily. Targeting these modifying enzymes *via* inhibitors may restore antimicrobial sensitivity and represents a promising target for an adjuvant to be used in combination therapy to overcome antimicrobial resistance.^{113, 285, 286}

Some kinases are essential for bacteria or involved in important cellular processes and are under investigation as drug targets, e.g. the Ser/Thr PASTA kinases PknA and PknB from *M. tuberculosis*.²⁸⁷ Numerous studies have attempted to target PknB, however, there are currently no single-drug clinical candidates.¹⁰⁶ One obstacle when developing kinase inhibitors is that the efficiency of the drug *in vivo* is lower than indicated by *in vitro* testing. This may be due to uptake of the drug or a result of the many more molecular interaction partners present in bacterial cells.¹⁰⁶ However, another *M. tuberculosis* kinase, PknG, was successfully targeted through inhibition of its ATP-binding site, and this resulted in effective clearance of the cells by macrophages.²⁷⁷ It has been suggested that combined β -lactam and Ser/Thr kinase inhibition could represent a new strategy to overcome β -lactam resistance.¹⁰⁶ In *Listeria monocytogenes*, the PASTA kinase PrkA is essential for resistance to β -lactam antibiotics and was successfully inhibited by the broad spectrum kinase inhibitor staurosporine.²⁸⁸ When staurosporine was used in combination with β -lactam antibiotics, cells showed a 100-fold increase in susceptibility to the antibiotics. This suggests that PASTA kinase inhibitors in combination with β -lactams is a novel and viable antibiotic development strategy.²⁸⁸

Histidine kinases of two-component systems are another potential drug target. Two-component systems have been linked to resistance through regulation of cell wall metabolism or expression of efflux pumps. They are considered attractive antibacterial targets as multiple members are found in nearly all bacteria, they are often essential and have highly conserved domains. Hundreds of inhibitors have been described in the literature.²⁸⁹ However, the ATP-binding domain Bergerat fold is also present in several human protein families and there is a likelihood of off-target inhibitory effects. Despite this, some progress has been made. For example,

walkmycins, inhibitors of Walk, part of an essential and highly conserved two-component system in Gram-positive bacteria, are in preclinical development.²⁹⁰ One such inhibitor prevents the auto-phosphorylation activity of Walk, is bactericidal, and restored sensitivity of drug-resistant isolates to amoxicillin and cefotaxime when used as an adjuvant in combination with the specified antimicrobial.²⁹¹ Tyrosine kinases have also been suggested as a potential drug target, with the advantage that they are structurally distinct from eukaryotic kinases.¹⁰⁵

Lnt is an apolipoprotein *N*-acyl transferase which adds the third fatty acid to apolipoproteins before they are trafficked to the outer membrane.²⁹² *Neisseria meningitidis* strains deficient in Lnt show increased susceptibility to antimicrobials, including a 64-fold increase in susceptibility to rifampicin and 16-fold increase towards ciprofloxacin.²⁹³ As such, Lnt has been described as a promising target for an adjuvant antimicrobial therapy. Finally, the pupylation-proteasome system of *M. tuberculosis* has been highlighted as an important potential drug target to combat emerging multi-drug resistant *M. tuberculosis* strains.²²⁴

PTMs and the enzymes performing them have the potential to be promising targets for antimicrobial therapy. However, before this can be realised, considerable work is needed to uncover the links between PTMs and antimicrobial resistance. While the post-translational modification of multiple proteins involved in antimicrobial resistance has been reported, there have been fewer studies characterising and confirming these associations. Therefore, investigating the relationship between post-translational modifications and antimicrobial resistance may be a valuable resource both for understanding a wider perspective of the mechanisms behind antimicrobial resistance and for uncovering future drug targets.

1.4 Characterising PTMs

There are various chemical biology approaches enabling the characterisation of PTMs.²⁹⁴ Post-translationally modified proteins can be extracted directly from cells, as they often are for mass spectrometry studies. However, the amount of proteins in the cellular pool subjected to the modification is often only a small proportion, and it is often difficult to obtain a pure sample.²⁹⁵ Instead, a heterogeneous mixture of modified and non-modified proteins is likely to be obtained. This is particularly true for dimeric or tetrameric proteins, as not all of the proteins in a complex may be uniformly modified yet they will be purified together. This method can be useful for characterising proteins *in vitro* and allows the proteins to be isolated in their natural conformation. However, it is not suitable for characterising the effect of PTMs in live cells due to the low amount of modification. It is possible to use methods to decrease or enhance the amount of PTM, *e.g.* by limiting or increasing the expression of modifying enzymes, but this is unlikely to obtain a homogeneous sample, and the enzymes performing the modifications are sometimes unknown.²⁹⁴

Another method of characterising PTMs is amino acid substitution. Many studies attempting to characterise PTMs substitute the amino acid subjected to a modification *in vivo* to a different amino acid which is analogous to the modification, *e.g.* it has the same charge state as the modification would confer.²⁹⁴ For example substitution of lysine with glutamine is commonly used to mimic lysine acetylation. This method has the advantage of being relatively simple to perform, however, it is not an exact replication of the modified amino acid and so there may be some characteristics of the modification which are not conferred by the substitute amino acid such as steric effects.²⁹⁵ Chemical synthesis allows the direct incorporation of modification into proteins, and this can be a useful approach.²⁹⁴ However, the size of the polypeptide chain can be limited in chemical synthesis, although this can be overcome by using semisynthetic methods, such as native chemical ligation, to produce full length proteins. Unfortunately, this approach is rarely useful for studying the effect of the protein modification on living cells, due to difficulties in delivering protein to cells.²⁹⁴ An approach which addresses some of these limitations, and allows direct substitution of the modified amino acid *in vivo*, is unnatural amino acid incorporation.^{294, 295}

1.4.1 Unnatural amino acid incorporation

Unnatural (non-canonical) amino acid incorporation employs genetic code expansion to site-specifically incorporate unnatural amino acids into a protein of interest.²⁹⁶ Here, 'unnatural' refers to any amino acid which is not one of the common 20 canonical amino acids. Genetic code expansion exploits DNA codons which are rarely used *in vivo*, and reassigns such 'blank' codons to encode the unnatural amino acid. The most commonly used blank codon is the amber stop codon, TAG, which is used as a stop codon ~8% of the time in *E. coli*.²⁹⁷ As this codon is rarely used, it can be utilised for unnatural amino acid incorporation with minimum off-target effects.²⁹⁷ To reassign the amber stop codon to encode for the non-canonical amino acid, a tRNA with a CUA anticodon (tRNA_{CUA}) and corresponding tRNA synthetase are used. The tRNA synthetase is subjected to directed evolution alongside the tRNA_{CUA} to ensure that it only aminoacylates the tRNA_{CUA} with the amino acid of interest.²⁹⁷ The tRNA and tRNA synthetase pair are therefore engineered to be completely orthogonal inside the host cell, *i.e.* the tRNA_{CUA} and the tRNA synthetase interact only with each other and the non-canonical amino acid, with no crosstalk with canonical tRNAs, tRNA synthetases or amino acids.²⁹⁸ They are, however, able to interact with the translation machinery of the host cell.

An example of a tRNA/synthetase pair orthogonal in both bacteria and mammalian cells is the pyrrolysyl-tRNA synthetase(PylRS)/tRNA_{CUA} pair from the archaea *Methanosarcina mazei* and *Methanosarcina barkeri*.^{298, 299} In these *Methanosarcina*, TAG is not used as a stop codon, as in other species, but is used to encode pyrrolysine, which is endogenously translated into proteins in these species³⁰⁰ To this end, PylRS naturally binds pyrrolysine, but none of the 20 canonical amino acids, and uses it to aminoacylate the tRNA_{CUA}.^{299, 300} PylRS has subsequently been engineered to recognise specific non-canonical amino acids through directed evolution, resulting in various PylRS variants responding to specific unnatural amino acids.^{298, 299} Thereby, utilisation of specific PylRS variants with the corresponding tRNA_{CUA} and non-canonical amino acid allows for easy experimental design, with only the target gene of interest requiring researcher manipulation. The codon corresponding to the amino acid of interest in the target gene must be mutated to TAG, which is often easily achieved by a PCR mutagenesis.

The host cell must then be provided with all of these components. This can be achieved by transforming the cell with both an expression vector, containing the gene of interest with an amber stop codon, and a second plasmid containing the tRNA_{CUA} and tRNA synthetase (**Figure 1.17**). The gene of interest can be placed downstream

of an inducible promoter, to allow control over gene expression. The unnatural amino acid itself can be chemically synthesised and provided to the cells during the exponential growth phase in the culture medium. Such a design requires that the unnatural amino acid can diffuse through the bacterial cell membrane and most are transported into *E. coli* cytoplasm, except for those which are highly charged.²⁹⁷ Inhibitors of enzymes such as deacetylases can also be provided in the medium, to prevent removal of the modification by the host cell.²⁹⁵

There are several advantages to this approach when studying post-translational modifications.^{294, 295} Incorporation of the unnatural acid is often high and, particularly if the protein is extracted and purified, it is possible to obtain a homogenously-modified sample. Another key advantage of this technique is the ability to modify proteins in live cells,²⁹⁶ allowing the effect of any modifications on cellular physiology to be characterised. This permits a broader representation of any effects compared to testing the effect of a modification on interaction between two proteins *in vitro*, as *in vivo* one protein may interact with multiple proteins, there may be interactions which have not yet been elucidated, or there may be physiological downstream effects of such interactions. Further potential applications include the *in vivo* control of protein function, the incorporation of multiple unnatural amino acids into a single protein, and therapeutic applications.^{296, 298, 301} However, a potential disadvantage of this approach is that although the amber stop codon is used infrequently in the bacterial genome, it is still used. As such, any TAG codon in the exon regions may be decoded with the unnatural amino acid instead of translation terminating. This may lead to read through and improper translation of affected genes, although essential genes are rarely terminated by TAG.²⁹⁷

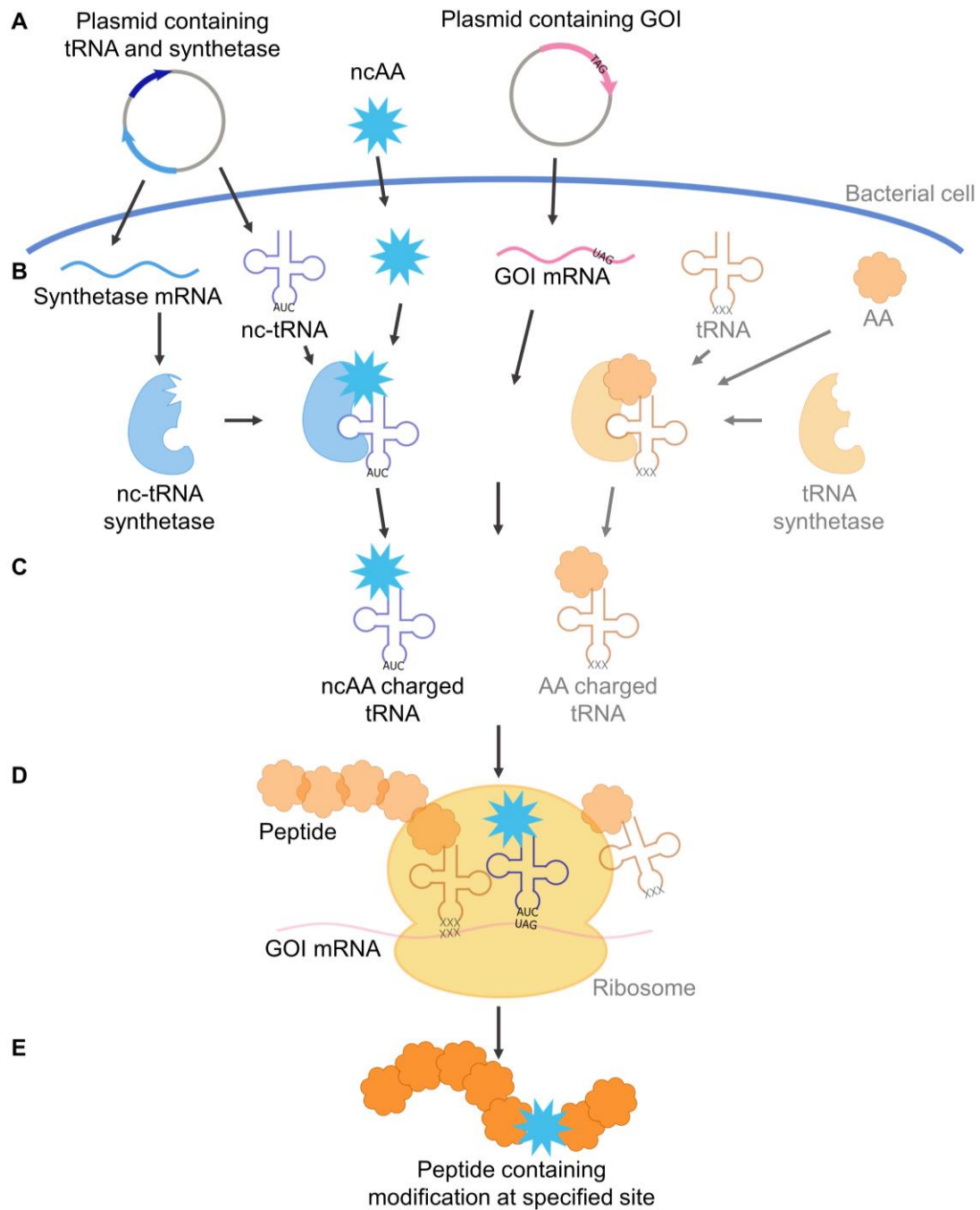


Figure 1.17 Schematic of genetic code expansion. **A** The bacterial cell is provided with a plasmid containing the non-canonical tRNA (nc-tRNA) and tRNA synthetase (nc-tRNA synthetase), a second plasmid containing the gene of interest (GOI) with a TAG codon, and the non-canonical amino acid (ncAA). **B** The nc-tRNA, nc-tRNA synthetase mRNA and GOI mRNA are transcribed by the cellular transcription machinery and the nc-tRNA synthetase mRNA is translated into the corresponding protein by the cellular translation machinery. **C** The nc-tRNA is charged with the ncAA by the nc-tRNA synthetase. The endogenous cellular mechanisms produce canonical tRNA charged with the 20 canonical amino acids. **D** The GOI mRNA is decoded by the ribosome with the endogenous translation machinery, with the TAG codon decoded by the ncAA-charged tRNA. **E** The resulting peptide contains the ncAA at the specified site, and is folded into the final protein.

1.5 Aims and objectives of thesis

The aim of this thesis is to investigate the largely unexplored role of post-translational modifications of bacterial proteins in antimicrobial resistance. Two proteins previously reported to undergo post-translational modification and with known roles in antibiotic resistance were selected for this purpose. In both cases, the protein of interest was produced in bacteria, with genetic code expansion for unnatural amino acid incorporation to produce the modified protein. Then, any effects of the modification on protein function or cellular physiology were characterised in comparison to the wildtype protein.

The first half of this thesis explores a specific resistance protein, AdeT1, which is a multi-drug efflux pump from the nosocomial pathogen *Acinetobacter baumannii*. This protein is post-translationally modified with lysine propionylation *in vivo* and here the effect of this modification on bacterial survival in the presence of antibiotics is assessed. The second half of the thesis investigates a ubiquitous bacterial DNA-binding protein, HU β , known to have wide roles in cellular physiology, including resistance phenotypes in various species. Specifically, this project investigates the effect of lysine acetylation on the DNA-binding affinity of *Escherichia coli* HU β .

Chapter 2 – Investigating the effects of lysine propionylation on the *Acinetobacter baumannii* AdeT1 protein

2.1 Summary

Acinetobacter baumannii is a prevalent source of hospital-acquired infections and rapidly acquires antimicrobial resistance. The *A. baumannii* AdeT1 protein is a membrane fusion protein which is part of a resistance-nodulation-division-type multidrug efflux pump. AdeT1 has a significant role in resistance to a range of antimicrobials and undergoes lysine propionylation *in vivo*. To investigate the effects of this post-translational modification on antimicrobial resistance, a minimum inhibitory concentration assay for characterising the effects of heterologous proteins in an *E. coli* host was developed. This chapter demonstrates that while AdeT1 does form part of a functional efflux pump in *E. coli*, expression of wildtype AdeT1 protein does not confer resistance to any antibiotics tested. Propionyl-lysine was then incorporated into AdeT1 protein and subsequent minimum inhibitory concentration assays demonstrated that when propionylated AdeT1 is expressed, erythromycin resistance is conferred to the *E. coli* host. It is likely that propionylation of AdeT1 regulates either the function of the AdeT1 protein or its interaction with other proteins in the resistance-nodulation-division-type complex in *A. baumannii*.

This chapter contributed towards the publication:

Barlow, V.L., Lai, S.J., Chen, C.Y., Tsai, C.H., Wu, S. H. and Tsai, Y.T. Effect of membrane fusion protein AdeT1 on the antimicrobial resistance of *Escherichia coli*. *Scientific Reports*, **10**, 20464 (2020).

2.2 Introduction

2.2.1 *Acinetobacter baumannii*

Acinetobacter baumannii is a Gram-negative bacterium which has various reservoirs including soil, water, animals and humans.³⁰² It is also considered as an opportunistic human pathogen associated with a range of diseases including pneumonia, blood stream infections, meningitis and urinary tract infections.³⁰³ The bacteria became known for being frequently recovered from military service members injured during both the Vietnam War and in Afghanistan and Iraq during the early 2000s, and is still commonly isolated from patients being treated for traumatic injuries.³⁰² Presently, *A. baumannii* is typically acquired in the health care setting and has become a prevalent source of hospital-acquired infections.³⁰⁴ Particularly, in intensive care units, the pathogen accounts for up to 10% of infections worldwide.³⁰⁵ Pathogenic infection with *A. baumannii* is often facilitated by invasive procedures which allow the bacteria to directly colonise the site of infection, such as the use of catheters or mechanical ventilation, and the use of broad-spectrum antimicrobials to treat a prior infection.³⁰³

Pathogenic *A. baumannii* possesses a variety of virulence factors enabling infection of the host.³⁰³ Yet, the major obstacle in treating infections is widespread antimicrobial resistance, which has developed with alarming speed. In fact, antibiotic resistance is the biggest determinant of clinical outcome in infections caused by *A. baumannii*.³⁰⁶ Increasing rates of drug resistance were first noticed in the 1970s, and have since become a widespread phenomenon.^{304, 307-309} Concerningly, *A. baumannii* is able to develop multidrug resistance at an unrivalled rate compared to other ESKAPE pathogens. Occurrences of multidrug resistance in *A. baumannii* increased from 23% to 63% of clinical isolates over a 10 year period while remaining relatively stable for the other pathogens tested.³¹⁰ Further, several strains of *A. baumannii* are completely resistant to most clinically available antibiotics, severely limiting viable treatment options.³¹¹ Today, about 45% of global isolates of *A. baumannii* are multi-drug resistant.³¹⁰ Indeed, the World Health Organization recently highlighted that infections caused by drug-resistant *A. baumannii* are one of the most dangerous threats to human society.³¹² As such, understanding the mechanisms that allow *A. baumannii* to exhibit such alarmingly prevalent and rapid resistance to antibiotics is of utmost value.

Multidrug-resistant strains of *A. baumannii* harbour a genomic island containing up to 45 resistance genes, and sequence analysis suggests frequent exchange of genetic information between *A. baumannii* and other bacterial species.³¹³ Rapid acquisition of resistance has also been attributed to the high plasticity of protein expression in *A. baumannii*.^{314, 315} Such dynamic protein expression allows the species to exhibit an arsenal of resistance mechanisms.³⁰⁹ *A. baumannii* has been documented to produce various antibiotic-degrading proteins, including oxacillinases³⁰⁶ as well as various β -lactamases from all described classes.³¹⁶ The bacteria can also modify cell membrane structure, permeability or stability to prevent antibiotic-membrane interactions.³¹⁷⁻³¹⁹ Similarly, loss of two different outer membrane proteins have been repeatedly associated with imipenem resistance,³²⁰⁻³²³ leading to speculation that these proteins transport imipenem into the cell and rapid downregulation of their expression provides resistance.³²⁰ Further, *A. baumannii* modifies proteins targeted by antimicrobials, such as modification to the regions of DNA gyrase and DNA topoisomerase IV targeted by fluoroquinolones.³¹⁶ Finally, dynamic production of both drug-specific efflux pumps, such as those providing resistance to tetracycline, but also of non-specific, multidrug efflux pumps provides resistance to a range of antimicrobials.^{316, 324}

2.2.2 Multidrug efflux pumps

Multidrug efflux pumps confer intrinsic, acquired, and induced resistance to antibiotics.^{19, 47} However, the use of antibiotics is very recent in terms of bacterial evolution. Multidrug efflux pumps evolved long before the application of antibiotics³²⁵ and have roles in bacterial interactions with plants, animal hosts and other bacteria, and maintenance of cell homeostasis.^{326, 327} They also have wider roles in infection, such as increasing pathogenicity through transport of virulence factors and aiding in biofilm formation.³²⁸ These broad ranging applications are facilitated through the wide substrate scope of most efflux pumps.³²⁷ There are five main classes of multidrug efflux pumps: the small multidrug resistance (SMR) family, major facilitator superfamily (MFS), multidrug and toxic efflux (MATE) family, ATP-binding cassette (ABC) family and resistance nodulation division (RND) superfamily (**Figure 2.1**). Most classes of multidrug efflux pumps are located in the inner membrane of Gram-negative bacteria, where they pump toxic compounds into the periplasm. From here, the toxic compounds leave the cell *via* outer membrane proteins, such as TolC.³²⁸ RND-type efflux pumps are composed of a protein complex, which spans both the inner and outer membranes, and extrude toxic compounds from the cytosol or periplasm directly into the extracellular space.³²⁹

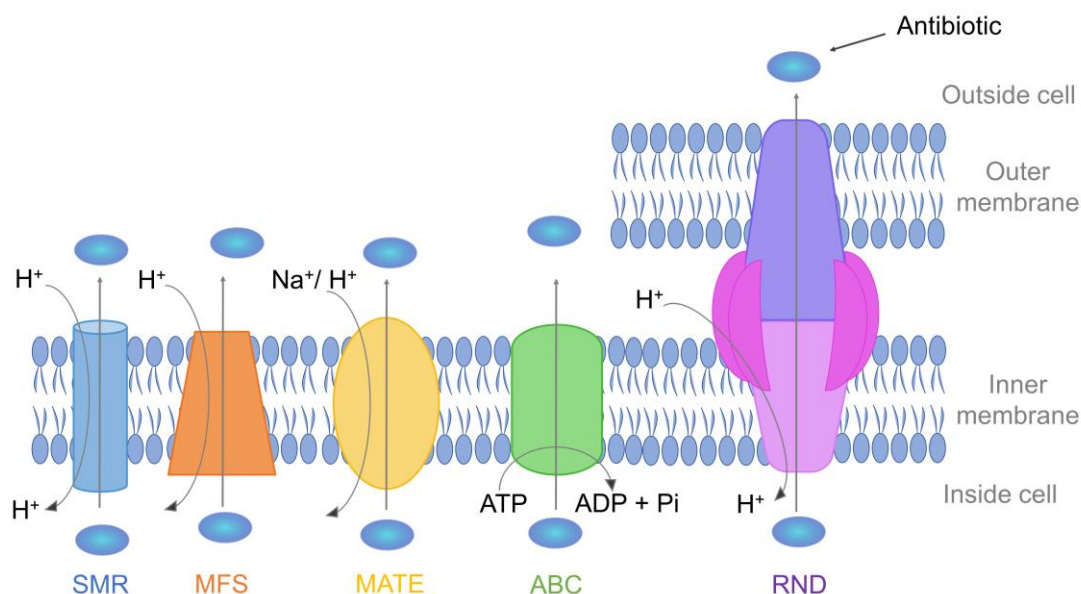


Figure 2.1 Classes of multidrug efflux pumps. From left to right: Small multidrug resistance (SMR); Major facilitator superfamily (MFS); multidrug and toxic efflux (MATE); ATP binding cassette (ABC) and resistance-nodulation-division (RND) efflux pumps. RND-type pumps are the only family to span both the inner and outer membranes.

Not surprisingly, overexpression of pumps has been documented in many clinical isolates of *A. baumannii*.^{324, 330} Particularly, the MFS and RND families are associated with resistance in this species.³³¹ Basal-level expression of RND pumps is commonly observed and provides the bacteria with broad intrinsic resistance.^{331, 332} This low-level resistance allows for selection of mutations in the regulatory genes controlling expression, inducing higher-level, acquired resistance.³³³⁻³³⁵

2.2.3 RND-type multidrug efflux pumps

RND-type transporters represent the highest clinical relevance in several species of multidrug resistant bacteria.^{46, 336-338} At the molecular level, RND transporters have a tripartite structure, composed of inner membrane proteins, membrane fusion proteins, and outer membrane proteins (**Figure 2.2**). Three inner membrane proteins transport substrates from the cytosol while the three outer membrane proteins form a barrel-like structure which creates a pore in the membrane. Multiple membrane fusion proteins connect the other two components, which do not otherwise interact, and are also anchored in the inner membrane. Together, the proteins form a functional transporter that extrudes a wide variety of toxic substrates from the cell using proton motive force as an energy source.^{19, 329, 338-340} RND type pumps have a considerably wider substrate scope than single component efflux pump families. Through multiple

substrate entrance channels and binding sites,³⁴¹ they allow extrusion of substrates often unrelated in structure, allowing broad resistance to be conferred by a single pump.^{19, 338, 340} Extrusion *via* RND type pumps can occur from the cytoplasm or from the periplasm,^{43, 342} enabling cooperative effects with other families of efflux pumps.³⁴³ In addition to providing resistance through direct extrusion of antibiotics, recent evidence suggests that RND-type pump activity may impact other antimicrobial resistance mechanisms such as regulation of resistance protein expression and DNA mutation rate.³⁴¹

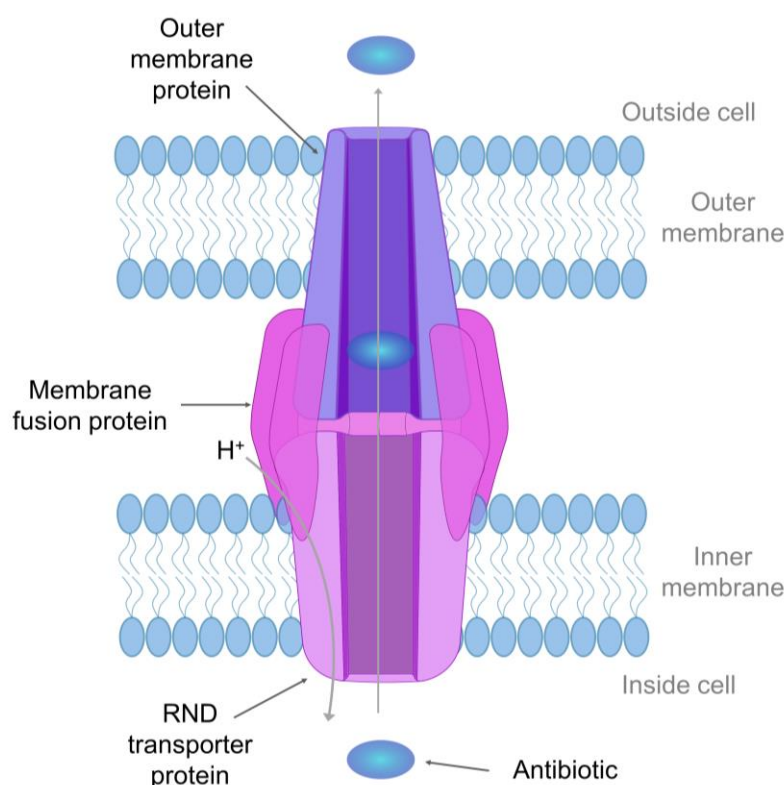


Figure 2.2 Schematic of a resistance nodulation division (RND)-type multidrug efflux pump. RND-type pumps have a tripartite structure composed of three different types of proteins. An RND transporter protein sits in the inner membrane and uses proton motive force to extrude substrates from the cytosol while an outer membrane protein forms a pore in the outer membrane which allows substrates to leave the cell. Multiple membrane fusion proteins anchored in the inner membrane connect these two components and are critical for complex formation.

In *A. baumannii*, RND-type efflux pumps play a critical role in conferring resistance to a wide range of antibiotics and detergents and are widespread among *A. baumannii* strains.^{333, 344, 345} AdeABC was the first RND system characterised in *A. baumannii* and consists of the membrane fusion protein AdeA, inner membrane protein AdeB, and outer membrane protein AdeC.³⁴⁶ Overexpression of *adeABC* was shown to

increase resistance to a wide range of substances including aminoglycosides, fluoroquinolones, cefotaxime, erythromycin, tetracycline, and chloramphenicol.^{332, 346-350} The operon is found in 80% of strains,³⁵¹ but notably not in environmental, as opposed to clinical, isolates.³⁵² Another RND pump system, AdeFGH, confers resistance to fluoroquinolones, tetracycline-tigecycline, chloramphenicol, SDS, ethidium bromide, and acridine orange, amongst others, when overexpressed.³⁵⁰ The *adeFGH* operon was found in 90% of strains tested,³⁵⁰ however, it is not constitutively expressed in wildtype strains and is therefore unlikely to contribute to intrinsic resistance.³²⁴ Similarly, RND pump AdeIJK was found to have a wide substrate scope and contributes towards resistance to β -lactams, chloramphenicol, tetracycline, erythromycin, fluoroquinolones, acridine, and SDS.³³² AdeIJK appears to be intrinsic to *A. baumannii*, the genes encoding this pump are present in all strains tested.³³² Further, it was reported that deletion of just a single component of an RND-type pump, the gene encoding membrane fusion protein AdeT1, could increase the antimicrobial susceptibility of *A. baumannii* to a wide range of substrates.³⁵³

In addition to the native effects in *A. baumannii*, heterologous expression of *adeABC*, *adeIJK* or *adeT1* in *E. coli* have also been demonstrated to increase bacterial resistance to antibiotics.^{353, 354} Bacterial resistance proteins are often functional in heterologous hosts, and *E. coli* has been commonly used for functional characterisation of antibiotic resistance proteins from other bacteria.³⁵⁵⁻³⁵⁷ Antibiotic hypersusceptible strains of *E. coli* are often used for such characterisations due to their low level intrinsic resistance to antimicrobials. For example, *E. coli* KAM32 strain lacks the genes *acrB*, encoding the pump protein of the major *E. coli* RND complex AcrAB-TolC, and *ydhE*, encoding a multidrug efflux pump of the MATE family.³⁵⁸

2.2.4 Post-translational modifications of multidrug efflux pumps

Investigations into the effects of post-translational modifications (PTMs) on efflux pumps are very much in their infancy. Recently, PTM of an RND-type pump in the pathogen *Campylobacter jejuni* was demonstrated to modulate efflux pump function. In the RND-type pump CmeABC, all three protein components are post-translationally modified with *N*-linked glycans. Such modification was found to increase protein thermostability, promote protein-protein interaction, and stabilise protein complexes. As such, when glycosylation was abrogated, *C. jejuni* displayed decreased efflux pump activity, manifesting as higher ethidium bromide accumulation and increased sensitivity to antimicrobials.²⁶⁸

In *A. baumannii*, PTMs occur on proteins involved in a wide range of functions and have been suggested as potential drug targets.¹⁰⁵ PTMs have been recorded on various proteins involved in drug resistance. For example, the phosphorylation of a number of proteins associated with drug resistance was detected in the multidrug-resistant clinical isolate AbH120-A2 but not in the susceptible reference strain.³⁵⁹ Furthermore, acylation, phosphorylation and glycosylation of *A. baumannii* lipid A has been shown to confer resistance to colistin.^{281, 360, 361} PTMs have also been revealed to occur on multidrug efflux pumps in this species. The phosphoproteome of *A. baumannii* revealed phosphorylation of an ABC type multidrug transporter.³⁵⁹ The MATE efflux pump AbeM which confers resistance to fluoroquinolones, tetracycline-tigecycline and chloramphenicol^{350, 362} is acetylated *in vivo*.²⁵⁵ The acetylome also reveals acetylation of an MFS permease and RND transporter in an imipenem-resistant but not imipenem-susceptible strain.³⁶³ Finally, the propionylome of *A. baumannii* revealed that the membrane fusion protein AdeT1 undergoes propionylation in this species.²⁵⁶ As yet, no published studies have characterised the effect of such modifications on efflux pump function in *A. baumannii*.

2.2.5 AdeT1

AdeT1 was identified in 2011 as a membrane-fusion protein component of an RND-type multidrug efflux pump by Srinivasan and colleagues.³⁵³ Deletion of the gene encoding the protein *in vivo* in *A. baumannii* resulted in increased susceptibility to a broad range of antibiotics including a 4-fold increase in susceptibility to chloramphenicol and acridine orange and a 2-fold increase to various other antimicrobials including erythromycin, minocycline, novobiocin, tetracycline and acriflavine. Subsequent provision of the gene encoding AdeT1 on a plasmid restored antimicrobial resistance to wildtype levels. The effect of AdeT1 on antimicrobial resistance was also characterised in *E. coli* KAM32, an antimicrobial hypersusceptible strain, where the results were even more striking. In KAM32, provision of *adeT1* on a plasmid provided increased resistance to a broad range of antimicrobials, most notably a 6-fold increase in the amount of erythromycin required to inhibit growth, 5-fold increases in the amount of chloramphenicol and novobiocin required, and 4-fold increases in acridine orange, acriflavine, deoxycholate, and SDS. As mentioned, AdeT1 was recently discovered to be propionylated *in vivo* in *A. baumannii*, but the effects of this modification remain unknown.²⁵⁶ As expression of this single component of an RND-type pump complex alone has such a profound effect on antimicrobial resistance, this provides an ideal opportunity for investigating

the effects, if any, of this PTM on the antimicrobial susceptibility conveyed by AdeT1 and any complexes in which it partakes.

2.2.6 Lysine propionylation of AdeT1

Lysine propionylation (**Figure 2.3**) is a PTM likely to have important functions in the regulation of prokaryotic biological processes including energy metabolism, translation, post-translational modifications and stress response.^{126, 198, 204} Lysine residues are positively charged at physiological pH, and it is anticipated that lysine propionylation may significantly alter protein function in response to physiological conditions.²⁰⁴ This is because propionylation would prevent formation of a positive side chain at physiological pH, thereby lowering the reactivity of the lysine residue and potentially altering interactions with other proteins. As mentioned in **Lysine acylation**, much remains unknown about the processes regulating lysine propionylation. However, propionyl-coenzyme A (CoA) is assumed to be required as a propionyl donor and the acetyltransferase PatZ and the sirtuin CobB have been shown to have propionylation and de-propionylation activity, respectively.^{198, 205}

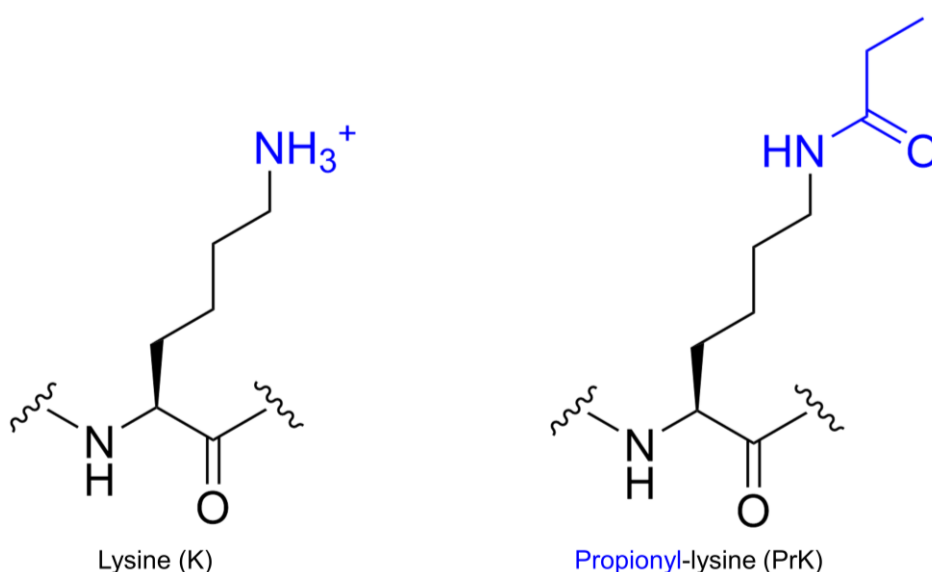


Figure 2.3 Schematic representation of lysine (K) and propionyl-lysine (PrK). Lysine propionylation is the addition of a propionyl group to the terminal nitrogen of the lysine side chain to afford propionyl-lysine.

Propionylation at Lys280 of AdeT1 was found in both an imipenem-susceptible and imipenem-resistant strain of *A. baumannii* (**Figure 2.4**).²⁵⁶ As AdeT1 protein likely forms an RND-type pump protein complex, it is possible that this modification could interfere with this interaction. However, the structure of membrane fusion proteins and RND-type pumps in *A. baumannii* remain unsolved. While much progress has been made in determining the structure of the *E. coli* RND pump AcrAB-TolC,^{339, 364-368} for other complexes progress has been slow. The structure of a singular component of AdeB from *A. baumannii* has been determined³⁶⁹ but, as of yet, there is no structural information available for *A. baumannii* membrane fusion proteins. Therefore, the location of this modification within the 3-dimensional structure of the protein and within its interaction with other proteins is unclear.

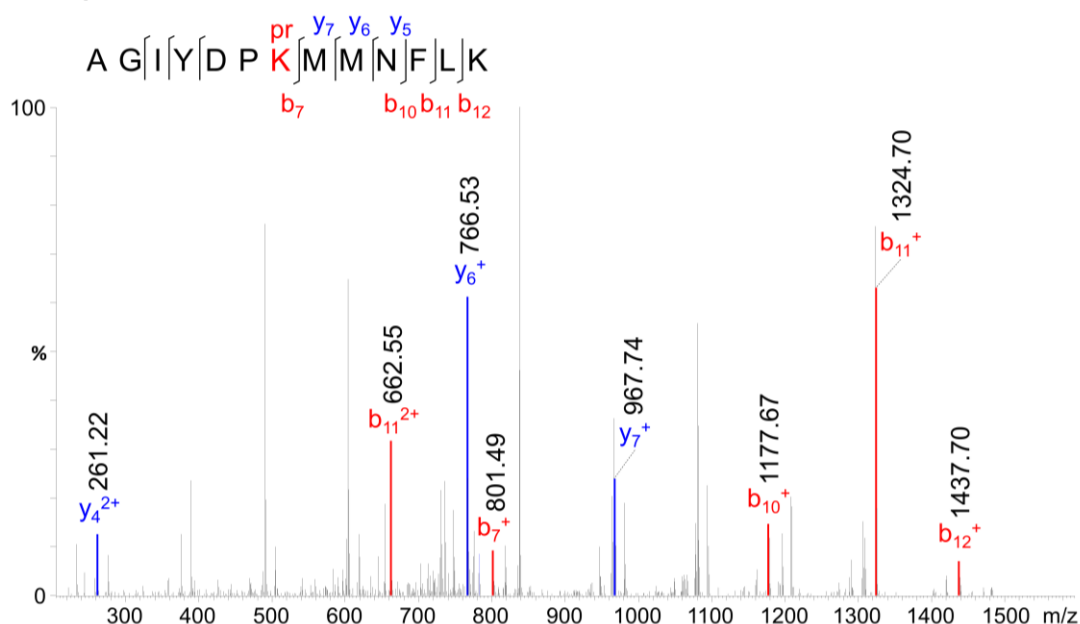
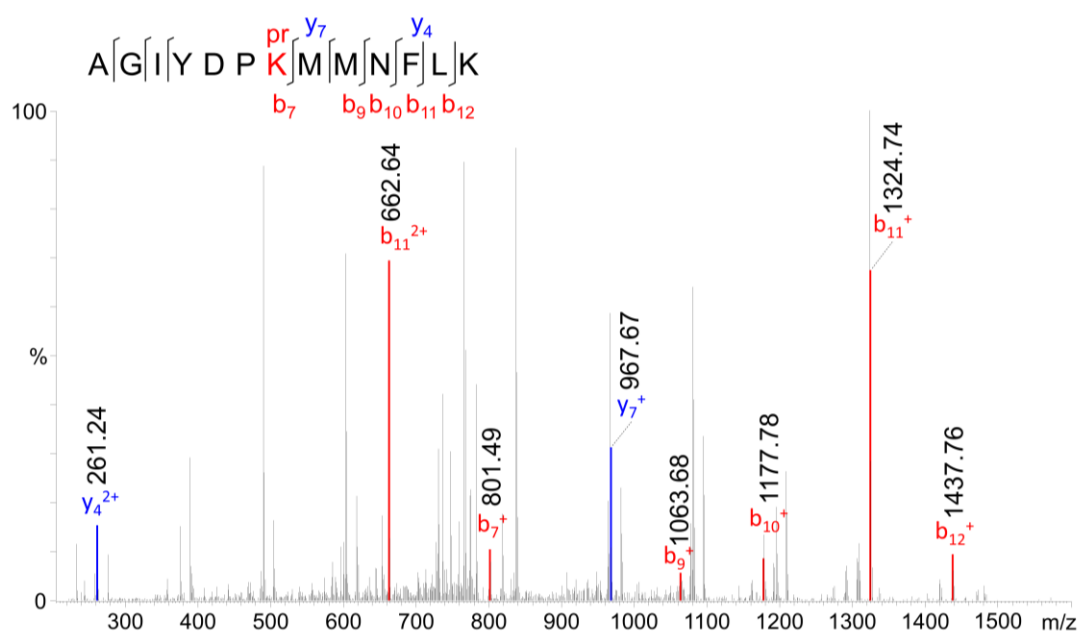
A Imipenem-resistant *Acinetobacter baumannii* strain SK17-R**B** Imipenem-susceptible *Acinetobacter baumannii* strain SK17-S

Figure 2.4 Tandem mass spectrometry of AGIYDPK^{pr}MMNFLK peptide from *Acinetobacter baumannii* strain **A**) SK17-R and **B**) SK17-S. The propionylated peptide from AdeT1 protein is found in both the imipenem-resistant and imipenem-susceptible strain. Reproduced from Barlow *et al.* with permission.³⁷⁰

While the structure of the *E. coli* membrane fusion protein AcrA has been solved,³⁶⁴ AdeT1 has low sequence similarity (24.4%) and identity (16.5%) with AcrA (**Figure 2.5**). Despite this low similarity, it is reasonable to assume based on the alignment that the general orientation of both proteins in relation to the outer membrane protein and the pump protein may be similar. The equivalent residue to Lys280 of AdeT1 is Val359 of AcrA, which is located in close proximity to the pump protein, AcrB, and may also be anchored in the inner membrane (**Figure 2.5**). If Lys280 of AdeT1 is similarly located in close proximity to the pump protein of its own RND-type pump complex and/or the inner membrane, propionylation may interfere with such interactions. Despite the uncertainties around the location of Lys280 in the tertiary structure of AdeT1, as the protein has a key role in multidrug resistance in *A. baumannii*,³⁵³ it is possible that propionylation of this protein may have regulatory effects on antimicrobial resistance.

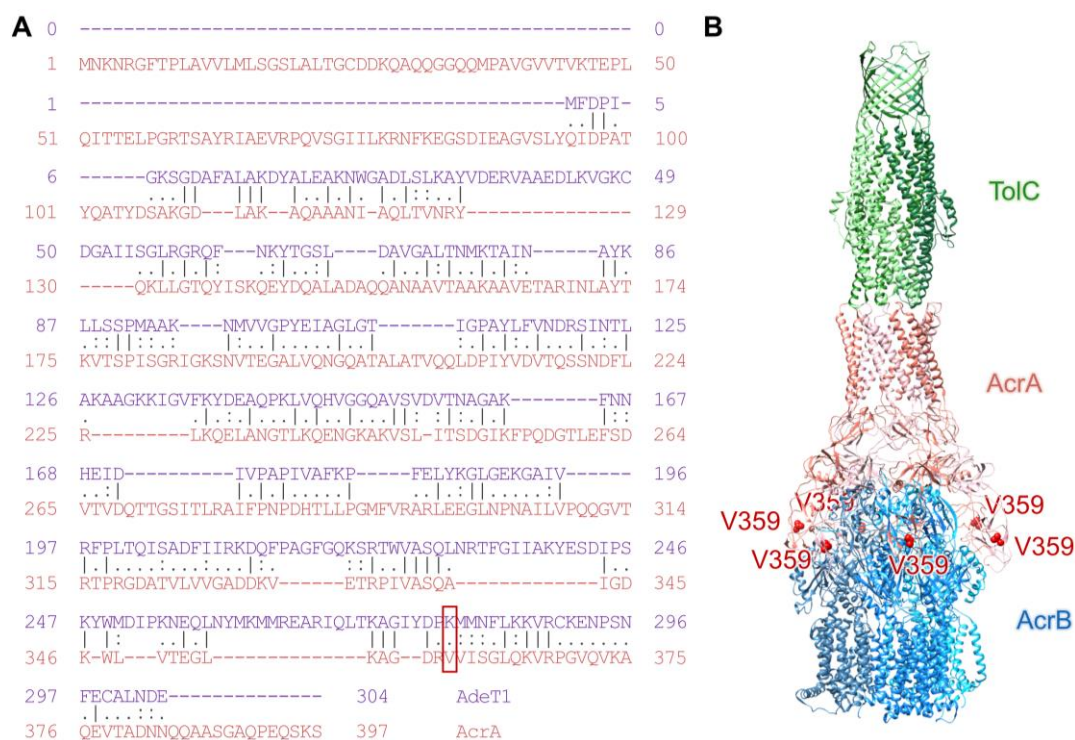


Figure 2.5 Alignment of AdeT1 with AcrA. **A** Pairwise sequence alignment of *A. baumannii* AdeT1 with *E. coli* AcrA.³⁷¹ The sequences have 16.5% identity and 24.4% similarity. A dash (-) represents mismatch or gap in the sequence, one dot (.) indicates a small positive similarity score between residues, two dots (:) represent a positive similarity score greater than 1, while a line (|) indicates that an identity has the same residue in both sequences. A red box highlights Lys280 in AdeT1 and the equivalent residue in AcrA, Val359. **B** Structure of *E. coli* RND-type efflux pump AcrAB-TolC.³⁶⁴ Val359 of AcrA is annotated in red.

2.2.5 Characterising the effects of PTMs on efflux pump function

When investigating the effects of post-translational modification on efflux pump function *in vivo*, there are several factors to be considered. Ideally, to obtain the most obvious presentation of any change in efflux pump function, all or most of the protein should be modified. While ensuring the protein of interest undergoes complete modification, this must be targeted, otherwise any observed effects may be the result of global protein modifications rather than the effect of a singular protein. Unnatural amino acid incorporation *via* genetic code expansion fulfils both these criteria, as only the protein of interest is modified in a targeted, site-specific manner.²⁹⁶ However, genetic code expansion has been primarily developed in *E. coli*, and has not been established in *A. baumannii*. In *E. coli*, genetic code expansion has been well documented as a successful tool for incorporating unnatural amino acids and has already been successfully used with propionyl-lysine.^{372, 373} While it may be possible to modify existing systems for use in *A. baumannii*, an alternative option is to characterise the protein heterologously in *E. coli*.

As mentioned, AdeT1 is heterologously functional in *E. coli*, where it increases resistance to a range of antimicrobials, and *E. coli* has frequently been used to characterise antibiotic resistance proteins from other species.^{353, 355-357} This provides several other advantages. For example, if propionylated AdeT1 (AdeT1^{Pr}) is expressed in a heterologous host, it is less likely that the cell will have innate mechanisms to recognise the protein and depropionylate it compared to if it were expressed in *A. baumannii*. Further, such experiments can be carried out in commensal laboratory *E. coli* strains which are safer and easier to handle than *A. baumannii*. Therefore, propionyl-lysine will be incorporated into AdeT1 *in vivo* in *E. coli* (**Figure 2.6**). Then, characterisation of the effect of the modification on efflux pump function will be carried out *via* ethidium bromide efflux assays and minimum inhibitory concentration testing.

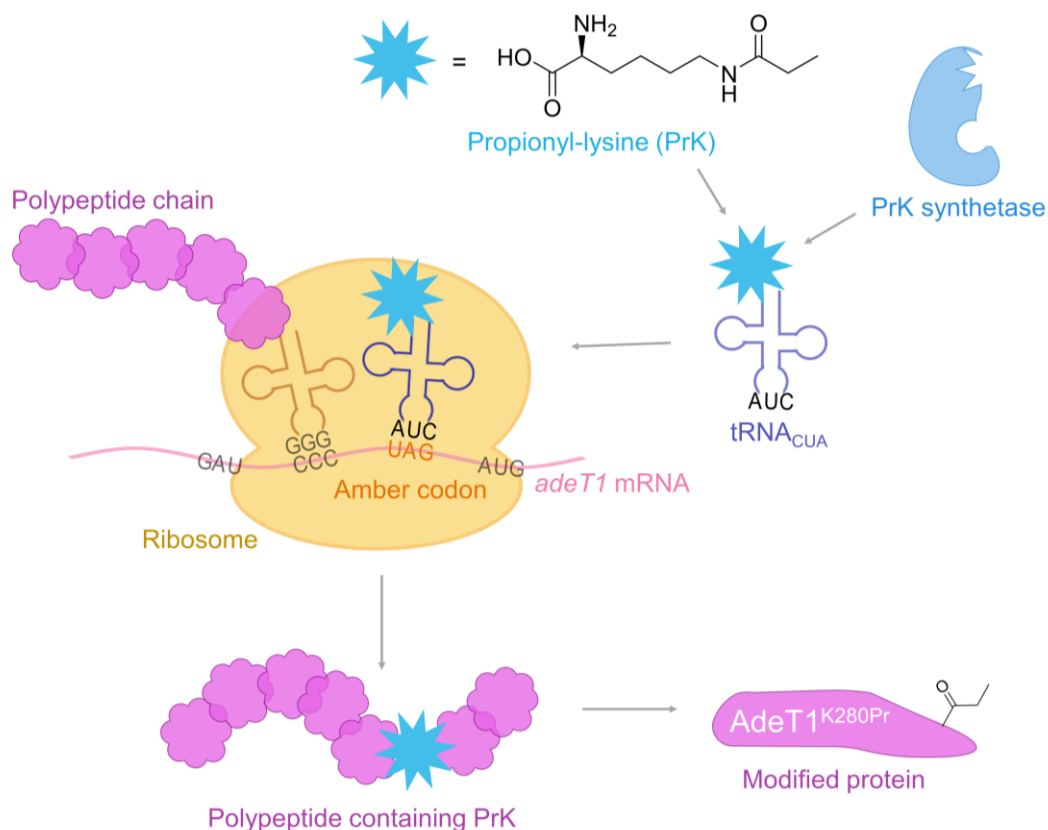


Figure 2.6 Schematic depicting incorporation of propionyl-lysine into position 280 of *A. baumannii* AdeT1 protein *in vivo* in *E. coli*. Mutation of the position encoding lysine 280 into TAG in the *adeT1* gene results in mRNA containing the amber codon UAG at the desired position. An orthogonal tRNA_{CUA} and tRNA synthetase pair are provided on a plasmid. When the cell growth media is supplemented with propionyl-lysine, the synthetase acylates the tRNA with propionyl-lysine and decodes the amber stop codon when *adeT1* tRNA is translated by the ribosome. The resulting protein, AdeT1^{K280Pr}, contains propionyl-lysine at position 280.

2.2.6 Assessing efflux pump activity

To confirm that AdeT1^{Pr} remains capable of forming an RND-type pump complex, assays to confirm efflux pump activity will be undertaken. Ethidium bromide is a well-known substrate of various efflux pumps and is commonly used in assaying efflux pump activity.³⁷⁴⁻³⁷⁶ In such purposes, it is particularly suitable as probe because it emits only weak fluorescence in aqueous solution whereas it becomes strongly fluorescent in a hydrophobic environment. In efflux pump assays, these qualities result in weak fluorescence when ethidium bromide is outside the cell and greatly increased fluorescence when ethidium bromide occupies the periplasmic space or is bound to DNA.^{375, 377} Consequently, ethidium bromide can be used for monitoring the activity of efflux pumps in living cells in real time. In such assays, cells are grown to

exponential phase before incubation with ethidium bromide under conditions which minimise efflux pump activity, such as the presence of an efflux pump inhibitor, the absence of glucose and a lowered temperature, e.g. 25 °C. Efflux pump activity is then restored by exchanging cells into fresh solution supplemented with glucose and incubation at 37 °C.³⁷⁸ Ethidium bromide efflux, and therefore efflux pump activity, can then be measured by monitoring the ethidium bromide fluorescence of the sample. This is most readily achieved by measuring fluorescence on a plate reader over time.

Once complex formation is confirmed, minimum inhibitory concentration (MIC) analysis will be employed to determine any effects of lysine propionylation on the antimicrobial resistance conferred by AdeT1 (**Figure 2.7**). MIC testing is an established procedure for determining the susceptibility of bacteria to antimicrobials *in vitro*.^{379, 380} A series of tubes or plates with varying concentrations of antimicrobials are prepared as broth or agar formulations. Then, a standardised amount of bacteria at low optical density is used to inoculate the conditions before incubation at 35 ±2 °C. Inhibition of growth is observed visually to determine the minimum concentration of antibiotic required. Usually, MIC testing is performed to determine the resistance of a species or strain of bacteria to certain antimicrobial agents. To determine the effects of a single protein on antimicrobial susceptibility, MIC testing can be used with strains where the gene encoding the protein of interest has been knocked out, or is provided on an expression vector.^{353, 355, 357, 381}

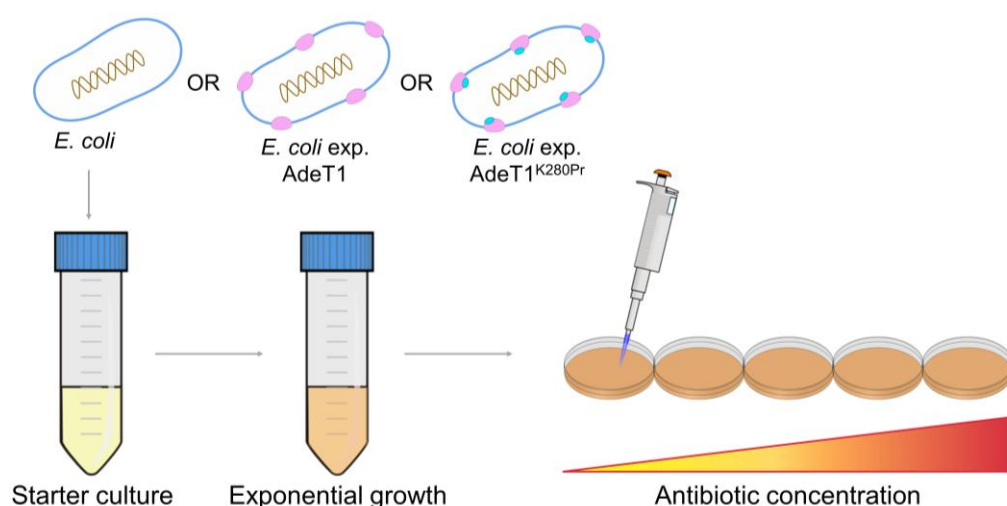


Figure 2.7 Investigating the effect of propionylation at lysine 280 of AdeT1 on minimum inhibitory concentration (MIC). Cultures containing either wildtype *E. coli* or *E. coli* expressing (exp.) AdeT1 or propionylated AdeT1 (AdeT1^{K280Pr}) are grown to the exponential phase before being plated on agar plates containing increasing concentrations of a test antibiotic or antimicrobial.

2.3 Aims and objectives

Here, the aim is to determine the effect of a protein post-translational modification, lysine propionylation, on the antimicrobial resistance protein AdeT1. To achieve this goal, the protein of interest will be provided to the antibiotic hypersusceptible *E. coli* strain KAM32 on an expression vector as reported by Srinivasan *et al.*³⁵³ Genetic code expansion for unnatural amino acid incorporation will be employed to insert propionyl-lysine at position 280 of AdeT1 protein. The formation of a functioning efflux pump will then be confirmed with ethidium bromide efflux assays. Finally, the cells expressing AdeT1 with propionylation at this lysine residue (AdeT1^{K280Pr}) will undergo MIC testing, allowing the functional characterisation of this PTM on antimicrobial resistance. Specific objectives are:

1. To establish an *E. coli* assay for determining the minimum inhibitory concentration upon AdeT1 expression.
2. To confirm that AdeT1^{Pr} is capable of complex formation *in vivo*
3. To investigate the effect of propionylation at Lys280 on bacterial growth in the presence of antibiotics

2.4 Results

2.4.1 Establishing an AdeT1 bioassay

Production of AdeT1 was reported to increase the resistance of *E. coli* KAM32 to various antimicrobial agents.³⁵³ Specifically, *E. coli* KAM32 expressing *adeT1* were demonstrated to have up to 6- and 5-fold higher MIC values for erythromycin and chloramphenicol, respectively, when compared to *E. coli* KAM32 that do not produce AdeT1. Therefore, this MIC assay could serve as an ideal means to characterise the effect of Lys280 propionylation on AdeT1 protein function.

Expression of AdeT1 with an inducible promoter in *E. coli* KAM32

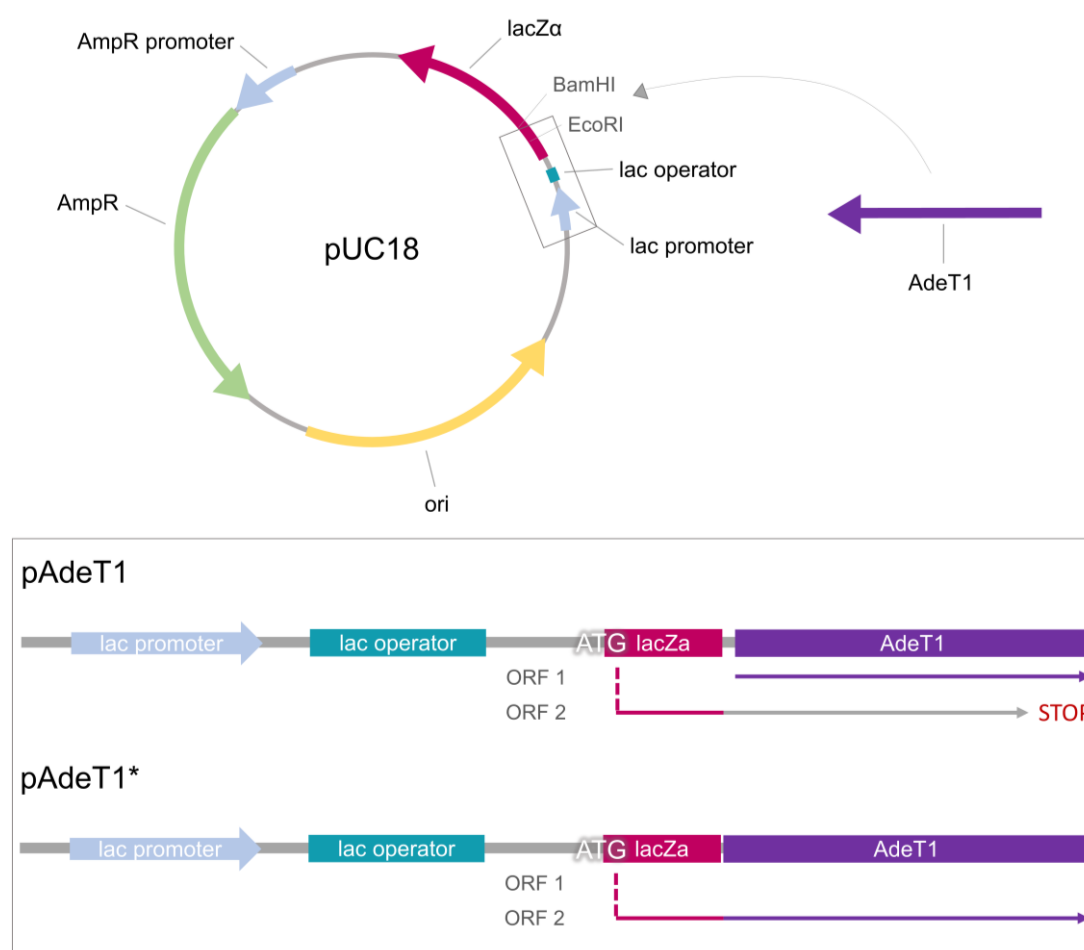


Figure 2.8 Cloning of pAdeT1 as described by Srinivasa *et al.*³⁵³ The *adeT1* gene fragment was inserted into pUC18 digested with restriction enzymes BamHI and EcoRI. An enlarged section of the plasmid (in box) highlights that the *adeT1* gene is inserted into a different ORF to the *lacZα* gene and is not transcribed. Another plasmid, pAdeT1*-His6, was constructed in a similar manner, but with the *adeT1* gene in frame with *lacZα*.

The *adeT1* gene was cloned into a pUC18 vector to construct pAdeT1 as described in the literature (**Figure 2.8**).³⁵³ As the *adeT1* gene in pAdeT1 is controlled by the lac promoter with a downstream lac operator, it was expected that gene expression would be observed upon addition of IPTG into the bacterial culture. However, no prominent band at the expected size (ca. 33.4 kDa) was observed in SDS-PAGE (**Figure 2.9**).

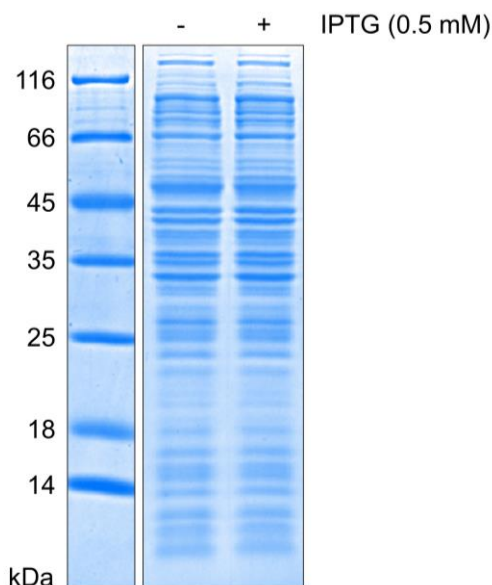


Figure 2.9 SDS-PAGE analysis of cell lysate from *E. coli* BL21(DE3) containing pAdeT1. Cells were cultured to A_{600} 0.6, when half of the culture was induced with 0.5 mM IPTG. Samples were taken after 18 hours induction at 20 °C. A band at ca. 33.4 kDa, the expected molecular weight of AdeT1 protein, is not observed.

Sequence analysis of pAdeT1 indicated that the *adeT1* gene was not in frame with the start codon (**Figure 2.8**). The *adeT1* sequence begins with GTG. This codon can be interpreted as a start codon, as happens in less than 5% of proteins in *A. baumannii*³⁸² and 14% in *E. coli*.³⁸³ However, an ATG codon lies 20 bp upstream of *adeT1*, initiating the now disrupted *lacZa* gene. This sequence is much more likely to be interpreted as a start codon, is in a different open reading frame to the *adeT1* gene and results in a premature stop codon after translation of 20 amino acids. Therefore, it is unlikely that the *adeT1* gene was translated from this construct.

Consequently, it became important to verify if pAdeT1 plasmid can result in production of AdeT1 protein. Detection of messenger RNA is not suitable for this purpose, as although the *adeT1* gene may be transcribed into mRNA, translation might start further upstream and in a different ORF to the *adeT1* gene. Therefore, it is necessary to analyse production at the protein level. As no protein could be detected by SDS-PAGE, a more sensitive technique such as immunoblot is required.

However, anti-AdeT1 antibodies are not commercially available. Therefore, a hexahistidine (His6) tag was inserted at the C-terminus of *adeT1* to produce pAdeT1-His6, and protein production was detected through this tag *via* anti-His antibodies. However, no protein could be detected by immunoblotting (**Figure 2.10**). Hence, it was concluded that the literature reported plasmid, pAdeT1, is not functional for production of AdeT1 protein. Instead, an alternative plasmid, pAdeT1*-His6, was constructed. This plasmid is similar to the literature reported pAdeT1, except the *adeT1* gene is placed in frame with the disrupted *lacZa* start codon and a His-tag is present on the C-terminal of *adeT1* (**Figure 2.8**). Immunoblotting with anti-His6 antibody clearly indicated the production of AdeT1 protein from pAdeT1*-His6 plasmid upon IPTG induction (**Figure 2.10**).

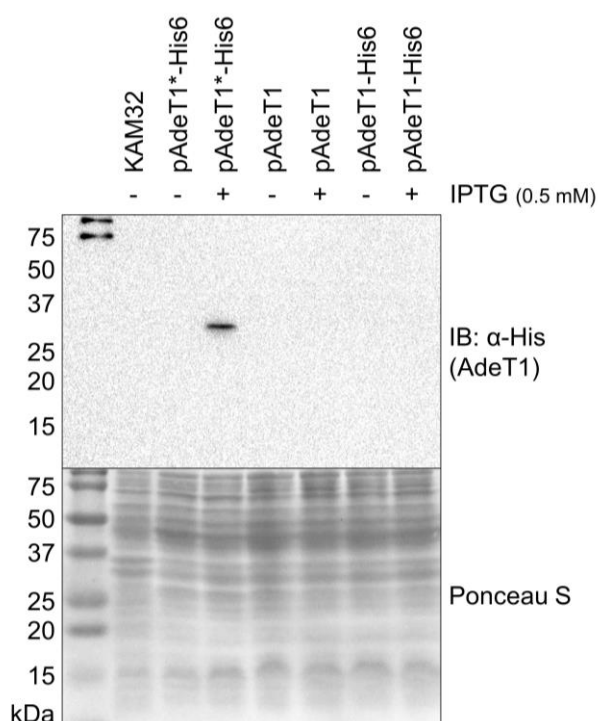


Figure 2.10 Immunoblot analysis of AdeT1 production in *E. coli* KAM32 from three plasmids. The pAdeT1 plasmid was constructed as described in the literature³⁵³ while pAdeT1-His6 contains a 6x Histidine tag on the C terminus of the protein encoding gene. Plasmid pAdeT1*-His6 is a similar construct, with the *adeT1* gene in frame with a start codon and with a 6x Histidine tag on the C-terminus. Cells were cultured until A_{600} 0.6, then divided into 2 halves, and 1 half induced with 0.5 mM IPTG. Samples were taken after 2 hours further incubation at 37 °C. Expression of AdeT1 was only observed from the pAdeT1*-His6 plasmid, when induced with 0.5 mM IPTG. Protein was detected through the 6x Histidine tag on the C-terminus.

Determining MIC using liquid culture

After confirming successful AdeT1 production in *E. coli* KAM32 with pAdeT1*-His, MIC testing was proceeded with. Before progressing with the incorporation of propionyl-lysine, it was particularly important to confirm the resistance conferred by AdeT1 protein in *E. coli*, due to the initial difficulties encountered when replicating the previous study.

MIC testing entails the dilution of cells to low optical density before addition of antibiotics to the culture and further incubation.³⁷⁹ This permits clear discrepancy between growth or inhibition of growth of bacterial cultures. Cells are usually cultured in low volumes, such as 100 μ L, for easier replication and to allow multiple antibiotics to be tested simultaneously, e.g. in a 96 well plate. This methodology results in A_{600} measurements being obtained from both plate readers and spectrophotometers at varying stages of growth. As different machines may give different values in absorbance, it is necessary to generate a calibration curve for comparison of values.³⁸⁴ Therefore, for accurate and comparable analysis of cell growth, a standard curve of A_{600} readings was generated from a serially diluted *E. coli* KAM32 culture measured with both a spectrophotometer and a plate reader (**Figure 2.11**).

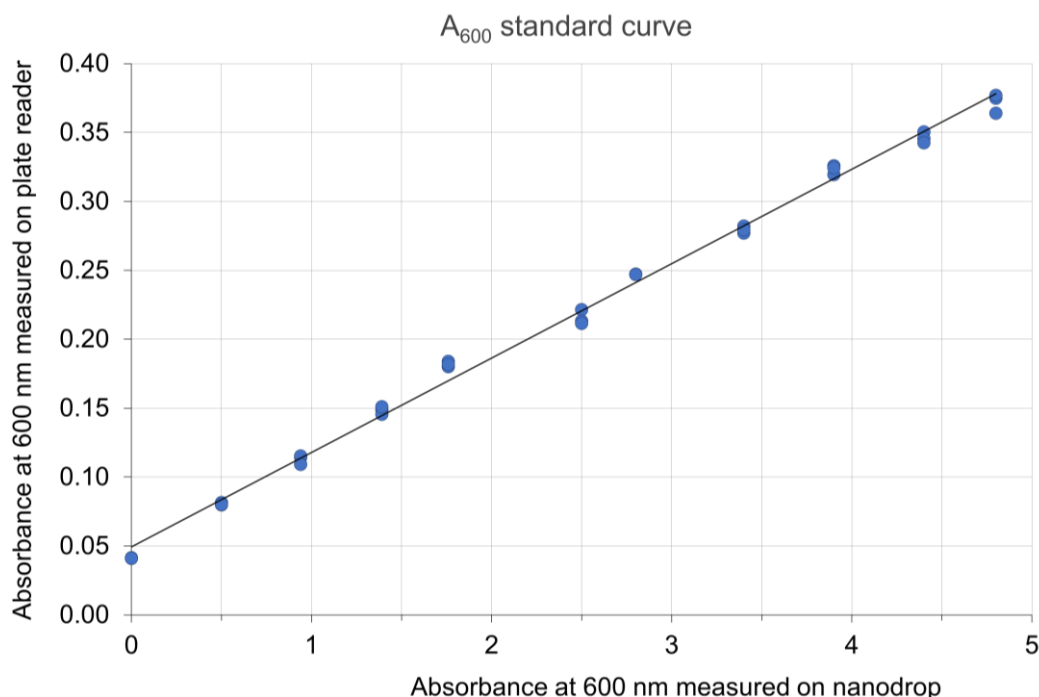


Figure 2.11 A_{600} standard curve for *E. coli* KAM32 cells. Cell densities were determined by measuring 1 mL of culture at 600 nm using a NanoDrop One (ThermoFisher). Three technical repeats (3x 100 μ L) of each culture were then plated in a transparent 96 well plate and measured on a Victor X (Perkin Elmer) plate reader using the A_{600} protocol (CW-lamp OG590, filter B7) with 5 seconds shaking before measurement. Each data point represents one plate reader measurement.

Using pAdeT1*-His6, preliminary MIC analysis with chloramphenicol was performed as described in the literature.³⁵³ However, no difference in MIC values was observed for cells expressing AdeT1 protein versus those in which expression had not been induced (**Table 2.1**). As pAdeT1*-His6 contains a histidine tag, and AdeT1 does not in nature, I wondered whether the histidine tag was interfering with AdeT1 folding or RND-pump complex formation. To this end, pAdeT1*, a construct where the *adeT1* gene is in a translated reading frame but does not contain a C-terminal histidine tag, was cloned. The microdilution MIC assays were repeated, but no difference between KAM32 cells expressing pUC18, pAdeT1* or pAdeT1*-His6 was found (**Figure 2.12**). Further, on probing for AdeT1 protein in cultures after MIC testing, although AdeT1 protein was observed in cells after IPTG induction, cells which had been subjected to dilution and growth in the presence of chloramphenicol had no detectable AdeT1 expression (**Figure 2.13**).

Table 2.1 Preliminary MIC results for *E. coli* KAM32 cells expressing pAdeT1*-His6. Cells were cultured until A_{600} 0.6, then split into 2 halves, and 1 half induced with 0.5 mM IPTG. Cultures were incubated for 2 hours at 37 °C, then diluted to A_{600} 0.01 into MHB containing various concentrations of chloramphenicol and incubated for 18 hours at 37 °C. Absorbance at 600 nm was recorded on a Victor X (Perkin Elmer) plate reader (CW-lamp OG590, filter B7) and converted to values equivalent to the plate reader measurements. Such values demonstrate no difference in the MIC when protein expression is or is not induced with IPTG. The results shown are an average of 2 independent transformations.

Chloramphenicol ($\mu\text{g/mL}$)	A_{600}							
	0	0.05	0.1	0.2	0.4	0.8	1.6	3.2
NO IPTG	2.97	3.00	2.42	0.00	0.00	0.00	0.00	0.00
0.5 mM IPTG	2.35	2.46	1.13	0.00	0.00	0.00	0.00	0.00

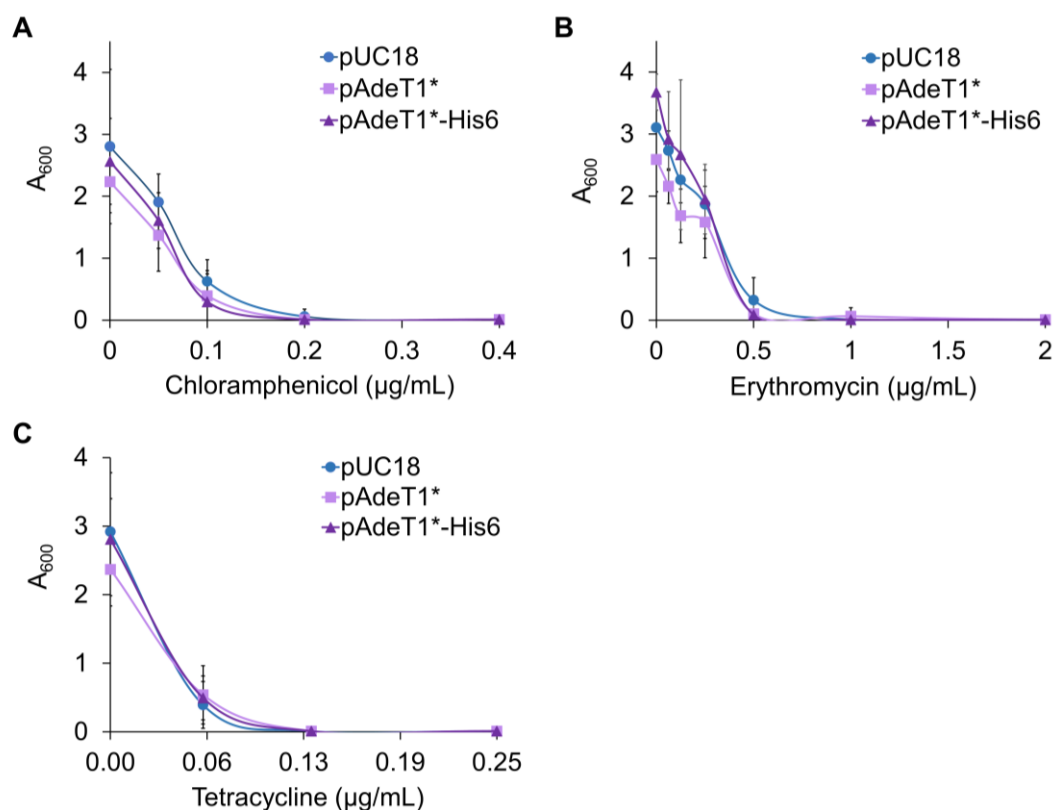


Figure 2.12 Preliminary MIC test of KAM32 cells expressing pUC18, pAdeT1* or pAdeT1*-His6. Cells were grown to A_{600} 0.6 before induction with IPTG. 1 hour post-induction, cells were diluted into fresh media containing various concentrations of **A** chloramphenicol, **B** erythromycin or **C** tetracycline according to CLSI standards. After overnight incubation, cell growth was analysed through absorbance at 600 nm on a plate reader.

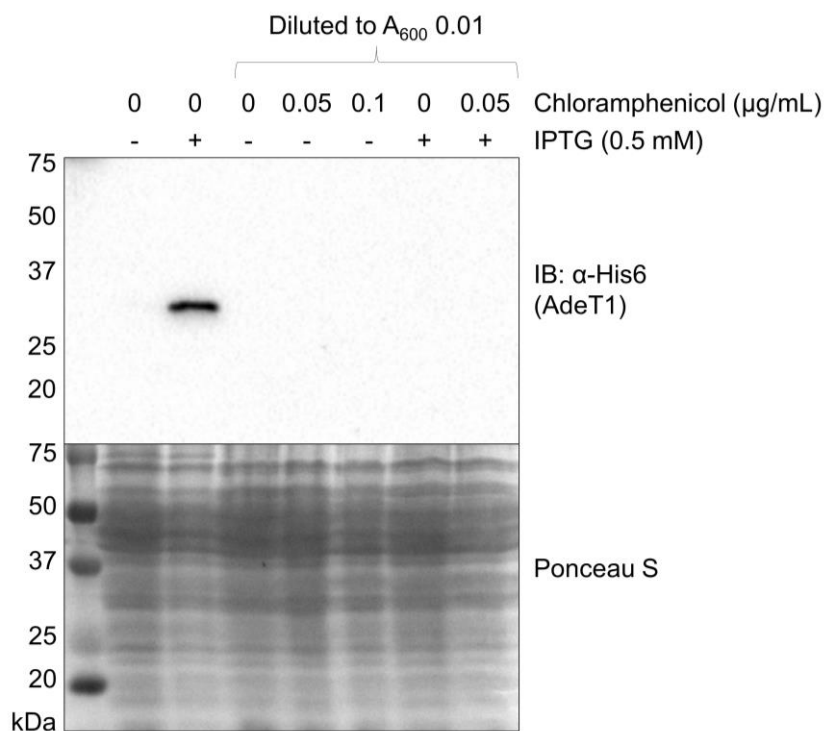


Figure 2.13 Immunoblot analysis of AdeT1 production during preliminary MIC test with chloramphenicol of *E. coli* KAM32 cells with or without induction of pAdeT1*-His6 (**Table 2.1**). Expression of AdeT1 was detected through the 6x Histidine tag on the C-terminus. AdeT1 protein was only detected in the original culture when induced with 0.5 mM IPTG, protein production was not maintained when this culture was diluted to A_{600} 0.01 and incubated overnight with or without chloramphenicol.

Further scrutiny of post-induction cultures revealed that dilution of cells expressing pAdeT1*-His6 into fresh IPTG-containing media does not reproducibly maintain the production of AdeT1 protein. This lack of reproducibility is independent of the dilution factor (to A_{600} 0.01 or 0.001), culture volume, or incubation container (*i.e.* 5 mL culture in a 50 mL falcon tube, 200 μL culture in an Eppendorf tube, or 100 μL culture in a 96 well plate) (**Figure 2.14**).

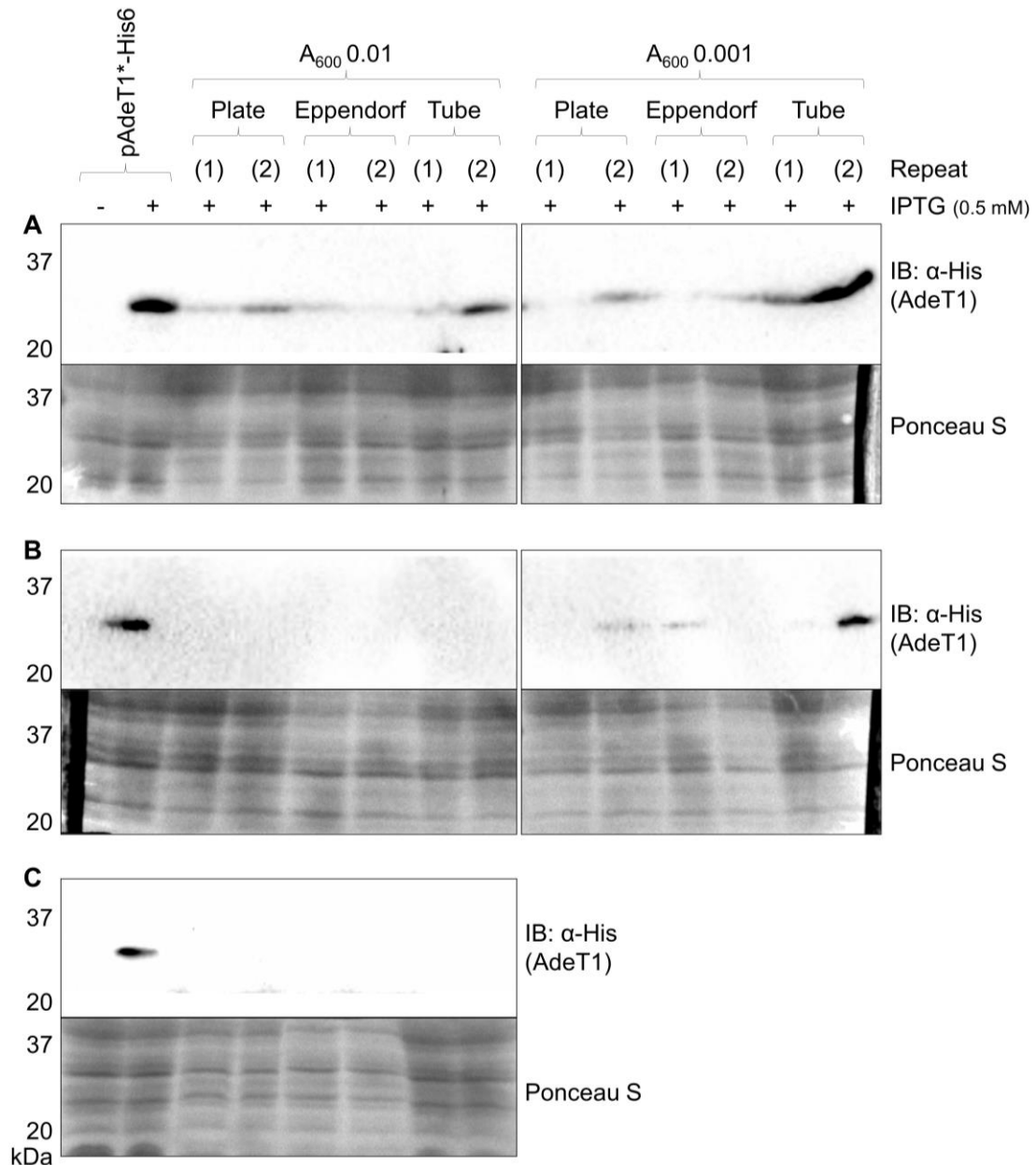


Figure 2.14 Immunoblot analysis of production of AdeT1 when diluted to two cellular densities (A_{600} 0.01 or 0.001). Protein was detected through the 6x Histidine tag on the C terminus. Cultures were grown until A_{600} 0.6 before induction with 0.5 mM IPTG. 2 hours post-induction, samples of the induced culture (+) and a no IPTG control (-) were taken and diluted to A_{600} 0.01 or 0.001 in 100 μ L (96 well plate), 200 μ L (Eppendorf), or 5 mL (falcon tube). Three biological repeats, **A**, **B**, and **C**, were conducted on consecutive days. On the third day (**C**), no bacterial growth was observed when the culture was diluted to A_{600} 0.001.

Expression of AdeT1 from a pET vector in *E. coli* BL21(DE3)

Alongside protein production from diluted cultures being highly variable, the immunoblot signal observed from cultures which had been diluted to low A_s was considerably smaller than that obtained from the original culture. With the aim of increasing the amount of protein present after dilution and the hope that protein production may be more reproducible in a commercial expression vector, the *adeT1* gene was cloned into the common expression vector, pET28a. However, this expression vector relies on production of the bacteriophage T7 DNA polymerase, which is not present in *E. coli* KAM32. Nevertheless, this system allowed overexpression of AdeT1 protein in *E. coli* BL21(DE3) when induced with 0.5 mM IPTG as analysed by SDS-PAGE (**Figure 2.15**).

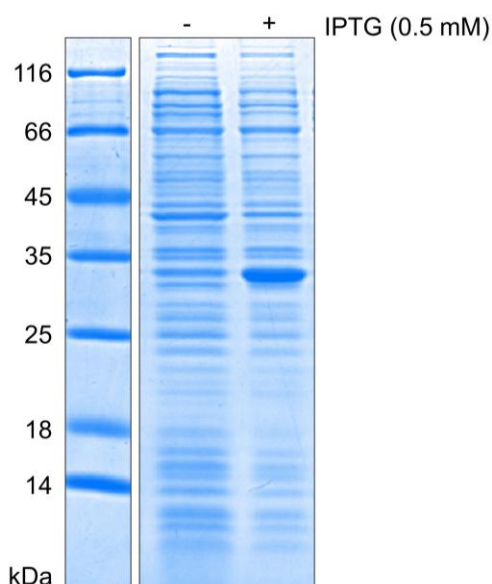


Figure 2.15 SDS-PAGE analysis of cell lysate from *E. coli* BL21(DE3) containing pET28a AdeT1-His6. Cells were cultured to A_{600} 0.6, when half of the culture was induced with 0.5 mM IPTG. Samples were taken after 18 hours induction at 20 °C. A band is observed at ca. 33.4 kDa, the expected molecular weight of AdeT1 protein.

Dilution of pET28a AdeT1-His6 into IPTG-containing solution

While expression of pET28a AdeT1-His6 resulted in a higher amount of protein production compared to pAdeT1*-His6, when cultures were diluted to low densities both protein production and bacterial growth were not reproducible. For example, when diluting cultures to an A_{600} of 0.001, bacterial growth was difficult to restore even in the absence of antibiotics. When diluting the culture to an A_{600} of 0.01, bacterial growth was consistently observed, but expression of AdeT1 was highly variable (**Figure 2.16**). This is an obvious problem for determining the effects of this protein on the minimum inhibitory concentration of antibiotics required.

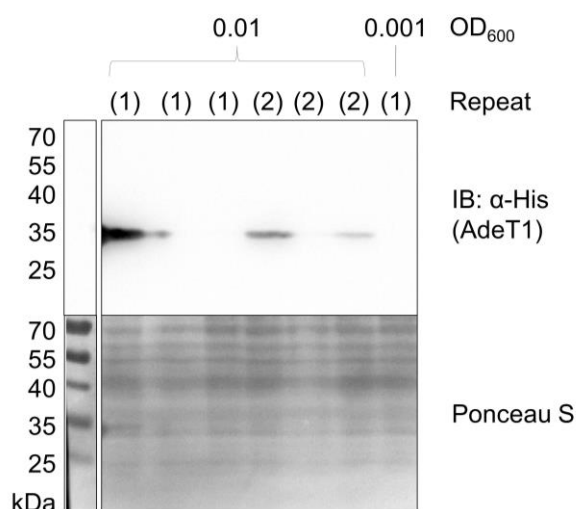


Figure 2.16 Western blot analysis of pET28a AdeT1-His6 expression after dilution to low cellular density. *E. coli* BL21(DE3) containing pET28a AdeT1-His6 were induced with 0.5 mM IPTG before dilution into MHB with 0.5 mM IPTG to A_{600} 0.01 and 0.001. Protein was detected through the 6x Histidine tag on the C terminus.

Dilution of pET28a sfGFP-His6 into IPTG-containing solution

To determine whether the highly variable protein expression observed when diluting bacterial cultures is unique to AdeT1 protein, or a more generalised phenomenon, dilution studies were performed using pET28a sfGFP-His6. Super-folded green fluorescent protein (sfGFP) is a convenient reporter, as expression can be measured through the fluorescence intensity of cultured cells. For dilution of post-induction cultures of *E. coli* BL21(DE3) expressing pET28a sfGFP-His6, the measured FI demonstrates an extremely variable range of protein production, from lower fluorescence than the non-induced cultures to relatively high fluorescence (**Figure 2.17**). Together, with the results of the experiments with cells producing AdeT1

protein, this data suggests that protein production from T7 and lac promoters is not reliably maintained after dilution of induced cultures to low cellular densities.

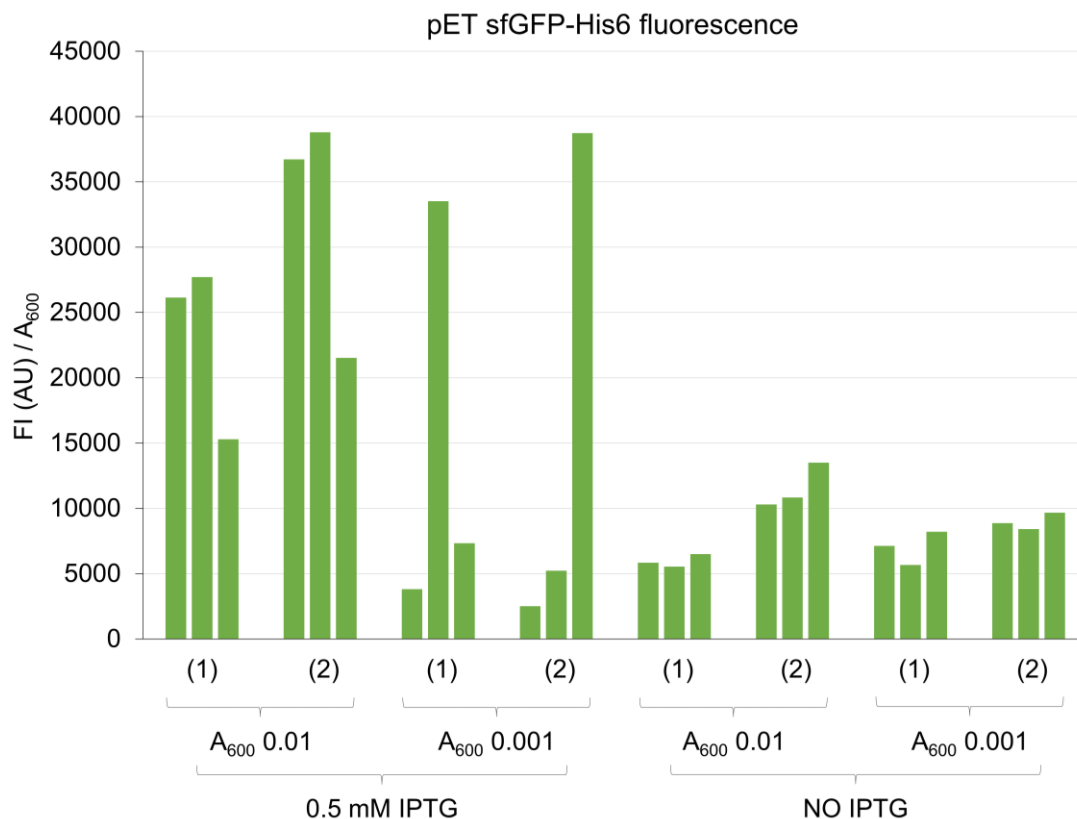


Figure 2.17 Fluorescence intensity of *E. coli* BL21(DE3) cells expressing pET28a sfGFP-His6 when diluted to A_{600} 0.01 or 0.001 into fresh IPTG-containing media, 1 hour post-induction with IPTG. Cells were then incubated for 18 hours before being pelleted and resuspended in PBS. Fluorescence intensity (FI) was measured with a FLUOstar (Optima) plate reader (ex 485 nm, em 520 nm, gain 804) and absorbance at 600 nm (A_{600}) was measured with a Victor X (Perkin Elmer) plate reader (CW-lamp OG590, filter B7). To normalise the FI relative to the cellular density, the FI in arbitrary units (AU) was divided by the A_{600} . For each condition, two independent transformations, (1) and (2), were diluted three times to produce three technical repeats (individual bars on chart). Expression of sfGFP is highly variable when cells are diluted to low A_{600} in IPTG-containing solutions.

Direct addition of chloramphenicol

Due to highly variable expression of AdeT1 protein in both pET28a and pUC18 vectors when diluted to low cellular densities, but consistent expression in liquid cultures after induction, an attempt was made to observe the effects on bacterial growth of adding chloramphenicol directly to liquid cultures 2 hours post-induction with IPTG. In contrast to the above dilution studies, expression of AdeT1 was

consistently maintained after overnight incubation with chloramphenicol in both pUC18 and pET28a constructs (**Figure 2.18** and **Figure 2.19**).

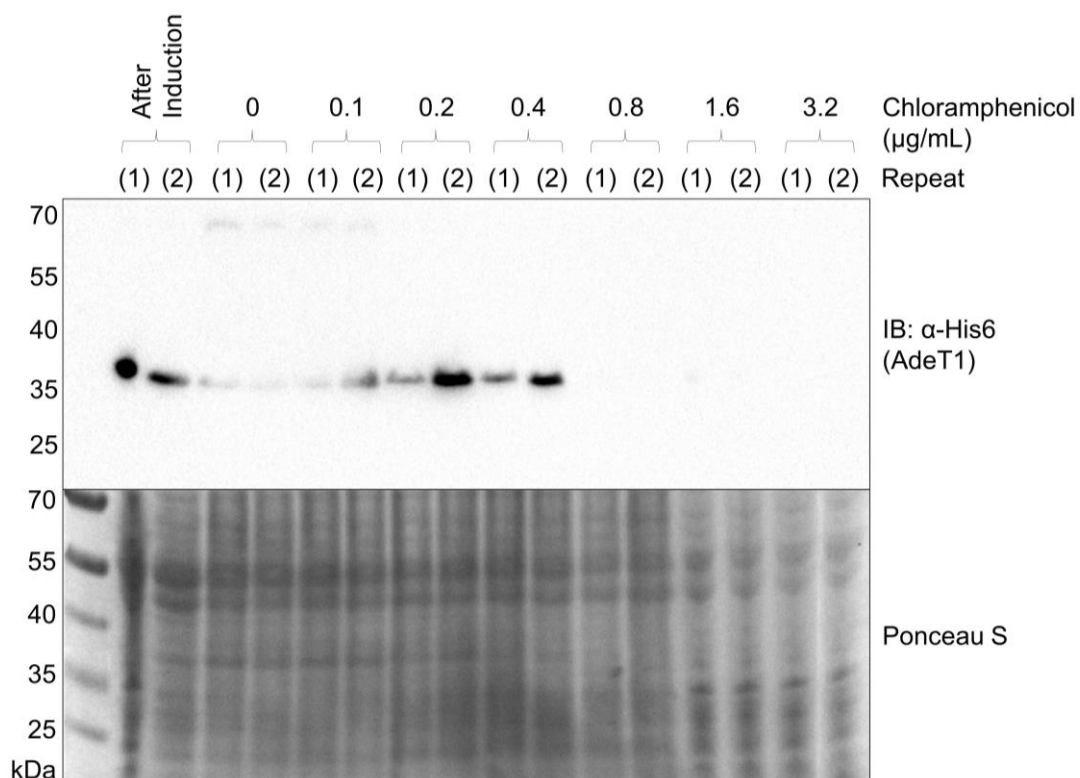


Figure 2.18 Immunoblot analysis of AdeT1 expression in liquid *E. coli* KAM32 pAdeT1*-His6 cultures to which varying concentrations of chloramphenicol have been added 2 hours post-induction with IPTG. Samples were taken after overnight incubation with chloramphenicol. Protein was detected through the 6x Histidine tag on the C terminus.

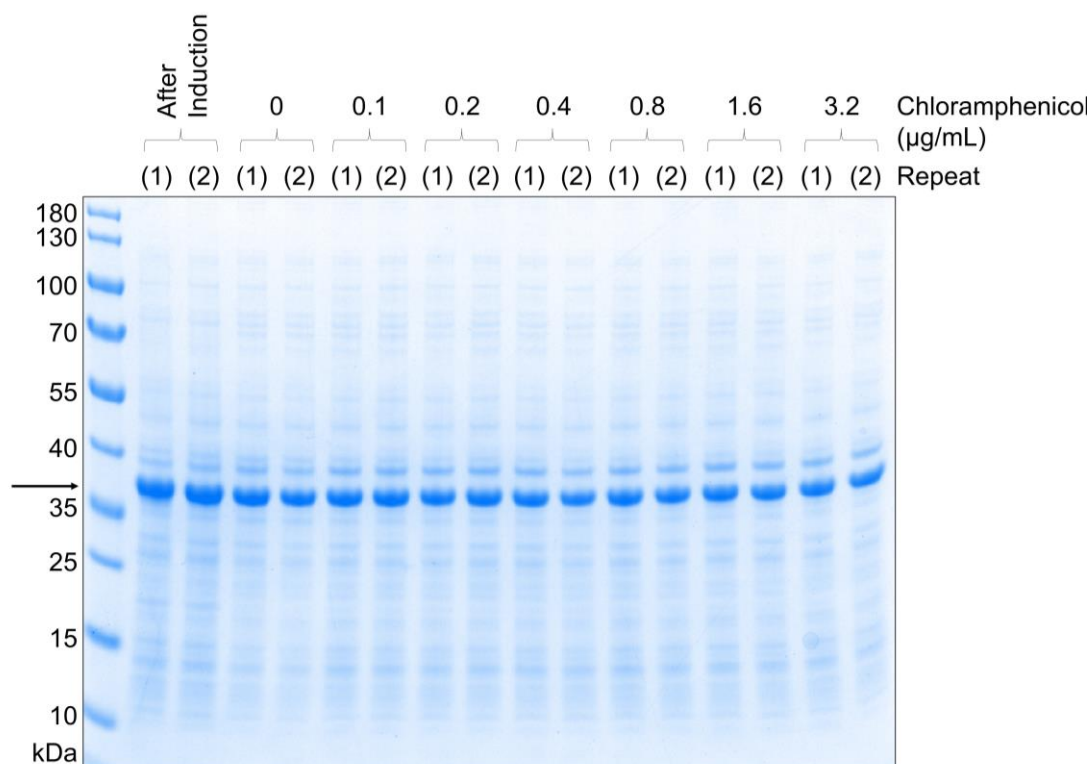


Figure 2.19 SDS-PAGE analysis of AdeT1 expression in liquid *E. coli* BL21(DE3) pET28a AdeT1-His6 cultures to which varying concentrations of chloramphenicol have been added 2 hours post-induction with IPTG. Samples were taken after overnight incubation with chloramphenicol. AdeT1 is visible as a band migrating slightly slower than the expected ca. 33 kDa, indicated by an arrow.

However, determining inhibition of bacterial growth from cultures with already high cellular densities proved difficult. As can be observed in **Figure 2.20** and **Figure 2.21**, the A_{600} of both cultures expressing pUC18 or pET28a control plasmids and experimental cultures expressing pAdeT1*-His6 or pET28a AdeT1-His6 reached different final A_{600} values, even when grown in the absence of chloramphenicol. For example, as observed in **Figure 2.20**, the control cultures grew to ca. A_{600} 1.25 in the absence of chloramphenicol, while the experimental cultures had a final A_{600} ca. 2.1.

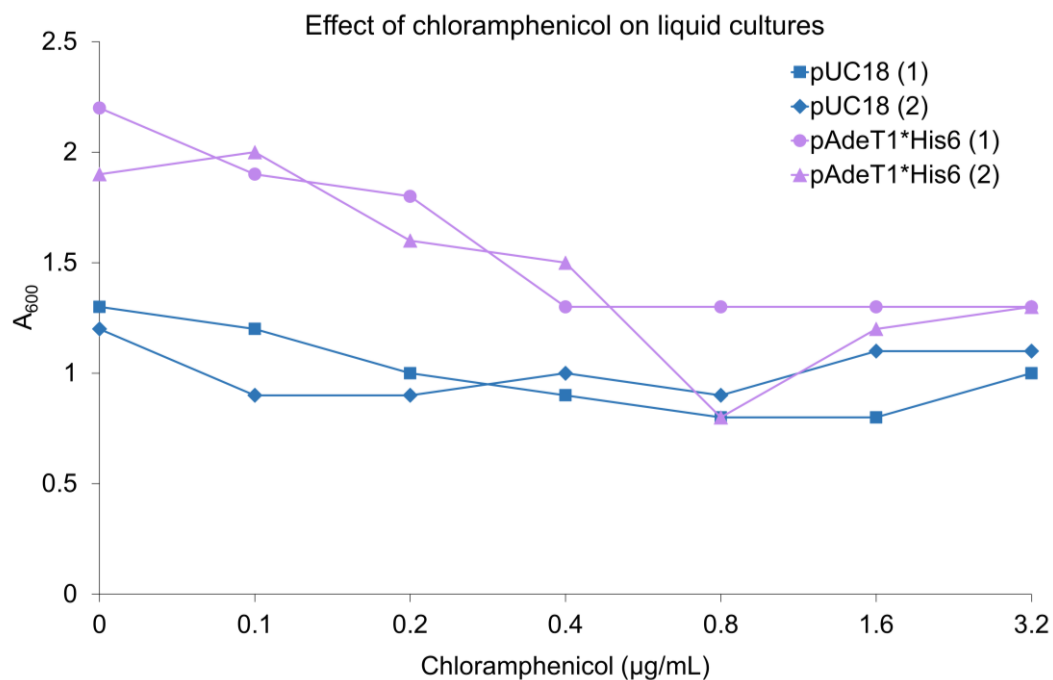


Figure 2.20 A_{600} measurements of cultures of *E. coli* KAM32 cells containing expression plasmid pAdeT1*-His6 or control plasmid pUC18 after overnight incubation in the presence of varying concentrations of chloramphenicol. Data from two independent transformations, (1) and (2), are shown. Inhibition of bacterial growth is difficult to determine as control cultures incubated in the absence of chloramphenicol reach different cellular densities and there is no clear cut off point for bacterial growth.

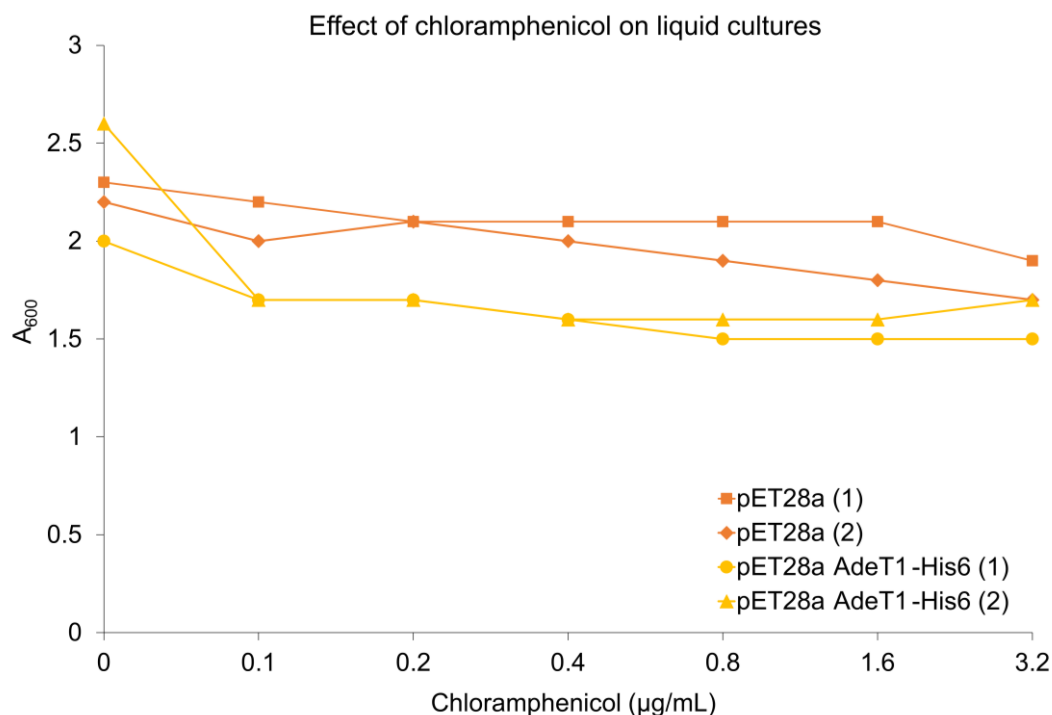


Figure 2.21 A_{600} measurements of cultures of *E. coli* BL21(DE3) cells containing expression plasmid pET28a AdeT1-His6 or control plasmid pET28a after overnight incubation in the presence of varying concentrations of chloramphenicol. Data from two independent transformations, (1) and (2), are shown. Inhibition of bacterial growth is difficult to determine as control cultures incubated in the absence of chloramphenicol reach different cellular densities and there is no clear cut off point for bacterial growth.

Expressing AdeT1 from a constitutively active promoter in *E. coli* KAM32

Due to the difficulties of maintaining protein production after dilution and determining inhibition of growth in cultures with high cellular densities, a new approach investigating whether constant expression of AdeT1 could be imposed, and whether this would allow AdeT1 expression from cultures diluted to low cellular densities was undertaken. To investigate this, the IPTG-induced lac or T7 promoters controlling AdeT1 expression would be replaced with constitutively active promoters. To easily verify whether constitutive expression of target protein is possible by this means, the gene encoding sfGFP was cloned downstream of various constitutively active promoters in pET21a vectors with the inducible T7 promoter removed.

Constitutively active super folder green fluorescent protein

Three constitutively active promoters were chosen to assess applicability for constitutive expression of proteins. The ampicillin resistance gene (AmpR) promoter is frequently used in bacterial expression plasmids for constitutive expression of the ampicillin resistance gene, encoding the β -lactamase enzyme. The LacI promoter is regularly used for constitutive expression of the lac repressor gene in pET expression systems. The LacUV5 promoter is a mutated version of the inducible lac promoter, containing 2 base pair mutations in the -10 hexamer region which enable stronger protein expression when compared with the original lac promoter. It is frequently used in recombinant protein expression whereby transcription of the target gene is induced with the addition of IPTG. I hypothesised that removal of the lac operon, where the lac repressor protein binds to inhibit transcription in the absence of an inducer molecule, would result in constitutive transcription of the gene of interest. Three constructs were created from pET21a vectors: pAmpR-sfGFP-His6, pLacI-sfGFP-His6, and pLacUV5-sfGFP-His6. Each contains one of the three promoters in replacement of the existing T7 promoter and *sfGFP* as the target gene.

Constitutive expression of sfGFP from these plasmids was analysed *via* fluorescence intensity, with all three promoters allowing constitutive production of the sfGFP protein (**Figure 2.22A**). The AmpR and LacUV5 promoters produced the highest fluorescence and therefore the most sfGFP protein. Fluorescence intensity was maintained after cultures were diluted to low cellular densities and re-cultured overnight (**Figure 2.22B**).

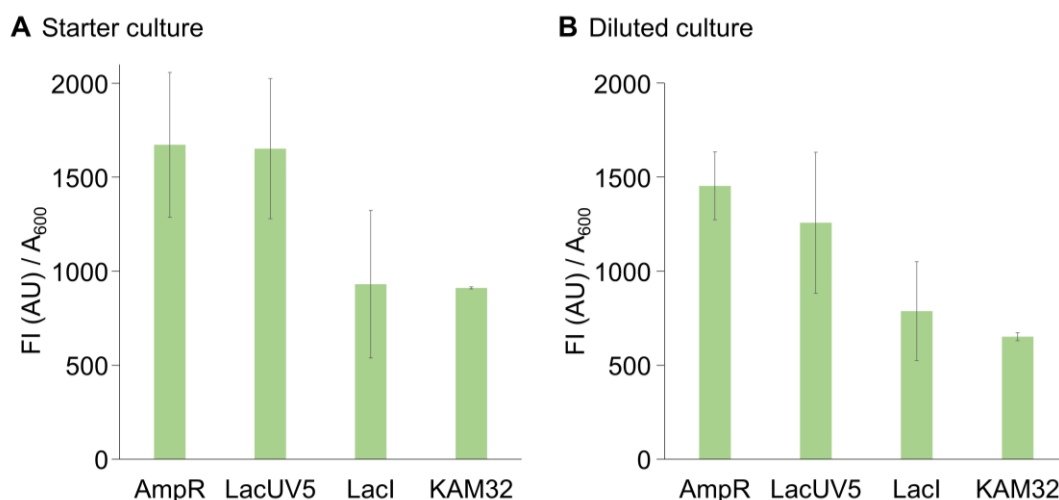


Figure 2.22 Fluorescence intensity (FI) of cells containing *sfGFP* under the control of three constitutive promoters: the ampicillin resistance gene promoter (AmpR); the LacUV5 promoter (LacUV5); or the Lac repressor promoter (LacI). FI was measured after incubation at 37 °C for 18 hours (**A**), and after dilution of the overnight culture to A₆₀₀ 0.01 and further incubation for 18 hours (**B**) using a FLUOstar (Optima) plate reader (ex 485 nm, em 520 nm, gain 804). Absorbance at 600 nm (A₆₀₀) was measured on a Victor X (Perkin Elmer) plate reader (CW-lamp OG590, filter B7). To normalise the FI relative to the cellular density, the FI in arbitrary units (AU) was divided by the A₆₀₀. Results shown are an average of two transformations, each with three technical repeats. The standard deviation is shown.

AdeT1 cannot be constitutively expressed

After demonstration that *sfGFP* can be constantly produced without induction under the control of constitutively active promoters, *adeT1* was subsequently cloned to replace *sfGFP* in the three vectors. All three constructs providing constitutive expression were chosen for continuation, as optimal levels of AdeT1 expression are not known. Endogenous *adeT1* expression in *A. baumannii* is likely to be relatively low, as suggested by the alternative start codon discussed earlier. However, when immediately replacing the *sfGFP* gene with *adeT1*, no expression of AdeT1 was observed under any of the promoters when analysed *via* immunoblot (**Figure 2.23**).

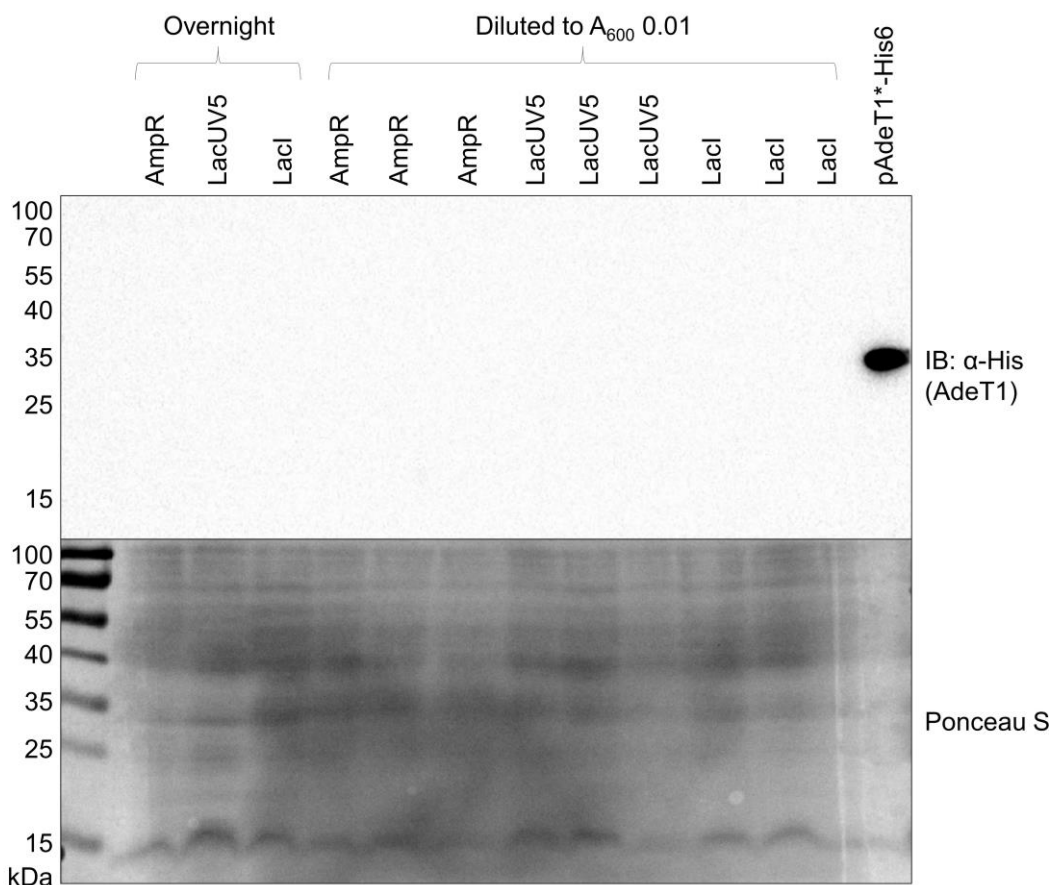


Figure 2.23 Immunoblot analysis of AdeT1 expression under the control of constitutively active promoters: ampicillin resistance gene promoter (AmpR), LacUV5 promoter, and the lac repressor gene promoter (LacI). A single colony was cultured overnight in MHB, then diluted to A_{600} 0.01 with three replicates and cultured overnight. Expression of AdeT1 was not observed through detection of the 6x Histidine tag on the C terminus under any condition.

Determining MIC using solid culture

As attempts to constitutively produce AdeT1 from cultures with low cellular densities proved unsuccessful, an alternative method of MIC analysis was explored. As AdeT1 expression from both pAdeT1*-His6 and pET28a AdeT1-His6 vectors is consistent post-induction, the agar dilution method³⁷⁹ was altered to exclude the dilution of cultures prior to MIC testing. Specifically, the A_{600} of cultures was measured 2 hours post-induction, before adjustment to A_{600} 4.0 by pelleting cells and resuspending in a smaller volume of fresh media. A defined amount of cells were then dropped onto LB agar plates containing 0.5 mM IPTG, antibiotics for plasmid selection, and varying concentrations of antimicrobials. Fortunately, with this method, AdeT1 protein was detectable by immunoblot after overnight incubation. This was true both of cultures of *E. coli* KAM32 cells expressing pAdeT1*-His6 (**Figure 2.25**, **Figure 2.27** and **Figure**

2.29) and *E. coli* BL21(DE3) cells expressing pET28a AdeT1-His6 (**Figure 2.32**, **Figure 2.34** and **Figure 2.36**). The MIC of chloramphenicol observed for *E. coli* KAM32 cells was 0.4 µg/mL for cells expressing pUC18 and 0.8 µg/mL for those expressing pAdeT1*-His6 (**Figure 2.24**). For erythromycin, the minimum concentration to inhibit growth was 4 µg/mL for both control and AdeT1 plasmids (**Figure 2.26**). For tetracycline, the MIC for both conditions was 0.5 µg/mL (**Figure 2.28**). For acridine orange, a toxic dye, cell growth was maintained with concentrations of acridine orange of more than 1 mg/mL for *E. coli* KAM32 cells (**Figure 2.30**). As cells were viable at this concentration of acridine orange, the minimum inhibitory concentration is arguably not relevant and was not determined. The data clearly demonstrate that expression of wildtype AdeT1 protein did not increase the minimum concentration of the compounds tested here.

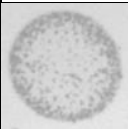
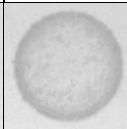
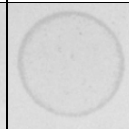
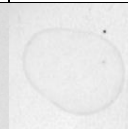

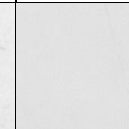

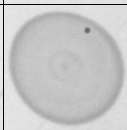

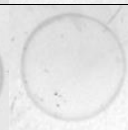

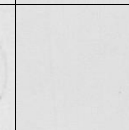
	Chloramphenicol (µg/mL)						MIC
	0	0.1	0.2	0.4	0.8	1.6	
pUC18							0.4
pAdeT1*-His6							0.8

Figure 2.24 Chloramphenicol MIC analysis of *E. coli* KAM32 carrying either pUC18 or pAdeT1*-His6. Cultures were grown to A_{600} 0.6 before induction with 0.5 mM IPTG. 2 hours post-induction, A_{600} of cultures were normalised to $\sim A_{600}$ 4.0 before 20 µL was dropped onto agar plates containing 0.5 mM IPTG, antibiotics for plasmid selection, and various concentrations of chloramphenicol. Plates were incubated at 37 °C overnight. The control and *adeT1*-containing plasmids show no difference in MIC for chloramphenicol. Data shown are representative of 6 biological repeats.

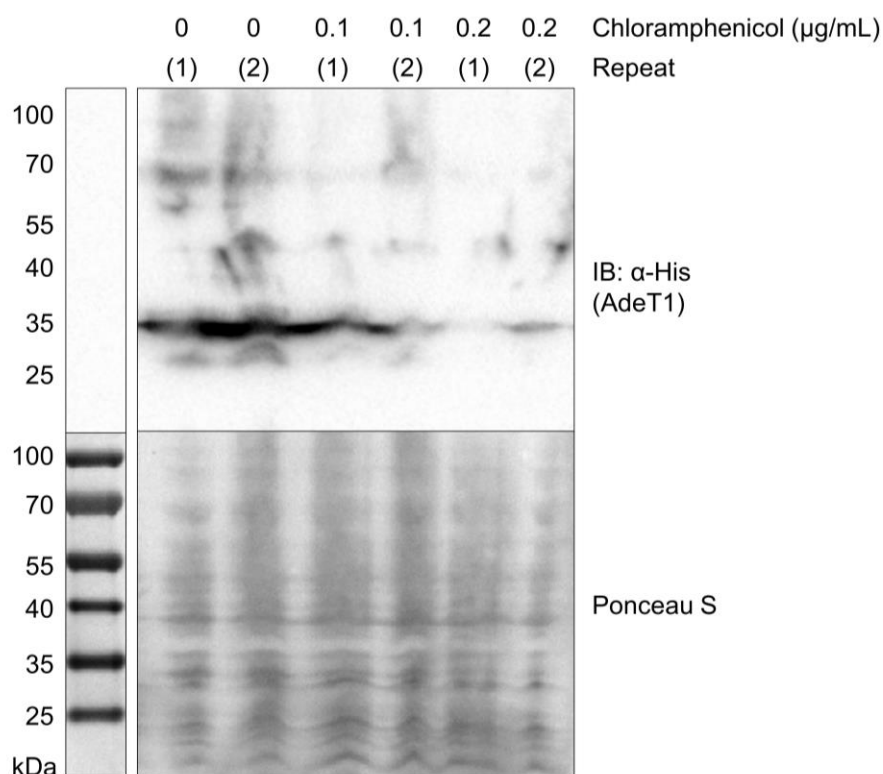


Figure 2.25 Immunoblot analysis of AdeT1 expression from *E. coli* KAM32 carrying pAdeT1*-His6 during MIC testing with chloramphenicol. Cultures were grown to A_{600} 0.6 before induction with 0.5 mM IPTG. 2 hours post-induction, A_{600} of cultures were normalised to $\sim A_{600}$ 4.0 before 20 μ L was dropped onto agar plates containing 0.5 mM IPTG, antibiotics for plasmid selection, and various concentrations of chloramphenicol. Plates were incubated at 37 °C overnight. Protein expression was detected through the 6x Histidine tag on the C terminus.

	Erythromycin (μg/mL)					
	0	10	20	40	80	MIC
pUC18						80
pAdeT1* His6						80

Figure 2.26 Erythromycin MIC analysis of *E. coli* KAM32 carrying either pUC18 or pAdeT1*-His6. Cultures were grown to A_{600} 0.6 before induction with 0.5 mM IPTG. 2 hours post-induction, A_{600} of cultures were normalised to $\sim A_{600}$ 4.0 before 20 μ L was dropped onto agar plates containing 0.5 mM IPTG, antibiotics for plasmid selection, and various concentrations of erythromycin. Plates were incubated at 37 °C overnight. The control and *adeT1*-containing plasmids show no difference in MIC for erythromycin. Data shown are representative of 6 biological repeats.

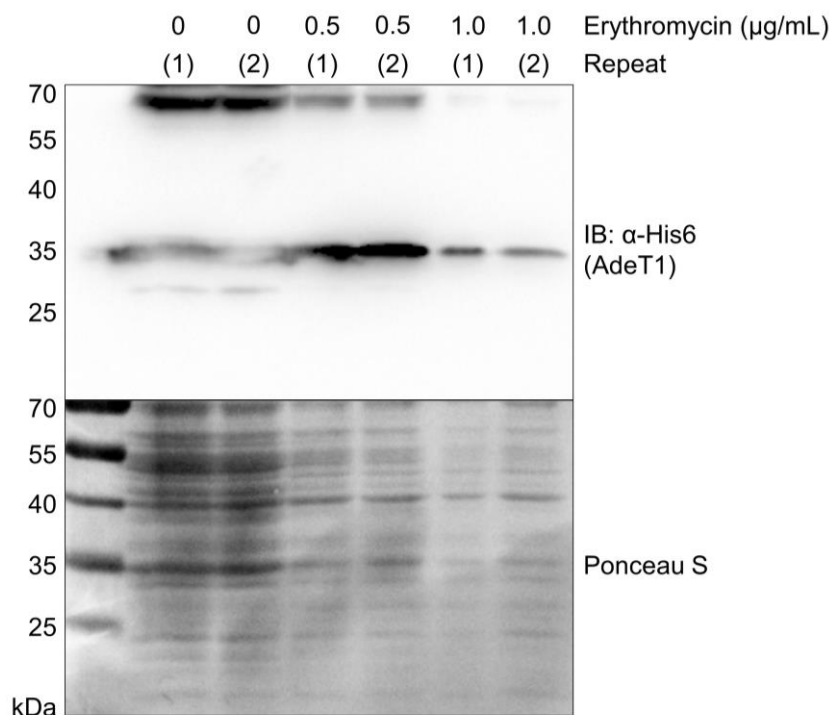


Figure 2.27 Immunoblot analysis of AdeT1 expression from *E. coli* KAM32 carrying pAdeT1*-His6 during MIC testing with erythromycin. Cultures were grown to A_{600} 0.6 before induction with 0.5 mM IPTG. 2 hours post-induction, A_{600} of cultures were normalised to $\sim A_{600}$ 4.0 before 20 μ L was dropped onto agar plates containing 0.5 mM IPTG, antibiotics for plasmid selection, and various concentrations of erythromycin. Plates were incubated at 37 °C overnight. Protein expression was detected through the 6x Histidine tag on the C terminus.

	Tetracycline (μ g/mL)						MIC
	0	0.125	0.25	0.5	1.0	2.0	
pUC18							0.5
pAdeT1* His6							0.5

Figure 2.28 Tetracycline MIC analysis of *E. coli* KAM32 carrying either pUC18 or pAdeT1*-His6. Cultures were grown to A_{600} 0.6 before induction with 0.5 mM IPTG. 2 hours post-induction, A_{600} of cultures were normalised to $\sim A_{600}$ 4.0 before 20 μ L was dropped onto agar plates containing 0.5 mM IPTG, antibiotics for plasmid selection, and various concentrations of tetracycline. Plates were incubated at 37 °C overnight. The control and *adeT1*-containing plasmids show no difference in MIC for tetracycline. Data shown are representative of 6 biological repeats.

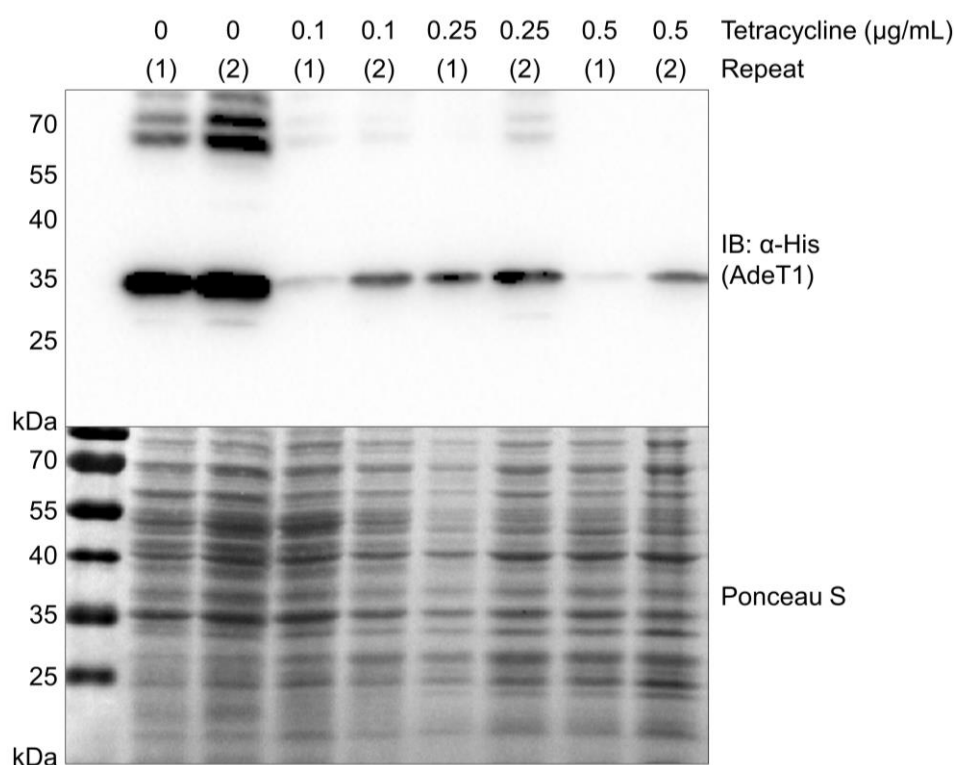


Figure 2.29 Immunoblot analysis of AdeT1 expression from *E. coli* KAM32 carrying pAdeT1*-His6 during MIC testing with tetracycline. Cultures were grown to A_{600} 0.6 before induction with 0.5 mM IPTG. 2 hours post-induction, A_{600} of cultures were normalised to $\sim A_{600}$ 4.0 before 20 μ L was dropped onto agar plates containing 0.5 mM IPTG, antibiotics for plasmid selection, and various concentrations of tetracycline. Plates were incubated at 37 °C overnight. Protein expression was detected through the 6x Histidine tag on the C terminus.

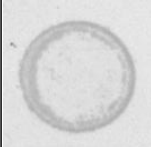
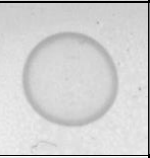
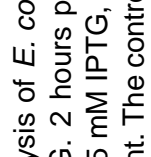





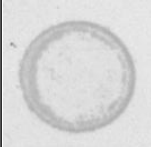
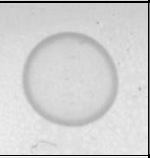
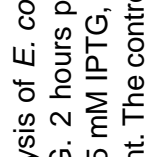





Acridine orange (µg/mL)										
	0	8	16	32	64	128	256	512	1024	MIC
pUC18										>1 mg/mL
pAdeT1*-His6										>1 mg/mL

Figure 2.30 Acridine orange MIC analysis of *E. coli* KAM32 carrying either pUC18 or pAdeT1*-His6. Cultures were grown to A₆₀₀ 0.6 before induction with 0.5 mM IPTG. 2 hours post-induction, A₆₀₀ of cultures were normalised to ~A₆₀₀ 4.0 before 20 µL was dropped onto agar plates containing 0.5 mM IPTG, antibiotics for plasmid selection, and various concentrations of acridine orange. Plates were incubated at 37 °C overnight. The control and *adeT1*-containing plasmids have an MIC of >1 mg/mL for acridine orange. Data shown are representative of 6 biological repeats.

MIC testing was also performed in *E. coli* BL21(DE3) cells containing either the control plasmid pET28a or pET28a AdeT1-His6. It was of interest to repeat the experiments using pET28a AdeT1-His6, as this construct results in greater production of AdeT1 protein in comparison to pAdeT1*-His6. The resulting data and MIC values are not directly comparable due to the use of an alternative *E. coli* strain. As previously mentioned, pET28a vectors necessitate the use of strains containing T7 polymerase. Further, *E. coli* BL21(DE3) are not antimicrobial hypersusceptible like KAM32. Nonetheless, the results were consistent with those obtained from pAdeT1*-His6.

For chloramphenicol, the MIC was 1.6 µg/mL for cells with pET28a and 0.8 µg/mL for those expressing pET28a AdeT1-His6 (**Figure 2.31**). The basal level of erythromycin resistance is higher in BL21(DE3) cells compared to KAM32, but this was unchanged with the addition of pET28a AdeT1-His6 and an MIC of 80 µg/mL was found in both conditions (Figure 2.33Error! Reference source not found.). Similarly, the MIC of tetracycline observed was 2 µg/mL for cells expressing pET28a and 1.0 µg/mL for those expressing pET28a AdeT1-His6 (**Figure 2.35Error! Reference source not found.**). For acridine orange, cell growth persisted in concentrations of >1 mg/mL (**Figure 2.37**). AdeT1 protein was detected in all solid cultures from plates after antibiotic testing (**Figure 2.32, Figure 2.34 and Figure 2.36**). These findings corroborate the previous indication that expression of wildtype AdeT1 protein does not confer increased resistance to antimicrobials in *E. coli*. Interestingly, *E. coli* expressing pET28a AdeT1-His6 had an altered colony morphology compared to that expressing pET28a. Particularly, *E. coli* expressing pET28a had a lawn appearance when dropped on agar whereas *E. coli* expressing pET28a AdeT1-His6 appeared as a collection of distinct colonies.






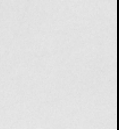
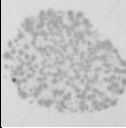
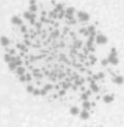
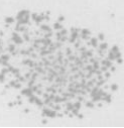
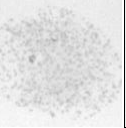
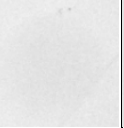
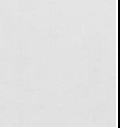
	Chloramphenicol ($\mu\text{g/mL}$)						
	0	0.1	0.2	0.4	0.8	1.6	MIC
pET28a							1.6
pET28a AdeT1-His6							0.8

Figure 2.31 Chloramphenicol MIC analysis of *E. coli* BL21(DE3) carrying either pET28a or pET28a AdeT1-His6. Cultures were grown to A_{600} 0.6 before induction with 0.5 mM IPTG. 2 hours post-induction, A_{600} of cultures were normalised to $\sim A_{600}$ 4.0 before 20 μL was dropped onto agar plates containing 0.5 mM IPTG, antibiotics for plasmid selection, and various concentrations of chloramphenicol. Plates were incubated at 37 °C overnight. The control and adeT1-containing plasmids show no difference in MIC for chloramphenicol. Data shown are representative of 4 biological repeats.

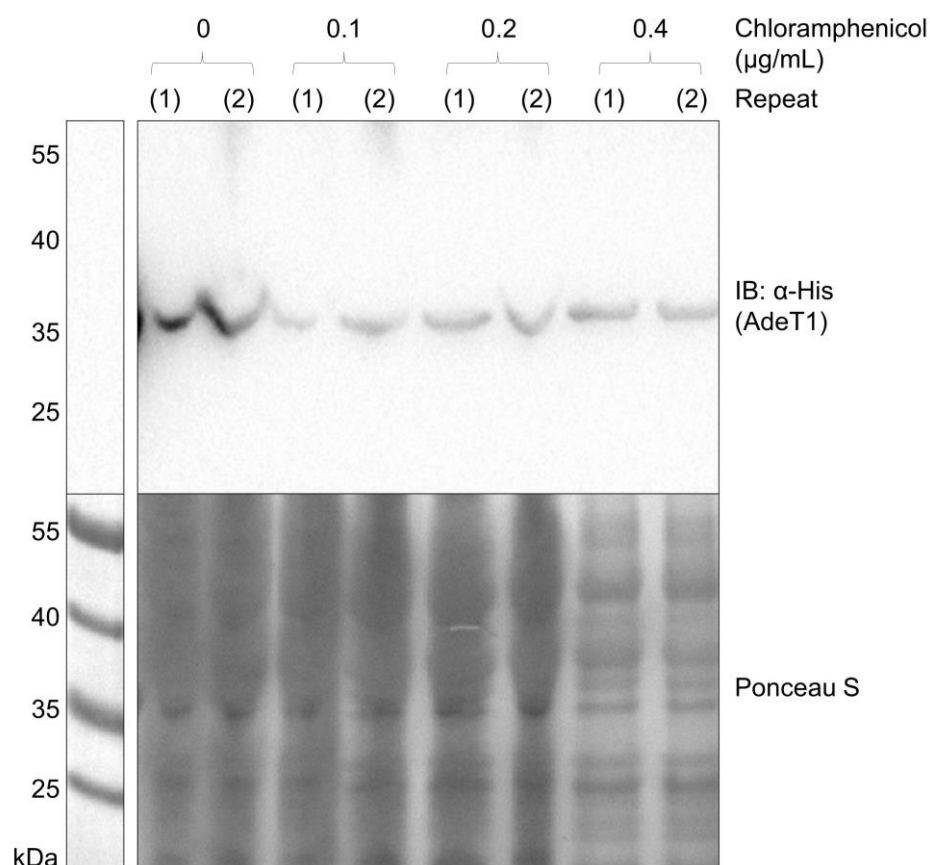


Figure 2.32 Immunoblot analysis of AdeT1 expression from *E. coli* BL21(DE3) carrying pET28a AdeT1-His6 during MIC testing with chloramphenicol. Cultures were grown to A_{600} 0.6 before induction with 0.5 mM IPTG. 2 hours post-induction, A_{600} of cultures were normalised to $\sim A_{600}$ 4.0 before 20 μ L was dropped onto agar plates containing 0.5 mM IPTG and various concentrations of chloramphenicol. Plates were incubated at 37 °C overnight. Protein expression was detected through the 6x Histidine tag on the C terminus.

	Erythromycin (μ g/mL)					
	0	10	20	40	80	MIC
pET28a						80
pET28a AdeT1-His6						80

Figure 2.33 Erythromycin MIC analysis of *E. coli* BL21(DE3) carrying either pET28a or pET28a AdeT1-His6. Cultures were grown to A_{600} 0.6 before induction with 0.5 mM IPTG. 2 hours post-induction, A_{600} of cultures were normalised to $\sim A_{600}$ 4.0 before 20 μ L was dropped onto agar plates containing 0.5 mM IPTG, antibiotics for plasmid selection, and various concentrations of erythromycin. Plates were incubated at 37 °C overnight. The control and *adeT1*-containing plasmids show no difference in MIC for erythromycin. Data shown are representative of 6 biological repeats.

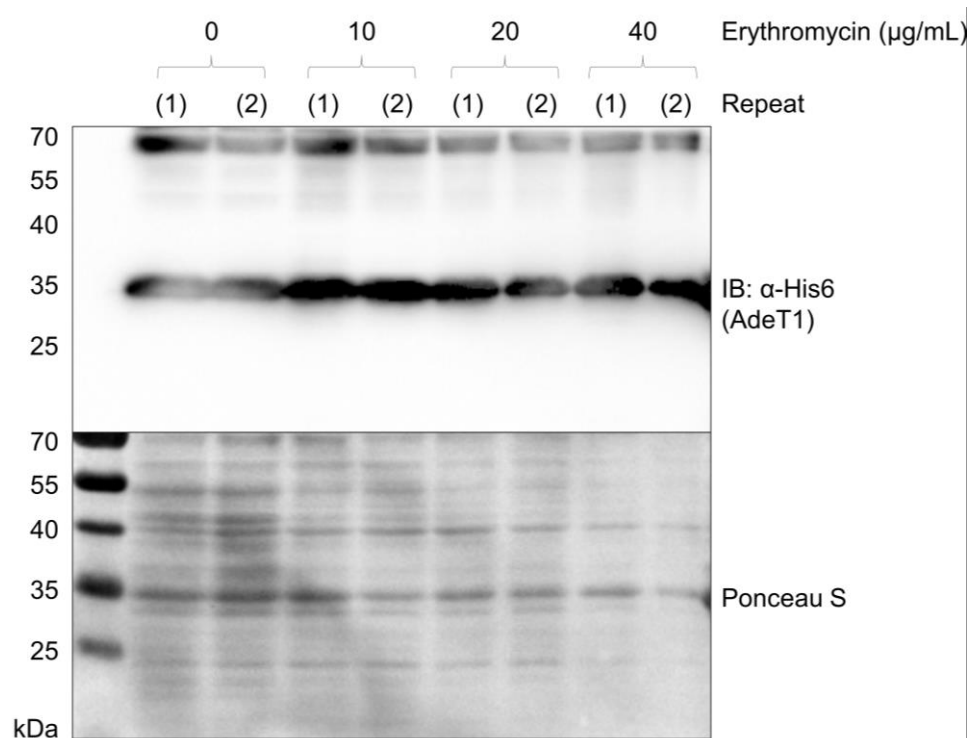


Figure 2.34 Immunoblot analysis of AdeT1 expression from *E. coli* BL21(DE3) carrying pET28a AdeT1-His6 during MIC testing with erythromycin. Cultures were grown to A_{600} 0.6 before induction with 0.5 mM IPTG. 2 hours post-induction, A_{600} of cultures were normalised to $\sim A_{600}$ 4.0 before 20 μ L was dropped onto agar plates containing 0.5 mM IPTG, antibiotics for plasmid selection, and various concentrations of erythromycin. Plates were incubated at 37 °C overnight. Protein expression was detected through the 6x Histidine tag on the C terminus.

	Tetracycline (μ g/mL)					
	0	0.25	0.5	1.0	2.0	MIC
pET28a						2.0
pET28a AdeT1-His6						1.0

Figure 2.35 Tetracycline MIC analysis of *E. coli* BL21(DE3) carrying either pET28a or pET28a AdeT1-His6. Cultures were grown to A_{600} 0.6 before induction with 0.5 mM IPTG. 2 hours post-induction, A_{600} of cultures were normalised to $\sim A_{600}$ 4.0 before 20 μ L was dropped onto agar plates containing 0.5 mM IPTG, antibiotics for plasmid selection, and various concentrations of tetracycline. Plates were incubated at 37 °C overnight. The control and *adeT1*-containing plasmids show no difference in MIC for tetracycline. Data shown are representative of 6 biological repeats.

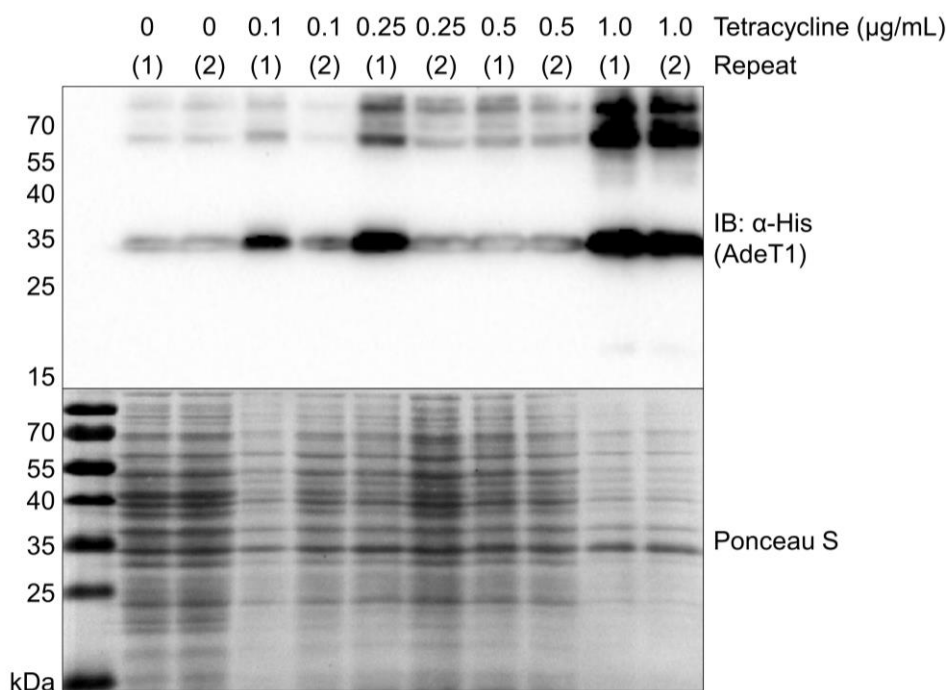


Figure 2.36 Immunoblot analysis of AdeT1 expression from *E. coli* BL21(DE3) carrying pET28a AdeT1-His6 during MIC testing with tetracycline. Cultures were grown to A_{600} 0.6 before induction with 0.5 mM IPTG. 2 hours post-induction, A_{600} of cultures were normalised to $\sim A_{600}$ 4.0 before 20 μ L was dropped onto agar plates containing 0.5 mM IPTG, antibiotics for plasmid selection, and various concentrations of tetracycline. Plates were incubated at 37 °C overnight. Protein expression was detected through the 6x Histidine tag on the C terminus.

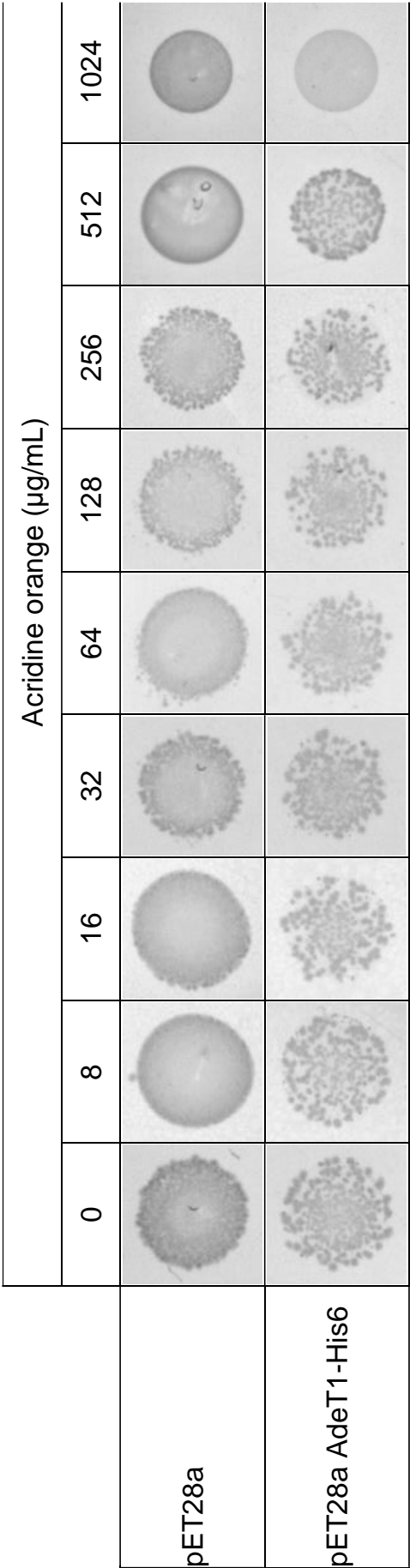


Figure 2.37 Acridine orange MIC analysis of *E. coli* BL21(DE3) carrying either pET28a or pET28a AdeT1-His6. Cultures were grown to A_{600} 0.6 before induction with 0.5 mM IPTG. 2 hours post-induction, A_{600} of cultures were normalised to $\sim A_{600}$ 4.0 before 20 µL was dropped onto agar plates containing 0.5 mM IPTG, antibiotics for plasmid selection, and various concentrations of acridine orange. Plates were incubated at 37 °C overnight. The control and *adeT1*-containing plasmids have an MIC of >1 mg/mL for acridine orange. Data shown are representative of 6 biological repeats

2.4.2 Confirmation of AdeT1 expression

Although a clear signal around the correct molecular weight was observed in immunoblots, it was important to confirm that AdeT1 protein was being produced as intended and that the lack of difference in MIC was not due to mis-production of the protein. To this end, a 1 L culture of BL21(DE3) cells containing pET28a AdeT1-His6 was expressed and then purified by nickel affinity chromatography (**Figure 2.38**). To overcome the insolubility of AdeT1, a membrane protein, all buffers used in purification contained 6 M urea. The resulting eluted fraction number 2 was sent for mass spectrometry analysis, where a peak at 34,278.50 Da was observed (**Figure 2.39**). This agreed with the expected average mass of 34,278.53 Da. Protein from the eluted fraction was also subjected to a trypsin digest, and the resulting peptide fragments analysed by mass spectrometry, where peptide fragments covering 63% of AdeT1 sequences were identified (**Figure 2.40**).

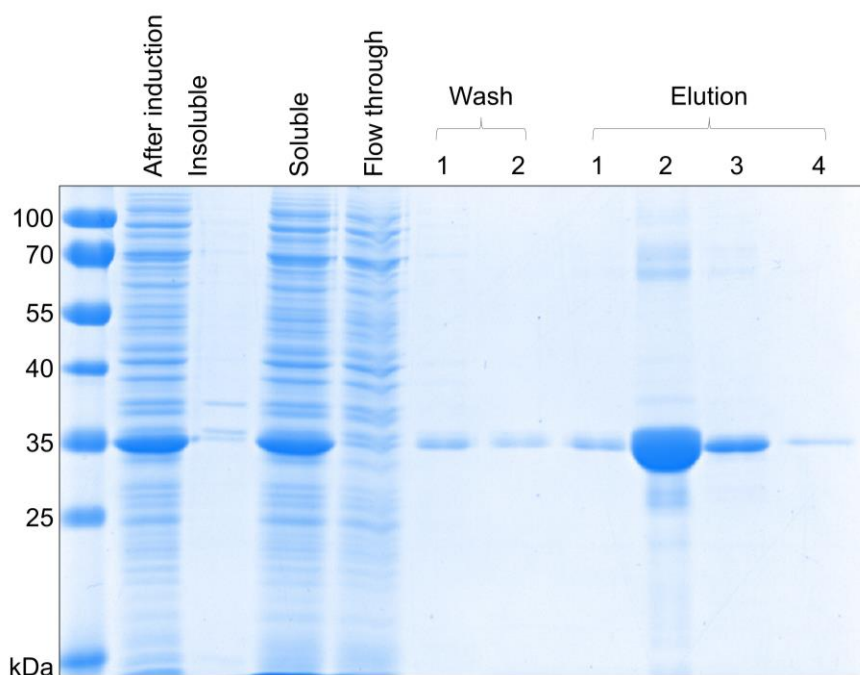


Figure 2.38 Nickel affinity chromatography of wildtype AdeT1 protein with a 6x Histidine tag on the protein C-terminus. Cells were pelleted by centrifugation and resuspended in lysis buffer containing 6 M urea before sonication. After high speed centrifugation, the insoluble fraction was discarded while the soluble supernatant was collected and incubated with nickel-NTA resin. The mixture was then loaded onto a gravity column and a sample of the flow through taken. The column was washed twice with wash buffer containing 6 M urea before protein was eluted in 4x 4 mL fractions using elution buffer containing 6 M urea. Samples were combined with SDS loading dye and analysed on 12% SDS-PAGE.

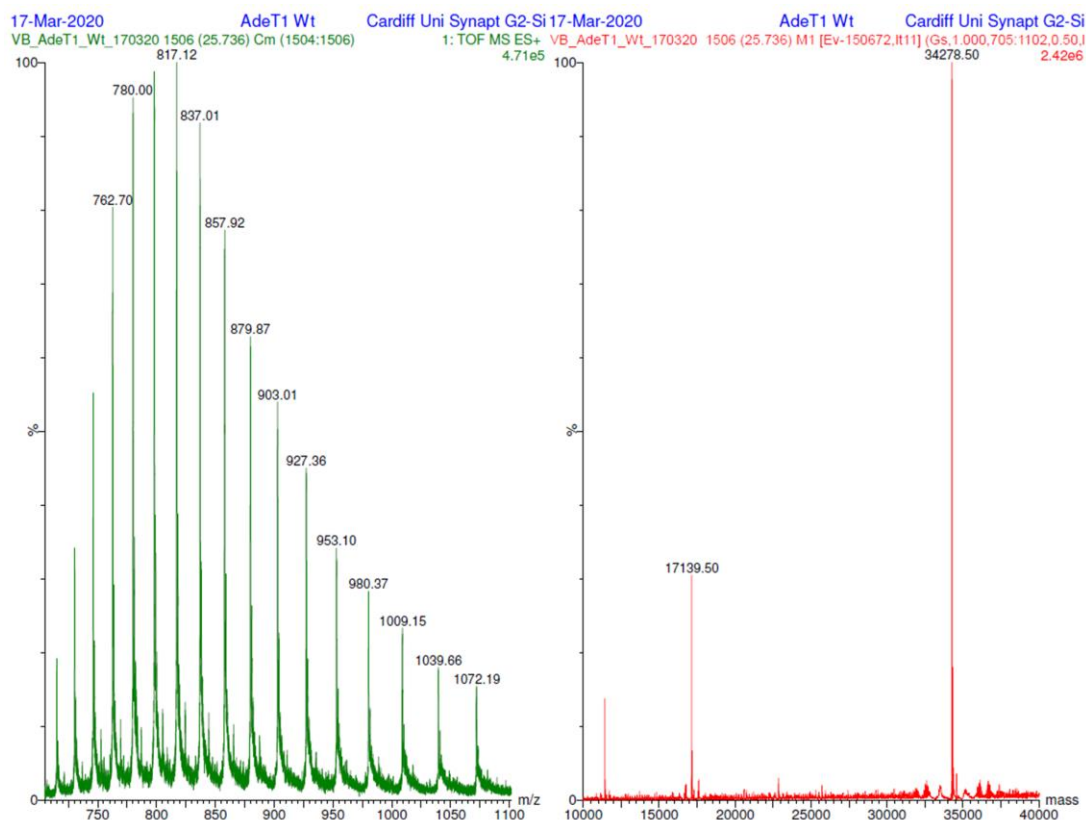


Figure 2.39 Mass spectrometry analysis of purified wild-type *A. baumannii* AdeT1 protein. *E. coli* BL21(DE3) cells expressing pET28a AdeT1-His6 were cultured to A_{600} 0.6, before induction with 0.5 mM IPTG and supplementation with 5 mM PrK. Cells were incubated for 18 hours at 20 °C before being harvested and purified by nickel affinity chromatography. The expected average mass is 34278.53 Da. A peak at 34278.50 Da can be observed. Samples were analysed using a SYNAPT G2-Si (Waters) mass spectrometer.

MFDP|GK|SGDAFALAK|DYALEAK|NWGADLSLK|AYVDER|VAAEDLK|
 VGK|CDGAIISGLR|GR|QFNK|YTGSLDAVGALTNMK|TAINAYK|LLSSP
 MAAK|NMVVGPEYIAGLGTIGPAYLFVNDR|SINTLAK|AAGKK|IGVFK|
 YDEAQPK|LVQHVGGQAVSVDVTNAGAK|FNNHEIDIVPAPIVAFKPFEL
 YK|GLGEK|GAIVR|FPLTQISADFIIR|K|DQFPAGFGQK|SR|TWVASQL
 NR|TFGIIAK|YESDIPSK|YWMDIPK|NEQLNYMK|MMREAR|IQLTK|AG
 IYDPK|MMNFLK|KVRCK|ENPSNFECALNDEHHHHH*

Figure 2.40 Peptide fragments of wild type AdeT1 digested with trypsin identified by mass spectrometry. Masses corresponding to peptide fragments colour coded blue were identified. Peptide fragments colour coded red were not identified. Peptide fragments colour coded grey have masses below 500 Da and were not analysed. Samples were analysed using a SYNAPT G2-Si (Waters) mass spectrometer.

2.4.3 Confirmation of AdeT1 efflux pump activity

Although it was confirmed that AdeT1 was produced in *E. coli* and that production of AdeT1 did not result in an increase in MIC, it remained unclear whether this was due to the protein not having an effect in *E. coli* or whether the protein was either misfolded or not functional in *E. coli*. As AdeT1 is a membrane fusion protein component of an efflux pump, AdeT1 alone is not assumed to possess efflux function. Thereby, several possibilities existed. The first was that AdeT1 was not correctly folded in *E. coli*, resulting in a non-functional polypeptide. Alternatively, AdeT1 was not trafficked to the membrane or, at the membrane, did not form a component of an efflux pump. In any of these cases, production of the protein would have no effect on the cell, or in fact, may be slightly detrimental to cells as resources are used to produce an ineffective protein. An alternative possibility is that AdeT1 does form part of an efflux pump, but this new hybrid pump does not confer antibiotic resistance. As AdeT1 is overexpressed in these experiments, if AdeT1 is forming part of an efflux pump it is likely that this would have some effect on efflux pump activity. Similarly, even if AdeT1 is not specifically trafficked to the membrane, the high amount of protein makes it likely that at least some would reach the membrane. Pump activity may either be reduced if AdeT1 is a less effective component when replacing an endogenous *E. coli* membrane fusion protein, or, pump activity may be increased if AdeT1 works more effectively in an *E. coli* RND-type complex.

To investigate these possibilities, an efflux assay with ethidium bromide was performed. When this assay was performed with *E. coli* KAM32 cells expressing either the control plasmid pUC18 or pAdeT1*, the results were not reproducible (**Figure 2.41**). The relative fluorescence of cells over the 15-min incubation period compared to the starting fluorescence was variable and although it appears to suggest a possible difference between *E. coli* KAM32 cells containing pUC18 or pAdeT1*, the difference was not reproducible nor consistent between repeats.

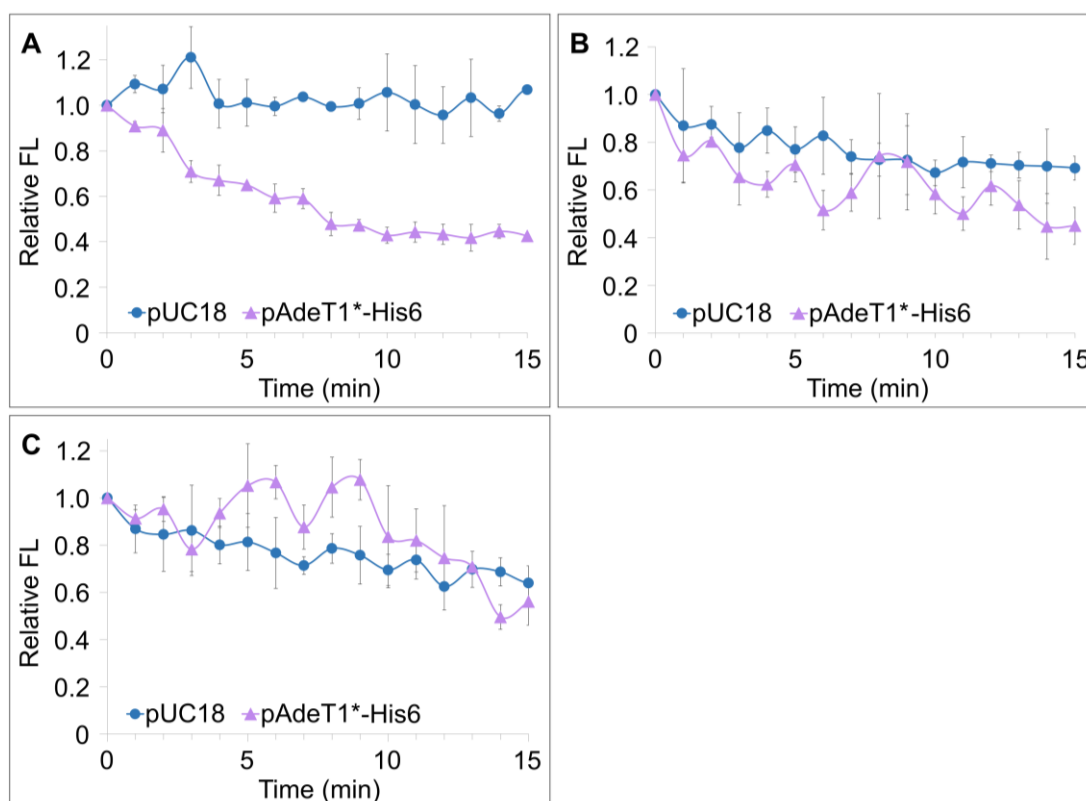


Figure 2.41 Efflux of ethidium bromide from *E. coli* cells expressing pUC18 or pAdeT1*. *E. coli* KAM32 cells were transformed with either pUC18 or pAdeT1*-His6 and grown to the log phase, when protein production was induced. 1 h later, cells were harvested and incubated with ethidium bromide, IPTG and an efflux pump inhibitor for 1 h at 25 °C. The ethidium bromide was then removed and cells exchanged into PBS containing glucose. Ethidium bromide efflux was monitored by measuring fluorescence at ex 500, em 590 nm for 15 minutes at 37 °C. For each condition, the fluorescence data was made relative to the starting fluorescence value (starting fluorescence = 1.0). Each datapoint represents an average of three technical replicates, standard deviation is annotated for each average. Three biological replicates (**A**, **B**, and **C**) are shown.

In contrast, when this assay was performed with *E. coli* BL21(DE3) cells containing either the control plasmid pET28a or pET28a AdeT1*-His6, a clear and reproducible effect was observed (**Figure 2.42**). For cells expressing the control plasmid, fluorescence decreased about 45% \pm 0.04 over the 15-min incubation compared to the starting fluorescence value. When cells were producing AdeT1, a greater decrease of about 74% \pm 0.03 was observed. This observation was consistent for four biological repeats, and the difference between the conditions was found to be statistically significant ($p < 0.001$).

The increased efflux of ethidium bromide from cells producing AdeT1 suggested that the protein formed part of a functional efflux pump with endogenous *E. coli* proteins. Although AdeT1 did not confer increased resistance to antimicrobials in *E. coli*, it appeared to form an efflux pump capable of ethidium bromide efflux. As it remained possible that propionylation of AdeT1 may have an effect on the function of this pump, and any information gained may provide insights into the effect of propionylation on AdeT1 in *A. baumannii*, it appeared worthwhile to continue the investigations and assess whether propionylation at Lys280 has any effect on efflux pump function.

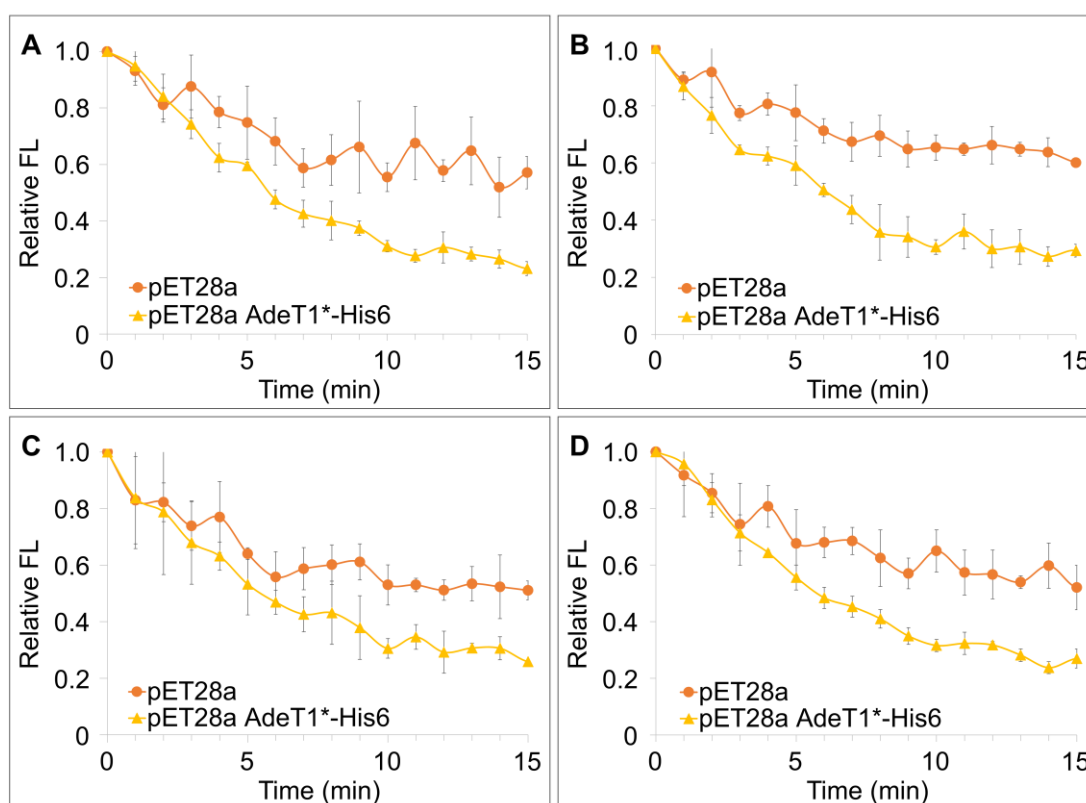


Figure 2.42 Efflux of ethidium bromide from *E. coli* cells expressing pET28a or pET28a AdeT1*-His6. *E. coli* BL21(DE3) cells were transformed with either pET28a or pET28a AdeT1*-His6 and grown to the log phase, when protein production was induced. 1 h later, cells were harvested and incubated with ethidium bromide, IPTG and an efflux pump inhibitor for 1 h at 25 °C. The ethidium bromide was then removed and cells exchanged into PBS containing glucose. Ethidium bromide efflux was monitored by measuring fluorescence at ex 500, em 590 nm for 15 minutes at 37 °C. For each condition, the fluorescence data was made relative to the starting fluorescence value (starting fluorescence = 1.0). Each datapoint represents an average of three technical replicates, standard deviation is annotated for each average. Four biological replicates (A, B, C, and D) are shown.

2.4.4 Producing AdeT1^{K280Pr}

In *A. baumannii*, AdeT1 protein is propionylated at the lysine residue in amino acid position 280 *in vivo*.²⁵⁶ To study the effects of this post-translational modification *in vitro*, genetic code expansion for unnatural amino acid incorporation was employed. Initially, propionyl-lysine was incorporated into sfGFP to confirm the feasibility of the approach.

Incorporation of propionyl-lysine into position 150 of sfGFP

Propionyl-lysine was incorporated into sfGFP in *E. coli* BL21(DE3) containing pET28a sfGFP(150TAG)-His6. The *E. coli* sirtuin CobB has been previously reported to remove lysine propionylation.²⁰⁵ As CobB is NAD⁺-dependent and is inhibited by nicotinamide,³⁸⁵ to assess whether de-propionylation was likely in these experiments, 20 mM nicotinamide was added to half of the culture at the point of induction with IPTG and supplementation with PrK. After incubation for 18 hours at 37 °C, the resulting two cultures were purified individually, with 20 mM nicotinamide present in the lysis buffer of the appropriate culture, and analysed by MS. The data obtained show that propionylated sfGFP at the expected size (27.9 kDa) was found regardless of addition of nicotinamide (**Figure 2.43** and **Figure 2.44**). Therefore, nicotinamide was not included in subsequent experiments.

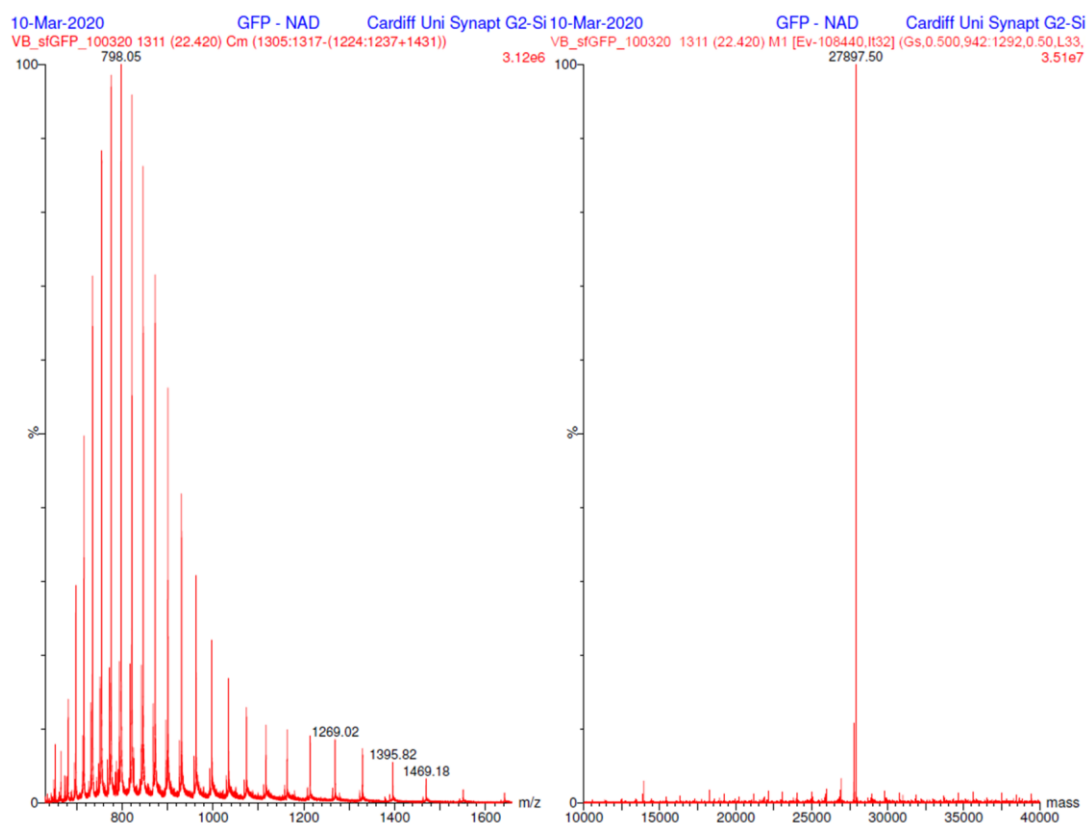


Figure 2.43 MS data of sfGFP(K150Pr) purified from cultures grown in the absence of nicotinamide. *E. coli* BL21(DE3) cells expressing pET28a sfGFP(150TAG) were cultured to A_{600} 0.6, before induction with 0.5 mM IPTG and supplementation with 5 mM PrK. Cells were incubated for 18 hours at 20 °C before being harvested and purified by nickel affinity chromatography. The expected average mass is 27897.39 Da, the observed mass is 27897.50 Da. Data was collected on a SYNAPT G2-Si (Waters) mass spectrometer.

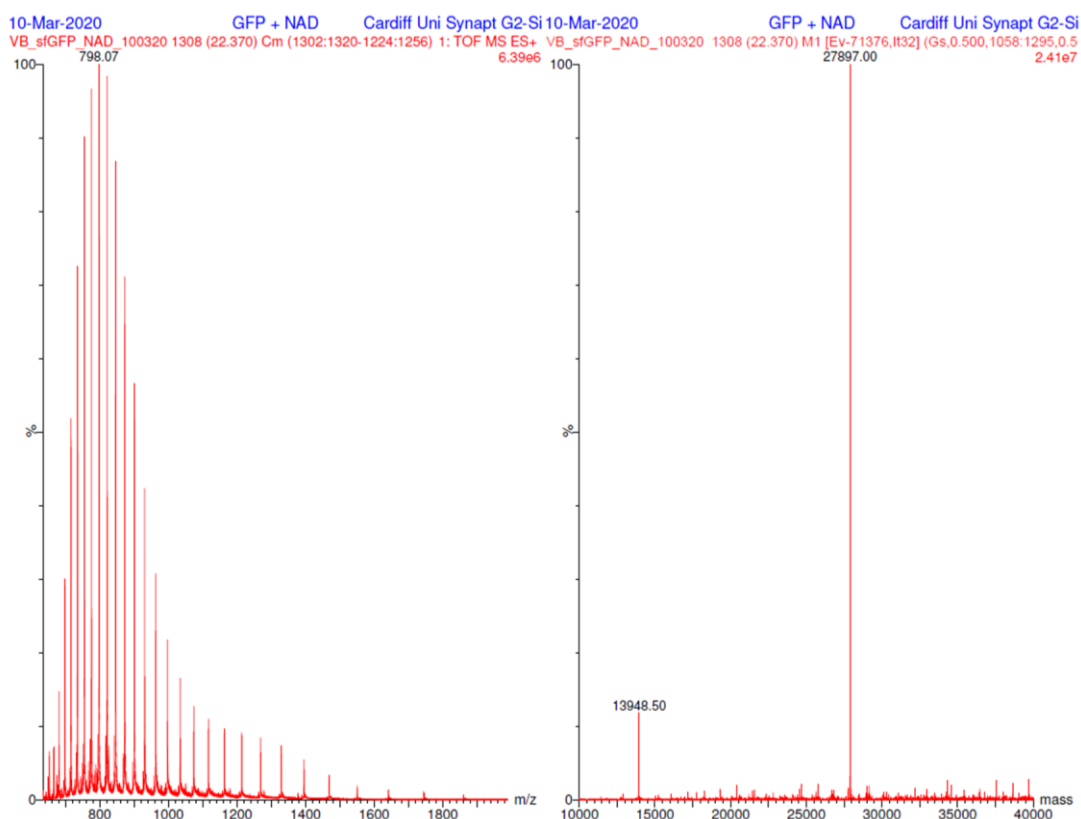


Figure 2.44 MS data of sfGFP(K150Pr) purified from cultures grown in the presence of nicotinamide. *E. coli* BL21(DE3) cells expressing pET28a sfGFP(150TAG) were cultured to A_{600} 0.6, before induction with 0.5 mM IPTG and supplementation with 5 mM PrK and 20 mM nicotinamide. Cells were incubated for 18 hours at 20 °C before being harvested and purified by nickel affinity chromatography. The expected average mass is 27897.39 Da, the observed mass is 27897.50 Da. Data was collected on a SYNAPT G2-Si (Waters) mass spectrometer.

Incorporation of propionyl-lysine into position 280 of AdeT1

The codon at position 280 in *adeT1* was mutated to the amber stop codon TAG in both pAdeT1*-His6 and pET28a AdeT1-His6 to generate pAdeT1*(K280TAG)-His6 and pET28a AdeT1(K280TAG)-His6, respectively. These plasmids were then co-expressed with a plasmid encoding either propionyl-lysine synthetase or acetyl-lysine synthetase and a corresponding orthogonal tRNA_{CUA} (pPrKST or pAckST, respectively). Preliminary expression tests with pET28a AdeT1(K280TAG)-His6 demonstrated that incorporation was most successful with AckST (**Figure 2.45**), so this synthetase and tRNA pair was used going forward.

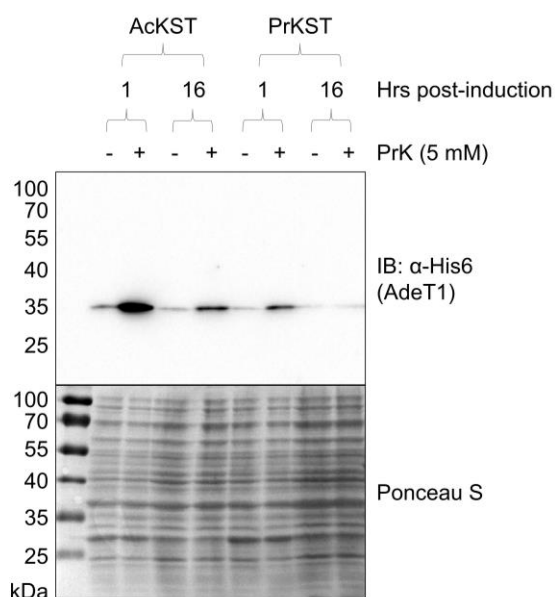


Figure 2.45 Immunoblot analysis of propionyl-lysine (PrK) incorporation into position 280 of AdeT1 protein in *E. coli* BL21(DE3). Incorporation was achieved through expression of plasmid pET28a AdeT1-His6 with co-expression of either propionyl-lysine synthetase (PrKST) or acetyl-lysine synthetase (AckST) in the presence or absence of 5 mM propionyl-lysine (PrK). Protein was detected through the 6x Histidine tag on the C terminus.

To confirm that expression of AdeT1^{K280Pr} would be maintained during MIC testing, a preliminary experiment was performed in which the cells were subjected to similar conditions as the MIC test, but without test antibiotics present in the agar plates. Cultures were grown until A_{600} 0.6 before induction with 0.5 mM IPTG. The culture was then divided into 2 halves, and 5 mM PrK added to one half. 2 hours after induction, the cell density was measured and adjusted to A_{600} 4.0 and 20 μ L dropped onto LB agar plates containing 0.5 mM IPTG, antibiotics for plasmid selection, and 5 mM PrK (as appropriate). The plates were incubated for 18 hours before samples were taken.

Such treatment of cells producing AdeT1^{K280Pr} yielded unexpected results. As can be observed in **Figure 2.46**, both the – and + PrK conditions gave a similar signal intensity in immunoblot. Due to the position of the TAG codon in pAdeT1*(K280TAG)-His6, if PrK is not incorporated protein translation should terminate at position 280. As the 6x Histidine tag is located on the C-terminus of the AdeT1 gene, downstream of the TAG codon, this should result in no translation of the 6x Histidine tag when the culture is not supplemented with PrK. Accordingly, no signal should be detected in the immunoblot using anti-8x Histidine antibodies. Interestingly, the signal from both

– and + PrK conditions is much stronger from samples obtained from solid cultures as opposed to those from liquid cultures. Nonetheless, the similar signal intensity obtained from both conditions causes uncertainty about whether the intended protein is being produced.

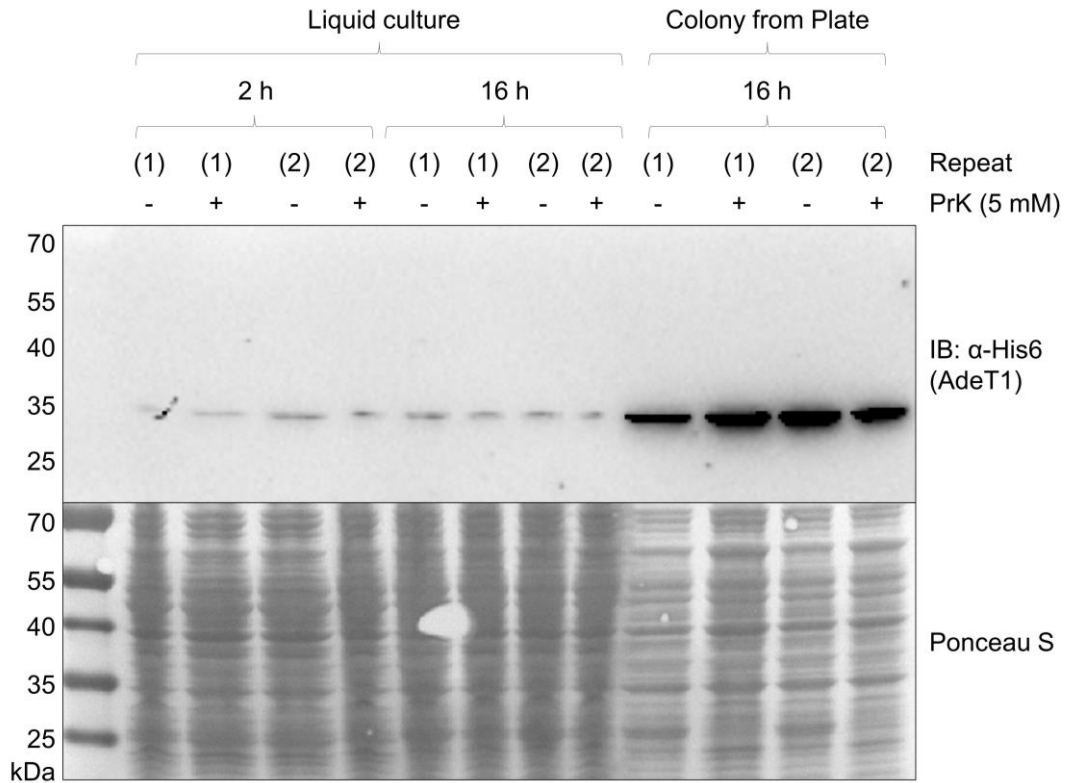


Figure 2.46 Immunoblot of PrK incorporation into AdeT1 protein in *E. coli* KAM32 expressing plasmids pAdeT1*(K280TAG)-His6 and pAckST. 5 mM PrK and 0.5mM IPTG were added to the culture at A_{600} 0.6. The culture was incubated for a further two hours, before a sample was taken and adjusted to A_{600} 4.0. Then, 20 μ L of this concentrated culture was dropped onto agar plates containing 0.5 mM IPTG and 5 mM PrK. These plates and the original culture were incubated for 16 h before samples were taken. Protein was detected through the 6x Histidine tag on the C-terminus.

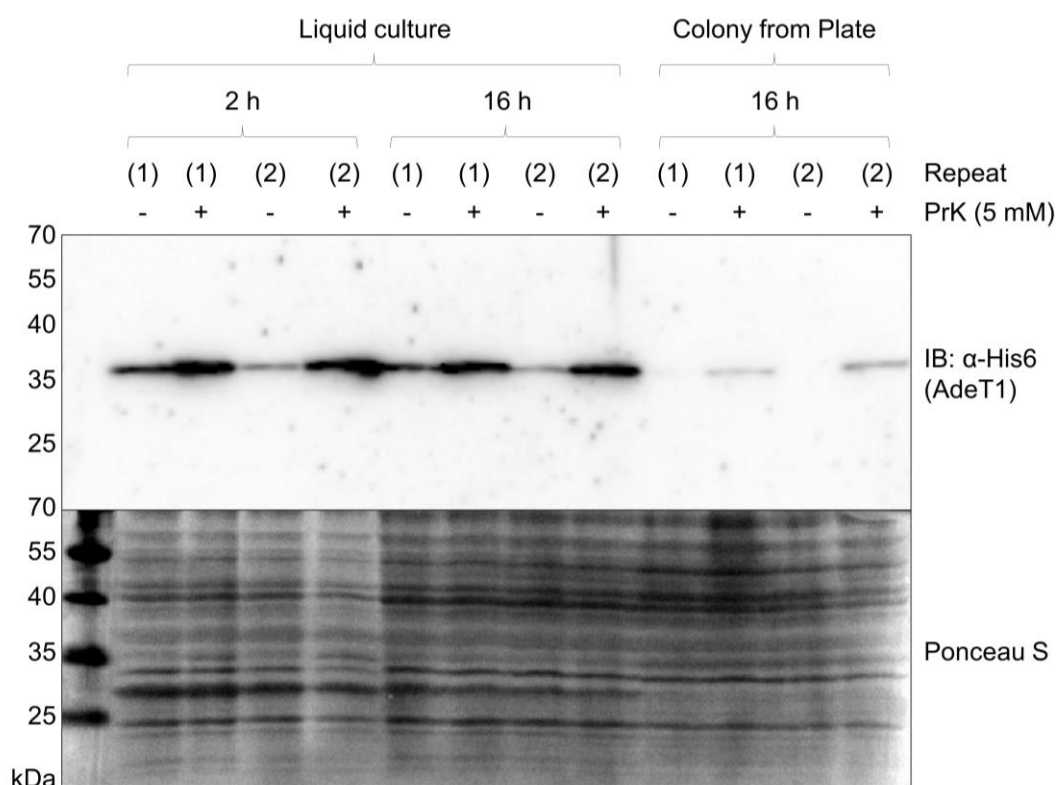


Figure 2.47 Immunoblot of PrK incorporation into AdeT1 protein in *E. coli* BL21(DE3) expressing plasmids pET28a AdeT1(K280TAG)-His6 and pAckST. 5 mM PrK and 0.5 mM IPTG were added to the culture at A_{600} 0.6. The culture was incubated for a further two hours, before a sample was taken and adjusted to A_{600} 4.0. Then, 20 μ L of this concentrated culture was dropped onto agar plates containing 0.5 mM IPTG and 5 mM PrK. These plates and the original culture were incubated for 16 h before samples were taken. Protein was detected through the 6x Histidine tag on the C-terminus.

For *E. coli* BL21(DE3) expressing pET28a AdeT1(K280TAG)-His6 and pAckST, a much greater disparity in signal intensity could be observed between the – and + PrK conditions (**Figure 2.47**). However, a signal was still observed in the conditions without supplementation of propionyl-lysine. When analysing samples collected from solid cultures, less protein was detected compared to liquid cultures. No signal was detected in the solid cultures expressed without propionyl-lysine. However, due to the smaller quantity of protein, it is likely that some protein was still present at below detectable levels. The presence of signal from cultures expressed without propionyl-lysine is concerning and necessitated confirmation that the intended proteins were being produced.

2.2.5 Confirmation of AdeT1^{K280Pr} production

To investigate AdeT1^{K280Pr} production, cells expressing pET28a AdeT1(K280TAG)-His6 and pAckST were cultured either in the absence or presence of 5 mM PrK before purification *via* nickel affinity chromatography (**Figure 2.48**). Purified protein was then sent for mass spectrometry analysis and spectra of both the full protein (**Figure 2.49**) and of a tryptic digest (**Figure 2.50**) were obtained. The recorded mass for the full protein agreed with the expected average mass (both 34.3 kDa) and the tryptic digest peptides covered 63% of the sequences.

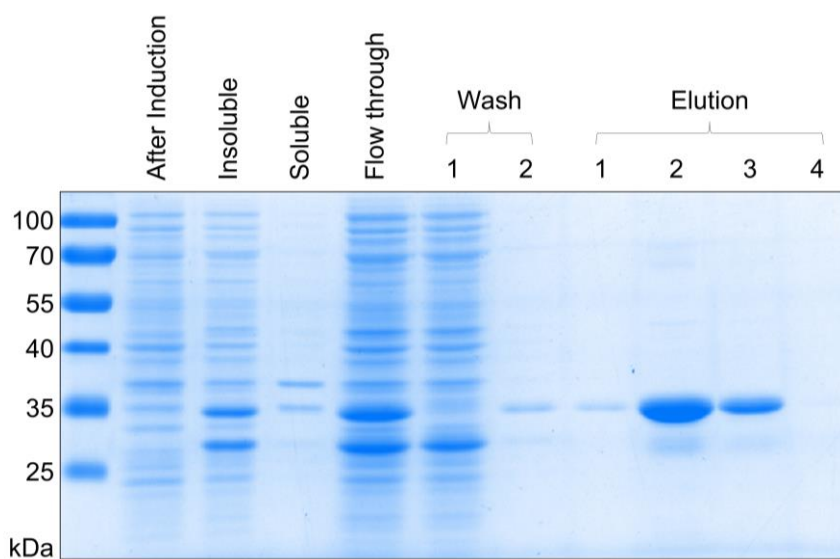


Figure 2.48 Nickel affinity chromatography of AdeT1^{K280Pr} with a 6x Histidine tag on the protein C-terminus. Cells were pelleted by centrifugation and resuspended in lysis buffer containing 6 M urea before sonication. After high speed centrifugation, the insoluble fraction was discarded while the soluble supernatant was collected and incubated with nickel-NTA resin. The mixture was then loaded onto a gravity column and a sample of the flow through taken. The column was washed twice with wash buffer containing 6 M urea before protein was eluted in 4x 4 mL fractions using elution buffer containing 6 M urea. Samples were combined with SDS loading dye and analysed on 12% SDS-PAGE.

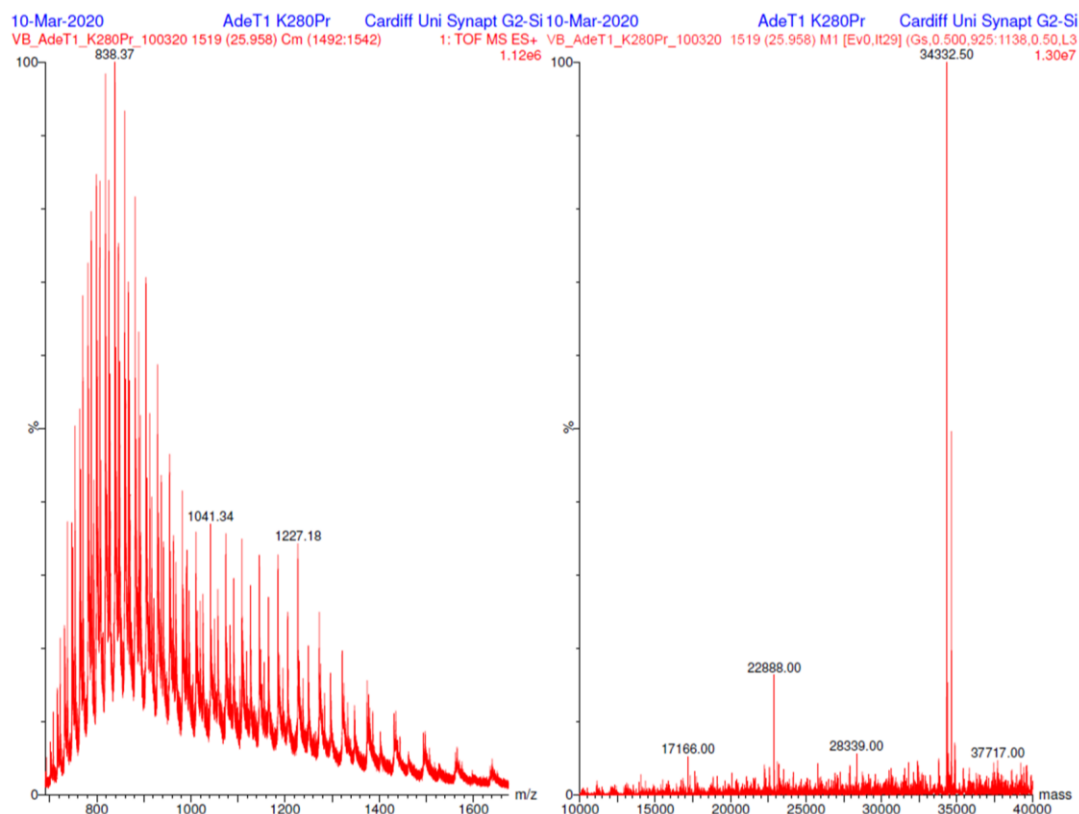


Figure 2.49 Mass spectrometry analysis of AdeT1 protein with propionyl-lysine incorporated into amino acid position 280. *E. coli* BL21(DE3) cells expressing pET28a AdeT1(K280TAG)-His6 were cultured to A_{600} 0.6, before induction with 0.5 mM IPTG and supplementation with 5 mM PrK. Cells were incubated for 18 hours at 20 °C before being harvested and purified by nickel affinity chromatography. The expected average mass is 34334.53 Da. A peak of 34332.50 Da can be observed. Samples were analysed using a SYNAPT G2-Si (Waters) mass spectrometer.

MFDPIGK|SGDAFALAK|DYALEAK|NWGADLSLK|AYVDER|VAAEDLK|
 VGK|CDGAIISGLR|GR|QFNK|YTGSLDAVGALTNMK|TAINAYK|LLSSP
 MAAK|NMVVGPEIAGLGTIGPAYLFVNDR|SINTLAK|AAGKK|IGVFK|
 YDEAQPK|LVQHVGQAVSVDVTNAGAK|FNNHEIDIVPAPIVAFKPFEL
 YK|GLGEK|GAIVR|FPLTQISADFIIR|K|DQFPAGFGQK|SR|TWVASQL
 NR|TFGIIAK|YESDIPSK|YWMDIPK|NEQLNYMK|MMREAR|IQLTK|AG
 IYDPKpr|MMNFLK|KVRCK|ENPSNFECALNDEHHHHH*

Figure 2.50 Peptide fragments of AdeT1^{K280Pr} digested with trypsin identified by mass spectrometry. Masses corresponding to peptide fragments colour coded blue were identified. Peptide fragments colour coded red were not identified. Peptide fragments colour coded grey have masses below 500 Da and were not analysed. Samples were analysed using a SYNAPT G2-Si (Waters) mass spectrometer.

2.2.6 Confirmation of AdeT1^{K280Pr} efflux activity

After confirming that AdeT1^{K280Pr} was produced by *E. coli* BL21(DE3) it was necessary to confirm that the modified protein was capable of forming part of an RND-type pump and to investigate whether propionylation had any effect on pump activity. To this end, preliminary ethidium bromide efflux assays with cells containing plasmid pET28a AdeT1(K280TAG)-His6 in the absence or presence of 5 mM PrK were performed (**Figure 2.51**). However, at the beginning of the assay, the fluorescence of cells cultured in the presence of 5 mM PrK was approximately half the fluorescence of those cultured in the absence of PrK. This prevented the assessment of efflux based on relative fluorescence to the starting value for two reasons. The first is that the starting fluorescence of the two conditions should be approximately equal to facilitate a valid comparison. The second is that as the baseline level of fluorescence for cells cultures in the absence of PrK was higher, any reduction in fluorescence, and thus the assumed efflux of ethidium bromide, for these cells would be artificially greater. The low starting fluorescence of cells cultured in the presence of PrK made me speculate that the lower fluorescence may be due to improved efflux of ethidium bromide even during the ethidium bromide accumulation part of the assay. If so, ethidium bromide would not accumulate in the cells to as high of a concentration, and there would be less ethidium bromide to pump out during the assay.

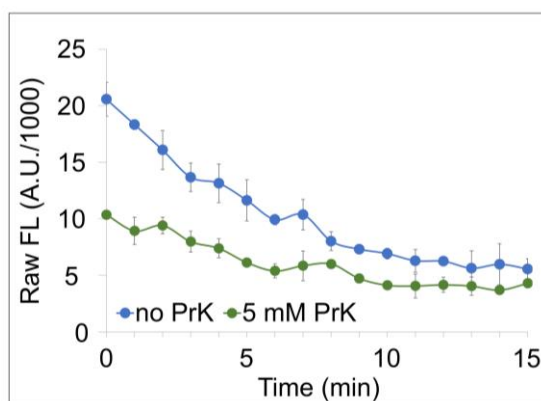


Figure 2.51 Efflux of ethidium bromide from *E. coli* cells expressing pET28a AdeT1(K280TAG)-His6. *E. coli* BL21(DE3) cells were transformed with pET28a AdeT1(K280TAG)-His6 and grown in the presence or absence of 5 mM PrK to the log phase, when protein production was induced. 1 h later, cells were harvested and incubated with ethidium bromide, IPTG and an efflux pump inhibitor for 1 h at 25 °C. Ethidium bromide was then removed and cells exchanged into PBS containing glucose. Ethidium bromide efflux was monitored by measuring fluorescence at ex 500, em 590 nm for 15 minutes at 37 °C. For each condition, the fluorescence data was made relative to the starting fluorescence value (starting fluorescence = 1.0). Each datapoint represents an average of three technical replicates, standard deviation is annotated for each average.

For these reasons, the assays were repeated with the fluorescence of the cells instead monitored during the 1-h incubation with ethidium bromide (**Figure 2.52**). In these ethidium bromide accumulation assays, cells cultured in the presence or absence of PrK started the assay with around the same fluorescence; the average of all repeats was 12806 ± 1343 A.U. for cells without PrK and 12843 ± 1229 A.U. for those cultured with PrK. However, during the 1-h incubation, cells cultured in the absence of PrK increased in fluorescence around 2.2-fold (average 27772 ± 2030 A.U.), while cells cultured in the presence of PrK increased only 1.5-fold (average 19416 ± 1534 A.U.). The difference in final fluorescence between the two conditions was found to be highly statistically significant ($p < 0.001$). This suggests that ethidium bromide was being more effectively removed from the cells during the incubation period when cells were producing AdeT1^{K280Pr} compared to control cells.

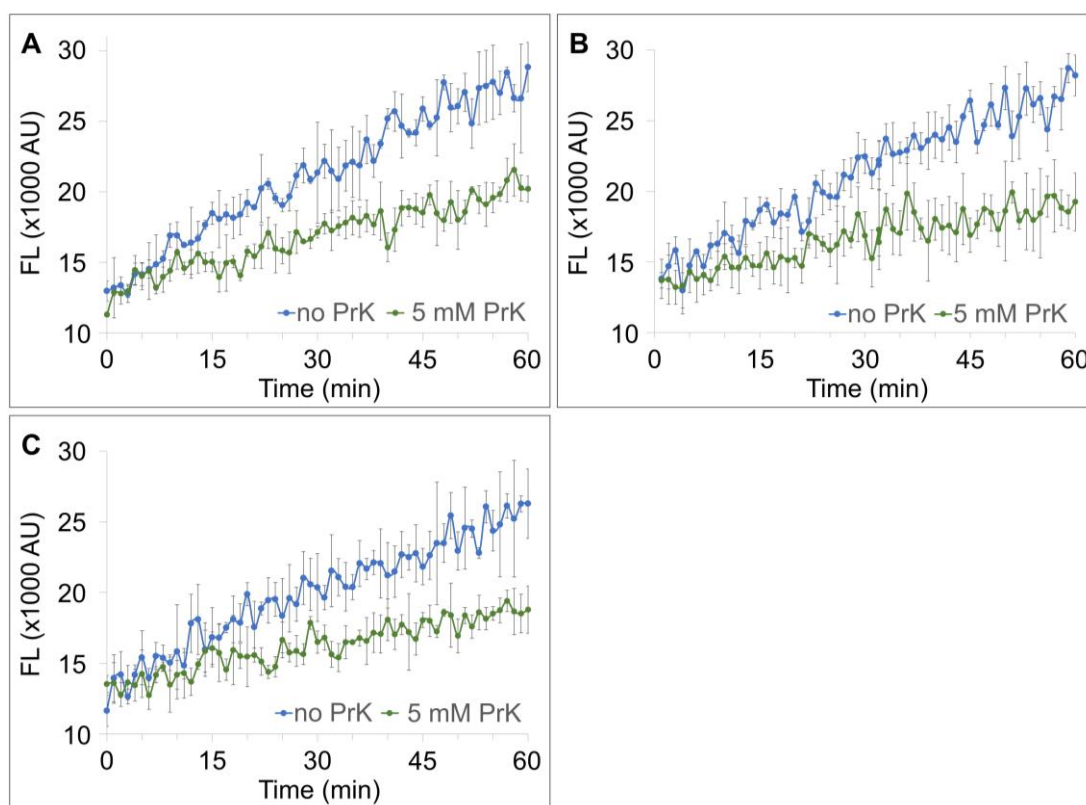


Figure 2.52 Accumulation of ethidium bromide in *E. coli* cells expressing pET28a AdeT1(K280TAG)-His6. *E. coli* BL21(DE3) cells were transformed with pET28a AdeT1(K280TAG)-His6 and grown in the presence or absence of 5 mM PrK to the log phase, when protein production was induced with IPTG. 1 h later, cells were harvested and incubated with ethidium bromide, IPTG and an efflux pump inhibitor for 1 h at 25 °C. Ethidium bromide accumulation was monitored by measuring fluorescence (FL) at ex 500, em 590 nm. Each datapoint represents an average of three technical replicates, standard deviation is annotated for each average. Three biological replicates (**A**, **B**, and **C**) are shown.

2.4.7 Minimum inhibitory concentration testing with AdeT1^{K280Pr}

As AdeT1^{K280Pr} appeared to improve efflux pump activity, it was worthwhile to proceed with MIC testing of cells producing AdeT1^{K280Pr} vs control cells. Initially, tests were performed with chloramphenicol and erythromycin, the two antibiotics to which wildtype AdeT1 conferred no increased resistance. With AdeT1^{K280Pr}, MIC testing with chloramphenicol revealed similar results to the wildtype protein. The MIC of chloramphenicol required for cultures without PrK was 0.4 µg/mL and was 0.8 µg/mL for cultures with PrK (**Figure 2.53** Error! Reference source not found.). It is noted that this concentration is slightly lower than the concentration recorded for cells expressing the wild-type AdeT1 protein. As the MIC is consistent across – and + amino acid conditions, it is likely that the additional stress imposed on the cell of carrying 2 plasmids may cause the slight reduction in MIC. Expression of protein was confirmed through immunoblot (**Figure 2.54**).

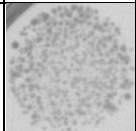
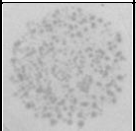
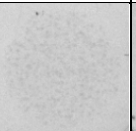
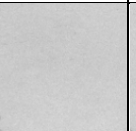
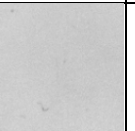
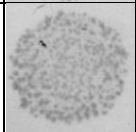
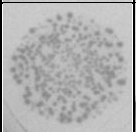
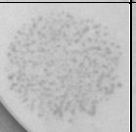
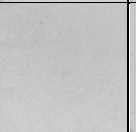
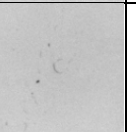
	Chloramphenicol (µg/mL)					
	0	0.2	0.4	0.8	1.6	MIC
No PrK						0.4
5 mM PrK						0.8

Figure 2.53 Chloramphenicol MIC analysis of *E. coli* BL21(DE3) expressing pET28a AdeT1(K280TAG)-His6 and pAckST. Cultures were grown to A₆₀₀ 0.6 before induction with 0.5 mM IPTG and divided into two halves. Half the culture was supplemented with 5 mM PrK while the other was left as a control. At 1 hour post-induction, A₆₀₀ of cultures were measured and adjusted to 4.0 before 20 µL was dropped onto agar plates containing antibiotics for plasmid selection, 0.5 mM IPTG, various concentrations of chloramphenicol, and 5 mM PrK (as appropriate). Plates were incubated at 37 °C overnight.

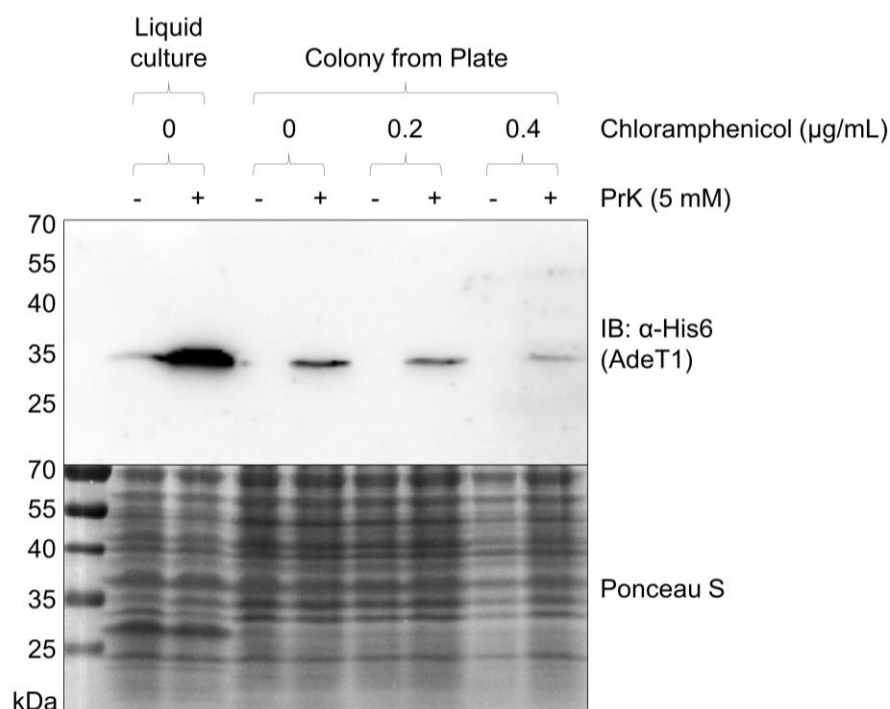


Figure 2.54 Immunoblot analysis of *E. coli* BL21(DE3) expressing pET28a AdeT1(K280TAG)-His6 and pAckST during MIC testing with chloramphenicol. Cultures were grown to A_{600} 0.6 before induction with 0.5 mM IPTG and divided into two. One half of the culture was supplemented with 5 mM PrK while the other was used as a control. At 1 hour post-induction, A_{600} of cultures were measured and adjusted to 4.0 before 20 μ L was dropped onto agar plates containing antibiotics for plasmid selection, 0.5 mM IPTG, various concentrations of chloramphenicol, and 5 mM PrK (as appropriate). Plates were incubated at 37 °C overnight before samples were taken. Protein was detected through the 6x Histidine tag on the C terminus.

When MIC testing was performed with erythromycin, a surprising result was obtained. The MIC of cells cultured without propionyl-lysine was 40 μ g/mL, the same as obtained for the wildtype protein (**Figure 2.55**). However, for cultures expressing AdeT1^{K280Pr} cell growth persisted in the presence of up to 240 μ g/mL of erythromycin. Expression of AdeT1^{K280Pr} was confirmed by immunoblotting (**Figure 2.56**). Additionally, the signal detected by immunoblotting increased with increasing concentrations of erythromycin, despite the amount of lysate loaded remaining constant.

Erythromycin (μ g/mL)						
0	40	80	160	240	320	MIC

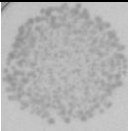
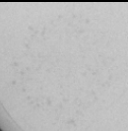


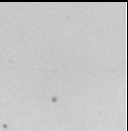

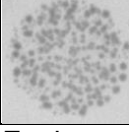


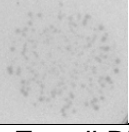
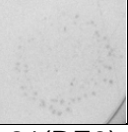
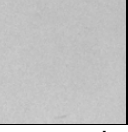
No PrK							40
5 mM PrK							240

Figure 2.55 Erythromycin MIC analysis of *E. coli* BL21(DE3) expressing pET28a AdeT1(K280TAG)-His6 and pAckST. Cultures were grown to A_{600} 0.6 before induction with 0.5 mM IPTG and half the culture supplemented with 5 mM PrK. At 1 hour post-induction, A_{600} of cultures were measure and adjusted to 4.0 before 20 μ L was dropped onto agar plates containing antibiotics for plasmid selection, 0.5 mM IPTG, various concentrations of erythromycin, and 5 mM PrK (as appropriate). Plates were incubated at 37 °C overnight.

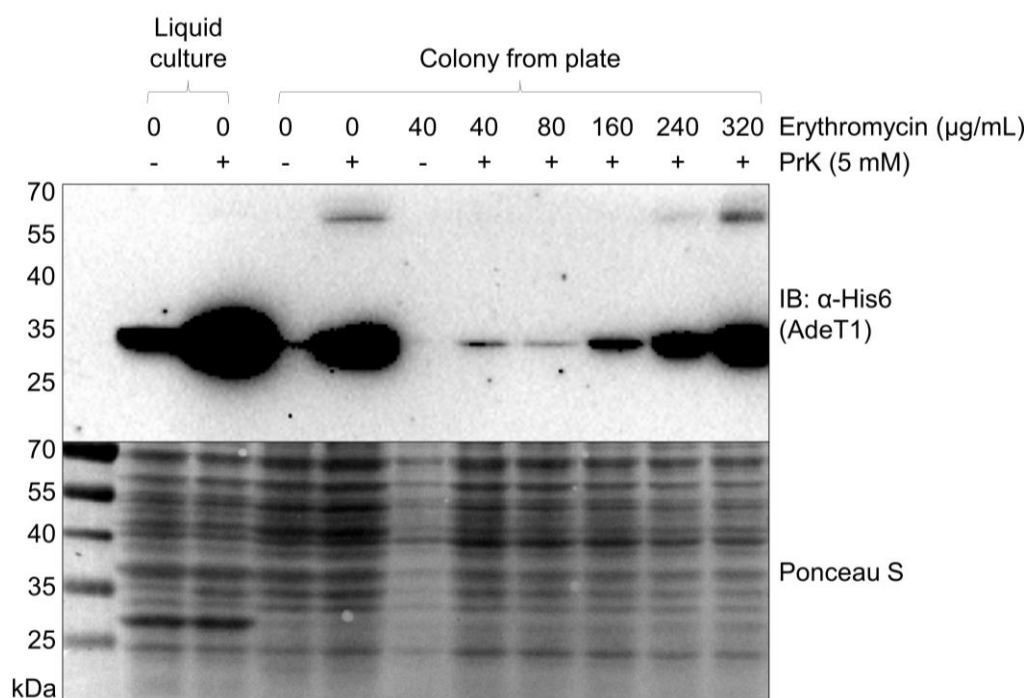


Figure 2.56 Immunoblot analysis of *E. coli* BL21(DE3) expressing pET28a AdeT1(K280TAG)-His6 and pAckST during MIC testing with erythromycin. Cultures were grown to A_{600} 0.6 before induction with 0.5 mM IPTG and divided into two. Half the culture was supplemented with 5 mM PrK. At 1 hour post-induction, A_{600} of cultures were measured and adjusted to 4.0 before 20 μ L was dropped onto agar plates containing antibiotics for plasmid selection, 0.5 mM IPTG, various concentrations of erythromycin, and 5 mM PrK (as appropriate). Plates were incubated at 37 °C overnight before samples were taken. Protein was detected through the 6x Histidine tag on the C terminus.

The results obtained with erythromycin suggested that lysine propionylation may have an effect in regulating function in this protein. Therefore, additional antibiotics were

used for MIC testing. However, no increase in MIC was observed for either tetracycline or ampicillin. For tetracycline, the MIC of both – and + PrK conditions was 0.25 µg/mL (**Figure 2.57**Error! Reference source not found.). AdeT1^{K280Pr} expression was confirmed through immunoblot (**Figure 2.58**). Similarly, for ampicillin, MIC of both conditions was 2.5 µg/mL (**Figure 2.59**) despite the presence of AdeT1^{K280Pr} as confirmed by immunoblot (**Figure 2.60**), while for ertapenem the MIC of both conditions was 0.15 µg/mL (**Figure 2.61**Error! Reference source not found.).

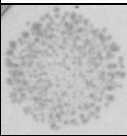
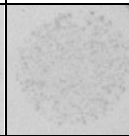
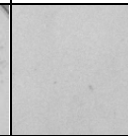
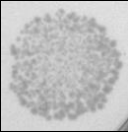
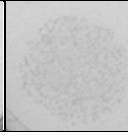
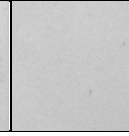
	Tetracycline (µg/mL)			
	0	0.125	0.250	MIC
No PrK				0.25
5 mM PrK				0.25

Figure 2.57 Tetracycline MIC analysis of *E. coli* BL21(DE3) expressing pET28a AdeT1(K280TAG)-His6 and pAckST. Cultures were grown to A_{600} 0.6 before induction with 0.5 mM IPTG and divided into two. Half the culture was supplemented with 5 mM PrK. 1 hour post-induction, A_{600} of cultures were measured and adjusted to 4.0 before 20 µL was dropped onto agar plates containing antibiotics for plasmid selection, 0.5 mM IPTG, various concentrations of tetracycline, and 5 mM PrK (as appropriate). Plates were incubated at 37 °C overnight.

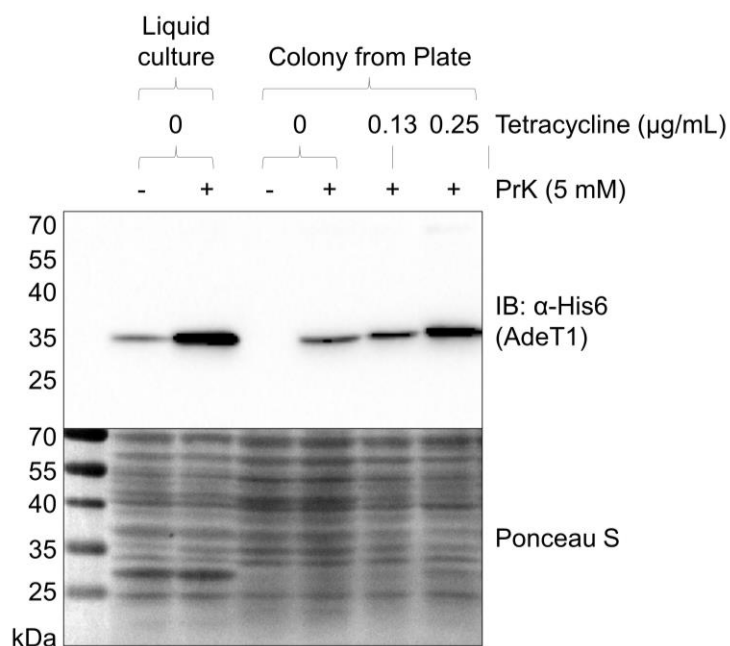


Figure 2.58 Immunoblot analysis of *E. coli* BL21(DE3) expressing pET28a AdeT1(K280TAG)-His6 and pAckST during MIC testing with tetracycline. Cultures were grown to A_{600} 0.6 before induction with 0.5 mM IPTG and divided into two. Half the culture was supplemented with 5 mM PrK. 1 hour post-induction, A_{600} of cultures were measured and adjusted to 4.0 before 20 µL was dropped onto agar plates containing antibiotics for plasmid selection, 0.5 mM IPTG, various concentrations of tetracycline, and 5 mM PrK (as appropriate). Plates were incubated at 37 °C overnight before samples were taken. Protein was detected through the 6x Histidine tag on the C-terminus.

	Ampicillin (µg/mL)						
	0	1.25	1.50	1.75	2.00	2.50	MIC
No PrK							2.5
5 mM PrK							2.5

Figure 2.59 Ampicillin MIC analysis of *E. coli* BL21(DE3) expressing pET28a AdeT1(K280TAG)-His6 and pAckST. Cultures were grown to A_{600} 0.6 before induction with 0.5 mM IPTG and divided into two. Half the culture was supplemented with 5 mM PrK. 1 hour post-induction, A_{600} of cultures were measured and adjusted to 4.0 before 20 µL was dropped onto agar plates containing antibiotics for plasmid selection (kanamycin and spectinomycin), 0.5 mM IPTG, various concentrations of ampicillin, and 5 mM PrK (as appropriate). Plates were incubated at 37 °C overnight.

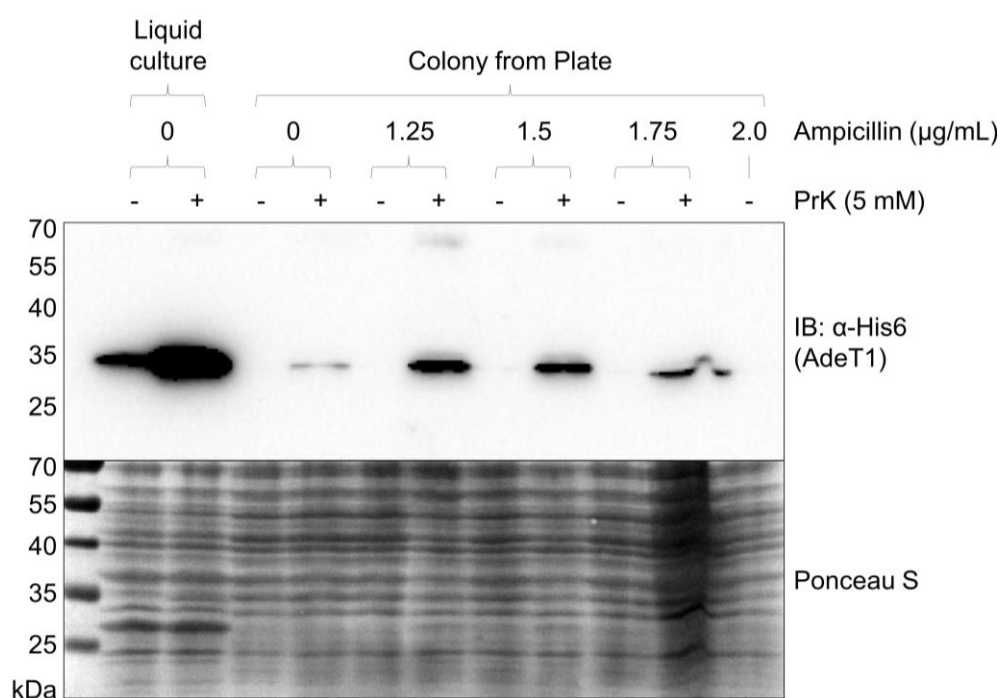


Figure 2.60 Immunoblot analysis of *E. coli* BL21(DE3) expressing pET28a-AdeT1*(K280TAG)-His6 and pAckST during MIC testing with ampicillin. Cultures were grown to A_{600} 0.6 before induction with 0.5 mM IPTG and divided into two. Half the culture was supplemented with 5 mM PrK. 1 hour post-induction, A_{600} of cultures were measured and adjusted to 4.0 before 20 μ L was dropped onto agar plates containing antibiotics for plasmid selection, 0.5 mM IPTG, various concentrations of ampicillin, and 5 mM PrK (as appropriate). Plates were incubated at 37 °C overnight before samples were taken. Protein was detected through the 6x Histidine tag on the C-terminus.

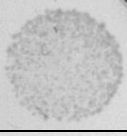

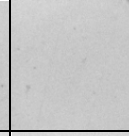
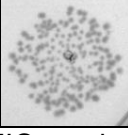


		Ertapenem (μ g/mL)			
		0	0.15	0.30	MIC
No PrK					0.15
5 mM PrK					0.15

Figure 2.61 Ertapenem MIC analysis of *E. coli* BL21(DE3) expressing pET28a AdeT1(K280TAG)-His6 and pAckST. Cultures were grown to A_{600} 0.6 before induction with 0.5 mM IPTG and divided into two. Half the culture was supplemented with 5 mM PrK. 1 hour post-induction, A_{600} of cultures were measured and adjusted to 4.0 before 20 μ L was dropped onto agar plates containing antibiotics for plasmid selection, 0.5 mM IPTG, various concentrations of ertapenem, and 5 mM PrK (as appropriate). Plates were incubated at 37 °C overnight.

2.5 Discussion

2.5.1 Producing AdeT1 in *E. coli*

AdeT1 was previously reported to be functional in *E. coli*, where it greatly enhanced resistance to a wide range of antimicrobials.³⁵³ However, several problems were encountered here when producing AdeT1 in *E. coli*. Primarily, it was discovered that the literature reported plasmid, pAdeT1, does not produce AdeT1 in *E. coli*, most likely due to the *adeT1* gene not being in frame with the start codon. Indeed, amendment of this by creating an in-frame plasmid, pAdeT1*-His6, allowed production of AdeT1 in *E. coli*. If pAdeT1 was constructed as described by Srinivasan *et al.*, it is unlikely that AdeT1 protein was actually present in their studies. Alternatively, it is possible that an error was made during the documentation of their methodology and the *adeT1* gene was placed within the correct reading frame during their cloning procedures. Nevertheless, Srinivasan *et al.* did not report detailed experimental procedures in their manuscript, such as whether IPTG was used to induce protein expression. As the *adeT1* gene in pAdeT1 is downstream of the lac promoter and the lac inhibitor, IPTG would be necessary to induce protein expression.

The second problem encountered with AdeT1 production related to the dilution of cultures in which protein expression had been induced. MIC assays necessitate the dilution of bacterial cultures to low cellular densities to permit unambiguous assessment of inhibition of bacterial growth after incubation in the presence of the tested antibiotic. When performing MIC assays with cultures that are producing recombinant proteins from expression vectors, this means diluting the culture post-induction with IPTG. When post-induction cultures were diluted to low cellular density, AdeT1 production was highly variable. Further, cultures diluted to A_{600} 0.001 were not able to reproducibly restore growth. For these reasons, I became sceptical of both the methodology and the results of Srinivasan *et al.* regarding the effect of AdeT1 on *E. coli*.³⁵³ It became imperative to establish a bioassay which maintains the production of AdeT1 post-dilution to low cellular density and to validate the effect of AdeT1 on antimicrobial resistance in *E. coli*.

To counter such variability in protein production, *adeT1* was first cloned into a common expression vector, pET28a. This vector is commonly used to overexpress recombinant proteins in an *E. coli* host for subsequent purification. As pET28a AdeT1-His6 produced a higher level of AdeT1 production than pAdeT1*-His6, it was possible that protein production would be preserved post-dilution. However, dilution of induced

cultures containing pET28a AdeT1-His6 again resulted in highly variable protein expression and cell growth.

Dilution of sfGFP-producing cultures

To establish whether such variable protein production in post-induced cultures was as a result of something specific to AdeT1 protein, or a more generalised phenomenon, dilution studies with pET28a sfGFP-His6 were performed. sfGFP is an ideal reporter as protein production can be easily assessed with fluorescence measured on plate readers. These assays revealed that protein production was highly variable in cultures containing pET28a sfGFP post-induction and post-dilution, suggesting that this may be a generalised occurrence. Indeed, it has been demonstrated that continuous dilution and sub-culturing of *E. coli* BL21(DE3) could lead to impaired production of active T7 RNA polymerase, likely through chromosomal mutations.³⁸⁶ In such experiments, subculturing cells before induction resulted in decreased protein expression when induced with IPTG. It is possible that subculturing after induction, as in the experiments presented here, may have exacerbated this selective pressure to undergo chromosomal mutations resulting in decreased protein expression of the target gene. This could explain why the protein of interest was not reproducibly detected in diluted cultures.

Unlike with AdeT1, when diluting post-induction cultures producing sfGFP, bacterial growth was consistent between all conditions. Cultures diluted to A_{600} 0.001 often grew to similar A_s as those diluted to A_{600} 0.01. This discrepancy may suggest that overexpression of AdeT1 at very low cellular densities causes cell death, possibly through extrusion of favourable compounds such as metabolites or those necessary for certain stress responses.³⁸⁷ For example, in *Pseudomonas aeruginosa*, overexpression of the RND-type pumps MexCD-OprJ or MexEF-OprJ shuts down the quorum sensing response through extrusion of signalling molecules.^{388, 389} Regardless, when expressing AdeT1 from either a pET28a or pUC18 vector, bacterial growth and protein expression are not guaranteed when cultures were diluted to low A_{260} . Therefore, alternative methods of MIC analysis that allowed consistent protein expression during dilution to low cellular densities were investigated.

Constitutive protein expression

There are few examples in the literature of others using recombinant protein expression during MIC assays.^{390, 391} Those who have reported such experiments either constitutively express the target gene on a vector or integrate it into the host genome. Constitutively active promoters have been successfully, albeit infrequently,

employed in *E. coli* for producing recombinant proteins.³⁹²⁻³⁹⁷ Here, it was demonstrated that two constitutive promoters allowed constant production of sfGFP at low levels in *E. coli*. Low levels refer to sfGFP production being undetectable upon visible observation of cultures, requiring a plate reader or similar, in contrast to sfGFP production under the T7 promoter in which cultures display obvious green fluorescence.

After confirming constitutive production of sfGFP, *sfGFP* was directly replaced with *adeT1* in the vector. However, culturing of cells containing the corresponding vector did not result in detectable AdeT1 production *via* immunoblotting. This result was unexpected as direct replacement of *sfGFP* with *adeT1* should result in constitutive production of AdeT1. This result may indicate endogenous *E. coli* control mechanisms to regulate expression of constitutively active proteins *e.g.* through the production of inhibitors or DNA-binding proteins. It is possible that something specific to the *adeT1* gene or the resulting protein is not compatible with constitutive expression. For example, constitutive expression of this protein may be toxic to the cells in early growth phases. Alternatively, protein expression may have occurred at levels too low to be detected by immunoblotting.

MIC assays without dilution of cultures

Due to the inability to produce AdeT1 through constitutively active promoters and the high variability in protein production when diluting induced cultures, MIC assays were attempted without prior dilution of cultures. First, antibiotics were added directly to post-induction cultures. However, even when culturing cells in the absence of antibiotics, cultures containing different plasmids reached different final A_{600} . This created difficulties in comparing growth between cultures in an objective manner and defining inhibition of growth without ambiguity. For example, as can be seen in **Figure 2.20**, for the cultures expressing pUC18 it could be interpreted that inhibition of growth results in an A_{600} value of around 1.0, as this is the lowest value observed. However, for the experimental AdeT1 cultures, it appears as though inhibition of growth results in an A_{600} value of 1.3. As both conditions were diluted to the same initial A_{600} , these differences cast uncertainty over defining when growth has been fully inhibited and makes it difficult to establish a standardised procedure for determining MIC. Furthermore, A_{600} values do not provide any information about the viability of cells in the culture. It was therefore concluded that this approach is not a suitable strategy for determination of MIC in this instance.

The final method tried involved adjusting the A_{600} of post-induction cultures to 4.0, usually resulting in an increase in cell density between 2 and 4-fold, and dropping a defined amount of these cultures on agar plates. Both in the presence and absence of antibiotics, this technique resulted in the reproducible production of AdeT1. Further, clear discrimination between growth and inhibition of growth was maintained. Therefore, established MIC protocols were successfully modified to permit characterisation of recombinant proteins from expression vectors. Additionally, this work highlights the importance of confirming target protein expression when investigating relationships between target proteins and drug resistance.

2.5.2 Functionality of AdeT1 in *E. coli*

To determine whether AdeT1 forms part of a functional efflux pump in *E. coli*, efflux assays with ethidium bromide were performed. The results obtained with KAM32 cells containing either pUC18 or pAdeT1 were inconsistent. While it appeared that the two conditions behaved distinctly, no conclusions could be drawn. In contrast, BL21(DE3) cells containing either pET28a or pET28 AdeT1-His6 showed significantly different fluorescence profiles. Cells containing pET28a AdeT1-His6 exhibited a higher decrease in fluorescence over the 15-min observation period, suggesting that they effluxed significantly more ethidium bromide than the control cells during this time. This indicates that AdeT1 likely forms part of a functional efflux pump in *E. coli*. The difference between the pUC18 and pET28a vectors may be due to the higher level of protein expression from the pET28a vector.

An RND transporter has three components: an inner membrane protein, a membrane fusion protein, and an outer membrane protein.³²⁹ Membrane fusion proteins, such as AdeT1, alone are not functional for drug efflux. However, individual proteins in RND-type complexes can be interchangeable.^{398, 399} Further, such interchangeability is true even with components from a heterologous host. For example, two components of *Haemophilus influenzae* multidrug efflux pump AcrAB were found to function with the *E. coli* outer membrane protein TolC⁴⁰⁰. Similarly, *P. aeruginosa* multidrug efflux pump MexXY can also assemble with *E. coli* TolC for drug efflux.⁴⁰¹ In addition, *P. aeruginosa* MexB is an inner membrane protein that can complex with *E. coli* AcrA and TolC to form a tripartite pump.³⁶⁶ Such interspecies assemblies are explained by a common mechanism of tripartite pump assembly.³⁶⁶ Thus, it would not be a surprise if AdeT1 can form a functional pump with endogenous *E. coli* RND pump components as indicated in the literature.³⁵³

2.5.3 Effect of AdeT1 on antimicrobial resistance in *E. coli*

On performing MIC assays with cultures producing AdeT1 protein, the previously reported result that production of AdeT1 increases the antimicrobial resistance of *E. coli*³⁵³ was unable to be replicated. Instead, cultures containing control plasmids and those containing AdeT1 exhibited the same MIC values, and this was true for both *E. coli* KAM32 and BL21(DE3) cells. The only antimicrobial where a small effect was observed was chloramphenicol, where the MIC was 0.4 µg/mL for cells expressing pUC18 and 0.8 µg/mL for those expressing pUC18-AdeT1*-His6 (**Figure 2.24**). However, this result is still in opposition to the literature describing an MIC of 0.2 µg/mL for KAM32 expressing pUC18, and a 5-fold increase to 1.0 µg/mL when expressing pAdeT1.³⁵³ Similarly, in these experiments the MIC of erythromycin to inhibit growth was 4 µg/mL for both control and AdeT1 plasmids (**Figure 2.26**). Again, this contrasts with the literature report of 4 and 24 µg/mL for the control and AdeT1-containing plasmids, respectively. For tetracycline, the MIC for both conditions was 0.5 µg/mL (**Figure 2.28**) in contrast with the literature report of 0.5 and 1.0 µg/mL for pUC18 and pAdeT1, respectively. Another compound, acridine orange, was described in the literature of having an MIC of 16 µg/mL in *E. coli* KAM32 cells expressing pUC18 and 64 µg/mL for those expressing pAdeT1. However, these experiments show that cell growth was maintained with concentrations of acridine orange of more than 1 mg/mL for *E. coli* KAM32 cells (**Figure 2.30**). Overall, the data obtained here are in stark contrast with the previous report of a 5-fold increase in MIC for chloramphenicol, a 6-fold increase for erythromycin, and a 4-fold increase for acridine orange.³⁵³ The disparity between the results described here and previously is concerning. As already mentioned in **2.5.1 Producing AdeT1 in *E. coli***, several problems with the previously reported plasmid and methodology were uncovered. As such, the results presented here indicate that production of wildtype *A. baumannii* AdeT1 protein does not confer antimicrobial resistance to *E. coli*.

In assays where chloramphenicol was added directly to post-induction cultures, KAM32 cultures producing AdeT1 exhibited higher final As in the absence of antibiotics compared to the controls (**Figure 2.20**). For BL21(DE3), this was not the case (**Figure 2.21**). This may suggest that AdeT1 provided a growth advantage in KAM32, a strain which otherwise lacks two major efflux pump components. However, in BL21(DE3), which does not lack any major efflux pumps, provision of AdeT1 did not provide any growth advantage. In fact, BL21(DE3) cells containing AdeT1 had lower final A values than the control cells, suggesting growth might be hindered due to diversion of resources to overproduce the protein. In any case, even if AdeT1

provided a growth advantage to KAM32 cells, it did not confer higher resistance to the tested compounds.

2.5.2 Production of AdeT1^{K280Pr} through incorporation of propionyl-lysine

AdeT1^{K280Pr} was successfully produced in *E. coli* using genetic code expansion for unnatural amino acid incorporation as analysed by immunoblot (**Figure 2.45**) and mass spectrometry (**Figure 2.49** and **Figure 2.50**). Surprisingly, a weak signal was repeatedly observed in immunoblots of lysates from cultures incubated in the absence of PrK. As the histidine tag used to detect AdeT1 production is located downstream of the TAG codon, the histidine tag should only be produced if PrK is incorporated during translation. This prompted an investigation whereby PrK was incorporated into a different protein, sfGFP, in *E. coli*. Immunoblots analysing eGFP^{K150Pr} production in the presence and absence of PrK also exhibited a weak signal in lysates from cells grown in the absence of PrK. It is likely that the weak signal is due to a low production of full-length protein *via* misread through of the amber stop codon.⁴⁰² Further, as most unnatural amino acid incorporation experiments analyse protein production in *E. coli* *via* SDS-PAGE, it is probable that such misread through occurs frequently but remains undetected.

It was previously reported that in *S. enterica*, CobB de-propionylates the propionyl-coenzyme A synthetase enzyme PrpE.²⁰⁵ To investigate whether *E. coli* CobB was likely to remove propionyl groups in this study, nicotinamide, an inhibitor of CobB activity,³⁸⁵ was provided to the cells during the preliminary incorporation of propionyl-lysine into sfGFP. Propionyl-lysine was also incorporated in the absence of nicotinamide for comparison. Analysis of the mass spectra of the purified proteins revealed that neither protein sample contained a mass equivalent to the expected mass of the wildtype or de-propionylated protein. In other words, the calculated mass corresponded to the expected mass for propionylated sfGFP (**Figure 2.43** and **Figure 2.44**). Therefore, it appears that sfGFP propionylated at Lys150 is not a substrate for de-propionylation by CobB. For AdeT1^{K280Pr}, the deconvoluted mass spectra also aligned with the expected mass for propionylated AdeT1 and a peak corresponding to wildtype AdeT1 was not observed (**Figure 2.49**). However, from these limited investigations it is not possible to draw wider conclusions on whether CobB acts to remove propionyl groups from native *E. coli* proteins.

2.5.3 Functionality of AdeT1^{K280Pr} in *E. coli*

When performing a preliminary ethidium bromide efflux assay, cells producing AdeT1^{K280Pr} had low starting fluorescence at the beginning of measurements. Specifically, the initial fluorescence reading for cells grown in the presence of 5 mM PrK was approximately half the value of that of the control cells grown in the absence of PrK. A large discrepancy in initial starting fluorescence prevents comparison between the two conditions. Measuring the rate and amount of ethidium bromide efflux over a set time period requires the initial amount of ethidium bromide in cells of both conditions to be equal. To investigate the discrepancy, the fluorescence of the cells during the 1-h incubation with ethidium bromide was measured. During this period cells are incubated under conditions which encourage ethidium bromide accumulation while maintaining cell viability. Namely, they were incubated at 200 rpm at 25 °C in the presence of an efflux pump inhibitor and 1 µg/mL ethidium bromide.

During such accumulation assays, cells producing AdeT1^{K280Pr} never increased in fluorescence to the same extent as control cells. Specifically, they exhibited a 1.5-fold increase while the fluorescence of control cells more than doubled with a 2.2-fold increase. This suggests that cells producing AdeT1^{K280Pr} were actively effluxing ethidium bromide during the incubation period. As the cellular environment should have encouraged ethidium bromide accumulation, this may suggest that cellular efflux pumps had greatly increased function or ethidium bromide recognition with AdeT1^{K280Pr}. Alternatively, it may suggest that propionylation of AdeT1 prevented the efflux pump inhibitor from interacting with AdeT1, thereby allowing efflux.

2.5.4 Effect AdeT1^{K280Pr} on antimicrobial resistance in *E. coli*

MIC testing with cells producing AdeT1^{K280Pr} revealed that production of AdeT1^{K280Pr} resulted in a 6-fold increase in erythromycin resistance in *E. coli* BL21(DE3) cells. A clear difference in concentration of erythromycin required to inhibit growth between cultures expressing AdeT1^{K280Pr} (240 µg/mL) and those expressing a truncated version of the protein (40 µg/mL), or indeed the wildtype protein and control cells (both 80 µg/mL) was observed. However, while there appeared a possible increase in chloramphenicol resistance, no increase in MIC was observed for tetracycline, ertapenem, or ampicillin. Coupled with the increased ethidium bromide efflux in cells producing AdeT1^{K280Pr}, the increase in erythromycin resistance suggests that propionylation of AdeT1 may regulate efflux pump activity or modify substrate recognition.

Interestingly, in the immunoblot analyses of cell lysates from MIC assays with erythromycin, AdeT1 signal increases with increasing erythromycin concentration. This phenomenon persists even as the amount of cell lysate decreases due to decreasing cell growth in the presence of higher concentrations of erythromycin. As expression of *adeT1(K280TAG)* was under control of the T7 promoter in this construct, it is unlikely that the cell upregulated expression of this protein. Although it is possible that cells experienced mutations which upregulated expression of either the T7 RNA polymerase or the T7 promoter under erythromycin selection.⁴⁰³ Alternatively, this result may suggest that the protein was less likely to be degraded when the cell was under increasing stress from the presence of erythromycin.

While an exciting result, it is important to remember that AdeT1 is an *A. baumannii* protein being expressed in *E. coli* in these experiments. Any implications inferred must be viewed in the context of AdeT1^{K280Pr} providing resistance to a heterologous species. As previously mentioned, it is likely that AdeT1 forms an efflux pump with endogenous *E. coli* RND-type pump components. Due to the position of membrane-fusion proteins in RND-type pumps, where they connect the outer and inner membrane proteins, it is unlikely that they provide efflux without interactions with any other proteins. In this scenario, propionylation of AdeT1 may cause a change in formation of the efflux pump complex or otherwise alter the interaction between complexed proteins. Such a change in conformation may result in increased efflux pump activity. Indeed, previous research suggests that membrane fusion proteins directly activate the inner membrane pump protein of RND complexes.³⁴² This would explain the high disparity of MIC required for erythromycin between *E. coli* producing wild type and propionylated AdeT1.

Erythromycin and ethidium bromide recognition may be conferred by the *E. coli* pump-protein rather than by AdeT1, as such, AdeT1 would not be directly responsible for conferring resistance to these substrates, but may be responsible for increasing the activity of an efflux pump which recognises them. On the other hand, propionylation of AdeT1 may directly alter substrate specificity. In more studied RND type pumps, substrate specificity has been shown to be conferred through the inner membrane pump protein.^{404, 405} Furthermore, resistance provided by RND-type pumps is cooperative and can be the result of additive interactions.^{343, 406} Thereby, the vastly increased resistance to erythromycin may not be due to this pump alone but in concert with other *E. coli* RND-type pumps. An alternative possibility is that AdeT1 may not form part of an RND-type pump in *E. coli* yet works synergistically with *E. coli* outer membrane proteins without necessarily forming a pump complex. In any case, the

results and conclusions drawn here are not directly applicable to any efflux pump occurring *in vivo*.

2.5.5 Propionylation of AdeT1 in *A. baumannii*

As this report investigates the effect of propionylation of AdeT1 in *E. coli*, this data may not be representative of the effects of AdeT1 propionylation in *A. baumannii*. As mentioned, erythromycin and ethidium bromide substrate specificity may be conferred by the RND-pump protein, in this instance an *E. coli* protein, and so AdeT1^{K280Pr} may not be directly related to erythromycin resistance in *A. baumannii*. Therefore, although from this data a relationship between AdeT1 propionylation and resistance to specific antimicrobials in *A. baumannii* cannot be inferred, it is likely that propionylation may regulate AdeT1 function or interaction with other proteins in a similar manner.

In *A. baumannii*, AdeT1 likely forms an RND-type pump with other RND-type proteins. To study the effect of propionylation of AdeT1 further, it would be of great interest to identify the outer and inner membrane proteins which naturally form a pump complex with AdeT1. Expression of all three components in *E. coli* would allow exploration of the effects of AdeT1 propionylation on the function of its endogenous RND-type pump. This would also allow more insights into whether propionylation increases resistance to specific antimicrobials through substrate recognition or whether it is a more general mechanism to increase efflux pump activity. Of course, studying propionylation in a heterologous species will always suffer from the drawback of a possible lack of synergistic effects between other native proteins. Hence, the development of methods of studying lysine propionylation in *A. baumannii* would provide valuable insights into how this modification regulates AdeT1 function *in vivo*.

2.5.6 Post-translational modification to regulate efflux pump function

It is already well documented that the regulation of expression of multidrug efflux pumps is kept under tight control through regulation by local or global transcriptional repressors or through two component systems, which allow regulation in response to environmental changes.^{328, 387} Under favourable growth conditions, such as in the laboratory, efflux pumps are expressed at only low basal levels. While the purpose of modulating efflux pump function remains speculative, it may have several advantages.³⁸⁷ Although increased efflux pump activity may increase cellular survival under stress from antimicrobial compounds, under favourable cellular environments over-activity of efflux pumps may be a disadvantage to cellular physiology. As mentioned, efflux pumps are used in many other cellular processes in addition to

antibiotic resistance mechanisms and in the absence of antibiotics, high efflux pump activity may result in the extrusion of beneficial compounds from the cell such as metabolites or signalling molecules. Modulating efflux pump function may allow control over the secretion of compounds involved in bacterial toxicity or biofilm formation. For ATP-dependent efflux pumps, lowering efflux activity when not required would conserve energy.

The data presented here indicate that lysine propionylation may also be used as a mechanism to modulate efflux pump activity. If this is the case, this reversible modification would permit tight regulation over efflux pump function, acting as a switch to alter activity as required. Such post-translational modification would allow more dynamic and faster regulation of pump activity compared to regulation by transcriptional repressors and two component systems, which control activity at the gene expression level. Propionylation may therefore be an additional level to tighten control on pump activity and allow rapid responses to environmental changes. Here, the RND-type pump containing AdeT1 was capable of ethidium bromide efflux when not propionylated, while propionylation greatly increased ethidium bromide and erythromycin efflux. Therefore, propionylation may serve as a mechanism to allow efflux activity to be fine-tuned as required, rather than binary control. As only cells producing AdeT1^{K280Pr} had increased erythromycin resistance, while those producing AdeT1 did not, propionylation may also modulate substrate specificity or recognition. Again, such modulation would provide delicate control over pump function without requiring the synthesis of new proteins or a complete cessation of pump activity. Clearly, more work is required to further unravel the intricate mechanisms controlling efflux pump function.

2.6. Conclusions

Multidrug efflux pumps are a major resistance mechanism in multidrug resistant pathogens. *A. baumannii* in particular utilises numerous RND-type efflux pumps for intrinsic resistance to a wide range of antimicrobials. Heterologous expression of resistance proteins in *E. coli* provides a convenient method of characterisation. However, in contrast to a previous report, the results presented here indicate that production of wildtype AdeT1 protein from *A. baumannii* does not confer antimicrobial resistance when expressed in *E. coli*. Further, these investigations revealed that methods used by others may not reliably result in the production of recombinant proteins during MIC assays. Modification of the standard MIC testing protocols allowed the development of an assay which maintains recombinant protein production from an expression vector during antimicrobial susceptibility testing. However, production of AdeT1 did not result in an increased MIC for any of the antimicrobials tested for *E. coli* KAM32 nor *E. coli* BL21(DE3). This highlights the importance of confirming protein production during MIC assays when characterising antimicrobial resistance proteins, particularly when characterising proteins in a heterologous species. Through more detailed investigations, it was found that production of AdeT1 in *E. coli* results in increased ethidium bromide efflux. This is most likely due to the formation of a chimeric RND-type pump composed of AdeT1 in concert with endogenous *E. coli* inner membrane pump proteins and outer membrane proteins.

As AdeT1 formed part of a functional pump in *E. coli*, the effects of lysine propionylation on the activity of this pump were characterised. AdeT1^{K280Pr} was successfully produced through genetic code expansion for unnatural amino acid incorporation in *E. coli*. Production of AdeT1^{K280Pr} resulted in high levels of ethidium bromide efflux, suggesting increased efflux pump activity. Subsequent MIC testing revealed that production of AdeT1^{K280Pr} conferred a 4-fold higher MIC value to cells in the presence of erythromycin. Together, this indicates that when produced in *E. coli*, lysine propionylation was able to modulate AdeT1 function. It is reasonable to assume that lysine propionylation may also be used to regulate the function of AdeT1 in *A. baumannii*, where this protein is propionylated *in vivo*. However, it is difficult to speculate on the exact physiological effect of this modification in *A. baumannii*. Particularly, the antimicrobial resistance profile of cells with this modification may be determined by the pump protein of an RND-type complex and AdeT1 was likely complexed with *E. coli* proteins in my studies. Nevertheless, it seems that lysine

propionylation may be used as a mechanism to regulate the activity or substrate recognition of efflux pumps involved in antimicrobial resistance.

2.7 Materials and methods

2.7.1 Plasmid construction

Plasmid **pBAD sfGFP⁴⁰⁷** was a kind gift from Dr D. Dafydd Jones. Plasmids **pPrKST** and **pAcKST** were cloned by Sanjay Patel. The pET28a control plasmid for **pET28a AdeT1*-His6** in this study is plasmid **pET28a sfGFP(150TAG)** (Addgene plasmid #133455). After IPTG induction, a 16.8 kDa protein is produced.

pAdeT1. AdeT1 in a pUC18 vector was reconstructed as described in Bharathi Srinivasan *et al*³⁵³. Vector pUC18 was digested with *Bam*HI and *Eco*RI. The *adeT1* gene was inserted using NEBuilder (New England Biolabs, #E2621S). The sequence was confirmed using primers YTS47 and YTS53.

pAdeT1-His6. Site-directed mutagenesis with primers VBF008 and VBR008 was used to insert a 6x Histidine tag at the C-terminus of the *adeT1* gene in pAdeT1 to construct pAdeT1-His6. The resulting sequence was confirmed using primers YTS47 and YTS53.

pAdeT1*-His6. The *adeT1* gene was amplified by PCR using primers VBF002 and VBR002. The resulting 973 bp fragment was cloned into a pUC18 vector linearised with restriction enzymes *Eco*RI and *Bam*HI using NEBuilder (New England Biolabs, #E2621S) to afford pAdeT1*-His6. The plasmid sequence was confirmed using primers YTS47 and YTS53.

pAdeT1*. A 3597 bp fragment was amplified from plasmid pAdeT1*-His6 using primers VBF035 and VBR033. The resulting sequence was confirmed using primers YTS47 and YTS53.

pET28a sfGFP-His6. To construct pET28a sfGFP-His6, both pET28a and pBAD sfGFP were digested with *Nco*I and *Xho*I to afford the vector and insert, respectively. The two fragments were assembled by T4 ligation (ThermoFisher Scientific, #EL0011). The resulting plasmid was sequenced with T7 promoter and T7 terminator primers.

pET28a AdeT1-His6. To construct pET28a AdeT1-His6, a 1000 bp fragment was PCR amplified and inserted into pET28a digested with *Bam*HI and *Nco*I using NEBuilder (New England BioLabs, #E2621S). The resulting plasmid was sequenced with primers YTS30 and YTS52.

pAmpR-sfGFP-His6. To construct the plasmid that constitutively expresses sfGFP by the AmpR (ampicillin resistance gene) promoter, a 3762 bp vector fragment was

PCR amplified from pET21a using primers VBF004 and VBR004, and an 827 bp fragment containing *sfGFP* was PCR amplified from pBAD *sfGFP* using primers VBF005 and VBR005. The two fragments were assembled using NEBuilder (New England BioLabs, #E2621S) to afford pAmpR-*sfGFP*-His6, which was confirmed by sequencing with primers YTS14 and YTS15.

pLac-*sfGFP*-His6. A 3728 bp vector fragment was amplified from pET21a using primers VBF007 and VBR004. A 797 bp fragment was amplified from pBAD *sfGFP* using primers VBF005 and VBR007. The two fragments were assembled using NEBuilder (New England BioLabs, #E2621S). The resulting plasmid was sequenced with primers YTS14 and YTS15.
pLacUV5-*sfGFP*-His6. The lac promoter in plasmid pLac-*sfGFP*-His6 was mutated to the LacUV5 promoter using primers VBF015 and VBR015 through site directed mutagenesis. The resulting plasmid was sequenced using primers YTS14 and YTS15.

pLacI-*sfGFP*-His6. A 4536 bp fragment was amplified using primers VBF016 and VBR016 and directly transformed into *E. coli* Stbl3 where homologous recombination afforded plasmid pLacI-*sfGFP*-His6. The plasmid sequence was confirmed using primers YTS14 and YTS15.

pAmpR-AdeT1-His6. The *adeT1* gene was cloned downstream of the constitutively active ampicillin resistance gene promoter by replacing the *sfGFP* gene in pAmpR-*sfGFP*-His6 with *adeT1*. The *adeT1* gene was amplified *via* PCR using primers VBF020 and VBR019. The resulting 991 bp fragment was inserted into pAmpR-*sfGFP*-His6 digested with restriction enzymes *XhoI* and *NcoI* and assembled using NEBuilder (New England BioLabs, #E2621S). The resulting plasmid, pAmpR-AdeT1-His6, was sequenced using primers VBS014 and VBS017.

pLacUV5-AdeT1-His6. The *adeT1* gene was amplified using primers VBF021 and VBR020 and the resulting 1000 bp fragment was inserted into pLacUV5-*sfGFP*-His6 plasmid digested with restriction enzymes *NcoI* and *XhoI*. The two fragments were assembled using NEBuilder (New England BioLabs, #E2621S) and the resulting plasmid sequenced using primers VBS014 and VBS017.

pLacI-AdeT1-His6. The *adeT1* gene was amplified using primers VBF022 and VBR020, resulting in a 1034 bp fragment and the pET21a vector was amplified using primers VBR016 and VBR004 to result in a 3717 bp plasmid. The two fragments were assembled using NEBuilder (New England BioLabs, #E2621S) and the resulting plasmid was sequenced using primers VBS014 and VBS017.

pAdeT1*(K280TAG)-His6. Site-directed mutagenesis was used to mutate the lysine codon at position 280 to the amber stop codon (TAG) using forward primer VBF027 and reverse primer VBR025. The resulting plasmid was sequenced with primers VBS014 and VBS017.

pET28a AdeT1(K280TAG)-His6. Site directed mutagenesis was used to construct plasmid pET28a AdeT1(K280TAG)-His6 using forward primer SPF001 and reverse primer SPR001 with pET28a AdeT1-His6 as a template. The resulting plasmid was sequenced with primers YTS30 and YTS52.

Table 2.2 Plasmids used in this study.

Plasmid	Vector	Insert	Antibiotic Selection	Cloning Sites	Notes
pAdeT1	pUC18	<i>adeT1</i>	Ampicillin	EcoRI BamHI	<i>adeT1</i> gene is not in frame with start codon
pAdeT1-His6	pUC18	<i>adeT1</i>	Ampicillin		
pAdeT1*-His6	pUC18	<i>adeT1</i>	Ampicillin	BamHI EcoRI	
pET28a	pET28a	<i>sfGFP</i> (150TAG)	Kanamycin		Induction of this gene results in truncated sfGFP (16.8 kDa)
pET28a-AdeT1*-His6	pET28a	<i>adeT1</i>	Kanamycin	BamHI NcoI	
pET28a-sfGFP-His6	pET28a	<i>sfGFP</i>	Kanamycin	NcoI XhoI	
pAmpR-sfGFP-His6	pET21a	<i>sfGFP</i>	Ampicillin		
pLac-sfGFP-His6	pET21a	<i>sfGFP</i>	Ampicillin		Lac promoter constitutively active due to removal of lac operator
pLacUV5-sfGFP-His6	pET21a	<i>sfGFP</i>	Ampicillin		LacUV5 promoter is constitutively active through removal of lac operator
pLacI-sfGFP-His6	pET21a	<i>sfGFP</i>	Ampicillin		
pAmpR-AdeT1-His6	pET21a	<i>adeT1</i>	Ampicillin	NcoI XhoI	
pLacUV5-AdeT1-His6	pET21a	<i>adeT1</i>	Ampicillin	NcoI XhoI	LacUV5 promoter is constitutively active through removal of lac operator

Table 2.15 continued.

Plasmid	Vector	Insert	Antibiotic Selection	Cloning Sites	Notes
pLacI-AdeT1-His6	pET21a	<i>adeT1</i>	Ampicillin		
pAdeT1(K280TAG)-His6	pUC18	<i>adeT1</i> (K280TAG)	Ampicillin		
pET28a AdeT1(K280TAG)-His6	pET28a	<i>adeT1</i> (K280TAG)	Kanamycin		
pPrKST		<i>MbPrKRS</i> , Pyl tRNA	Spectinomycin		
pAcKST		<i>MbAcKRS</i> , Pyl tRNA	Spectinomycin		MbAcKRS is a variant of MbPylRS with mutations: D76G/S123G/L266M/L270I/Y271F/L274A/C313F

Table 2.3 Primers used for PCR.

Primer	Sequence (5' – 3')	Purpose
VBF002	CAGCTATGACCATGATTACGGTGTTTGATCCGAT TGGTAAAAGCGGTGATGC	Amplification of <i>adeT1</i>
VBR002	CCTGCAGGTCGACTCTAGAGTCAGTGGTGGTGAT GATGATGTTTCATCGTTCAGG	Amplification of <i>adeT1</i>
VBF004	GTTATTGTCTCATGAGCGGATACATATTTGAATG TATTTAGAAAAATAAACAAATAGGGGTTCCGCGG ATCCAAGGAGGAACATATATCCGGATTGGCGAATG G	Amplification of pET21a backbone and addition of AmpR promoter
VBR004	TAAAGCTCGAGATCTGCAGCTGGCGCAACGCAAT TAATGTAAGTTAGC	Amplification of pET21a backbone
VBF005	CCAGCTGCAGATCTCGAGCTTTAATG	Amplification of <i>sfGFP</i>
VBR005	GTATCCGCTCATGAGACAATAACCCTGATAAATG CTTCAATAATATTGAAAAAGGAAGAGTCCATGGT TAGCAAAGGTGAAGAACTG	Amplification of <i>sfGFP</i> and addition of AmpR promoter
VBF006	ATCTTATAAGCGGGACAGGCTGACAAGAATTCAA AGGAGGAACATATATCCGGATTGG	Amplification of pET21a backbone and addition of GlnS promoter
VBR006	TTGTCAGCCTGTCCCGCTTATAAGATCCATGGTT AGCAAAGGTGAAGAACTG	Amplification of <i>sfGFP</i> and addition of GlnS promoter
VBF007	CAACATACGAGCCGGAAGCATAAAGTGTAAGAA TTCAAAGGAGGAACATATATCCGGATTGG	Amplification of pET21a backbone and addition of Lac promoter
VBR007	TTTACACTTTTATGCTTCCGGCTCGTATGTTGCCA TGGTTAGCAAAGGTGAAGAACTG	Amplification of <i>sfGFP</i> and addition of Lac promoter
VBF008	GAATGTGCCCTGAACGATGAACACCATCATCATC ACCATTAAGGATCCTCTAGAGTCGACCTG	Addition of 6x His tag to <i>adeT1</i>
VBR008	TCATCGTTCAGGGCACATTC	Addition of 6x His tag to <i>adeT1</i>
VBF015	ACATTATACGAGCCGGAAGCATAAAGTGTAAGC CTGGGGTGCCCTAATGAGTGAGAATTCAAAGGAGG AACTATATCCGGATTGG	Conversion of Lac promoter to LacUV5 promoter
VBR015	GCTTCCGGCTCGTATAATGTGTGGAAAAGCTTGG ATCCCATGGTTTCACACAGGAAACAGCTATGGTT AGCAAAGGTGAAGAACTG	Conversion of Lac promoter to LacUV5 promoter

VBF016	GACACCATCGAATGGCGCAAAACCTTTCGCGGTA TGGCATGATAGCGCCCGGAAGAGAGTCAATTCAG GGTGGTGAATATGGTTAGCAAAGGTGAAGAACTG	Amplification of <i>sfGFP</i> and addition of LacI promoter
VBR016	TTGCGCCATTCGATGGTGTCTGAATTCAAAGGAGG AACTATATCCGGATTGG	Amplification of pET21a and addition of LacI promoter
VBR019	CGTTGCGCCAGCTGCAGATCTCGAGCTTCAGTGG TGGTGATGATGATGTTTCATCGTTCAGG	Amplification of <i>adeT1</i> for LacI promoter
VBF020	TGCTTCAATAATATTGAAAAAGGAAGAGTCCATG TTTGATCCGATTGGTAAAAGCGGTG	Amplification of <i>adeT1</i> and addition of AmpR promoter
VBR020	GCGCCAGCTGCAGATCTCGAGCTTTAGTGGTGGT GATGATGATGTTTCATCGTTCAGG	Amplification of <i>adeT1</i> for pET21a vector
VBF021	GTGTGGAAAAGCTTGGATCCCATGGTTTTCACACA GGAAACAGCTATGTTTGATCCGATTGGTAAAAGC GGTGATGC	Amplification of <i>adeT1</i> and addition of LacUV5 promoter
VBF022	GACACCATCGAATGGCGCAAAACCTTTCGCGGTA TGGCATGATAGCGCCCGGAAGAGAGTCAATTCAG GGTGGTGAATATGTTTGATCCGATTGGTAAAAGC GGTGATGC	Amplification of <i>adeT1</i> and addition of LacI promoter
VBR025	GGGATCATAAATACCTGCTTTGGTC	Insertion of TAG codon into <i>adeT1</i>
VBF027	AAGCAGGTATTTATGATCCCTAGATGATGAACTT CCTGAAGAAAGTGC	Insertion of TAG codon into <i>adeT1</i>
VBR033	TGCAGGTCGACTCTAGAGTCATTCATCGTTCAGG GCACATTC	Removal of His tag from <i>adeT1</i>
VBF035	TGACTCTAGAGTCGACCTGCAG	Removal of His tag from <i>adeT1</i>
SPF001	TTCATCATCTAGGGATCATAAATACCTGCTTTGG TCAG	Insertion of TAG codon into <i>adeT1</i>
SPR001	TATGATCCCTAGATGATGAACTTCCTGAAGAAAG TGC	Insertion of TAG codon into <i>adeT1</i>

Table 2.4 Primers used for sequencing.

Primer	Sequence	Aligns to
YTS14	CCGATTCTGGTGGAACTG	<i>sfGFP</i>
YTS15	TAGGTCAGGGTGGTCAC	<i>sfGFP</i>
YTS30	ATGGTGTCCGGGATCTC	<i>lacI</i> promoter/pET28a vector
YTS47	GCCTTTTGCTCACATGTTC	pUC18 vector
YTS52	TTAATGCGCCGCTACAG	f1 ori
YTS53	AAATACCGCACAGATGC	<i>lacZ</i> α
VBS014	CATTGGTCCGGCATAACC	<i>adeT1</i>
VBS017	CAATCGGTGCCGGAAC	<i>adeT1</i>

2.7.2 Bacterial protein expression

Chemical transformation

Most plasmids in this study were transformed into *E. coli* TG1 KAM32 (Δ *acrB*, Δ *ydhE*) cells, which were provided as a kind gift from Professor Teruo Kuroda, Hiroshima University. Plasmids containing the T7 promoter (pET28a, pET28a AdeT1-His6, pET28a AdeT1(K280TAG)-His6 and pET28a sfGFP-His6) were transformed into *E. coli* BL21(DE3) cells.

Constitutive expression

A single colony was used to inoculate 5 mL Mueller Hinton Broth (MHB), Sigma-Aldrich #70192) and incubated at 37 °C, 180 rpm, for 16-18 hours. Culture was then diluted to A₆₀₀ 0.01 into 5 mL fresh MHB and 100 μ L/well of this dilution was plated in 3 wells of a 96-well plate and incubated at 37 °C, 180 rpm, for 16-18 hours.

Inducible protein expression

For all expressions, a starter culture was prepared by inoculating a single colony into 5 mL media and incubated at 37 °C, 180 rpm, for 16-18 hours. The starter culture was then diluted in fresh media to an A₆₀₀ of 0.05 and incubated at 37 °C, 180 rpm. At A₆₀₀ 0.6, protein expression was induced with a final concentration of 0.5 mM IPTG.

For MIC testing, MHB was used and cultures were incubated at 37 °C, 180 rpm, for 2 hours after induction before MIC testing.

When expressing protein for purification, terrific broth (TB) medium was used. When supplementing with 20 mM nicotinamide, this was added with IPTG at A_{600} 0.6. The temperature after induction was lowered to 20 °C and cultures incubated at 180 rpm for 16-18 hours.

PrK incorporation

Cells were co-transformed with both the expression plasmid containing the TAG codon (*i.e.*, pAdeT1*(K280TAG)-His6 or pET28a AdeT1(K280TAG)-His6) and a second plasmid containing either acetyl-lysine (AcK) or propionyl-lysine (PrK) synthetase and 1 copy of the corresponding tRNA (*i.e.*, pAcKST or pPrKST). Transformation protocol was followed as above, and 500 μ L of the transformation mixture was used to directly inoculate 5 mL of MHB supplemented with appropriate antibiotics for plasmid selection and incubated at 37 °C, 180 rpm, for 16-18 hours.

For MIC testing, the culture was then diluted to A_{600} 0.05 in 12.5 mL fresh MHB and incubated at 37 °C until A_{600} 0.6. At this point, 0.5 mM IPTG was added to the culture, which was split in half equally. To one half, 5 mM PrK was added and the other left as a negative control. Both cultures were incubated at 37 °C, 180 rpm for 2 hours before antibiotic testing.

For protein expression, the overnight culture was diluted to A_{600} 0.05 in 100 mL fresh TB and incubated at 37 °C until A_{600} 0.6. At this point, 0.5 mM IPTG and 5 mM PrK were added to the culture. The incubation temperature was lowered to 20 °C and the culture incubated at 180 rpm for 16-18 hours.

2.7.3 Minimum Inhibitory Concentration testing

For dilution studies, 2 hours post-induction the culture was diluted to A_{600} 0.01 or 0.001 as appropriate in fresh MHB containing plasmid selection antibiotics, 0.5 mM IPTG and varying concentrations of the test antibiotic. Cultures were then incubated at 37 °C, 180 rpm, overnight.

When test antibiotics were added directly to the liquid culture, 2 hours post induction the culture was divided into 10 mL fractions, and chloramphenicol added directly. The culture was then incubated for 18 hours at 37 °C, 180 rpm.

For solid media MIC testing, 2 hours post-induction, the A_{600} of all cultures were normalised to A_{600} 4.0 and 20 μ L of these adjusted cultures were then dropped onto LB agar plates containing 0.5 mM IPTG, plasmid selection antibiotics, and various

test antibiotic concentrations and incubated at 37 °C for 18 hours. When genetic code expansion was implemented, the agar plates also contained \pm 5 mM PrK as appropriate.

2.7.4 SDS-PAGE and Western blot

Samples from liquid cultures were taken by normalising the A_{600} to 1.5 and taking 1 mL. Cells were then pelleted and resuspended in 50 μ L of SDS loading dye. For low volume liquid cultures, e.g. cultures in 96 well plate or Eppendorf tubes, where normalising the A_{600} was not possible, the whole culture was pelleted and resuspended in 10 μ L loading dye. For solid cultures from agar plates, the whole colony was resuspended in PBS, pelleted and resuspended in 10-50 μ L loading dye depending on cell density of colony.

Samples were heated (95 °C, 5 minutes) and 10 μ L of all samples were loaded onto 12% SDS-PAGE and electrophoresed with 155 V, 55 mA, for 1 hour. The gel was transferred to a 0.2 μ M nitrocellulose membrane (BioRad, #1704158) using a Trans-Blot Turbo Transfer System (BioRad, #1704150) with mixed molecular weight setting applied. Membrane was then stained with Ponceau S (0.1% Ponceau S in 5% acetic acid), then blocked in 5% (w/v) milk (Sigma-Aldrich, #70166) PBST for 1-2 hours at 18 °C with gentle agitation. Membrane was then transferred to 5% milk PBST containing primary mouse 6x His tag monoclonal antibody (ThermoFisher, #MA121315, 1:1000 (v/v) dilution) and incubated overnight at 4 °C. Membrane was then washed for 5 minutes in PBST 3 times, before incubation with 5% milk PBST containing goat anti-mouse IgG (H+L) secondary antibody (ThermoFisher #32430, 1:1000 (v/v) dilution) for 1-2 hours at 18 °C with gentle agitation. Membrane was then washed for 5 minutes in PBST 3 times. Signal was developed using Clarity Max (Bio-Rad, #1705062) and imaged using a ChemiDoc XRS+ system (Bio-Rad, #1708265).

2.7.5 Fluorescence intensity measurements

Samples of the culture after overnight expression were taken by normalising the A_{600} to 1.5 and taking 1 mL of culture, which was pelleted and resuspended in 1 mL PBS. Then, 3x 100 μ L was loaded onto a 96 well plate (Fisher Scientific, #167008). Samples from cultures grown in a 96 well plate were taken by centrifuging cultures in plate, discarding supernatant and resuspending in 100 μ L PBS. A_{600} was measured on a Victor X (Perkin Elmer) plate reader using the OD₆₀₀ protocol (CW-lamp OG590, filter B7) with 5 seconds shaking before measurement. Fluorescence intensity was measured on FLUOstar (Optima) plate reader with excitation at 485 nm and emission at 520 nm and gain set to 804.

2.7.6 Ethidium bromide efflux and accumulation assays

Ethidium bromide efflux assays were performed as described by Viveiros *et al.*, 2008.³⁷⁸ *E. coli* BL21(DE3) cells were transformed with the specified plasmid and appropriate antibiotics were used in the media for plasmid selection. Cells were grown to A_{600} 0.6 before 0.5 mM IPTG was added to cultures. For PrK incorporation, PrK was added at A_{600} 0.5 and IPTG was added 30 min later. 1 h post protein induction, cells were transferred to microcentrifuge tubes and centrifuged at 13,000 $\times g$ for 3 minutes and resuspended in PBS containing 0.5 mM IPTG, 100 $\mu\text{g/mL}$ 1-(1-naphthylmethyl)-piperazine and 0.5 $\mu\text{g/mL}$ ethidium bromide. 1-(1-Naphthylmethyl)-piperazine is an efflux pump inhibitor.⁴⁰⁸ When incorporating PrK, the PBS was also supplemented with 5 mM PrK.

For accumulation assays, at this point 100 μL of cells were transferred to a black 96-well microplate in triplicate. Fluorescence was measured every minute for 1 hour while cells were incubated with constant shaking at 25 °C. For efflux assays, cells were incubated at 25 °C for 1 h at 180 rpm. After incubation, cells were centrifuged at 13,000 $\times g$ for 3 minutes and resuspended in PBS containing 0.4% glucose. 100 μL of cells was then transferred to a black 96-well microplate in triplicate and fluorescence was measured every minute for 15 minutes while cells were incubated with constant shaking at 37 °C. In both instances, fluorescence measurements were obtained with a FLUOStar (Optima) plate reader (ex 500, em 590, gain 4095). Each experiment contains three technical replica for each condition, and at least three biological repeats of each experiment were conducted.

2.7.7 Protein purification

Nickel affinity purification

As described in **Chapter 5 - General materials and methods**. For purification of AdeT1 protein, all buffers also contained 6 M urea.

Buffer exchange

A desalting column was equilibrated in 3 column volumes phosphate buffer. The protein to be exchanged was diluted to 10 mL and loaded onto the column and eluted using phosphate buffer in 1 mL fractions. Protein concentration of collected fractions were briefly analysed at the bench using Bradford's Reagent (ThermoFisher, #23236) and then analysed using SDS-PAGE.

Concentrating

To concentrate protein samples, Vivaspin ultrafiltration units with 10,000 Da molecular weight cut off and polyethersulfone (PES) membranes were used (Sartorius, #VS2001 and #VS0102) as per manufacturer's instructions.

2.7.8 Mass spectrometry

Samples were analysed using SYNAPT G2-Si Mass Spectrometry (Waters) as described in **Chapter 5 - General materials and methods**.

Trypsin Digestion

1 µg of trypsin (Melford, #T70010) was added to 100 µg of AdeT1 protein at 100 µg/mL concentration and incubated for 18 hours at 37 °C. The digest was then diluted 1:1 with acetonitrile before analysis.

Chapter 3 – Investigating the effects of lysine acetylation on the *Escherichia coli* DNA-binding HU protein

3.1 Summary

HU is a prevalent DNA binding protein ubiquitous among bacteria and has been implicated in a wide range of cellular processes and phenotypes, including antimicrobial resistance. Lysine acetylation is a prominent post-translational modification with significant biological importance. *Escherichia coli* HU is acetylated on several lysine residues *in vivo*. Two of these residues are on the DNA binding-loop and the DNA binding interface, respectively. This chapter investigates the effect of acetylation of these two residues on DNA binding affinity. It was discovered that acetylation of one residue, Lys86, significantly reduces the DNA binding affinity of the homodimer HU β_2 . This result provides a clear example of post-translational modification directly impacting protein function and adds to the growing body of knowledge about HU-DNA interactions.

This chapter contributed towards the publication:

Barlow, V.L. and Tsai, Y.T. Acetylation at lysine 86 of *Escherichia coli* HU β modulates the DNA-binding capability of the protein. *Front. Microbiol.* 12, 809030 (2022).

3.2 Introduction

3.2.1 *Escherichia coli*

Escherichia coli is perhaps the most well documented bacteria to date. This is partially facilitated by its ease of handling and manipulation; it is a well known workhorse of molecular biology laboratories.⁴⁰⁹ However, the common laboratory strains comprise only a small subset of *E. coli*. A very diverse bacterium with many niches, the core genome shared by all strains represents only 20% of all analysed *E. coli* gene clusters.⁴¹⁰ In nature, *E. coli* principally forms part of the gut microbiota of humans and warm-blooded animals. The bacterium colonises the lower intestine, where it has a commensal relationship with its host.⁴¹¹ However, some strains of these commensal bacteria act as opportunistic pathogens under appropriate conditions. In total, six pathotypes have been identified which are capable of causing human disease.⁴¹² These diseases can be enteric, e.g. diarrhoea and dysentery, or extra-intestinal infections, e.g. urinary tract infections and meningitis.⁴¹³ Diseases can range from mild to severe; *E. coli* are by far the most common cause of urinary tract infections⁴¹⁴ but are also the most common cause of Gram-negative neonatal meningitis, which has case fatality rates of 15-40% and leaves severe neurological defects in survivors.⁴¹⁵

An array of virulence factors distinguishes pathogenic *E. coli* from their commensal relatives. For example, adhesins allow colonisation of sites normally inhabitable by *E. coli* and toxin excretion causes wide ranging disruption to host cells.⁴¹² Particularly, possession of the type VI secretion system, a protein nanomachine which facilitates direct injection of toxins into adjacent cells, allows potent pathogenicity.⁴¹⁶ Genes encoding virulence factors are often located on plasmids, bacteriophages, transposons and pathogenicity islands. The mobilisation of these elements through horizontal gene transfer facilitates the spread and combination of virulence factors.⁴¹⁷ For example, no single phenotypic profile has been determined that causes urinary tract infections, several adhesins and toxins are thought to be important and are found in varying percentages among isolates.^{418, 419}

Urinary tract infections caused by *E. coli* are one of the most common infections in the world. Multi-drug resistance is a prevalent problem in such diseases, particularly in developing countries but also with increasing speed in developed countries, and is considered a serious health concern.⁴²⁰⁻⁴²⁴ Multi-drug resistant strains are also commonly isolated from animals and food products, due to the use of antibiotics in

farming.⁴²³ Multi-drug resistant pathogenic *E. coli* strains display resistance to antimicrobials through a variety of mechanisms including production of antibiotic-degrading enzymes, expression of efflux pumps, reduced membrane permeability and decreased uptake of antibiotics.⁴²¹ The rapid spread of antimicrobial resistance is mainly facilitated through horizontal gene transfer of primarily plasmid-encoded genes.⁴²³ Of greatest concern are the rapid spread of genes encoding extended spectrum β -lactamases, carbapenemases, 16S rRNA methylases, and plasmid-mediated quinolone resistance genes.⁴²⁴ *E. coli* is quickly obtaining a large number of defences against current antimicrobials, necessitating new and alternative therapies.^{417, 423, 425}

In contrast to the previous chapter which focussed on a protein with known and direct activity against antimicrobials, this chapter will explore a broader antimicrobial target. DNA-binding proteins are ubiquitous in bacteria, where they have wide ranging effects on cellular transcription. Inhibiting DNA-binding proteins may weaken bacterial survival and interfere with gene regulation in response to stressors such as antibiotics. As such, DNA-binding proteins are a promising antimicrobial target for standalone use or in combination with existing antimicrobials. Here, the effects of post-translational modification of the DNA-binding protein HU will be investigated. A highly conserved protein, understanding the complex mechanisms regulating HU will enable insights into potential antimicrobial targets not just for *E. coli*, but for an array of bacterial species.

3.2.2 Histone-like HU protein

The HU protein is a prevalent DNA-binding protein ubiquitous among bacterial species. The small, basic protein exists as a dimer, composed of two 9 kDa monomeric units. HU is also capable of forming larger structures such as trimers and tetramers *in vitro*.⁴²⁶ The protein structure is highly conserved across species, consisting of an α -helical 'body' and two β -sheets that are extended to β -ribbon 'arms' which interact directly with DNA (**Figure 3.1**).⁴²⁷ HU is one of the most abundant proteins in *E. coli*, where an average of 30,000 dimers can be found per bacterial cell.⁴²⁸

The majority of bacterial species express one HU protein, which forms homodimers. *E. coli* is unique in expressing two variants of the HU protein: HU α and HU β , encoded by *hupA* and *hupB*, respectively. Consequently, three distinct dimeric forms of HU exist. HU α and HU β can each form homodimers (HU α_2 and HU β_2) alongside a heterodimer (HU $\alpha\beta$) (**Figure 3.1**). The majority of HU species found in *E. coli* are

HU $\alpha\beta$ heterodimers, which accumulate in the exponential phase and account for the vast majority (ca. 95%) of species in the stationary phase.⁴²⁹ Indeed, when purified HU α_2 and HU β_2 are combined in a 1:1 molar ratio *in vitro*, the chains will spontaneously rearrange to form the heterodimer.⁴³⁰ The proportion of each dimer changes throughout the cell cycle.⁴²⁹ In the lag and early exponential growth phase, HU α_2 accumulates. In the late exponential and stationary phase, HU $\alpha\beta$ predominates. HU β_2 is the least prevalent dimer and accounts for 5% of dimers in the stationary phase. For the remainder of this chapter, unless otherwise stated, 'HU' refers to the *E. coli* HU protein.

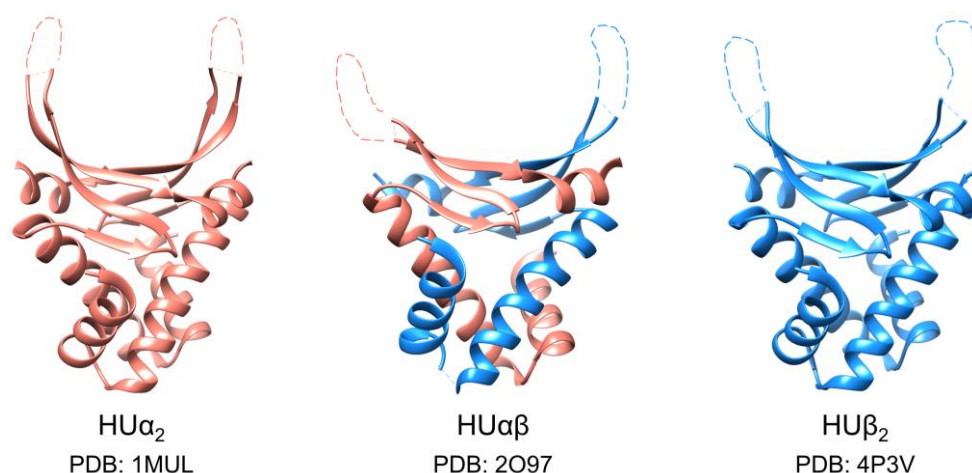


Figure 3.1. Crystal structures of the three dimeric forms of *E. coli* HU. HU α_2 (PDB #1MUL), HU $\alpha\beta$ (PDB #2O97), and HU β_2 (PDB #4P3V) share a highly similar structure composed of an α -helical body with β -sheet arms. As electron density data is not available for the β -sheet arms, likely due to their flexible nature in solution, they are illustrated for visualisation purposes with a dashed line.

3.2.3 DNA binding by HU protein

HU binds DNA in a sequence-independent manner and is capable of binding both single- and double-stranded DNA with a preference for double stranded. In the *E. coli* cell, HU is found to be randomly distributed across the genome. Although HU does not seem to preferentially bind to specific DNA sequences, it displays a strong preference for specific DNA structures. HU will preferentially bind supercoiled DNA over native B-form DNA.⁴³¹ HU demonstrates the highest affinity for DNA with structural deformities such as gaps, nicks, bends, hairpins, and cruciform DNA.⁴³² When bound to DNA, HU can induce flexible bends of 10 to 180°. ^{427, 433-435} The heterodimer displays greatly higher affinity for DNA than either homodimer. ^{436, 437}

Although HU-DNA interaction is well established, the exact molecular interaction between *E. coli* HU and DNA remains uncertain. Attempts to obtain high resolution crystal structures of *E. coli* HU bound to DNA have been thwarted. When high resolution structures of *E. coli* HU in the absence of DNA have been obtained, electron density data is not available for the β -ribbon arms, likely due to their mobility in solution. Despite these difficulties, two domains of HU have been identified as important for DNA binding (**Figure 3.2**). Swinger and colleagues succeeded in obtaining a crystal structure of *Anabaena* HU bound to a pseudo-self-complementary duplex containing three thymine to thymine mismatches and four unpaired thymine bases (**Figure 3.2A**).⁴²⁷ The β -ribbon arms of HU wrap around the DNA minor groove, with a conserved proline residue at the tip of each arm intercalating between base pairs to introduce and/or stabilise two kinks in the DNA duplex. The β -ribbon arms composed of residues 52 to 74 contain many positively charged amino acids (**Figure 3.3**), which interact directly with the negatively charged phosphate backbone of DNA. Due to the high structural similarities between the two proteins, it is likely that *E. coli* HU will interact with DNA in a similar manner. The α -helical body also contains a DNA binding interface consisting of two lysine residues, Lys83 and Lys86.^{438, 439} In the *Anabaena* HU-DNA co-crystal structure, this region interacts not only with directly bound DNA but also with DNA bound to nearby dimers in adjacent crystalline units, with the DNA forming a pseudo-continuous helix.⁴²⁷ The importance of this domain was also emphasised when Hammel and colleagues managed to use small angle X-ray scattering to obtain crystal structures of HU $\alpha\beta$ and HU α_2 interacting with 19 bp and 20 bp B-form DNA complexes in solution (**Figure 3.2B**).⁴³⁸ Interestingly, loss or modification of either DNA binding interface is tolerated by HU, but simultaneous alteration of both eliminates DNA binding capacity.⁴³⁹ These interfaces have been interpreted by others to be one larger DNA binding domain, consisting of the entire β -ribbon arms and the α -helical C-terminal of the protein.^{440, 441}

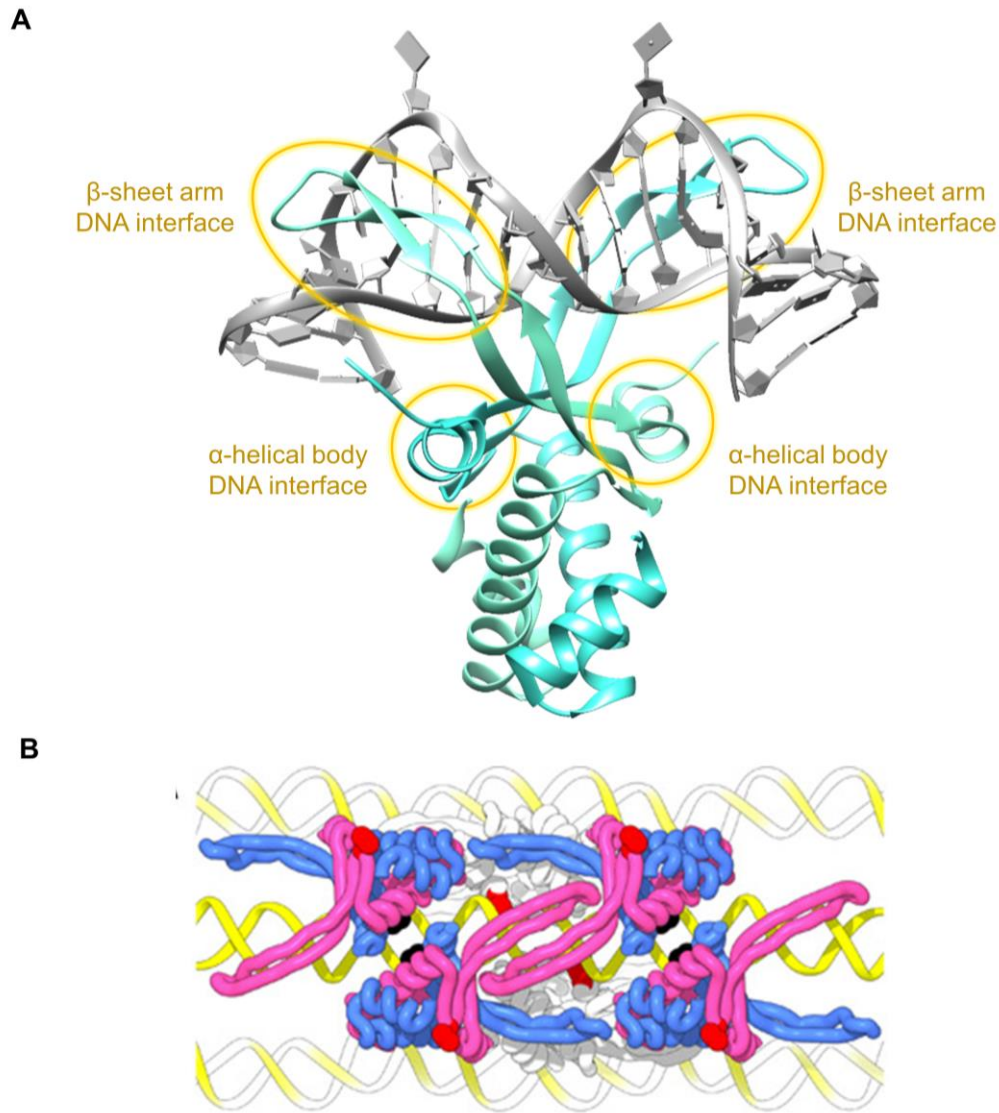


Figure 3.2 Alternative DNA-binding modes of HU. **A** Cocrystal structure of *Anabaena* HU bound to a pseudo-self-complementary DNA duplex containing three T:T mismatches and four unpaired Ts (PDB #1P71). The two highly conserved DNA binding interfaces of each HU monomer are shown in yellow circles. The β -ribbon arms of each monomer contains positively charged amino acid residues which interact directly with DNA. The α -helical body of each monomer also contains a positively charged DNA binding interface which interacts with DNA. When bound to structurally deformed DNA, HU interacts with the DNA primarily through its β -arms, inducing and stabilising a flexible hinge or bend in the DNA. **B** Small angle X-ray scattering crystal structure of *E. coli* HU $\alpha\beta$ bound to a 19 bp B-form DNA complex (PDB #4YEW). When interacting with native DNA, HU primarily interacts through the DNA binding interface of its α -helical body. Reproduced under license [CC BY-NC 4.0](#).⁴³⁸

Existing crystal structures have revealed that HU exhibits at least two alternative DNA binding modes (**Figure 3.2**). As evidenced in the crystal structure of *Anabaena* HU with DNA, when interacting with structurally deformed DNA, HU primarily interacts with the DNA through its β -ribbon arms, bending the DNA around its α -helical body through interactions with the DNA binding interface. Due to the high sequence similarity between *Anabaena* HU and *E. coli* HU (**Figure 3.3**), it is likely that *E. coli* HU will also interact with structurally deformed DNA in a similar manner. Indeed, multiple studies have found evidence of *E. coli* HU bending structurally deformed DNA.^{427, 433, 434} When interacting with native B-form DNA, *E. coli* HU primarily interacts through the α -helical body. The positively charged residues in the DNA binding interface form interactions with the DNA. Interaction with native DNA does not stabilise the β -ribbon arms, distinguishing the two alternative binding modes. When interacting with B-form DNA, pairs of dimers also interact across the DNA strand, primarily through hydrogen bonds. Notably, these interactions induce straightening of the DNA axis as opposed to the bending observed in complexes with structurally aberrant DNA. Intriguingly, HU α_2 is also capable of forming networks and of DNA bundling while this was not observed for the heterodimer.⁴³⁸

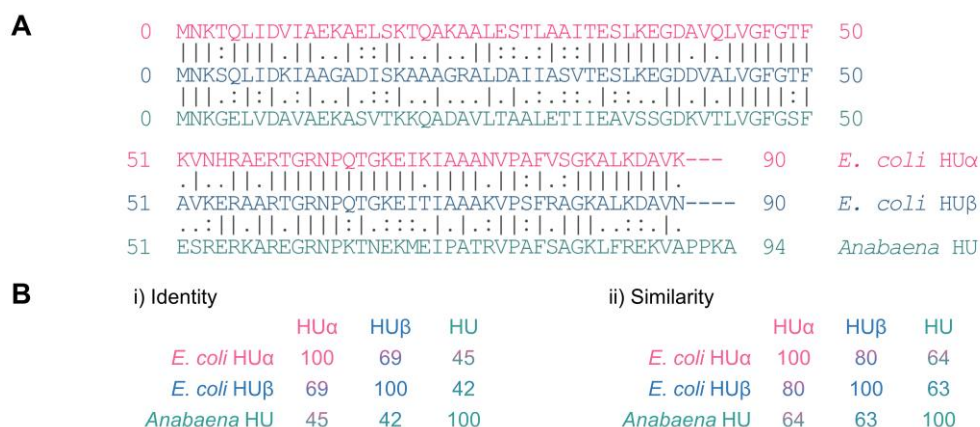


Figure 3.3 Sequence alignment of *E. coli* HU α , *E. coli* HU β and *Anabaena* HU. **A** Amino acid sequence alignment of *E. coli* HU α with *E. coli* HU β and *E. coli* HU β with *Anabaena* HU. A dash (-) represents mismatch or gap in the sequence, one dot (.) indicates a small positive similarity score between residues, two dots (:) represent a positive similarity score greater than 1, while a line (|) indicates that an identity has the same residue in both sequences. **B** The sequence i) identity and ii) similarity of the three sequences are shown.

3.2.4 Physiological roles of HU

HU is classified as a nucleoid associated protein yet the exact role of HU in the nucleosome is subject to debate.⁴⁴² HU has been indicated by various studies to have roles in both DNA compaction and relaxation. For example, when the *hupA* and *hupB* genes are deleted from *E. coli*, mutant strains display genome decompaction, whereby DNA is distributed randomly and evenly across the cell.^{443, 444} Conversely, high concentrations of HU protein have been shown to expand plasmid DNA from supercoiled into an open circular shape.⁴⁴² A later study clarified that at high concentrations HU initially causes DNA to form rigid filaments, but this effect is no longer observed after 2 h, when DNA returns to the pre-treated state.⁴⁴⁵ At low concentrations, HU induces very flexible bends in DNA responsible for compaction but at high concentrations rigid nucleoprotein filaments are formed, in which HU arranges helically around the DNA without condensing it.⁴⁴⁶ HU binds duplex DNA in different modes depending on concentration of HU, DNA length and DNA structure.^{438, 447} It has been suggested that HU performs both roles, under certain conditions compacting and in others relaxing the DNA with the conversing actions resulting in the wildtype nucleosome phenotype.⁴⁴⁸

As previously mentioned, HU has the highest affinity for structurally deformed DNA, such as DNA with cruciform structure, containing nucleotide gaps or nicks in the phosphate backbone. These DNA structures are those of DNA repair intermediates, indicating that HU may be involved in DNA repair mechanisms.⁴³² The affinity of HU for such DNA is so high that it specifically recognises and preferentially binds cruciform DNA even in the presence of a 100-fold excess of linear DNA.⁴⁴⁹ Further, when bound to such DNA repair intermediates, HU protects the DNA from the activity of exonucleases, preventing DNA degradation.⁴³² HU has a role in the repair of closely located lesions on opposite DNA strands, and prevents them leading to a double-stranded break in the DNA.⁴⁵⁰ Cells deficient in HU are extremely sensitive to UV irradiation⁴⁵¹⁻⁴⁵³ and it is highly likely that this sensitivity is due to an inhibited ability to repair damaged DNA.

Deleting either *hupA* or *hupB* from the *E. coli* genome does not significantly impair cell growth. However, when both are removed, the $\Delta hupAB$ mutant is highly pleiotropic: cell division, initiation of DNA replication, transposition and other biochemical functions are altered, causing a slow-growth phenotype.^{444, 454} In *Bacillus subtilis*, which has no other histone-like protein, the HU knockout is unviable.⁴⁵⁵ Expression of a mutant version of the HU α_2 heterodimer, HU $\alpha^{E38K, V42L}$, induces a variety of changes to the *E. coli* cell, including major changes to cellular morphology

from rods to cocci, altered transcription of hundreds of genes, and conversion of the laboratory strain *E. coli* K-12 from commensal to invasive. This phenotypic change is reversed when the gene encoding wildtype HU α_2 is provided on a plasmid.⁴⁵⁶

HU has also been heavily implicated in transcription and transcriptional regulation. HU has been demonstrated to control the transcription of 353 genes, comprising 8% of the *E. coli* genome.⁴⁵⁷ As a transcription factor, HU influences important metabolic cycles such as virulence, initiation of DNA replication, cell division, SOS response and galactose metabolism.⁴⁵⁸ For example, HU is essential for the formation of the Gal repressosome complex,⁴⁵⁹⁻⁴⁶¹ whereby looping of the DNA by the Gal repressor and HU prevents initiation of transcription of the *gal* operon.⁴⁶² HU can constrain transcription-induced supercoiling,⁴⁶³ yet also has the ability to induce negative supercoiling into relaxed DNA in the presence of topoisomerase I.⁴⁶⁴ This dual role in constraining or allowing negative supercoiling on DNA affects access by transcription factors⁴³⁸ and directly affects gene expression.^{463, 464} The homodimeric and heterodimeric forms influence gene expression differently. The HU α_2 homodimer forms DNA networks early in cell division; HU $\alpha\beta$ does not form these networks, allowing for topoisomerase to supercoil and condense the DNA more.⁴³⁸ The two mechanisms influence the altered gene expression during cell growth stages, evidenced by a correlation between nucleoid remodelling by HU and the altered regulation of hundreds of genes.⁴⁶⁵ Nucleoids of cells expressing the HU $\alpha^{E38K, V42L}$ mutant are considerably more condensed compared to wildtype cells. This mutant also altered the global transcription profile, providing evidence that HU directly regulates gene expression.⁴⁵⁶ HU $\alpha^{E38K, V42L}$ forms a multimeric complex which wraps DNA around the protein core surface to form nucleosome-like structures and also bound to different regions of genome compared to wildtype.⁴⁶⁶

HU also interacts with various other proteins in the cell, although knowledge of these interactions is still incomplete. HU modulates the formation of pre-replication complexes,⁴⁶⁷ repressosomes,⁴⁶⁸ and may play a role in the formation of higher protein complexes that regulate the initiation of gene transcription.⁴⁵⁸ HU also facilitates binding of integration host factor, a sequence specific nucleoid associated protein, to DNA *in vitro*.⁴²⁶ In *Mycobacterium tuberculosis*, HU forms a complex with another nucleoid associated protein; the complex has novel transcriptional regulatory properties which the two individual proteins do not.⁴⁶⁹ This versatile protein also acts as a molecular glue, allowing close interactions of negatively charged bacterial membranes with extracellular DNA in biofilms.⁴³⁹

3.2.5 Role in antimicrobial resistance

HU has been implicated in antimicrobial resistance in various bacterial species. For example, carbapenemase-producing *E. coli* and other *Enterobacteria* have been found to overexpress HU.⁴⁷⁰ While *E. coli* strains lacking *hupA* and *hupB* exhibit extreme sensitivity to chloramphenicol.⁴⁴⁴ In *Mycobacteria*, mutation of Lys86 to arginine resulted in significantly fewer colonies when plated on agar with concentrations of antibiotic near to the minimum inhibitory concentration and specifically resulted in the loss of the small colony variant phenotype implicated in reduced antimicrobial susceptibility.¹⁰⁴ The wide biological roles of HU in transcription, genome replication, DNA repair, virulence, and regulation of metabolism have led to the suggestion that HU should be given more attention as an antimicrobial response modulating protein⁴⁵⁸ and be considered as a target for controlling microbial systems.⁴³⁸

HU has been a target for preventing cell growth in the highly antimicrobial resistant *Mycobacterium tuberculosis*; Bhowmick and colleagues designed an inhibitor which specifically targets DNA binding interface of *M. tuberculosis* HU protein.⁴⁴⁰ Their inhibitor prevented HU binding DNA and was demonstrated *in vivo* to affect nucleoid architecture and inhibit cell growth. Another inhibitor design was employed by Agapova *et al.*, where the inhibitors successfully prevented DNA binding by HU from *E. coli*, *Spiroplasma melliferum* and *Mycoplasma gallicepticum*.⁴⁴¹ The inhibitor also demonstrated antimicrobial properties against the mycoplasma species, albeit not against *E. coli* due to the compensatory role of other nucleoid associated proteins. Even in species where HU is not essential for cell viability, inhibiting HU may negatively affect bacterial survival due to its involvement in gene expression and DNA repair mechanisms. Due to the highly conserved structure of HU protein, any inhibitor or other therapy to target HU is likely to be easily adapted to target HU in other bacterial species. HU therefore represents a promising avenue to complement antimicrobial therapy.

3.2.6 Post-translational modifications of DNA-binding proteins

In the eukaryotic DNA-binding proteins, histones, PTMs have impactful effects on DNA replication, compaction and levels of transcription.⁴⁷¹⁻⁴⁷³ The four most abundant bacterial DNA binding proteins (HU, H-NS, IHF and FIS) all undergo extensive PTM, leading to a mostly unanswered question of whether these modifications have similar functional implications for bacterial DNA binding proteins.⁴⁷⁴ For example, H-NS undergoes many PTMs including lysine acetylation and succinylation; arginine methylation; serine, tyrosine and threonine phosphorylation; asparagine deamidation;

and methionine oxidation, although the functional implications of such modifications remain speculative.⁴⁷⁵ HU itself is subjected to several PTMs, undergoing phosphorylation, methylation, succinylation, and acetylation in various species.⁴⁵⁸

There have been only a handful of studies characterising such modifications. In three *M. tuberculosis* transcriptional regulators, phosphorylation was demonstrated to abolish interactions with promoters of transcriptional targets.¹⁶² Similarly, phosphorylation at Thr112 of *M. tuberculosis* Lsr2 decreased DNA binding, resulting in altered expression of genes involved in growth in survival.⁴⁷⁶ On the other hand, tyrosine phosphorylation of a *B. subtilis* single-stranded DNA-binding protein increased single-stranded DNA binding 200-fold through an unknown mechanism.¹⁵⁶ S-nitrosylation was also found to decrease DNA binding in the *E. coli* and *P. aeruginosa* transcriptional regulator OxyR, which undergoes S-nitrosylation during nitrosative stress.⁴⁷⁷ For both *M. tuberculosis* and *Myxococcus xanthus* HU it has been demonstrated that phosphorylation diminishes the interaction with DNA.^{272, 478} Finally, acetylation at Lys13 of *A. baumannii* HU was demonstrated to affect both thermal stability and DNA binding kinetics.³⁶³

PTMs of DNA-binding proteins have been predicted to influence DNA-binding affinity, oligomerisation and protein-protein interactions.⁴⁷⁴ While recently many advances have been made in identifying which DNA-binding proteins are subjected to PTM, there have been fewer studies characterising the effects of these modifications on protein function and interaction with DNA.^{272, 478} For HU, there exists a strong need for further studies focused on roles of PTM of HU in interactions with nucleic acids.⁴⁵⁸ Particularly, lysine acetylation accounts for a large proportion of identified PTMs of HU and other bacterial DNA-binding proteins, yet has received little characterisation.

3.2.7 Lysine acetylation

Lysine acetylation (**Figure 3.4**) is a key post-translational modification in cell signalling and metabolism.¹⁷² About 8% of *E. coli* proteins undergo acetylation, which is particularly prominent in proteins involved in metabolism and translation.¹¹⁹ In eukaryotes, much work has been done to elucidate the physiological significance of this modification, and it has been implicated in many cellular processes.¹⁷² Despite acetylation occurring more frequently than in eukaryotes,¹⁷⁸ in prokaryotes the physiological importance of lysine acetylation remains largely unknown. However, it is thought to have roles in various metabolic pathways, adaptation and virulence.¹⁸³ The primary PTM affecting DNA-binding proteins is lysine acetylation.⁴⁷⁴ Lysine acetylation is reversible, allowing both activation and deactivation of cellular

pathways. Acetylation in *E. coli* is regulated by the acetylase YfiQ and chemically by acetyl-phosphate while deacetylation is almost entirely regulated by the deacetylase CobB.^{177, 178} The prominence of non-enzymatic acetylation by acetyl-phosphate may suggest an ancient form of protein function modulation in response to change in nutrient availability.⁴⁷⁴

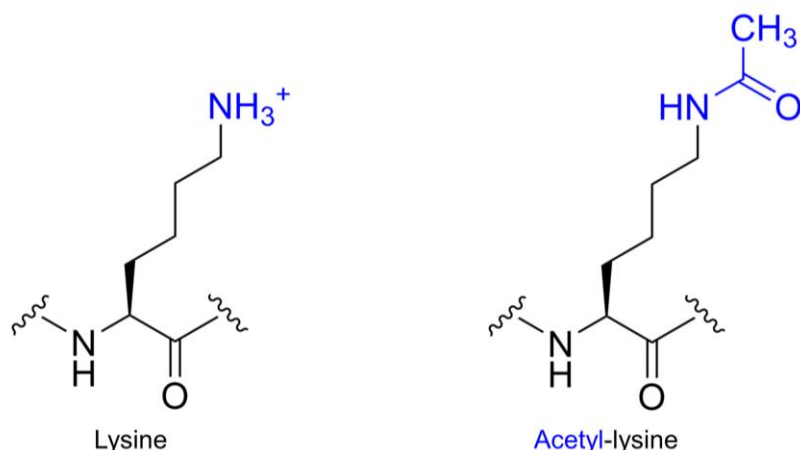


Figure 3.4 Schematic representation of lysine (K) and acetyl-lysine (AcK). Lysine acetylation is the addition of an acetyl group to the terminal nitrogen of the lysine side chain to afford acetyl-lysine.

The HU protein undergoes acetylation at various sites in *E. coli in vivo*. The α subunits are acetylated at 6 sites (Lys3, Lys13, Lys18, Lys67, Lys83, Lys86) while the β subunits undergo acetylation at 5 sites (Lys3, Lys9, Lys18, Lys67, Lys86).^{178, 185, 479} Four sites of acetylation are the same in both subunits. Of particular interest are acetylation of Lys67 and Lys86; Lys67 is located on the DNA-binding β -arms of the protein while Lys86 is located on the DNA binding interface (**Figure 3.5**). In eukaryotic histone proteins, neutralisation of lysine's positive charge weakens the interaction with negatively charged DNA backbones. Although not analogous to histone proteins, as a DNA binding protein, acetylation of *E. coli* HU protein may also weaken the interaction with DNA. For example, in HU from *Mycobacterium*, acetylation leads to decreased affinity for DNA.²⁷¹ However, *Mycobacterium* HU is more similar to eukaryotic histones than HU from other bacterial species; it is almost double the size at 214 amino acids and contains a C-terminal tail. In *Mycobacterium*, acetylation and deacetylation are used to regulate DNA binding capacity of HU in this way.⁴⁸⁰ It has been previously suggested that such modification, particularly of Lys86, may be used to modulate DNA binding of HU,⁴⁷⁴ but there has been no experimental validation thus far.

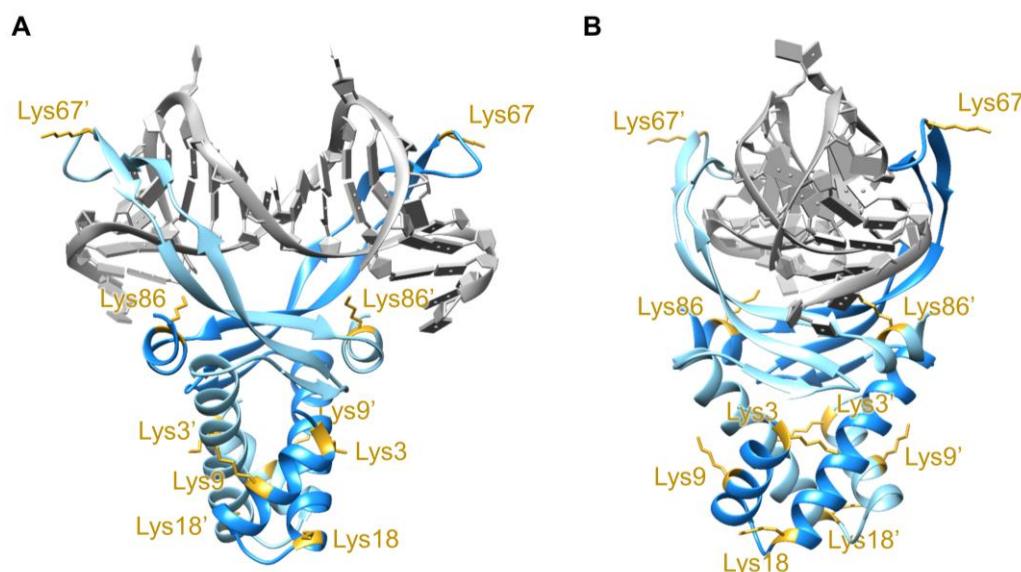


Figure 3.5 Homology model of *Escherichia coli* HU β_2 bound to DNA. The model was generated using SWISS-MODEL using the amino acid sequence of *E. coli* HU β_2 (Swiss-Prot/TrEMBL accession number P0ACF4) and PDB 1P51 (*Anabaena* HU) as the template. Two rotations of the model, **A** and **B**, are shown. Five lysine residues, K3/9/18/67/86 are annotated in yellow and are subjected to acetylation *in vivo*.

To site-specifically modify the protein at Lys67 and Lys86, unnatural amino acid incorporation through genetic code expansion was employed.²⁹⁶ In brief, the DNA codon corresponding to the residue of interest was mutated to the amber stop codon (TAG). The construct was then co-transformed into *E. coli* cells alongside a plasmid containing AcKRS, an engineered *Methanosarcina barkeri* pyrrolysyl-tRNA synthetase recognising acetyl lysine, and a cognate tRNA with a CUA anticodon. The synthetase and tRNA_{CUA} pair are completely orthogonal *in vivo*; AcKRS only acylates tRNA_{CUA} with AcK, no interactions with endogenous amino acids or tRNAs occur. Therefore, supplementation of the cell growth medium with AcK allows site-specific incorporation of the unnatural amino acid into HU protein. Cultures were also supplemented with nicotinamide, an inhibitor of lysine deacetylases, to prevent deacetylation of the residues *in vivo*.

3.3 Aims and objectives

This chapter investigates the effect of acetylation of Lys67 and Lys86 of the *E. coli* HU β on DNA binding. Acetylation of the residues will be achieved *via* genetic code expansion and subsequent unnatural amino acid incorporation during protein expression in *E. coli*. Here, four HU variants will be expressed and purified: HU α_2 , HU β_2 , HU β^{K67ac}_2 and HU β^{K86ac}_2 ; three additional dimers, HU $\alpha\beta$, HU $\alpha\beta^{K67ac}$ and HU $\alpha\beta^{K86ac}$ will be created through recombination of the purified proteins *in vitro*. The DNA binding characteristics of each dimer towards various types of DNA will be analysed by electrophoretic mobility shift assay. Specific objectives are:

1. Incorporate acetyl-lysine into the *E. coli* HU β protein
2. Compare the DNA binding efficiency of wildtype and acetylated HU β
3. Compare the effects of acetylation on the homodimer and the heterodimer
4. Compare the effects of acetylation on interactions with different DNA types

3.4 Results

3.4.1 Expression and purification of wild-type HU protein

HU α_2

To construct a plasmid containing *hupA*, the genomic DNA of *E. coli* BL21(DE3) was extracted and amplified by PCR with primers specific to the 5' and 3' ends of *hupA* and that would incorporate a hexahistidine (His6) tag and 20 bp homology regions for Gibson assembly. The PCR product was cloned into a pBAD expression vector and the resulting construct, pBAD *hupA*-His6 was confirmed *via* sanger sequencing. The plasmid was then expressed in *E. coli* BL21 AI, with visible over expression of a protein with a molecular weight of ca. 10.5 kDa when analysed by SDS-PAGE (**Figure 3.6**). The expression cultures were purified by nickel chromatography (**Figure 3.6**) and cation exchange chromatography (**Figure 3.7**). Molecular weight of the purified product was confirmed by mass spectrometry, where a peak at 10,357.5 Da was observed, in close agreement with the calculated average mass of 10,357.8 Da (**Figure 3.8**).

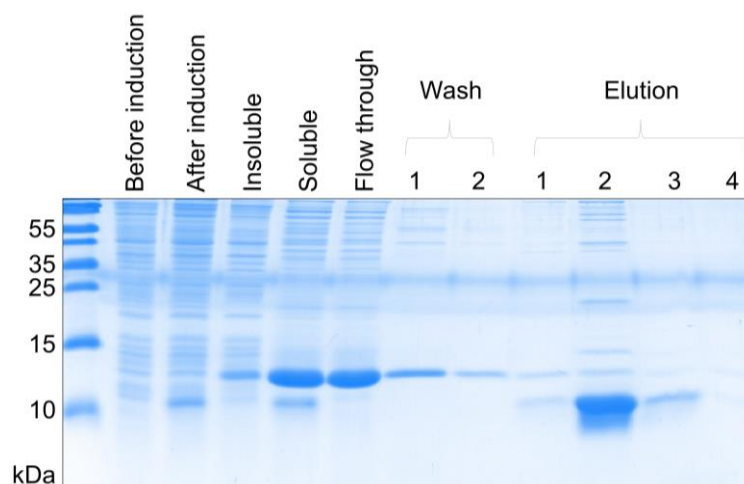


Figure 3.6 SDS-PAGE analysis of pBAD *hupA*-His6 expression and subsequent nickel affinity chromatography purification. *E. coli* BL21 AI were chemically transformed with pBAD *hupA*-His6 and a starter culture inoculated. Cells were grown to A_{600} 0.6 (before induction), before protein expression induced with 0.5 mM IPTG and 0.2% arabinose and the culture incubated overnight at 20 °C (after induction). Cells were pelleted by centrifugation and resuspended in lysis buffer before sonication. After high speed centrifugation, the insoluble fraction was discarded while the soluble supernatant was collected and incubated with nickel-NTA resin. The mixture was then loaded onto a gravity column and a sample of the flow through taken. The column was washed twice with wash buffer before protein was eluted in fractions using elution buffer. Samples were combined with SDS loading dye and analysed on 20% SDS-PAGE. The lysis buffer contained lysozyme, which can be observed in some lanes as a band with a molecular weight around 14 kDa.

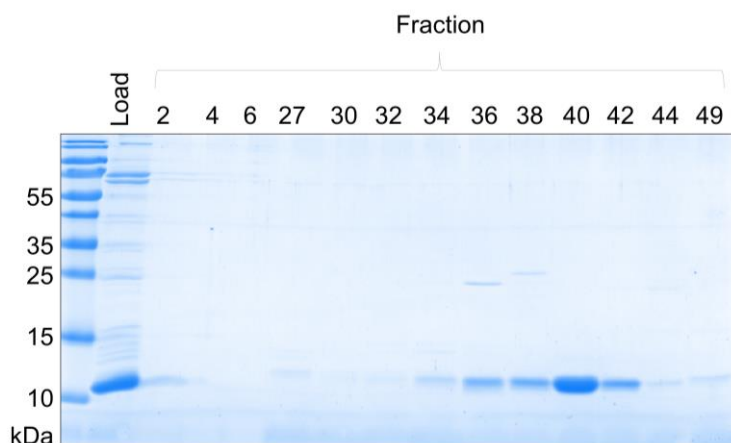


Figure 3.7 SDS-PAGE analysis of HU α cation exchange chromatography. Purified HU α from nickel chromatography was exchanged into phosphate buffer. A Resource STM column was equilibrated with phosphate buffer. The HU α sample was loaded onto the column. Protein was purified using a gradient elution from 0-0.5 M NaCl in phosphate buffer. Fractions displaying a peak at 214 nm were collected and analysed by 20% SDS-PAGE.

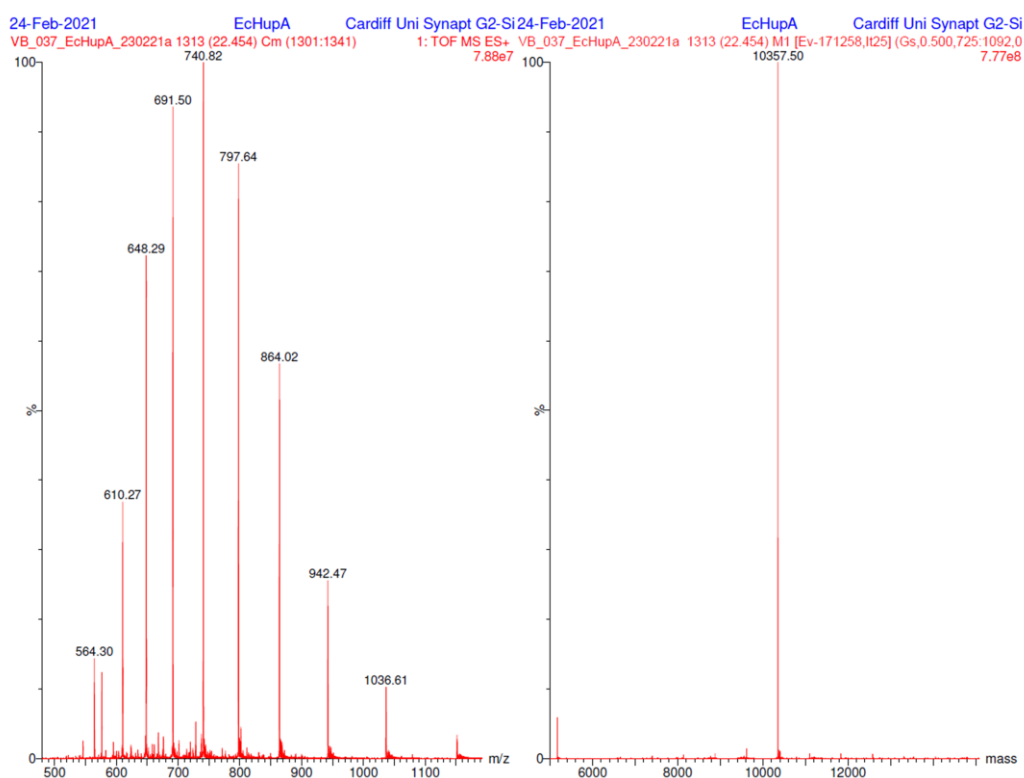


Figure 3.8 Mass spectrometry analysis of purified wildtype HU α protein. *E. coli* BL21 AI cells expressing pBAD hupA-His6 were cultured to A_{600} 0.6, before induction with 0.5 mM IPTG and 0.2% arabinose. Cells were incubated for 18 hours at 20 °C before being harvested and purified by nickel affinity chromatography and cation exchange chromatography. The expected average mass is 10357.83 Da. A peak at 10357.5 Da can be observed. Samples were analysed using a SYNAPT G2-Si (Waters) mass spectrometer.

HU β ₂

hupB was cloned into an expression vector to create pBAD *hupB*-His6 by Sanjay Patel. I expressed the construct in *E. coli* BL21 AI, with visible overexpression of a protein with a molecular weight of ca. 10.5 kDa when analysed by SDS-PAGE (**Figure 3.9**). The expression cultures were purified by nickel chromatography (**Figure 3.9**) and cation exchange chromatography (**Figure 3.10**) and the molecular weight of the purified product confirmed by mass spectrometry, where a peak at 10,290.5 Da was observed, in close agreement with the calculated average mass of 10,290.7 Da (**Figure 3.11**).

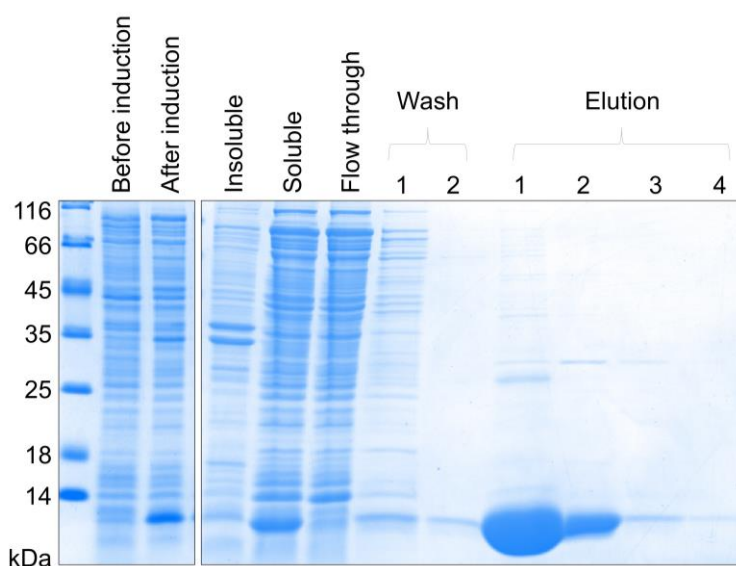


Figure 3.9 SDS-PAGE analysis of pBAD *hupB*-His6 expression and subsequent nickel affinity chromatography purification. *E. coli* BL21 AI were chemically transformed with pBAD *hupB*-His6 and a starter culture inoculated. Cells were grown to A_{600} 0.6 (before induction), before protein expression was induced with 0.5 mM IPTG and 0.2% arabinose and the culture incubated overnight at 20 °C (after induction). Cells were pelleted by centrifugation and resuspended in lysis buffer before sonication. After high speed centrifugation, the insoluble fraction was discarded while the soluble supernatant was collected and incubated with nickel-NTA resin. The mixture was then loaded onto a gravity column and a sample of the flow through taken. The column was washed twice with wash buffer before protein was eluted in fractions using elution buffer. Samples were combined with SDS loading dye and analysed on 15% SDS-PAGE. The lysis buffer contained lysozyme, which can be observed in some lanes as a band with a molecular weight around 14 kDa.

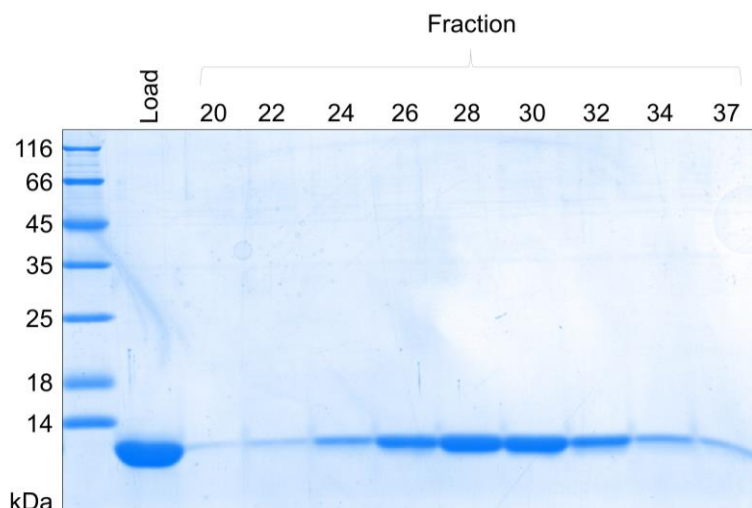


Figure 3.10 SDS-PAGE analysis of HU β cation exchange chromatography. Purified HU β from nickel chromatography was exchanged into phosphate buffer. A Resource STM column was equilibrated with phosphate buffer. The HU β sample was loaded onto the column. Protein was purified using a gradient elution from 0-0.5 M NaCl in phosphate buffer. Fractions displaying a peak at 214 nm were collected and analysed by 15% SDS-PAGE.

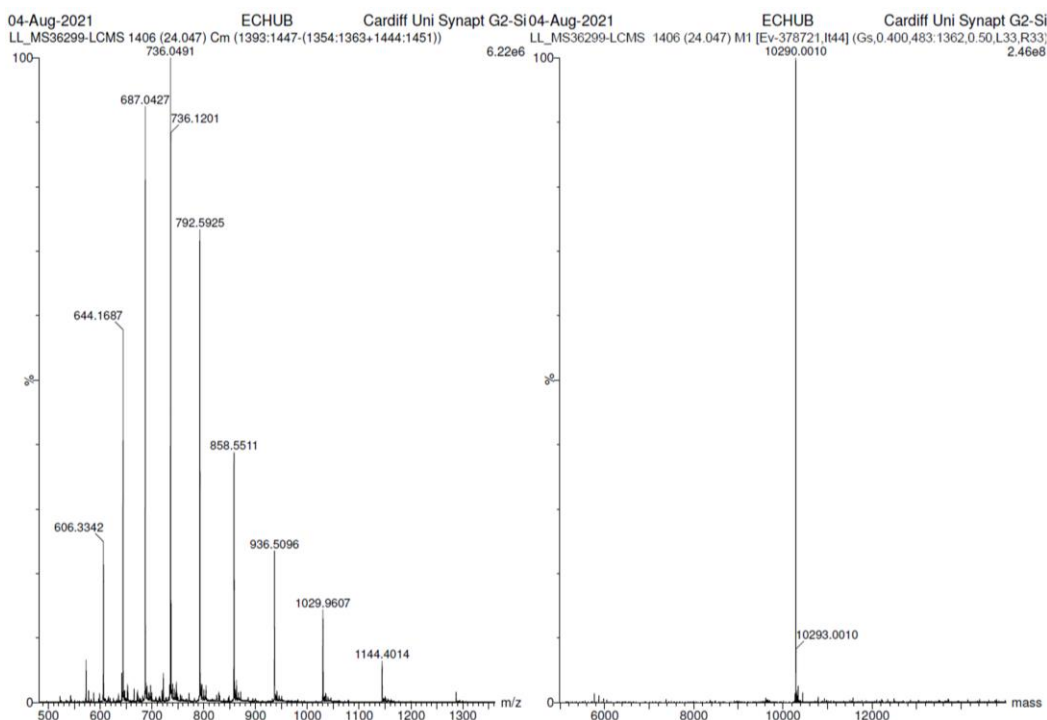


Figure 3.11 Mass spectrometry analysis of purified wildtype HU β protein. *E. coli* BL21 AI cells expressing pBAD hupB-His6 were cultured to A_{600} 0.6, before induction with 0.5 mM IPTG and 0.2% arabinose. Cells were incubated for 18 hours at 20 °C before being harvested and purified by nickel affinity chromatography and cation exchange chromatography. The expected average mass is 10290.7 Da. A peak at 10290.0 Da can be observed. Samples were analysed using a SYNAPT G2-Si (Waters) mass spectrometer.

3.4.2 Expression and purification of acetylated HU proteins

If acetylation affects protein function, it is expected that this effect will be most pronounced when both subunits are acetylated. This can be achieved by expressing an acetylated HU subunit, which will form homodimers *in vivo*. Thus, acetylation was primarily investigated in the HU β_2 homodimer.

Site-directed mutagenesis was used to mutate the DNA codon corresponding to Lys67 or Lys86 to TAG in pBAD hupB-His6 resulting in plasmids pBAD hupB(K67TAG)-His6 and pBAD hupB(K86TAG)-His6, respectively. Each construct was co-transformed with pAckRS in *E. coli* BL21 AI. During protein expression, the media was supplemented with 5 mM AcK and 20 mM nicotinamide, an inhibitor of NAD-dependent deacetylases. Due to the location of the amber stop codon, the hexahistidine tag will only be translated upon successful incorporation of AcK. Thereby, only the full-length protein will have affinity for the nickel during subsequent purification.

HU β^{K67ac_2}

Expression of pBAD hupB(K67TAG)-His6 resulted in moderate overexpression of a protein with a molecular weight ca.10 kDa as analysed by SDS-PAGE (**Figure 3.12**). Nickel purification of the culture demonstrated that the recombinant protein bound to and could be eluted from the nickel column as expected (**Figure 3.12**). Further purification *via* cation exchange resulted in a single band purity product (**Figure 3.13**). The molecular weight of the final purified protein was confirmed by mass spectrometry; a clear peak at 10,332 Da aligned with the calculated average mass of 10,332.7 Da (**Figure 3.14**). If the acetyl group were removed *in vivo* by lysine deacetylases, the expected average mass would be that of the wildtype, 10,290.7 Da. A peak corresponding to this molecular mass was found for in the spectrum with approximately 10% intensity in comparison to the peak of acetylated protein.

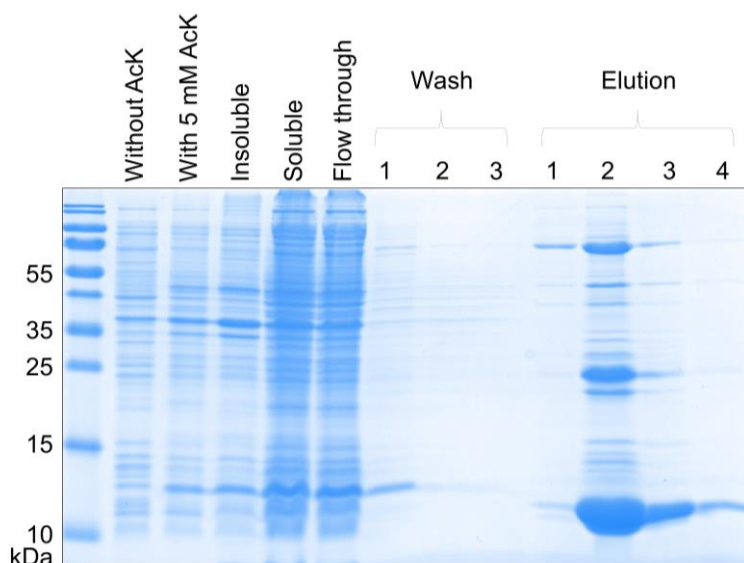


Figure 3.12 SDS-PAGE analysis of pBAD hupB(K67TAG)-His6 expression and subsequent nickel affinity chromatography purification. *E. coli* BL21 AI were chemically transformed with pBAD hupB(K67TAG)-His6 and pAckRS and a starter culture inoculated. Cells were grown to A_{600} 0.5 before the culture was split in half. One half was supplemented with 5 mM AcK and 20 mM nicotinamide (with 5 mM AcK), while the other remained as a control (without AcK). At A_{600} 0.8, or 30 min later, protein expression was induced with 0.5 mM IPTG and 0.2% arabinose and the culture incubated overnight at 20 °C. Cells were pelleted by centrifugation and resuspended in lysis buffer before sonication. After high speed centrifugation, the insoluble fraction was discarded while the soluble supernatant was collected and incubated with nickel-NTA resin. The mixture was then loaded onto a gravity column and a sample of the flow through taken. The column was washed twice with wash buffer before protein was eluted in fractions using elution buffer. Samples were combined with SDS loading dye and analysed on 20% SDS-PAGE. The lysis buffer contained lysozyme, which can be observed in some lanes as a band with a molecular weight around 14 kDa.

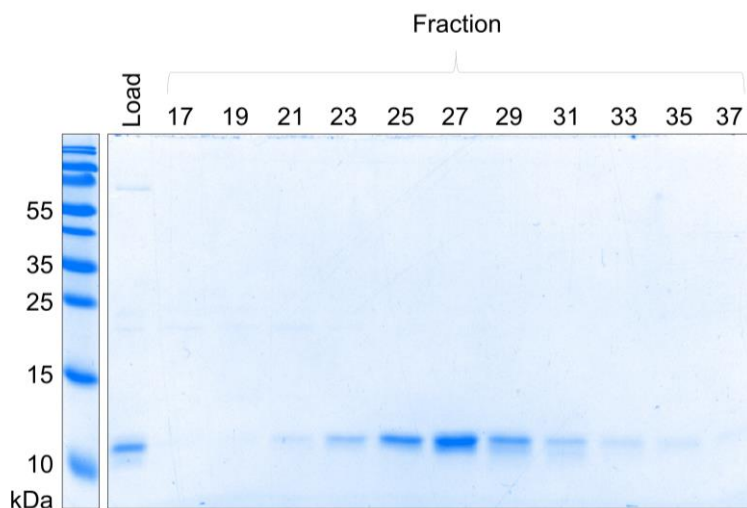


Figure 3.13 SDS-PAGE analysis of HU β^{K67ac} cation exchange chromatography. Purified HU β^{K67ac} from nickel chromatography was exchanged into phosphate buffer. A Resource STM column was equilibrated with phosphate buffer. The HU β^{K67ac} sample was loaded onto the column. Protein was purified using a gradient elution from 0-0.5 M NaCl in phosphate buffer. Fractions displaying a peak at 214 nm were collected and analysed by 20% SDS-PAGE.

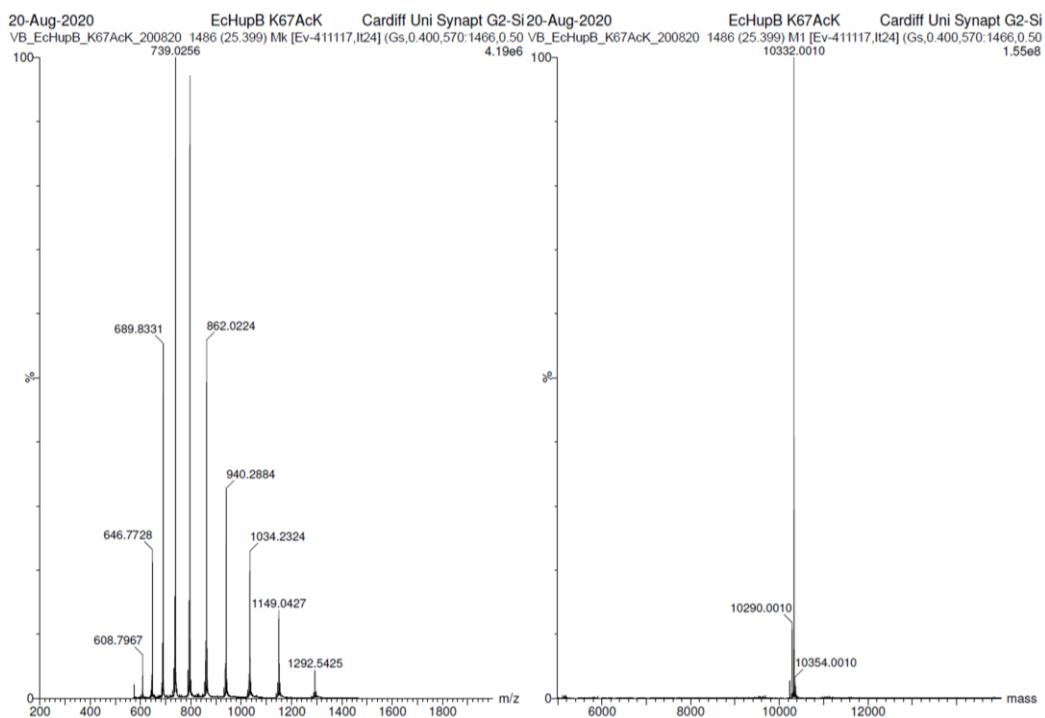


Figure 3.14 Mass spectrometry analysis of purified wildtype HU β^{K67ac} protein. *E. coli* BL21 AI cells expressing pBAD hupB(K67TAG)-His6 and pAckRS were cultured to A_{600} 0.5, before supplementation with 5 mM AcK and 20 mM nicotinamide. At A_{600} 0.8, or 30 min later, culture was induced with 0.5 mM IPTG and 0.2% arabinose. Cells were incubated for 18 hours at 20 °C before being harvested and purified by nickel affinity chromatography and cation exchange chromatography. The expected average mass is 10332.7 Da. A peak at 10332 Da can be observed. Samples were analysed using a SYNAPT G2-Si (Waters) mass spectrometer.

HU β ^{K86ac}₂

Expression of pBAD hupB(K86TAG)-His6 resulted in low overexpression of a protein with a molecular weight ca. 10 kDa as analysed by SDS-PAGE (**Figure 3.15**). As the TAG codon is in the 86th amino acid position out of a total 90 amino acids, in the absence of AcK a prominent band at around 10 kDa can be observed. This suggests that while overexpression of HU is effective, incorporation of AcK into position 86 has low efficiency. Nickel purification of the cultures demonstrated that the recombinant protein bound to and could be eluted from the nickel column as expected (**Figure 3.15**). However, further purification *via* cation exchange revealed a product with double band purity when analysed by SDS-PAGE (**Figure 3.16**). This is likely because, as the truncated version of the HU protein is only missing 4 amino acids, it can form a dimer with the full-length protein. Closer scrutiny of the fractions surrounding fraction 26 revealed that these fractions have almost single band purity, with the vast majority of the fractions composed of the band corresponding to a higher molecular weight (**Figure 3.17**). Accordingly, only these four fractions were pooled. The molecular weight of the final purified product was confirmed *via* mass spectrometry (**Figure 3.18**). A clear peak at 10,332.5 Da aligned with the calculate average mass of 10,332.7 Da. If the acetyl group were removed *in vivo* by lysine deacetylases, the expected average mass would be that of the wildtype, 10,290.7 Da. No peak corresponding to this molecular mass was found in the purified product, suggesting that this recombinant protein was not subjected to deacetylation *in vivo* when expressed in the presence of 20 mM nicotinamide. Nevertheless, contamination in the spectra can be observed, ~7% of the purified product is a peak at 9535 Da. This peak aligns very closely with the molecular mass of native *E. coli* HU α protein (9535 Da). It is likely that HU α formed dimers with HU β ^{K86ac} and a small amount was co-purified.

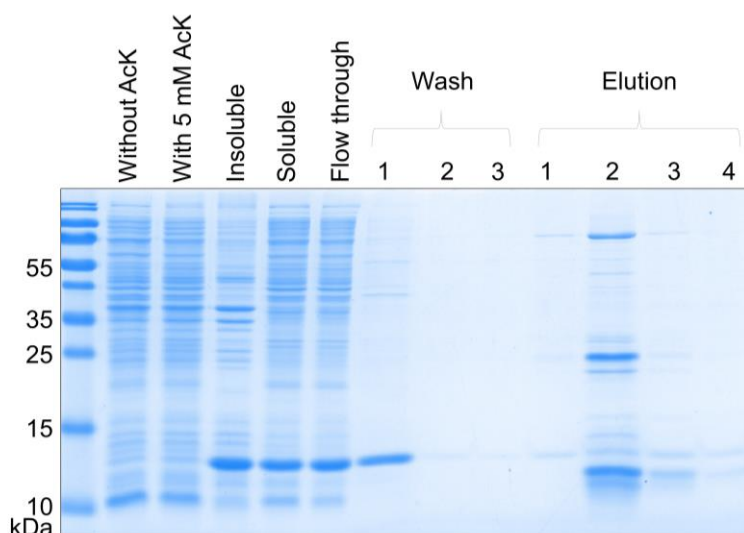


Figure 3.15 SDS-PAGE analysis of pBAD hupB(K86TAG)-His6 expression and subsequent nickel affinity chromatography purification. *E. coli* BL21 AI were chemically transformed with pBAD hupB(K86TAG)-His6 and pAckRS and a starter culture inoculated. Cells were grown to A_{600} 0.5 before the culture was split in half. One half was supplemented with 5 mM AcK and 20 mM nicotinamide (with 5 mM AcK), while the other remained as a control (without AcK). At A_{600} 0.8, or 30 min later, protein expression was induced with 0.5 mM IPTG and 0.2% arabinose and the culture incubated overnight at 20 °C. Cells were pelleted by centrifugation and resuspended in lysis buffer before sonication. After high speed centrifugation, the insoluble fraction was discarded while the soluble supernatant was collected and incubated with nickel-NTA resin. The mixture was then loaded onto a gravity column and a sample of the flow through taken. The column was washed twice with wash buffer before protein was eluted in fractions using elution buffer. Samples were combined with SDS loading dye and analysed on 20% SDS-PAGE. The lysis buffer contained lysozyme, which can be observed in some lanes as a band with a molecular weight around 14 kDa.

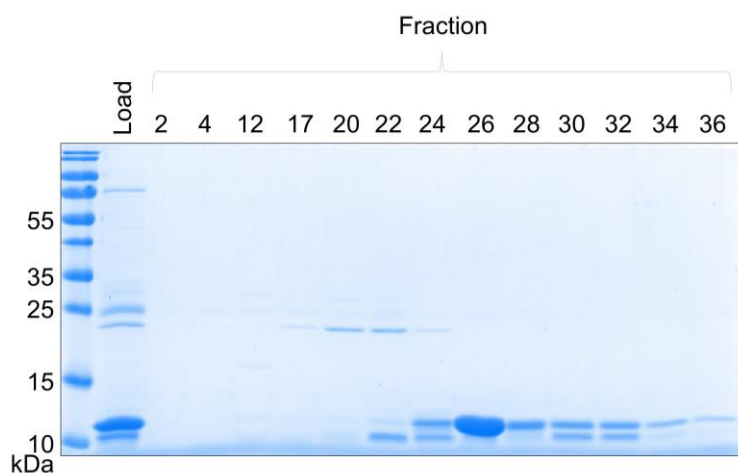


Figure 3.16 SDS-PAGE analysis of HU β^{K86ac} cation exchange chromatography. Purified HU β^{K86ac} from nickel chromatography was exchanged into phosphate buffer. A Resource S™ column was equilibrated with phosphate buffer. The HU β^{K86ac} sample was loaded onto the column. Protein was purified using a gradient elution from 0-0.5 M NaCl in phosphate buffer. Fractions displaying a peak at 214 nm were collected and analysed by 20% SDS-PAGE.

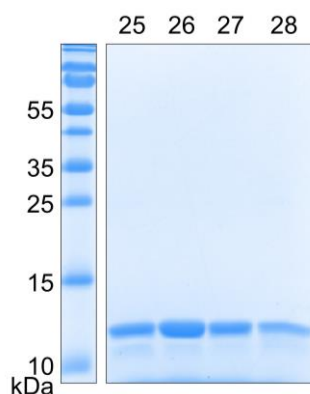


Figure 3.17 SDS-PAGE analysis of HU β^{K86ac} cation exchange chromatography fractions 25-28. Purified HU β^{K86ac} from nickel chromatography was exchanged into phosphate buffer. A Resource S™ column was equilibrated with phosphate buffer. The HU β^{K86ac} sample was loaded onto the column. Protein was purified using a gradient elution from 0-0.5 M NaCl in phosphate buffer. Fractions displaying a peak at 214 nm were collected and analysed by 20% SDS-PAGE.

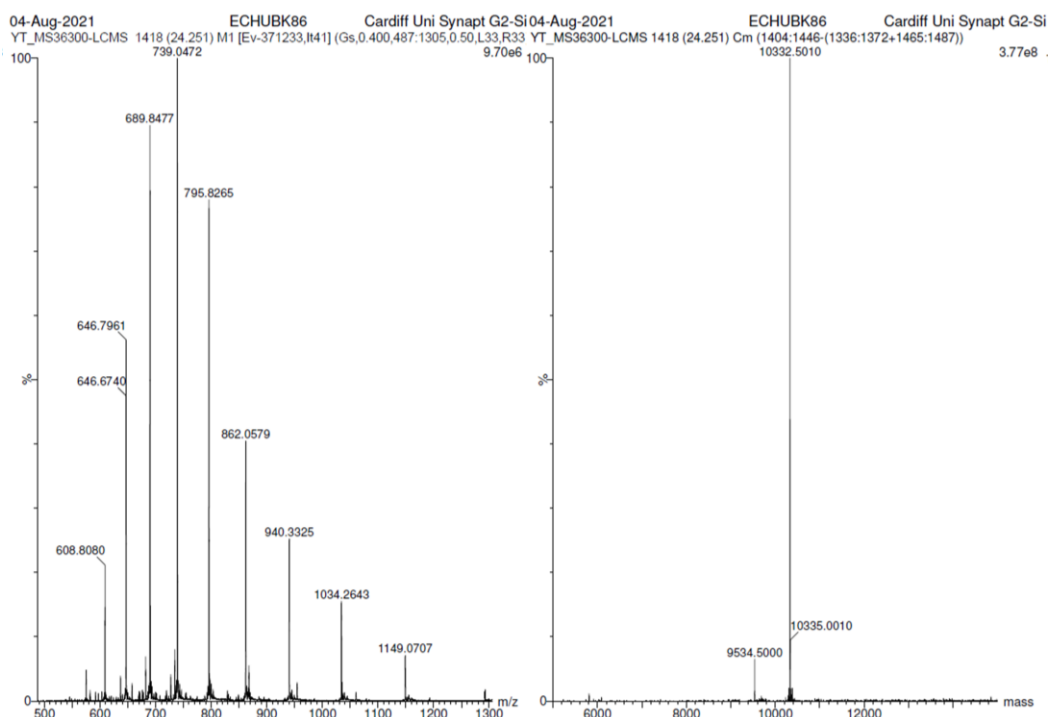


Figure 3.18 Mass spectrometry analysis of purified wildtype HU β^{K86ac} protein. *E. coli* BL21 AI cells expressing pBAD hupB(K86TAG)-His6 and pAcKRS were cultured to A₆₀₀ 0.5, before supplementation with 5 mM AcK and 20 mM nicotinamide. At A₆₀₀ 0.8, or 30 min later, culture was induced with 0.5 mM IPTG and 0.2% arabinose. Cells were incubated for 18 hours at 20 °C before being harvested and purified by nickel affinity chromatography and cation exchange chromatography. The expected average mass is 10332.7 Da. A peak at 10332.5 Da can be observed. Samples were analysed using a SYNAPT G2-Si (Waters) mass spectrometer.

3.4.3 Verifying dimer formation

As mentioned earlier, when combined *in vitro* HU α and HU β homodimers will spontaneously switch chains and form HU $\alpha\beta$ heterodimers.⁴³⁰ To this end, purified HU α and HU β were combined in a 1:1 molar ratio and formation of the heterodimer was analysed *via* native PAGE (**Figure 3.19**), where the observed bands correlated with those reported in the literature.⁴³⁰

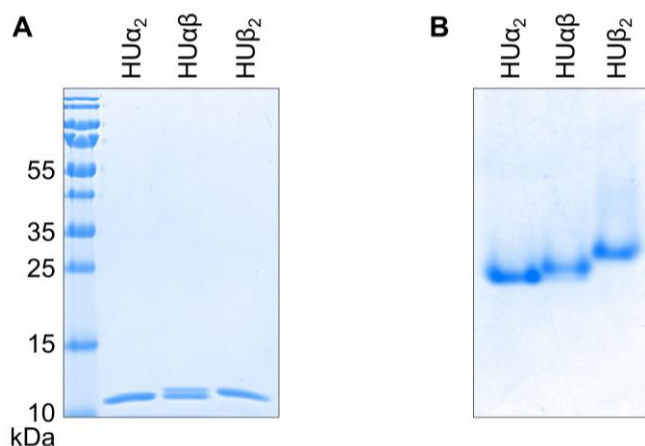


Figure 3.19 SDS and native PAGE analysis of HU α_2 , HU $\alpha\beta$, and HU β_2 dimer formation. For the heterodimer, purified HU α and HU β were combined in a 1:1 molar ratio. The resulting protein samples were analysed on **A** 15% SDS-PAGE and **B** 15% native PAGE to confirm dimer formation.

HU α_2 was also combined with HU β^{K67ac}_2 and HU β^{K86ac}_2 . Consequently, three heterodimers were obtained: HU $\alpha\beta$, HU $\alpha\beta^{K67ac}$ and HU $\alpha\beta^{K86ac}$. Notably, in this design only the β chain in each heterodimer contains an acetylated site. In total, seven different HU dimers were produced: HU α_2 , HU $\alpha\beta$, HU $\alpha\beta^{K67ac}$, HU $\alpha\beta^{K86ac}$, HU β_2 , HU β^{K67ac}_2 , and HU β^{K86ac}_2 . To confirm that the produced proteins were in their dimeric form and the successful recombination of HU α and β chains in the heterodimer, all proteins were subjected to native PAGE analysis (**Figure 3.20**). For dimers containing acetylated Lys86, the acetylated version of the dimer migrated to approximately the same distance in the gel as the non-acetylated dimer. In contrast, the mobility of dimers containing acetylated Lys67 was notably reduced compared to the corresponding non-acetylated dimer. The effect was most pronounced in the homodimer, where the migration of HU β^{K67ac}_2 is considerably less than that of HU β_2 . This is likely because in the homodimer both chains are acetylated whereas in the heterodimer only the β chain is acetylated. The reduced mobility in dimers containing acetylated Lys67 but not in those containing acetylated Lys86 may be due to the location of Lys67 on the β -ribbon arms of HU, which are flexible in solution. Acetylation of this site neutralises an exposed lysine residue. As the conditions used for native PAGE separated the proteins both on size and charge, with the current running from positive to the negative, the loss of this exposed charged residue may be the loss of mobility. In contrast, Lys86 is less exposed and loss of this charge may not affect migration.

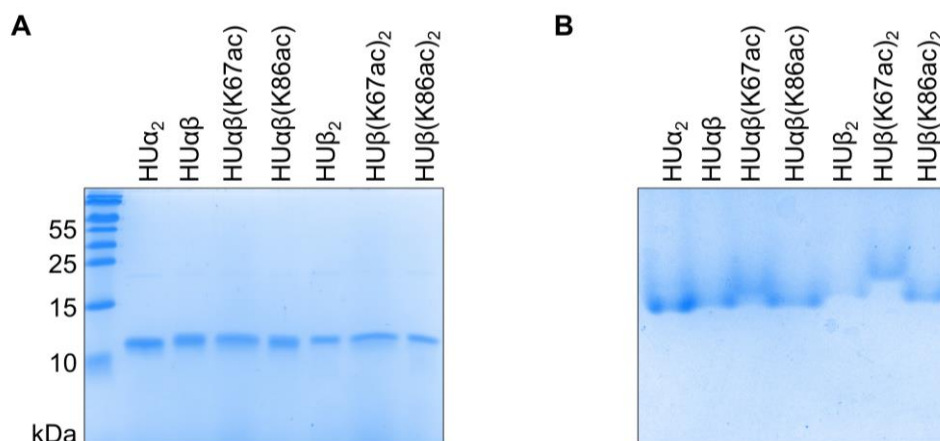


Figure 3.20 SDS and native PAGE analysis of all HU dimers. All homodimeric proteins were produced recombinantly in *E. coli* and purified by successive nickel affinity and cation exchange chromatography. For heterodimers, purified homodimer α and β proteins were combined in a 1:1 molar ratio. All dimers were analysed on **A** 20% SDS-PAGE and **B** 10% native PAGE to confirm dimer formation.

The purified dimers were also subjected to analytical size exclusion chromatography (**Figure 3.21**). All dimers showed very similar profiles on the chromatogram and eluted from the column between 7.90 and 7.95 min. A protein standard containing 5 proteins of known molecular weight were used to generate a calibration curve. The retention times of the five protein standards were plotted against the log of their molecular weights to generate a calibration curve. However, the calibration plot was not linear, resulting in an inaccurate line of best fit (**Figure 3.21C**). A second calibration curve was plotted using only the retention times of the three smallest protein standards, which resulted in a line of best fit with good approximation (**Figure 3.21D**). The two equations generated from the two calibration curves were used to calculate the estimated molecular weights of the protein standards of known molecular weights (**Table 3.1**). This revealed that the equation generated from the calibration curve of only the three smaller protein standards provided a better approximation of molecular weights in the range 1350 – 44,000 Da. As the HU dimers are ca. 20,000 Da and the monomers ca. 10,000 Da, this equation was used to estimate the molecular weights of the protein samples. Based on these calculations, the estimated molecular weights were between 23.3 and 24 kDa, in line with the expected molecular weights of between 20.6 and 20.7 kDa if the proteins are dimers (

Table 3.2). Further, the retention times of the HU dimers (between 7.9 and 7.95 min) are in between the retention times of the 44,000 Da standard (7.13 min) and the 17,000 Da standard (8.13 min).

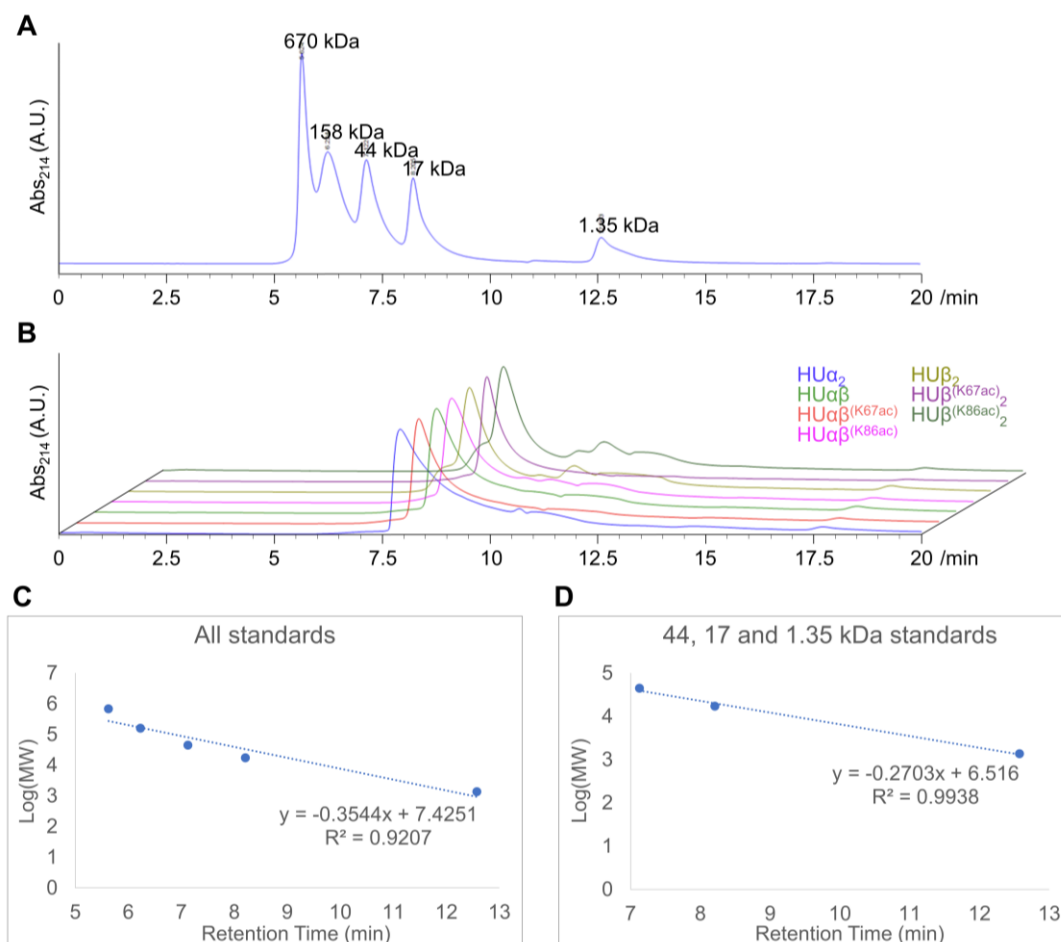


Figure 3.21 Analytical size exclusion high-performance liquid chromatography of HU protein samples. **A** Elution profile of Bio-Rad Gel Filtration standards of known molecular weights. **B** Overlay of elution profiles of $HU\alpha_2$, $HU\alpha\beta$, $HU\alpha\beta^{K67ac}$, $HU\alpha\beta^{K86ac}$, $HU\beta_2$, $HU\beta^{K67ac}_2$, and $HU\beta^{K86ac}_2$. Elution was measured at 214 nm for all proteins and is provided in arbitrary units (A.U.). Following sample injection, PBS was passed through the column at a flow rate of 0.35 mL/min for 20 minutes. **C** Standard curve generated by plotting the retention time of all 5 protein standards against the log of their molecular weights. **D** Standard curve generated by plotting the retention time of the 44, 17 and 1.35 kDa standards against the log of their molecular weights.

Table 3.1 Verifying the accuracy of a molecular weight (MW) calibration curve. The curve was generated by plotting the retention time of Bio-Rad Gel Filtration standards in analytical size exclusion high-performance liquid chromatography against their log molecular weight (**Figure 3.21**).

	MW (Da)	Log MW	Average RT (min)	Equation 1		Equation 2	
				Log MW	MW (Da)	Log MW	MW (Da)
Thyroglobulin	670000	5.826	5.629	5.430	269340	4.995	98758
y-globulin	158000	5.199	6.233	5.216	164529	4.831	67813
Ovalbumin	44000	4.643	7.127	4.899	79282	4.589	38858
Myoglobin	17000	4.230	8.210	4.516	32779	4.297	19812
Vitamin B12	1350	3.130	12.577	2.968	929	3.116	1307

Table 3.2 Calculated molecular weights (MW) of HU proteins based on analytical size exclusion high-performance liquid chromatography. An estimated molecular weight was calculated based on a standard curve derived from retention times of Bio-Rad gel filtration standards (**Figure 3.21**).

	Expected dimer MW (Da)	Expected monomer MW (Da)	RT (min)	Log (MW)	Calculated MW (Da)
HU α_2	20716	10358	7.908	4.378	23904
HU $\alpha\beta$	20649	10358+10291	7.952	4.367	23258
HU $\alpha\beta^{K67ac}$	20691	10358+10333	7.94	4.370	23432
HU $\alpha\beta^{K86ac}$	20691	10358+10333	7.902	4.380	23993
HU β_2	20582	10291	7.915	4.377	23800
HU β^{K67ac}_2	20666	10333	7.916	4.376	23785
HU β^{K86ac}_2	20666	10333	7.901	4.380	24008

3.4.4 Electrophoretic mobility shift assay

Electrophoretic mobility assays (EMSA) were performed with the purified proteins to analyse DNA binding affinity. In the assay, HU protein is incubated with DNA in a buffer which favours DNA binding. After incubation, the sample is analysed by electrophoresis and the gel stained for DNA. Free DNA will migrate the furthest, whereas DNA bound by HU will have reduced mobility in the gel.

EMSAs with HU β_2 and a 30-bp DNA fragment with a 2-nt gap

To gain insight into the role of acetylation of HU on DNA binding affinity, EMSA experiments with a small DNA fragment of 30 bp in length containing a 2-nucleotide (2-nt) gap were performed (**Figure 3.22**). HU was previously shown to have high affinity for DNA with this deformity.⁴³⁷ EMSA with 30-bp fragments allows analysis of

HU-DNA binding with high resolution on non-denaturing acrylamide gels. As the binding site for HU is estimated to be 9 bp, binding of a single HU dimer to one 30-bp fragment can be observed.⁴²⁶ As can be seen in **Figure 3.23**, when 1 μM of a 30-bp DNA fragment containing a 2-nt gap was incubated with 0.5 μM HU β_2 , a complex that migrates in line with the 100-bp DNA marker appears and the amount of free DNA decreases slightly. With increasing concentrations of HU, the intensity of this first complex increases while the free DNA continues to decrease, peaking at around 2-2.5 μM HU. At around 3 μM HU, the intensity of this first complex begins to decrease, as the intensity of a second complex, representing 2 HU dimers per 30-bp fragment, appears. In these experiments, HU DNA binding affinity was characterised by analysing the amount of free DNA remaining in each condition. The relative amount of free DNA remaining was calculated by setting the intensity of the band in the DNA only lane as a reference (100%) and measuring the relative quantity of free DNA in the corresponding bands in the HU containing conditions (see **3.7 Materials and methods, Figure 3.38**).

30 bp DNA fragments:

A 2-nucleotide gap:

```

T-A-C-G-G-A-T-C-G-C-A-G-C      G-G-T-T-A-G-G-G-A-A-G-T-T-G-G
| | | | | | | | | | | | | | | |
A-T-G-C-C-T-A-G-C-G-T-C-G-A-C-C-C-A-A-T-C-C-C-T-T-C-A-A-C-C

```

B nicked phosphate backbone:

```

T-A-C-G-G-A-T-C-G-C-A-G-C      T-G-G-G-T-T-A-G-G-G-A-A-G-T-T-G-G
| | | | | | | | | | | | | | | |
A-T-G-C-C-T-A-G-C-G-T-C-G-A-C-C-C-A-A-T-C-C-C-T-T-C-A-A-C-C

```

C whole complementary duplex:

```

T-A-C-G-G-A-T-C-G-C-A-G-C-T-G-G-G-T-T-A-G-G-G-A-A-G-T-T-G-G
| | | | | | | | | | | | | | | |
A-T-G-C-C-T-A-G-C-G-T-C-G-A-C-C-C-A-A-T-C-C-C-T-T-C-A-A-C-C

```

Figure 3.22 30 bp DNA fragments used in EMSAs. HU protein was incubated with either **A** a 30 bp DNA fragment with a 2-nucleotide gap, **B** a 30 bp fragment with a nick (\downarrow) in the phosphate backbone, or **C** a 30 bp fragment with a complete complementary duplex.⁴³⁷

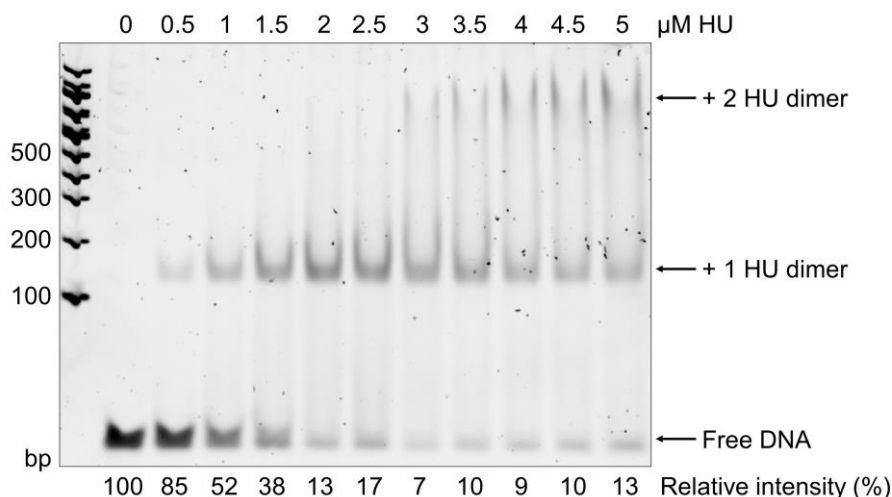


Figure 3.23 EMSA of HU β_2 with a 30 bp DNA fragment containing a 2-nt gap. Each reaction contained 1 μ M DNA, a buffer which facilitates DNA binding, and varying concentrations of HU protein. Reactions were incubated for 10 minutes at 18 °C before analysis on non-denaturing 10% PAGE. DNA was visualised via staining with PAGE GelRed and UV transillumination. An estimate of free DNA remaining in each condition was calculated using the intensity of DNA in the control reaction (0 μ M HU) as a reference (100%) and measuring the intensity of the corresponding band in other lanes relative to this.

When the three HU variants are compared, the HU β_2 and HU β^{K67ac}_2 again display very similar DNA binding capacities through their similar DNA migration patterns. With HU β^{K86ac}_2 , a distinct migration pattern was observed (**Figure 3.24**). This high-resolution analysis revealed that HU β^{K86ac}_2 binds significantly less DNA than the other variants. At 4 μ M, in the HU β_2 condition 12% \pm 0.6 of the DNA is unbound, HU β^{K67ac}_2 has 15% \pm 0.6 DNA unbound while for HU β^{K86ac}_2 57% \pm 8 of the DNA remains unbound. A t-test found significant difference between HU β_2 and HU β^{K67ac}_2 ($t(4) = 6.4$, $p=0.003$) and also between HU β_2 and HU β^{K86ac}_2 ($t(2) = 8.1$, $p=0.015$). However, the large difference in average free DNA remaining between HU β_2 and HU β^{K86ac}_2 demonstrates that the magnitude of difference is much greater here, almost 5x more DNA remained unbound with HU β^{K86ac}_2 . It is also notable DNA incubated with the wildtype HU β_2 displays a different migration pattern to both of the acetylated versions. Specifically, the band corresponding to a complex of one DNA molecule to 1 HU dimer has reduced mobility in the gel. This is likely due to the acetylated HU dimers having 2 fewer positive charges due to the acetyl group on each subunit.

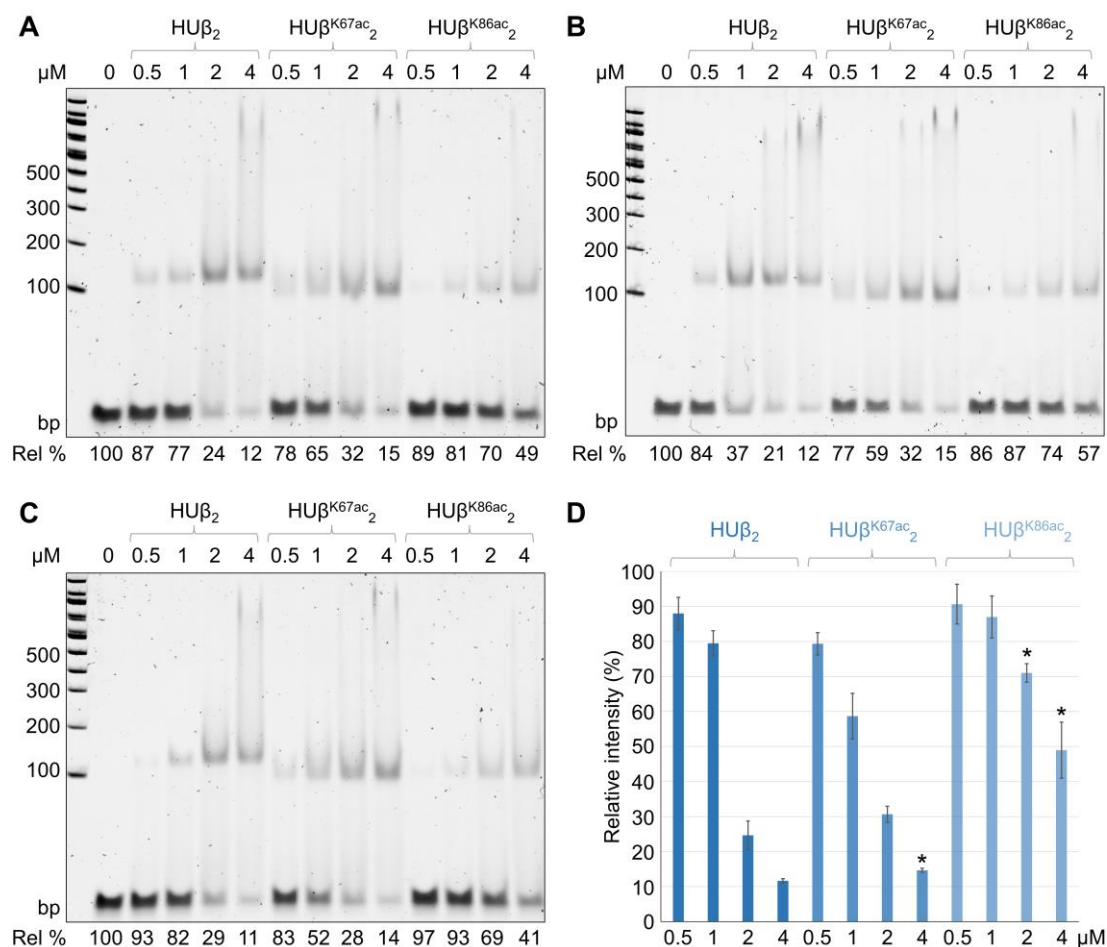


Figure 3.24 EMSA of HUβ₂, HUβ^{K67ac}₂ and HUβ^{K86ac}₂ with a 30 bp DNA fragment containing a 2-nt gap. Three repeats, **A**, **B** and **C** are shown. Each reaction contained 1 μM DNA, a buffer which facilitates DNA binding, and varying concentrations of HU protein. Reactions were incubated for 10 minutes at 18 °C before analysis on non-denaturing 10% PAGE. DNA was visualised via staining with PAGE GelRed and UV transillumination. An estimate of free DNA remaining in each condition was calculated using the intensity of DNA in the control reaction (0 μM HU) as a reference and measuring the intensity of the corresponding band in other lanes relative to this (Rel %). **D** The average relative intensity of free DNA remaining of **A**, **B** and **C** alongside the standard deviation. Statistically significant differences ($p < 0.05$) between HUβ^{K67ac}₂ or HUβ^{K86ac}₂ conditions compared to the corresponding HUβ₂ condition are denoted with an Asterisk (*).

EMSAs with HUαβ and 30 bp DNA fragments with a 2-nt gap

In vivo HU is mostly present in the heterodimeric form, HUαβ.⁴²⁹ This dimer may be considered more physiologically relevant due to its higher prevalence. Therefore, it is of interest to determine whether the discrepancy in DNA binding affinity exists between acetylated and non-acetylated versions of the heterodimer. EMSAs were performed with the three heterodimers. It is well established that the HU heterodimers

have stronger DNA binding affinity than the homodimers,^{436, 437} a phenomenon that was clear in these results. Intriguingly, acetylation at Lys86 on the β subunit of the heterodimer had a negligible effect on DNA binding affinity. As can be seen in **Figure 3.25**, conditions containing HU $\alpha\beta$, HU $\alpha\beta^{K67ac}$ and HU $\alpha\beta^{K86ac}$ have similar amounts of free DNA. At 4 μ M, in the HU $\alpha\beta$ condition 2.7% \pm 1.2 of the DNA is unbound, HU $\alpha\beta^{K67ac}$ has 5.7% \pm 2.9 DNA unbound while for HU $\alpha\beta^{K86ac}$ 5% \pm 3 of the DNA remains unbound. A t-test found no significant difference between HU $\alpha\beta$ and HU $\alpha\beta^{K67ac}$ ($t(3) = 1.7$, $p=0.193$) nor between HU $\alpha\beta$ and HU $\alpha\beta^{K86ac}$ ($t(3) = 1.3$, $p=0.298$).

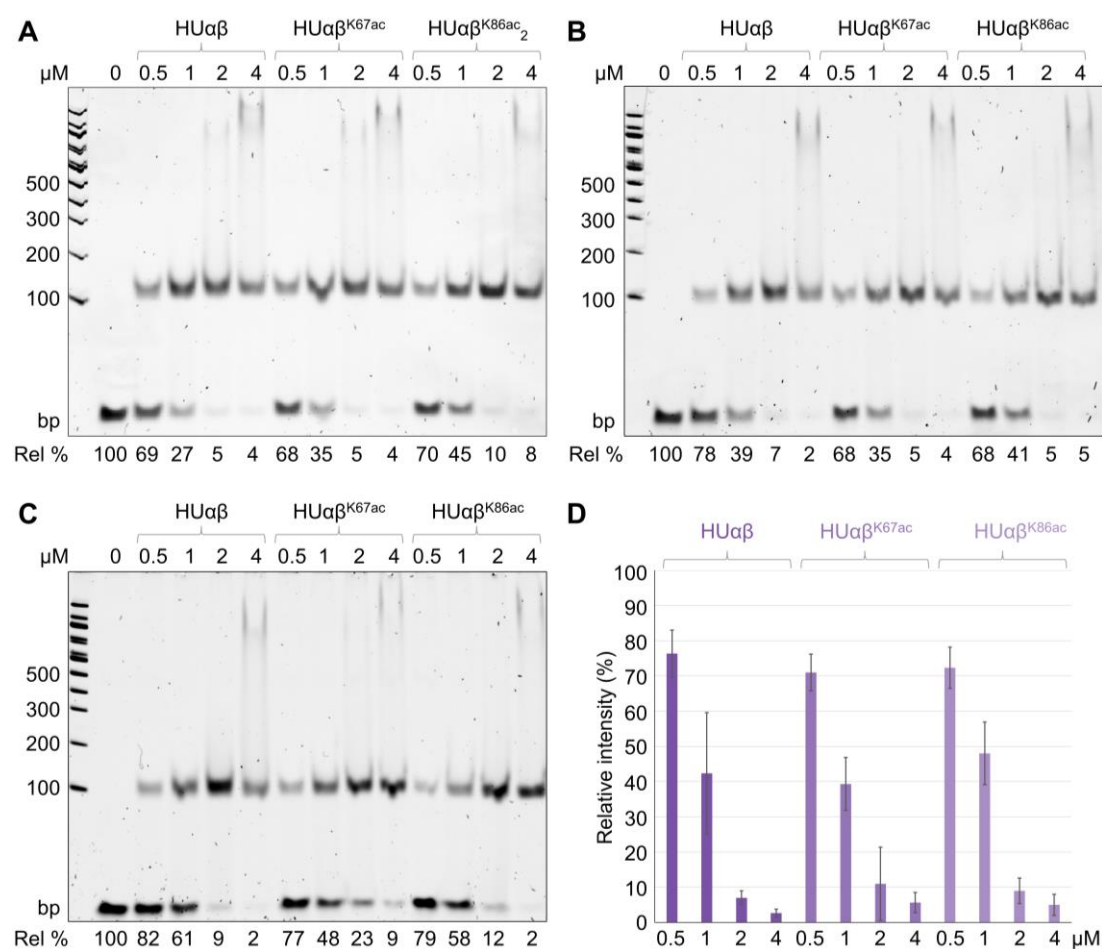


Figure 3.25 EMSA of HU $\alpha\beta$, HU $\alpha\beta^{K67ac}$ and HU $\alpha\beta^{K86ac}$ with a 30 bp DNA fragment containing a 2-nt gap. Three repeats **A**, **B**, and **C** are shown. Each reaction contained 1 μ M DNA, a buffer which facilitates DNA binding, and varying concentrations of HU protein. Reactions were incubated for 10 minutes at 18 °C before analysis on non-denaturing 10% PAGE. DNA was visualised via staining with PAGE GelRed and UV transillumination. An estimate of free DNA remaining in each condition was calculated using the intensity of DNA in the control reaction (0 μ M HU) as a reference and measuring the intensity of the corresponding band in other lanes relative to this (Rel %). **D** The average relative intensity of free DNA remaining in **A**, **B**, and **C** are shown alongside the standard deviation. There were no statistically significant differences between the conditions.

Comparing HU $\alpha\beta$ and HU β_2

For a more direct comparison between the HU homodimers and heterodimers, EMSAs comparing the acetylated and non-acetylated forms were performed and analysed simultaneously. **Figure 3.26** demonstrates the difference in effect of acetylation at Lys86 on DNA binding affinity between the homodimer and the heterodimer. At 2 μ M, in the HU $\alpha\beta$ condition 7% \pm 2.6 of the DNA is unbound, while HU $\alpha\beta^{K86ac}$ 9% \pm 6 of the DNA remains unbound. As expected, a t-test found no significant difference between HU $\alpha\beta$ and HU $\alpha\beta^{K86ac}$ ($t(3) = 0.5$, $p=0.633$). For HU β_2 at 2 μ M 30% \pm 11 of the DNA was unbound while for HU β^{K86ac}_2 66% \pm 6 remained free. As before, a t-test found significant difference between these groups ($t(3) = 5$, $p=0.016$). The averages for all conditions were extremely close to the averages when HU $\alpha\beta$ and HU β_2 were assayed individually and run on individual gels, demonstrating the reliability and reproducibility of this assay.

To enable a greater understanding of how acetylated HU interacts with different types of DNA, EMSA was also performed with a 30 bp DNA fragment containing a nicked phosphate backbone (**Figure 3.22**). At 4 μ M, in the HU $\alpha\beta$ condition 7.7% \pm 1.5 of the DNA is unbound, while HU $\alpha\beta^{K86ac}$ 4.7% \pm 1.5 of the DNA remains unbound (**Figure 3.27**). As before, a t-test found no significant difference between HU $\alpha\beta$ and HU $\alpha\beta^{K86ac}$ ($t(4) = 2.4$, $p=0.739$). For HU β_2 at 4 μ M 36% \pm 1.4 of the DNA was unbound and for HU β^{K86ac}_2 47% \pm 1.4 was free. As before, a t-test found significant difference between these groups ($t(2) = 7.8$, $p=0.016$).

Additionally, EMSA was performed with a 30 bp DNA fragment with a complete duplex (**Figure 3.22**). As expected, all HU variants bound this type of DNA at lower affinity and slightly higher concentrations were necessary. At 6 μ M, in the HU $\alpha\beta$ condition 14% \pm 7 of the DNA is unbound, while HU $\alpha\beta^{K86ac}$ 12% \pm 2 of the DNA remains unbound (**Figure 3.28**). As expected, a t-test found no significant difference between HU $\alpha\beta$ and HU $\alpha\beta^{K86ac}$ ($t(2) = 0.6$, $p=0.635$). For HU β_2 at 6 μ M 59% \pm 19 of the DNA was unbound and for HU β^{K86ac}_2 70% \pm 3 was free. A t-test found no significant difference between these groups ($t(2) = 1.0$, $p=0.409$). Acetylation of Lys86 therefore had no significant effect on interaction with a 30 bp DNA containing a complete complementary duplex.

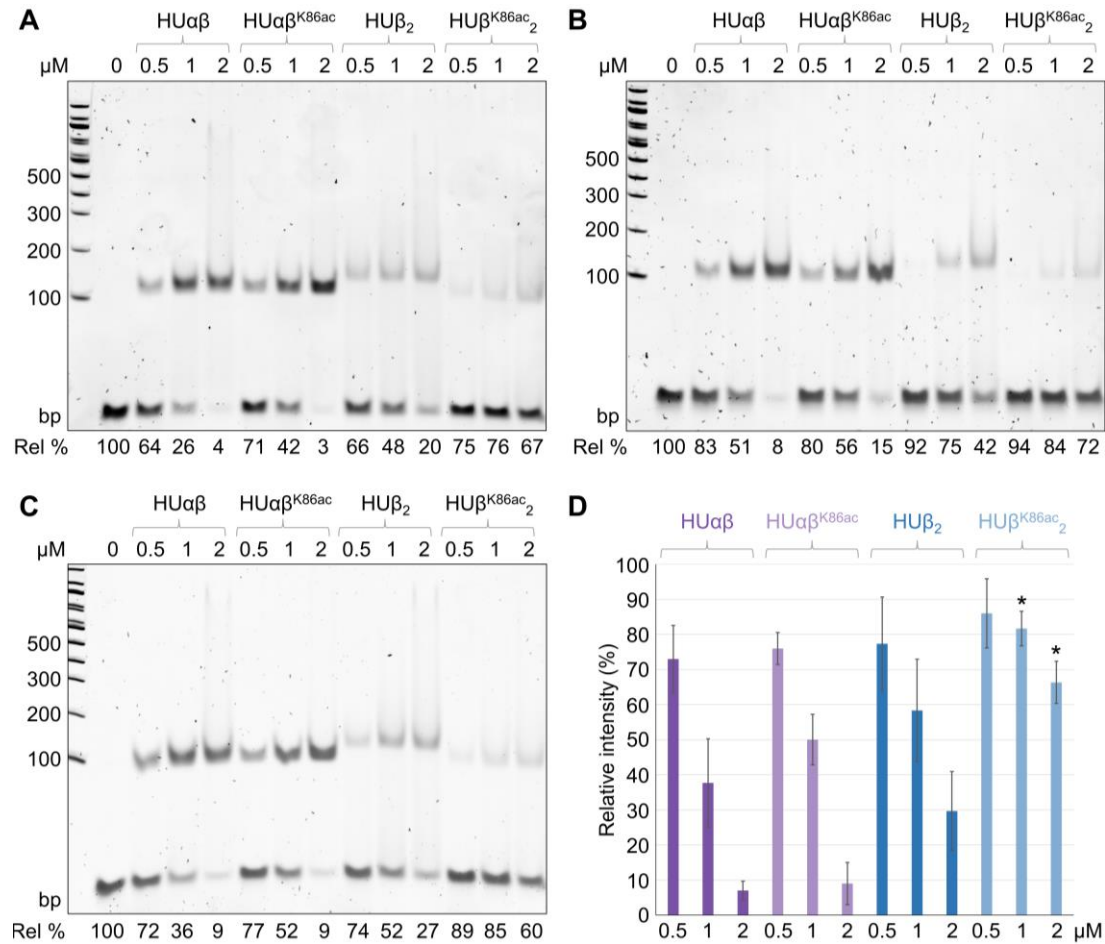


Figure 3.26 EMSA of HUαβ, HUαβ^{K86ac}, HUβ₂, and HUβ^{K86ac}₂ with a 30 bp DNA fragment containing a 2-nt gap. Three repeats **A**, **B**, and **C** are shown. Each reaction contained 1 μM DNA, a buffer which facilitates DNA binding, and varying concentrations of HU protein. Reactions were incubated for 10 minutes at 18 °C before analysis on non-denaturing 10% PAGE. DNA was visualised via staining with PAGE GelRed and UV transillumination. An estimate of free DNA remaining in each condition was calculated using the intensity of DNA in the control reaction (0 μM HU) as a reference and measuring the intensity of the corresponding band in other lanes relative to this (Rel %). **D** The average relative intensity of free DNA remaining in **A**, **B** and **C** is shown alongside the standard deviation. Statistically significant ($p < 0.05$) differences between HUβ^{K86ac}₂ conditions compared to the corresponding HUβ₂ condition are denoted with an Asterix (*).

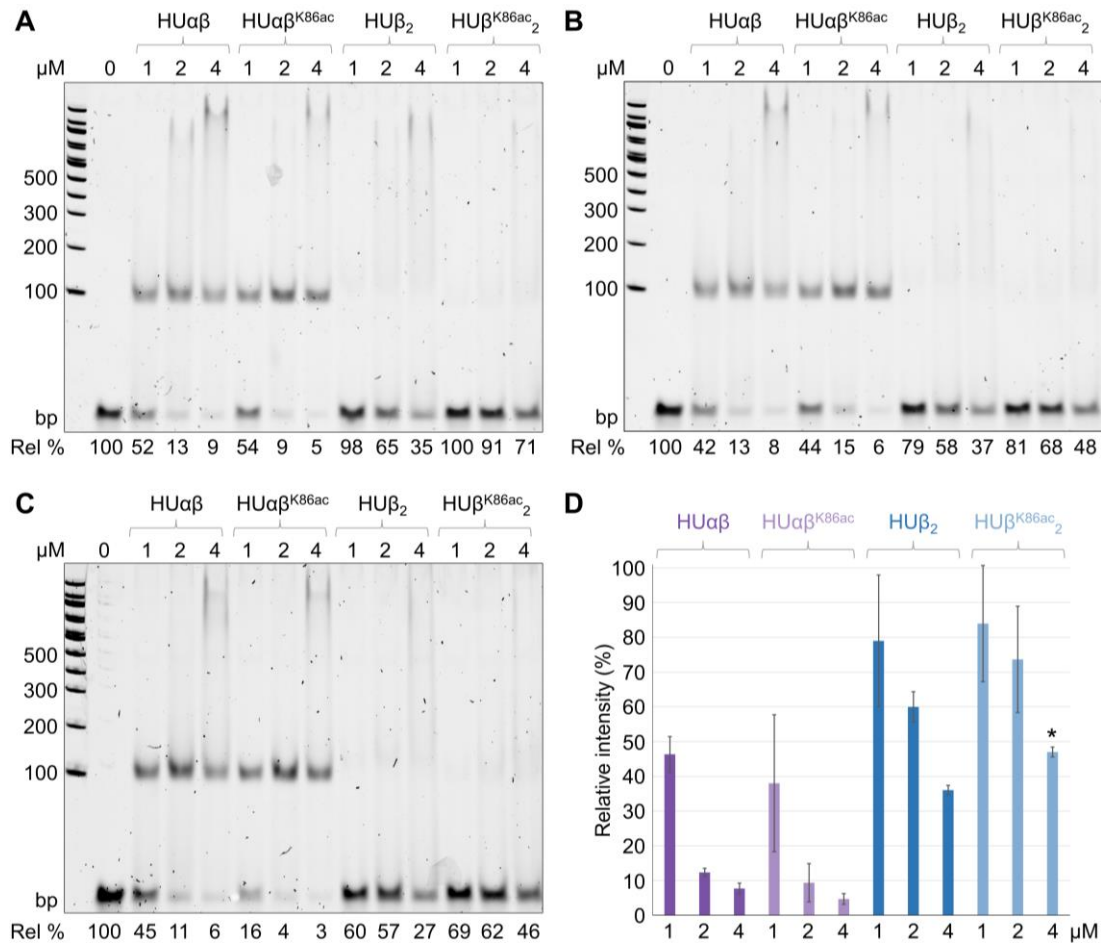


Figure 3.27 EMSA of HUαβ, HUαβ^{K86ac}, HUβ₂, and HUβ^{K86ac}₂ with a 30 bp DNA fragment containing a nicked backbone. Three repeats **A**, **B**, and **C** are shown. Each reaction contained 1 μM DNA, a buffer which facilitates DNA binding, and varying concentrations of HU protein. Reactions were incubated for 10 minutes at 18 °C before analysis on non-denaturing 10% PAGE. DNA was visualised via staining with PAGE GelRed and UV transillumination. An estimate of free DNA remaining in each condition was calculated using the intensity of DNA in the control reaction (0 μM HU) as a reference and measuring the intensity of the corresponding band in other lanes relative to this (Rel %). **D** The average relative intensity of free DNA remaining in **A**, **B**, and **C** is shown alongside the standard deviation. Statistically significant ($p < 0.05$) differences between HUβ^{K86ac}₂ conditions compared to the corresponding HUβ₂ condition are denoted with an Asterix (*).

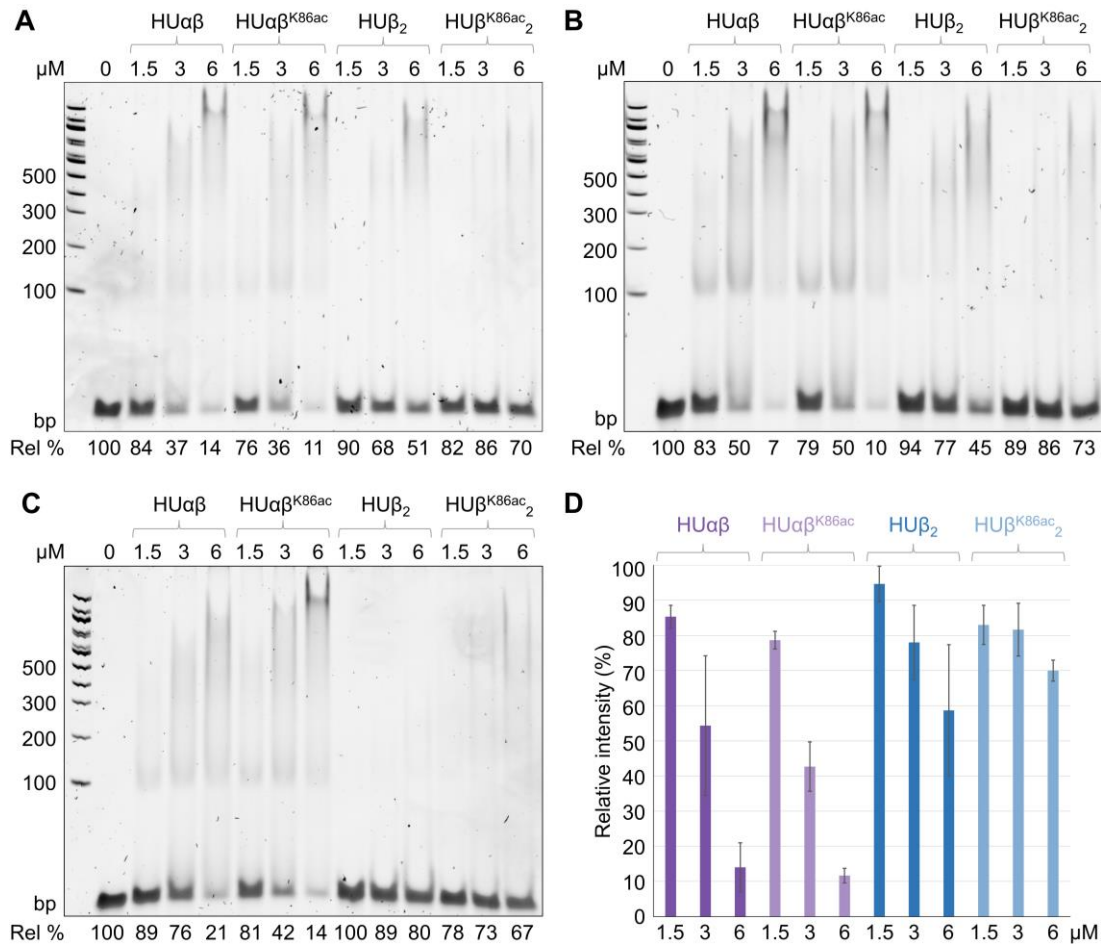


Figure 3.28 EMSA of HUαβ, HUαβ^{K86ac}, HUβ₂, and HUβ^{K86ac}₂ with a 30 bp DNA fragment with a complete duplex. Three repeats **A**, **B**, and **C** are shown. Each reaction contained 1 μM DNA, a buffer which facilitates DNA binding, and varying concentrations of HU protein. Reactions were incubated for 10 minutes at 18 °C before analysis on non-denaturing 10% PAGE. DNA was visualised via staining with PAGE GelRed and UV transillumination. An estimate of free DNA remaining in each condition was calculated using the intensity of DNA in the control reaction (0 μM HU) as a reference and measuring the intensity of the corresponding band in other lanes relative to this (Rel %). **D** The average relative free DNA remaining in **A**, **B**, and **C** is shown alongside the standard deviation. There was no significant difference ($p < 0.05$) between HUαβ and HUαβ^{K86ac} or HUβ₂ and HUβ^{K86ac}₂.

As summarised in **Figure 3.29**, for HUβ₂ acetylation at Lys86 caused a significant increase in the amount of free DNA remaining when interacting with 30 bp DNA containing a 2-nt gap or nicked phosphate backbone. For 30 bp DNA with a complete complementary duplex, acetylation at Lys86 caused no significant change in the amount of free DNA remaining. For HUαβ, acetylation at Lys86 of the HUβ subunit had no significant effect on the amount of free DNA remaining for any of the types of 30-bp DNA fragments assayed.

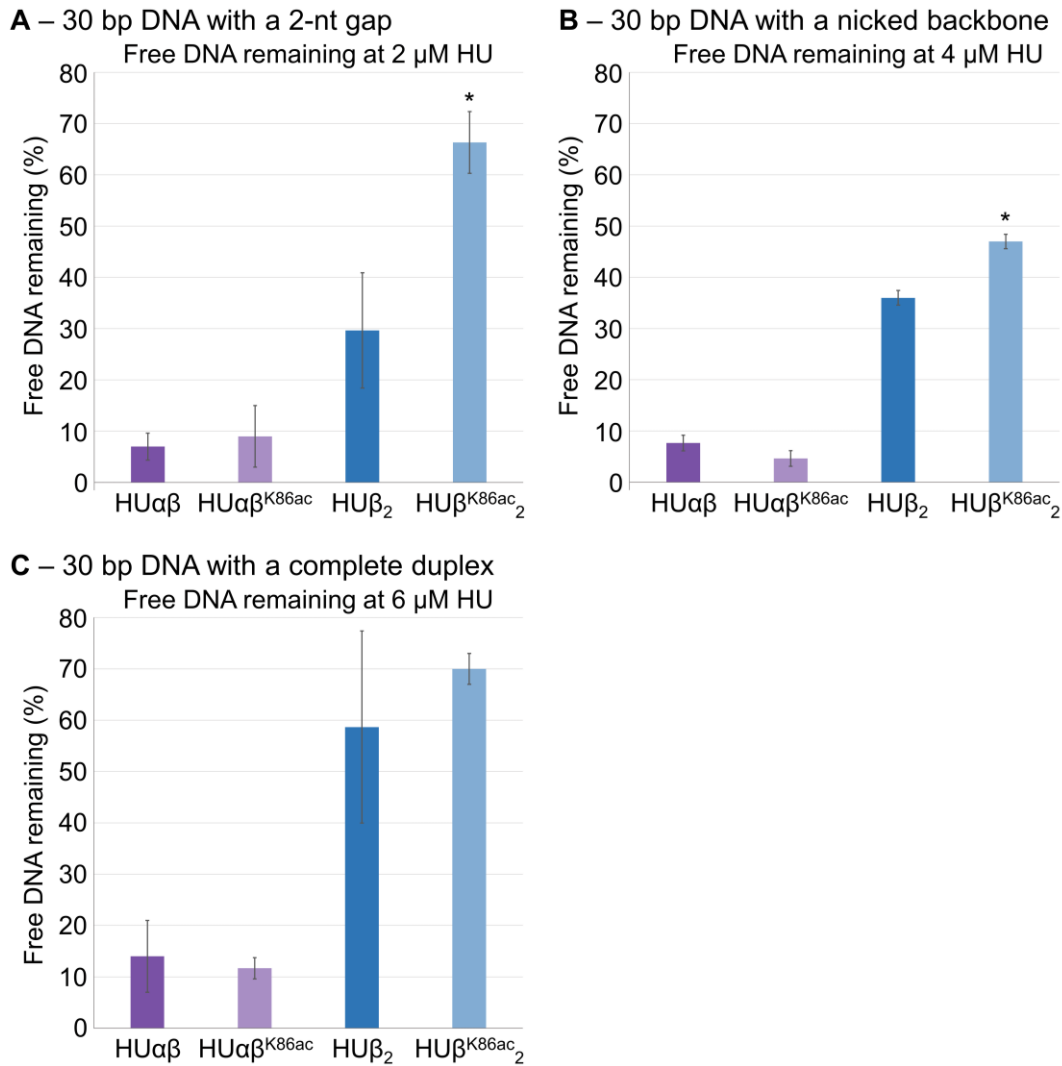


Figure 3.29 Effect of HU acetylation on interaction with different types of DNA. **A** 30 bp DNA fragment with a 2-nucleotide gap at 2 μ M HU. **B** 30 bp DNA fragment with a nicked phosphate backbone at 4 μ M HU. **C** 30 bp DNA fragment with a complete complementary duplex at 6 μ M HU. EMSAs were performed with 1 μ M of the specified 30 bp DNA fragment, varying concentrations of HU $\alpha\beta$, HU $\alpha\beta^{K86ac}$, HU β_2 and HU β^{K86ac}_2 in a buffer which facilitates DNA binding. Reactions were incubated for 10 minutes at 18 °C before analysis on non-denaturing 10% PAGE. An estimate of free DNA remaining in each condition was calculated using the intensity of DNA in the control reaction (0 μ M HU) as a reference and measuring the intensity of the corresponding band in other lanes relative to this. The data provided here is the average free DNA remaining for 3 independent repeats. The error bars represent the standard deviation, an asterisk (*) denotes a statistically significant difference ($p < 0.05$) in free DNA remaining between HU $\alpha\beta$ and HU $\alpha\beta^{K86ac}$ or HU β_2 and HU β^{K86ac}_2 .

EMSAs with HU β_2 and large DNA fragments

To gain insight into how HU interacts with longer DNA fragments, linearised plasmid DNA was used in further EMSAs. As significant differences in DNA binding affinity were only observed when the HU β_2 homodimer was acetylated at Lys67 or Lys86, only these dimers were used in further experiments. As can be seen in **Figure 3.30**, linearised 5500 bp plasmid DNA incubated with HU β_2 or HU β^{K67ac}_2 have very similar migration patterns. The migration pattern observed with HU β^{K86ac}_2 is noticeably different. The DNA displays both reduced mobility in the gel and a more smeared band appearance. The most mobile end of the smear is in line with free DNA, and the band extends past the most mobility-restricted DNA in the HU β_2 or HU β^{K67ac}_2 . In contrast, DNA incubated with HU β_2 or HU β^{K67ac}_2 , migrates as a compact band. EMSA was also performed with 2700 bp linearised plasmid DNA (**Figure 3.31**), where similar results were obtained.

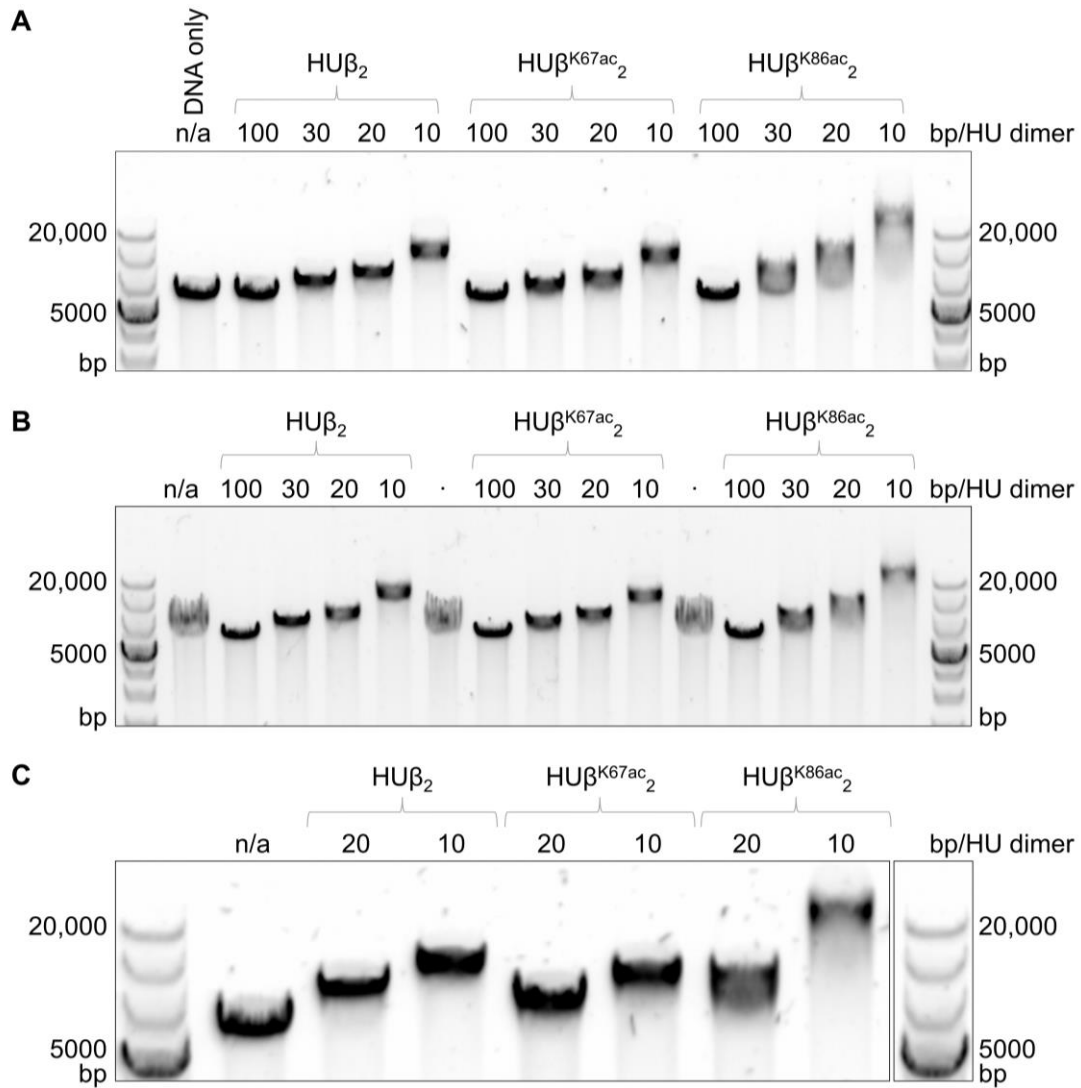


Figure 3.30 EMSA of HU β_2 , HU β^{K67ac}_2 and HU β^{K86ac}_2 incubated with linearised 5500 bp plasmid DNA. Three repeats, **A**, **B**, and **C**, are shown. Each reaction contained 125 ng of linearised plasmid DNA, a buffer that facilitates DNA binding and varying amounts of HU protein to provide the indicated ratio of DNA base pairs between HU dimers. The reaction was incubated at 37 °C for 1 hour before analysis *via* 0.5% agarose gel electrophoresis.

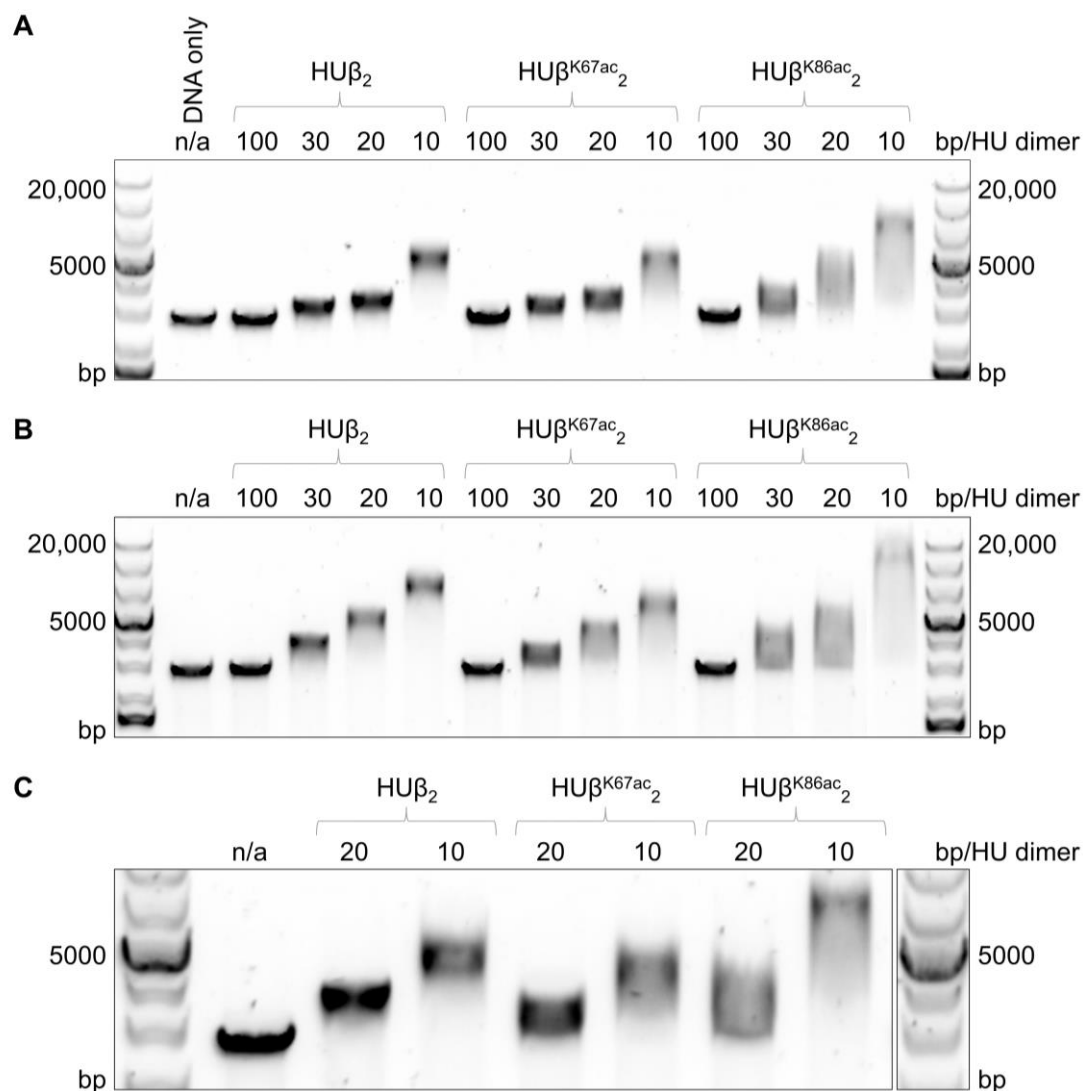


Figure 3.31 EMSA of HU β_2 , HU β^{K67ac}_2 and HU β^{K86ac}_2 incubated with linearised 2700 bp plasmid DNA. Three repeats, **A**, **B**, and **C**, are shown. Each reaction contained 125 ng of linearised plasmid DNA, a buffer that facilitates DNA binding and varying amounts of HU protein to provide the indicated ratio of DNA base pairs between HU dimers. The reaction was incubated at 37 °C for 1 hour before analysis *via* 0.5% agarose gel electrophoresis.

EMSA was also performed with a 1300 bp PCR fragment (**Figure 3.32**). When compared to EMSA with linearised plasmid, EMSA with the PCR fragment results in a greater level of retardation of the DNA in all HU containing conditions. However, this increase in retardation and mobility is even more pronounced when the DNA is incubated with HU β^{K86ac}_2 compared to the other two variants, in line with the results from the linearised plasmid DNA.

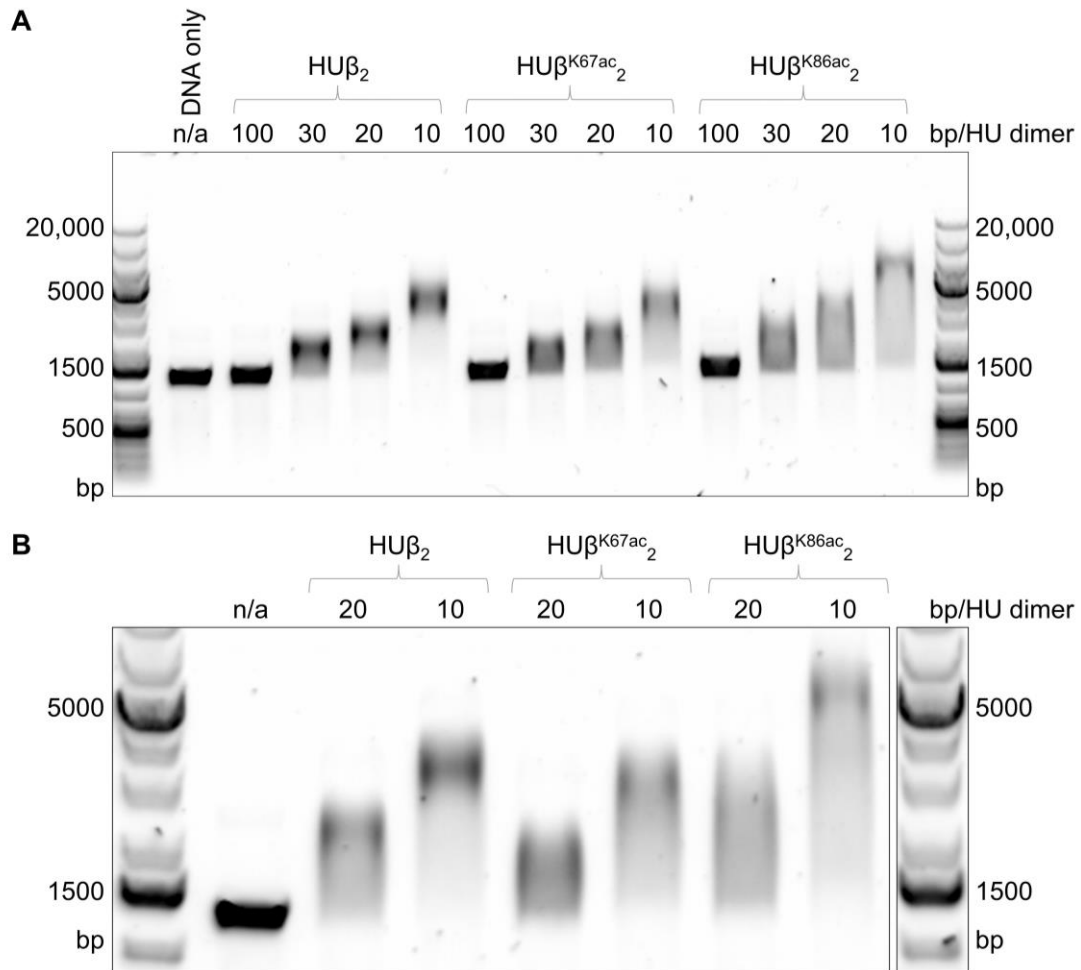


Figure 3.32 EMSA of HU β_2 , HU β^{K67ac}_2 and HU β^{K86ac}_2 incubated with a 1300 bp PCR fragment. Two repeats, **A** and **B**, are shown. Each reaction contained 125 ng of linearised plasmid DNA, a buffer that facilitates DNA binding and varying amounts of HU protein to provide the indicated ratio of DNA base pairs between HU dimers. The reaction was incubated at 37 °C for 1 hour before analysis *via* 0.5% agarose gel electrophoresis.

3.4.5 Circular dichroism

To investigate whether Lys86 acetylation modulates DNA binding through a change in protein secondary structure or thermal stability, characterization of these physical properties was carried out using circular dichroism (CD). At 20 °C, there were negligible differences in the CD spectra, indicating the preservation of the α -helix secondary structure (**Figure 3.33**). Additionally, by measuring CD spectra across increasing temperatures, the melting temperature of the proteins could be calculated (**Figure 3.34**). Measurement of CD spectra at 200, 208, 218 and 222 nm found no significant difference in thermal stability between HU β_2 and HU β^{K86ac}_2 (**Table 3.3**).

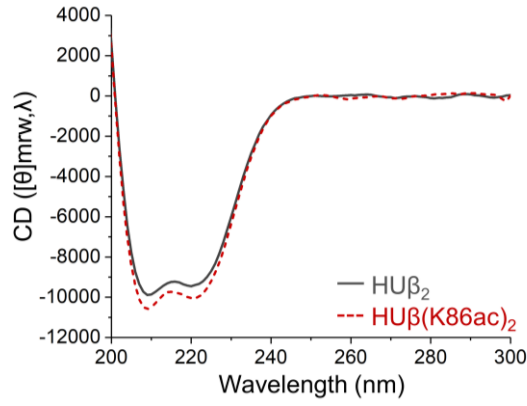


Figure 3.33 Effect of acetylation at Lys86 of *E. coli* HU β_2 homodimer on secondary structure. Circular dichroism spectra of HU β_2 (solid grey line) and HU β^{K86ac}_2 (dashed red line) from 200 to 300 nm measured at 20 °C showing the characteristic α -helix signals with two negative bands of similar magnitude around 210 and 220 nm.

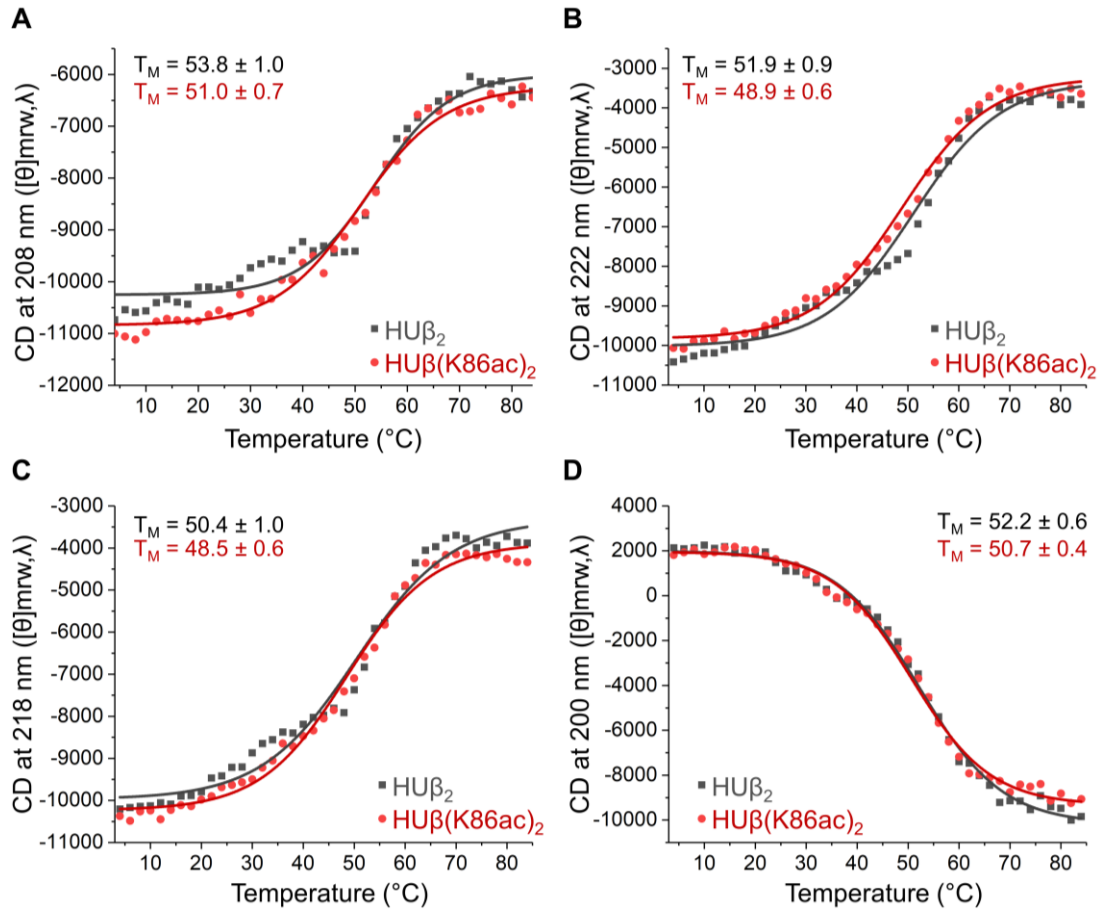


Figure 3.34 Effect of acetylation at Lys86 of *E. coli* HU β_2 homodimer on thermal stability analysed by circular dichroism. Data of wild-type and acetylated dimers are shown in grey or red lines, respectively. **A-D** Melting temperature T_M of the proteins as determined by CD signal from 4 °C to 84 °C at 208 (**A**), 222 (**B**), 218 (**C**) and 200 (**D**) nm.

Table 3.3 Average melting temperatures of HU β_2 and HU β^{K86ac_2} as determined by measuring circular dichroism at four different wavelengths.

	Repeat 1		Repeat 2		Repeat 3	
nm	HU β_2	HU β^{K86ac_2}	HU β_2	HU β^{K86ac_2}	HU β_2	HU β^{K86ac_2}
200			45.3 \pm 0.3	40.9 \pm 0.3	49.7 \pm 0.4	48.3 \pm 0.4
208	44.4 \pm 1.2	45.4 \pm 0.6	46.7 \pm 0.4	39.3 \pm 0.4	51.2 \pm 1.0	48.6 \pm 0.6
218	43.7 \pm 0.4	43.5 \pm 0.4	44.9 \pm 0.3	38.3 \pm 0.3	48.0 \pm 1.0	46.2 \pm 0.6
222	43.1 \pm 0.6	43.7 \pm 0.3	45.4 \pm 0.3	39.1 \pm 0.3	48.6 \pm 0.9	46.6 \pm 0.6

3.5 Discussion

3.5.1 Acetylation of Lys67 and Lys86

Of the five HU β_2 residues subjected to acetylation *in vivo*, Lys67 and Lys86 were chosen due to their locations on the DNA binding β -arms and DNA binding interface, respectively. As the β -arms interact most directly with DNA, it may have been reasonable to hypothesise that acetylation of Lys67 would be most likely to have an effect on DNA binding affinity. However, while the EMSAs comparing HU β_2 , HU β^{K67ac}_2 and HU β^{K86ac}_2 demonstrate that both acetylated versions have significantly reduced DNA binding affinity compared to the wildtype, the difference observed is much greater with HU β^{K86ac}_2 . This result was initially surprising. However, Lys86 has previously been identified as a key residue involved in HU-DNA interactions across bacterial species and is also highly conserved.^{440, 481, 482} On the rare occasions position 86 is not conserved as lysine, then it is occupied by arginine, another positively charged amino acid. In contrast, Lys67 is not always conserved.^{481, 482} The position often contains glutamic acid which has a negative charge, suggesting that the charge of the functional group of the amino acid in this position is not as necessary for, or directly related to, protein function.

Neutralisation of the positive charge at position 86 can also be achieved by amino acid substitution. Indeed, when replaced with alanine, DNA binding affinity was reduced in *E. coli* HU $\alpha\beta$.⁴³⁹ A similar effect was found with HU from *Bacillus subtilis*; when Lys86 was replaced with alanine, DNA binding affinity was reduced to 20% of the wildtype.⁴⁸³ In an HU homolog, replacement of Lys86 with glutamine reduced the DNA binding affinity.⁴⁸² Lys86 is also subjected to methylation¹⁰⁴ and succinylation¹⁹⁴ in various species. Lys86, among other residues, was also a target in the design of an effective inhibitor, which prevented interaction with DNA and reduced binding affinity.⁴⁴⁰

In vivo multiple residues may undergo post translational modification simultaneously. Therefore, Lys67 and Lys86 may be acetylated at the same time and the altered DNA binding affinity observed for each mutant may have an additive effect, as has been previously suggested for modifications of HU in mycobacteria.¹⁰⁴ Indeed, Thakur and co-workers investigated modifications of the DNA binding interface of HU, Lys83 and Lys86, and the DNA binding β -arms. When either Lys83 or Lys86 was replaced with alanine, or when the β -arms were deleted, HU could still bind DNA albeit with reduced affinity. When one residue was replaced with alanine and the DNA binding loop was

deleted, no DNA binding capacity remained.⁴³⁹ In this case, compromise of either site was tolerated but simultaneous modification of both sites rendered HU unable to bind DNA. It is possible that simultaneous acetylation of Lys67 and Lys86 may have a compound effect and reduce DNA binding further, or eliminate it altogether. It would be interesting to incorporate AcK into both position 67 and 86 of HU to study this possible effect. However, due to the observed decrease in production of HU protein here when AcK is incorporated into one position, it is likely that double incorporation of AcK into two sites would be challenging.

Circular dichroism of the wildtype and acetylated protein revealed that acetylation of Lys86 did not significantly affect the secondary structure nor the thermal melting temperature of HU β_2 . Further, analytical size exclusion chromatography confirmed that all proteins tested were in their dimeric states. Together, this suggests that the observed discrepancies in DNA binding affinity were not due to an alteration in secondary structure, thermal stability, or dimer formation. Therefore, the observed effect of acetylation on interaction on DNA must be due to a different mechanism.

3.5.2 Effect of acetylation on interaction with 30-bp DNA

EMSAs with short DNA were initially performed with a 30 bp DNA complex with a 2-nt gap on one strand. This DNA was chosen as both the homodimer and the heterodimer have very high affinity for 30 bp fragments with this deformity.⁴³⁷ Arguably, the high affinity HU exhibits towards this DNA may make it the most relevant for evaluating HU-DNA interactions and allows easier evaluation of reductions in binding affinity as such alterations should be more apparent than trying to estimate a decline in an already weak interaction.

For the HU β_2 homodimer, acetylation at either Lys67 or Lys86 significantly reduced DNA binding affinity towards 30 bp DNA with a 2-nt gap. This effect was most pronounced for HU β^{K86ac}_2 where an average reduction in free DNA remaining of 4.75-fold was observed at 4 μ M HU. For the HU $\alpha\beta$ heterodimer, no significant difference in DNA binding affinity was observed for HU $\alpha\beta^{K67ac}$ nor HU $\alpha\beta^{K86ac}$. The difference between the homodimer and heterodimer is discussed in more detail below. When incubated with 30 bp DNA with a nicked phosphate backbone, both the homodimer and heterodimer displayed reduced overall affinity compared to the 30 bp complex with a 2-nt gap, as expected. The effect of acetylation was also less pronounced. For the heterodimer, no significant effect of acetylation at either Lys67 or Lys86 on DNA binding affinity was observed. For the homodimer, a significant reduction in DNA binding of HU β^{K86ac}_2 was observed, but this reduction was only 1.3-fold compared to

the wildtype. For 30 bp DNA with a complete complementary duplex, the binding affinity by HU overall was greatly reduced. Interestingly, no significance alteration to DNA binding was observed for the homodimer nor the heterodimer.

These high-resolution assays on 10% non-denaturing acrylamide gels allow the observation of HU binding DNA at the single molecule level. Acetylation of the HU β_2 homodimer at Lys86 clearly and significantly reduces affinity for 30 bp fragments with gaps and nicks. This effect is most apparent for DNA with nucleotide gaps, and less so for DNA with nicks or a complete duplex. From this, it can be concluded that acetylation reduces the affinity of HU β_2 for damaged DNA. It can also be inferred that acetylation may be involved in controlling DNA damage repair mechanisms. When unacetylated, HU protein would have a high affinity for structurally deformed DNA. This DNA would be bound by HU and less likely to be degraded by exonucleases.⁴³² Acetylation of HU protein would reduce this affinity for damaged DNA, resulting in more damaged DNA being degraded.

In the only existing high resolution cocrystal structure of HU with DNA bound, *Anabaena* HU has introduced a bend into the DNA.⁴²⁷ The DNA wraps around the α -helical body of the HU protein, interacting with the DNA binding interface. It is possible that unacetylated HU protein would be more capable of bending bound DNA, as positively charged lysine residues allow a tighter interaction, and, in the case of Lys86, stronger attraction between the bound DNA and the α -helical body. Interruption of such DNA bending may result in an increased likelihood of HU to release bound DNA, as has been previously suggested.⁴⁷⁴ As such, acetylation may not interfere with HUs recognition of DNA, but if HU is unable to introduce a bend into the DNA it may increase the probability of a transient interaction rather than a stable bound DNA-protein complex.

An interesting observation from these assays is that in EMSAs with the HU β_2 homodimer, the complex corresponding to one HU β_2 dimer per one DNA molecule has slightly reduced mobility in the gel compared the same complex for HU β^{K67ac}_2 or HU β^{K86ac}_2 (**Figure 3.24**). This is likely due to the wildtype homodimer containing 2 additional positive charges compared to the acetylated dimers. As such, DNA-protein complexes containing the wildtype protein would experience slightly less repulsion from the negative electrode compared to those containing the acetylated proteins.

In the EMSAs with complete 30 bp duplex DNA, a band corresponding to one HU dimer bound to one molecule of DNA is not observed (**Figure 3.28**). Instead, as the amount of free DNA remaining decreases, a complex assumed to correspond to two HU dimers per DNA molecule appears. This is in contrast to EMSAs with gapped or nicked 30 bp DNA, where this complex appears sequentially after the first. Whole duplex DNA would be more difficult to bend or distort compared to the DNA with a 2-nt gap on one strand. This discrepancy may be representative of the alternative binding modes of HU depending on the type of DNA being interacted with. Here, for structurally deficient DNA, HU has a higher affinity and is more likely to bind one dimer to one DNA molecule at lower concentrations. For whole duplex DNA, HU has reduced affinity and HU molecules are likely to bind simultaneously. To investigate this further, it would be useful to analyse the EMSAs on a gel with a lower acrylamide concentration. Others have used 6.5% acrylamide gels to analyse EMSAs with short DNA fragments and have observed up to 5, decreasingly mobile and increasingly retarded complexes.^{426, 484}

With all of the 30 bp DNA fragments tested, the complex corresponding to one HU dimer per one DNA molecule is more prominent when DNA is incubated with HU $\alpha\beta$ compared to HU β_2 (**Figure 3.26**, **Figure 3.27** and **Figure 3.28**). In EMSAs with HU β_2 the first complex is fainter, even when comparing conditions with a similar amount of free DNA remaining. HU α_2 forms networks of stacked DNA while HU $\alpha\beta$ does not.⁴³⁸ It is possible that HU β_2 is also capable of forming such networks, which would display reduced mobility in the gel due to their increased molecular weight. It is also possible that HU β_2 is more likely to bind 2 HU dimers to one DNA relative to HU $\alpha\beta$. Together with the decreased prominence of the first complex when HU is incubated with whole duplex DNA compared to that with a 2-nt gap, this suggests that reduced affinity for DNA by HU results in a reduced possibility of a single dimer binding a single DNA fragment.

3.5.3 Acetylation in the HU β_2 homodimer vs the HU $\alpha\beta$ heterodimer

As others have noted, the HU $\alpha\beta$ heterodimer has a significantly greater affinity for dsDNA compared to the HU β_2 homodimer⁴³⁶ and the results presented here are in strong agreement with this observation. Acetylation of either Lys67 or Lys86 significantly reduces the binding affinity of the homodimer when incubated with a 30 bp DNA fragment containing a complete duplex, a nicked phosphate backbone or a 2-nt gap on one strand. Interestingly, the effect of acetylation on the heterodimer is not significant when either residue is acetylated.

It is important to consider that in this experimental design, the homodimer is acetylated on the lysine residue of both monomers, while in the heterodimer only the residue on the HU β monomer is modified. When the residue is acetylated on both monomers, any effect of acetylation on DNA binding will be magnified compared to acetylation of just one monomer. For example, the proposed effect of acetylation on the ability of HU to bend bound DNA would be emphasised if DNA has reduced attraction to the α -helical bodies of both monomers rather than just one. Further, HU may still be able to introduce a partial bend or hinge in the DNA when only one monomer is compromised, and this may allow for a prolonged complex formation (**Figure 3.35**). This may account for the lack of significant decrease in DNA binding affinity for HU $\alpha\beta^{K67ac}$ and HU $\alpha\beta^{K86ac}$ compared to the wildtype. On the other hand, the different types of dimers are known to interact differently with DNA⁴³⁶ and acetylation may have less of an effect on DNA binding mechanisms in the heterodimer.

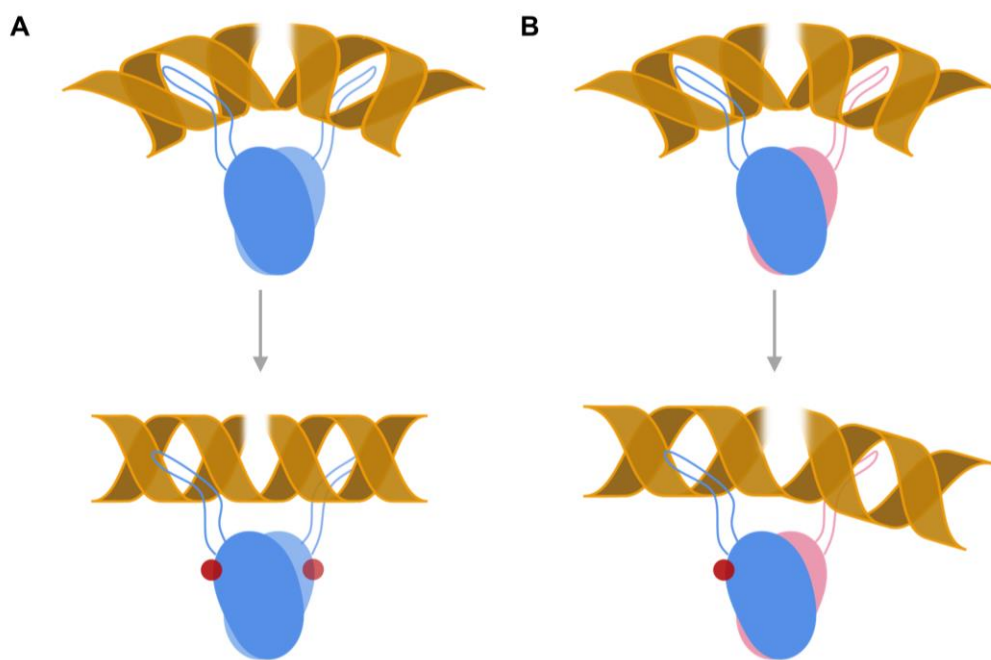


Figure 3.35 Schematic representation of possible effects of acetylation on binding to a 30 bp DNA fragment with a 2-nt gap by HU. **A** In the homodimer HU β_2 , acetylation may prevent bending of DNA by HU due to reduced attraction between the DNA binding interface and the negatively charged phosphate backbone resulting in a transient interaction between the β -ribbon arms of HU and DNA. **B** In the heterodimer HU $\alpha\beta$ acetylation of only one subunit may allow for some degree of DNA bending by HU and a more stable complex.

When interacting with native DNA, HU $\alpha\beta$ interacts with the DNA primarily through the α -helical body. The assembly of two heterogeneous chains in the heterodimer results in two distinct ‘faces’ in the resulting asymmetric dimer, with HU able to interact with B-form DNA through either face (**Figure 3.36**).⁴³⁸ When interacting with 30 bp whole duplex DNA in this study, HU $\alpha\beta$ and HU $\alpha\beta^{K86ac}$ had identical profiles. It is likely that acetylation of the β subunit did not considerably impede the interaction with DNA, as the other ‘face’ of the dimer would remain unaffected (**Figure 3.37**). It is possible that HU $\alpha\beta$ also interacts with structurally deformed DNA with one subunit more than the other. This may explain the reduced effect of acetylation in the heterodimer.

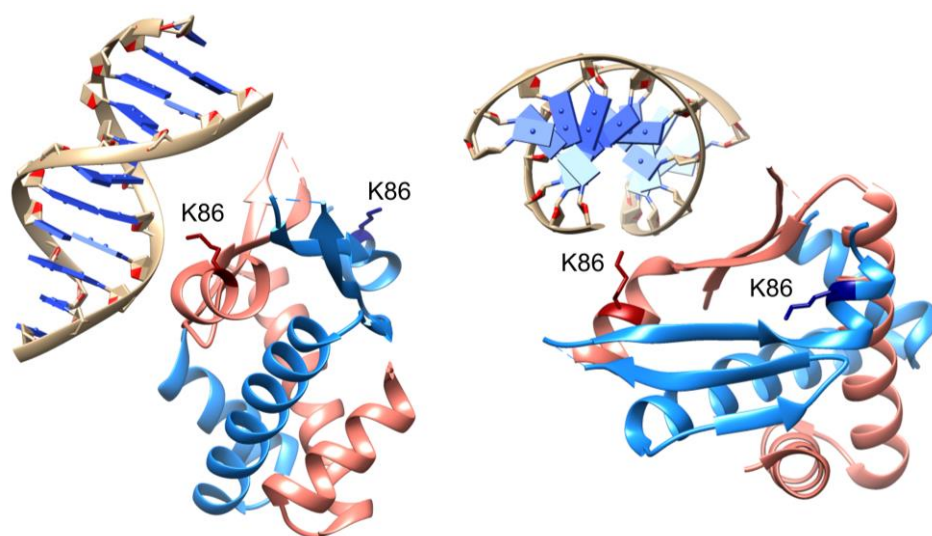


Figure 3.36 Cocystal structure of *E. coli* HU $\alpha\beta$ with a native β -form 19 bp DNA duplex (PDB #4YEW). Two alternative viewpoints are shown. HU $\alpha\beta$ primarily interacts with native form DNA through the α -helical body. HU can interact with B-form DNA through either of its two faces. In this conformation, the DNA binding interface of the α subunit (pink) is in close interaction with the DNA while the DNA binding interface of the β subunit (blue) faces into solution. Lys86 of each subunit is annotated.

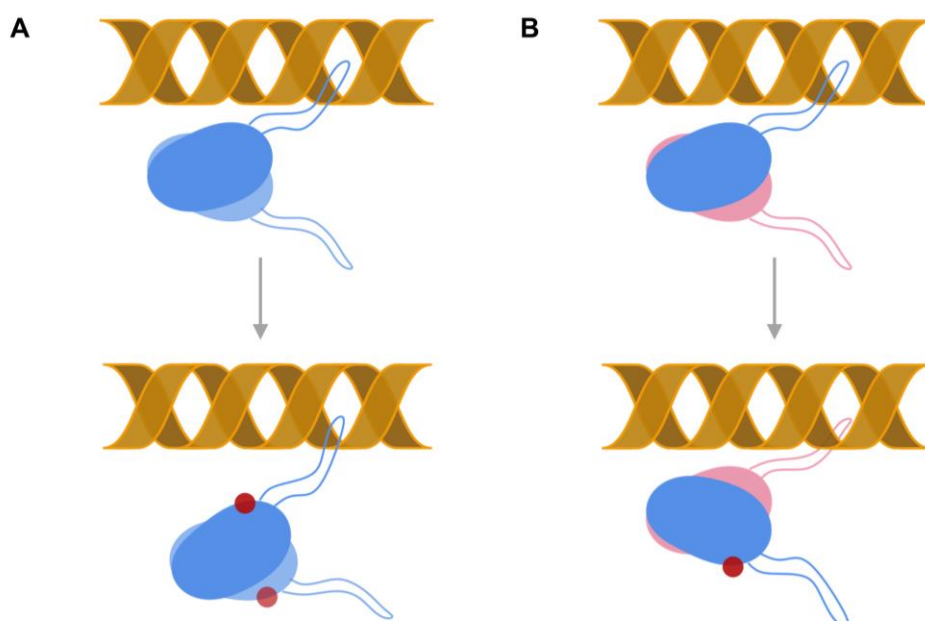


Figure 3.37 Schematic representation of possible effects of acetylation on the interaction of HU with a 30 bp whole duplex DNA fragment. **A.** In the homodimer $\text{HU}\beta_2$, acetylation may diminish interaction between the DNA duplex and HU due to reduced attraction forces between the DNA binding interface of the α -helical body of HU and the negatively charged phosphate backbone of DNA. **B.** In the heterodimer $\text{HU}\alpha\beta$ acetylation may not have an effect on DNA binding as HU can interact with DNA through the $\text{HU}\alpha$ subunit 'face' which is not acetylated.

To investigate the discrepancies further, it would be ideal to produce either a homodimer with only one monomer acetylated or a heterodimer with both subunits acetylated. Production of such a homodimer presents various challenges. As HU dimers automatically assemble, the acetylated and non-acetylated subunits could not be expressed within the same bacterial cell, as there would be no control over ensuring that each dimer has one acetylated and one non-acetylated subunit. Further, it is not known if mixing acetylated and non-acetylated HU in a 1:1 molar ratio *in vitro* would result in the chains spontaneously recombining. Unlike when mixing $\text{HU}\alpha$ with $\text{HU}\beta$, it is likely that that $\text{HU}\beta$ monomers will not have higher affinity for $\text{HU}\beta^{\text{K86ac}}$ monomers and the chains will not recombine. Nevertheless, it may be possible to construct a fusion protein whereby two $\text{HU}\beta$ monomers are connected *via* a linker sequence and only the first monomer contains an amber codon. In this design, the full sequence will only be translated if AcK is incorporated into the primary monomer, and the linker would need to be sufficiently long to allow the two monomers to form a dimer. This of course presents its own limitations; the linker may interfere with protein

conformation and DNA binding and may not be representative of native HU behaviour.

It would be considerably easier to produce a heterodimer with both subunits acetylated. Similarly to production of $\text{HU}\beta^{\text{K86ac}}_2$, mutation of the codon corresponding to Lys86 to TAG in *hupA* and subsequent incorporation of AcK would produce $\text{HU}\alpha^{\text{K86ac}}_2$. The resulting protein can then be combined with $\text{HU}\beta^{\text{K86ac}}_2$ and the chains will spontaneously recombine producing $\text{HU}\alpha^{\text{K86ac}}\beta^{\text{K86ac}}$. Performing EMSAs with this double-acetylated heterodimer would uncover whether the pronounced effect of acetylation on the homodimer compared to the heterodimer is due to the combined effect of acetylation on both monomers or an alternative mechanism. If time had allowed, I would have liked to investigate acetylation of Lys86 in the $\text{HU}\alpha$ homodimer and in the heterodimer. However, another study replaced Lys86 with alanine in $\text{HU}\alpha$ and found that this significantly reduced DNA binding capacity,⁴³⁹ suggesting that acetylation of $\text{HU}\alpha$ is likely to have a comparable effect to $\text{HU}\beta$ and that the one sided acetylation may indeed be the cause of the observed discrepancy between the homodimer and the heterodimer.

3.5.4 Effect of acetylation on interaction with longer DNA

EMSAs with 3800 bp and 5500 bp linearised plasmid DNA and with a 1300 bp PCR fragment revealed a clear and reproducible difference in migration between DNA incubated with $\text{HU}\beta_2$ and $\text{HU}\beta^{\text{K86ac}}_2$ whereby DNA incubated with $\text{HU}\beta^{\text{K86ac}}_2$ consistently displayed decreased migration in the agarose gel and increased smearing. A small difference was also observed between $\text{HU}\beta^{\text{K67ac}}_2$ and $\text{HU}\beta_2$, whereby DNA incubated with $\text{HU}\beta^{\text{K67ac}}_2$ appeared to have slightly increased migration compared to that of $\text{HU}\beta_2$. This suggests that fewer HU dimers bound the DNA compared to the wildtype protein, which is in line with the EMSAs with the 30 bp DNA fragments containing a 2-nt gap. However, the difference here was small and as with the EMSAs with shorter DNA fragments, acetylation of Lys86 appears to have a greater effect on interaction with DNA of $\text{HU}\beta$ than acetylation of Lys67.

However, in contrast to the EMSAs with 30 bp DNA fragments, acetylation of Lys86 appears to increase the DNA binding affinity of $\text{HU}\beta_2$. Complexes consistently displayed decreased mobility and increased retardation in the gel, suggesting a higher number of dimers were bound to the DNA. Increased smearing may also be a consequence of alteration in DNA bending or conformation by HU, resulting in reduced uniformity of DNA fragments in the sample. Due to the nature of analysing EMSAs with plasmid DNA on 0.5% agarose gels, the resolution is markedly

decreased compared to the EMSAs with 30 bp DNA fragments. The analysis is no longer at the single molecule level and, particularly with the ambiguity around the cause of band smearing, it is more difficult to form conclusions about what the observations imply about the interaction between HU and DNA.

When comparing the EMSAs with linearised plasmid or with PCR products, considerably more smearing and decreased migration is observed when any HU β dimer is incubated with the PCR product. Unlike purified plasmid DNA, purified PCR products have not undergone cellular DNA repair mechanisms and are likely to contain some gaps or mismatched base pairs. Therefore, as the PCR product is more likely to have structural deficiencies, HU is likely to have greater affinity for the PCR product over the linearised plasmid. These deformities also make the PCR product more flexible and more likely to be subjected to bending by HU. Thus, it may be that the increased smearing of the PCR product when incubated by HU compared to that of plasmid DNA is indicative of an increase in bound HU protein. With both linearised plasmid DNA and PCR products, DNA incubated with HU β^{K86ac}_2 appears more smeared and retarded compared to that incubated with HU β_2 or HU β^{K67ac}_2 . Therefore, it is possible that the increased smearing and decreased migration observed when DNA is incubated with HU β^{K86ac}_2 indicates an increase in HU-bound DNA.

It is interesting that both the EMSAs with 30 bp fragments and with plasmid DNA seem to suggest differing effects of acetylation depending on the type of DNA that HU is interacting with. It is well documented that HU has distinct interactions with different DNA types, and it is reasonable that acetylation may have alternative effects depending on the mechanism of interaction. HU exhibits differential binding modes when interacting with various types of DNA and interacts with native B-form DNA with no structural specificity through its α -helical body.^{438, 485} Acetylation of Lys86 is likely to reduce the affinity of the body for DNA, as the DNA binding interface would contain one fewer positive charge. This may result in an increase in transient interactions with DNA and a reduction in stable protein-DNA complexes. On the other hand, when HU does bind such DNA, acetylation of Lys86 would slightly decrease repulsion between positively charged HU dimers. HU α_2 is known to form networks between DNA strands⁴³⁸ and if HU β_2 also enables such networking, acetylation may permit easier network formation and closer stacking between HU dimers. Indeed, it has been demonstrated that changes in surface charge can cause repulsive separation of HU dimers and disruption of DNA bundling in HU α_2 .⁴⁶⁵ Both HU $\alpha\beta$ and HU α_2 are capable of packing tightly onto a DNA strand and forming rigid filaments.^{438, 446, 465} In these filaments, pairs of HU dimers interact closely across the DNA strand with one of the

arms of each dimer interacting with each other across the strand and the other arm interacting with the body of the opposite dimer.⁴³⁸ If the same occurs with HU β_2 , acetylation would allow even closer interactions between dimers.

This suggestion is somewhat supported by a study investigating acetylation in *M. tuberculosis* HU (MtHU). The authors found that acetylated MtHU had reduced DNA binding capacity in EMSAs. They also used transmission electron microscopy and observed that at a ratio of 1:60 dimer/bp, wildtype MtHU formed intramolecular loops in DNA while MtHU^{ac} coated the DNA. Intriguingly, at a ratio of 1:10 dimer/bp, MtHU formed large condensed DNA complexes while MtHU^{ac} formed rigid filaments. Their results suggest that acetylation resulted in reduced compaction ability of MtHU and induced coating of DNA. They also demonstrated decompaction of the nucleoid in cells producing a high amount of acetylated HU; with subsequent deacetylation reversing this effect.⁴⁸⁰ Their results demonstrate an increased packing of HU onto DNA and a decrease in bending of the bound DNA when HU is acetylated, in agreement with hypotheses postulated here. However, it must be noted that MtHU is structurally different to EchU, the 214 aa protein is considerably larger and contains a carboxy-terminal domain tail similar to that of eukaryotic histones.²⁷¹

HU binds linear DNA without specificity with a higher dissociation constant (K_D) while the K_D for DNA with gaps and nicks is much lower.⁴³⁶ For example, at low salt concentrations HU $\alpha\beta$ binds DNA with a K_D of around 400 nM for linear DNA, 4 nM for nicked DNA and 1-2 nM for DNA with gaps.⁴³⁶ When bound, HU either bends linear DNA only slightly or not at all^{438, 486} while it introduces flexible kinks from 65° to 140° into DNA containing structural deformities.^{427, 487, 488} If acetylation does interfere with bending of bound DNA, it would not negatively impact native DNA binding as much as it does with DNA fragments containing structural deformities. Acetylation may therefore be a mechanism to switch HU's preference, conveying lower affinity for cruciform and structurally deficient DNA and an increased affinity for genomic and plasmid DNA. This would explain the observed discrepancy between EMSAs with 30 bp structurally deficient DNA and with linearised plasmid DNA. Acetylation may also be a mechanism for controlling the local concentration of HU in the cell. Deacetylating HU protein would increase the concentration in the cytosol by decreasing affinity for genomic and plasmid DNA, making more HU available to bind DNA damage repair intermediates. Clearly, considerably more work is needed to unveil the molecular mechanism behind the effect of acetylation on interaction with different types of DNA. However, it is clear that acetylation of HU β_2 alters the interaction with DNA compared to the wildtype.

3.5.5 Physiological effects of acetylation

It appears that acetylation of HU may have contrasting effects depending on the type of DNA involved in the interaction. If so, this is in keeping with the seemingly contrasting effects of the HU protein mentioned before, having roles in both compaction and decompaction of DNA depending on concentration and time of incubation. It is possible that acetylation may also have alternating effects depending on the location of acetylation on HU and on the location of HU within the cell, *i.e.* whether HU is free in the cytosol or in close proximity to genomic DNA. Further, acetylation of HU may influence the DNA binding mode that is employed. Considering the discussion above, HU acetylated at Lys86 may have reduced affinity to DNA with structural deformities and increased affinity to genomic or plasmid DNA while HU acetylated at Lys67 appears to have decreased affinity for all DNA types. Acetylation could therefore provide spatial and/or temporal control of the affinity of HU for DNA and of the binding mode employed to invoke different functions of HU. As mentioned, acetylation may be a method of controlling local concentrations of HU protein on the DNA molecule. Acetylation may also influence DNA repair mechanisms by moderating the amount of damaged DNA fragments bound by HU and thereby influencing the amount of DNA which is targeted for degradation.

The results presented here demonstrate that acetylation has a pronounced effect on the HU-DNA interaction. This provides a very interesting insight into the role of acetylation in modulating protein function. However, it remains unclear what role acetylation will have at a physiological level in the cell. Investigating the effect of acetylation of HU *in vitro* with EMSAs provides a straightforward and relatively fast means to determine the effect of this modification on the protein's interaction with DNA. These assays are also not vulnerable to variables such as the effect of other proteins, small molecules, and cellular growth state, thereby allowing insight into the interaction with minimal interference. However, *in vivo*, all of these factors may have an effect on the interaction of HU with DNA.

HU is known to affect the transcription of many genes, including those involved in antimicrobial resistance. If acetylation interferes with HU binding to genomic DNA, it is likely that this will have implications on gene transcription. In mycobacterial HU, Lys86 is subjected to acetylation and methylation. When Lys86 was replaced with arginine, cells displayed a wildtype phenotype when grown in media. However, when plated on antibiotic plates at concentrations near to the minimum inhibitory concentration, cells carrying the mutated HU formed significantly fewer colonies than the wildtype and specifically lost small colony variants. The authors concluded that

this change in phenotype was due to a lack of either methylated or acetylated lysine.¹⁰⁴

Analysis of the transcriptome of cells expressing acetylated HU vs those expressing the wildtype protein would allow for insight as to whether acetylation of HU has an effect on gene transcription and regulation. As the greatest effect was seen with HU β^{K86ac}_2 vs HU β_2 , comparing cells expressing these two variants would be a good starting point. Transcriptomic studies using RNA-seq are easy, cheap and provide a large volume of data about the differential expression of genes between two samples.⁴⁸⁹ This would perhaps be the easiest way to gather a large amount of data about potential physiological effects of acetylation of HU. If differential regulation of any genes were revealed by these studies, assays investigating specific phenotypic changes could then be employed based on this.

3.6 Conclusions

This chapter provides evidence in agreement with previous works that Lys86 is a key residue involved in the HU proteins interaction with DNA. Others have shown that the elimination of the positive charge of this residue by amino acid substitution greatly reduces DNA binding. The results presented here reveal that neutralisation of the positive charge via acetylation causes a similar reduction in DNA binding affinity when interacting with structurally deficient DNA. However, when interacting with native DNA acetylation may increase DNA binding affinity. This report also reveals Lys67 as a key residue involved in DNA binding by HU protein. Acetylation of this residue consistently introduced a small but significant reduction in DNA binding affinity when interacting with either native or structurally deficient DNA. As HU is acetylated *in vivo*, this suggests that acetylation may be used as a mechanism by the cell to reduce the DNA binding affinity of the HU protein. The effect could be reversed with deacetylation, providing a real-time mechanism of modulating protein function.

HU exhibits a minimum of two binding modes. For short, structurally deformed DNA fragments, HU binds the DNA with its arms and bends the DNA around the protein body. Acetylation greatly reduces the DNA binding affinity of HU β_2 towards this type of DNA, likely by interfering with the interaction between the DNA binding interface and the DNA, preventing HU from bending the DNA and forming a stable complex. As HU protects such fragments from degradation by exonucleases, acetylation may have a role in the regulation of DNA repair mechanisms. When binding native DNA, HU mainly interacts with DNA through its α -helical body and pairs of dimers interact across the DNA strand. In this case, acetylation may allow closer interactions between dimers due to decreased repulsion and allow tighter packing of HU onto the DNA strand. If acetylation induces HU to coat the DNA and form rigid filaments, this will result in reduced access to DNA by transcriptional machinery and could significantly alter gene expression. As modifications to HU can affect antimicrobial resistance phenotypes, investigation into the effects of HU acetylation on the transcriptome is a key area for future research.

HU is a truly versatile protein serving many different and sometimes contrasting functions in the cell. It seems appropriate that the effect of acetylation may also have contrasting consequences depending on the type of DNA being interacted with and therefore may influence cellular processes in different ways. This work has provided an exciting glimpse into the effects of post-translational modification of HU on protein

function. However, considerably more work is needed to characterise the specific effects at the molecular level on the interaction with DNA, both to determine precisely how acetylation reduces DNA binding affinity for structurally deficient DNA and to determine the effect on binding native DNA. Investigation into transcriptomic and phenotypic consequences of HU acetylation is also of utmost importance to clarify the role of this modification on cellular processes.

3.7 Materials and methods

3.7.1 Genomic DNA extraction

E. coli whole genomic DNA extraction was performed using PureLink™ Genomic DNA Mini Kit (Invitrogen, #K182000) according to the manufacturer's instructions.

3.7.2 Plasmid construction

Plasmids **pBAD hupB-His6** and **pAcKRS** were cloned by Sanjay Patel.

pBAD hupB(K67TAG)-His6. Site-directed mutagenesis with primers VBF032 and VBR030 was used to mutate the Lys (AAA) codon at amino acid position 67 of pBAD hupB-His6 to TAG. The resulting sequence was confirmed using primer YTS35.

pBAD hupB(K86TAG)-His6. Site-directed mutagenesis with primers VBF033 and VBR031 was used to mutate the Lys (AAA) codon at amino acid position 86 of pBAD hupB-His6 to TAG. The resulting sequence was confirmed using primer YTS35.

pBAD hupA-His6. *hupA* was PCR amplified from the *E. coli* BL21(DE3) genome using primers VBF036 and VBR035, resulting in a 323 bp fragment. The pBAD vector was amplified from pBAD hupB-His6 using primers VBF037 and VBR034, resulting in a 3996 bp fragment. The two fragments were assembled using NEBuilder. The resulting plasmid was sequenced using primer YTS35.

Table 3.4 Plasmids used in this study.

Plasmid	Vector	Insert	Antibiotic Selection
pBAD hupB-His6	pBAD	<i>hupB</i>	Ampicillin
pBAD hupB(K67TAG)-His6	pBAD	<i>hupB(K67TAG)</i>	Ampicillin
pBAD hupB(K86TAG)-His6	pBAD	<i>hupB(K86TAG)</i>	Ampicillin
pBAD hupA-His6	pBAD	<i>hupA</i>	Ampicillin
pAcKRS		<i>MbAcKRS</i> , Pyl tRNA	Spectinomycin

Table 3.5 Primers for PCR.

Primer	Sequence (5' – 3')	Purpose
VBR030	GCAGCAGCGATGGTGATCTCCTAACCGGTCTGCG GGTTGC	Insertion of TAG codon into <i>hupB</i>
VBR031	TGCTCGAGGTTTACCGCGTCTACAGTGCTTTAC CTGCACGGAAGC	Insertion of TAG codon into <i>hupB</i>
VBF032	GAGATCACCATCGCTGCTGCTAAAGTAC	Insertion of TAG codon into <i>hupB</i>
VBF033	GACGCGGTAAACCTCGAGCAC	Insertion of TAG codon into <i>hupB</i>
VBR035	CAGCTGCAGATCTCAGTGGTGGTGGTGGTGGTGC TTAACTGCGTCTTTCAGTGCCTTG	Amplification of <i>hupA</i>
VBF036	GGCTAACAGGAGGAATTAACATGAACAAGACTCA ACTGATTGATGTAATTGC	Amplification of <i>hupA</i>
VBF037	ACCACTGAGATCTGCAGCTG	Amplification of pBAD vector
VBR037	GTTTACCGCGTCTTTCAGTGC	Amplification of <i>hupB</i>
VBF038	AGCGATTACGACATCCCCACTACTGAGAATCTTT ATTTTCAGGGCGCCATGAATAAATCTCAATTGAT CGACAAGATTGC	Amplification of <i>hupB</i>

Table 3.6 Primers for sequencing.

Primer	Sequence	Aligns to
YTS35	TGTCTCATGAGCGGATAC	AmpR promoter
VBS018	ACTTTGCTATGCCATAGC	araBAD promoter

3.7.3 Bacterial protein expression

Plasmids encoding *hupA* or *hupB* were chemically transformed into *E. coli* BL21(DE3) AI. For unnatural amino acid incorporation, cells were co-transformed with **pAckRS**. After transformation, all medium used was supplemented with antibiotics for plasmid selection based on plasmid resistance genes (for a list, see **Table 3.4**). The transformation mixture was used to inoculate a 15 mL starter culture in TB medium and incubated at 37 °C, 180 rpm, for 16-18 hours. The starter culture was then diluted

to A_{600} 0.05 in 1 L TB and incubated at 37 °C, 180 rpm. When incorporating unnatural amino acids, at A_{600} 0.5 the culture was supplemented with 5 mM AcK and 20 mM nicotinamide. At A_{600} 0.9, or 30 min after amino acid supplementation, protein expression was induced with 0.5 mM IPTG and 0.2% arabinose. Cultures were then incubated at 20 °C, 180 rpm, for 16-18 hours.

3.7.4 Protein purification

Nickel affinity purification

As described in **Chapter 5 - General materials and methods**.

Buffer exchange

Protein was buffer exchanged either using a desalting column or with a 3 kDa cut-off dialysis membrane. For the desalting, a HiPrep™ 26/10 desalting column (Cytiva, #17-5087-01) was equilibrated with phosphate buffer. Protein sample was loaded onto the column, which was then washed with phosphate buffer. The flow through was collected when a peak at 214 nm was observed and the fraction analysed by SDS-PAGE. For dialysis, protein samples were placed in 3.5 kDa cut-off SnakeSkin™ dialysis tubing. The tubing was incubated in at least 1000x the volume of the protein sample of the desired buffer and incubated at 4 °C for 16-18 hours.

Cation exchange

Further purification of protein samples obtained by nickel chromatography was achieved with cation exchange. Protein was loaded onto a 6 mL RESOURCE™ S column (Cytiva, #17118001) and separated with linear gradient elution from 0 to 0.5 M NaCl over 20 column volumes, according to manufacturer's instructions. The start buffer was phosphate buffer and the elution buffer phosphate buffer containing 1 M NaCl. Fractions were collected in 0.5 column volumes and those containing a peak at 214 nm were analysed by SDS-PAGE.

Concentrating protein

Protein samples were concentrated using a VivaSpin ultrafiltration unit with a 3000 MWCO PES membrane (Sartorius, #VS2092) according to manufacturers instructions at 4 °C.

Protein storage

For long term storage, the final concentration of glycerol in the sample was adjusted to 15%. Protein was aliquoted and stored at -80 °C.

BCA assay

The protein sample to be measured was diluted 1:10, 1:50 and 1:100 in PBS. To create known concentration standards, 2 mg/mL BSA stock was diluted to 800, 400, 200, 100, 50, 25, 12.5 and 6.25 µg/mL in PBS by serial dilution. BCA working solution was prepared by mixing Bicinchoninic Acid solution (Sigma, #B9643) with saturated CuSO₄ in a 50:1 ratio, respectively. Then, 90 µL of BCA working solution was added to each well in a clear 96 well plate. A negative control of 10 µL PBS was dispensed into the first 3 wells. Next, 10 µL of each BSA standard was dispensed in triplicate into the following wells. Finally, 10 µL of each dilution of the protein sample was added in triplicate. The plate was incubated at 37 °C for 30 min. The absorbance at 562 nm of each well was then measured on a Victor X (Perkin Elmer) plate reader.

3.7.5 Heterodimer formation

Purified HUα₂ was combined with HUβ₂, HUβ^{K67ac}₂ or HUβ^{K86ac}₂ in a 1:1 molar ratio and incubated on ice for 5 minutes.⁴³⁰ The resulting heterodimer was confirmed *via* native PAGE analysis and analytical size exclusion chromatography.

3.7.6 Native PAGE

Protein samples were prepared in 1X native loading dye. A discontinuous buffer system was used. For the resolving gel, between 10 to 15% acrylamide in native resolving buffer was polymerised with 0.1% APS and 0.5% TEMED. For the stacking gel, 8% acrylamide in native stacking buffer was polymerised with 0.1% APS and 0.1% TEMED. Electrophoresis was performed on ice with the electrodes reversed (positive to negative) in native running buffer with constant voltage at 100 V for 2.5 h.

Table 3.7 Buffers for native PAGE.

Buffer	Composition
4X native loading dye	0.24 M KOH, 0.24 M acetic acid, 0.04% w/v) pyronine Y, 40% glycerol
4X native resolving buffer	0.24 M KOH, pH 4.3, 1.44 M acetic acid
4X native stacking buffer	0.384 M KOH, pH 6.8, 0.4 M acetic acid
10X native running buffer	3.5 M 6-amino caproic acid, 1.4 M acetic acid pH 4.5

3.7.7. Analytical size exclusion high-performance liquid chromatography

Analytical size exclusion chromatography was performed with a high-performance liquid chromatography system (Agilent). A Bio SEC-3 column (Agilent) was equilibrated in PBS (10 mM Na_3PO_4 pH 7.4, 154 mM NaCl). For generating the standard curve of molecular weights, Gel Filtration Standard (Bio-Rad, #1511901) was diluted 1:10 in potassium phosphate buffer and 1 μL of the diluted standard was injected into the column using an autosampler. PBS was passed through the column at a rate of 0.35 mL/min and the elution profile of the standards was analysed at 214 nm. For analyses of HU protein, protein samples were prepared at 0.6 mg/mL and 20 μL of samples was injected into the column using an autosampler. PBS was passed through the column at a rate of 0.35 mL/min and the elution profile of the proteins were analysed at 214 nm.

For the standard curve, the log molecular weights of the protein standards were plotted against their retention time and a line of best fit generated. The equation of the line of best fit was then used to calculate an estimated molecular weight of the HU protein samples.

3.7.8 Electrophoretic mobility shift assay

EMSA with linearised plasmids and PCR products

The amount of protein required to give one HU dimer per a defined number of base pairs was calculated as follows:

$$\text{no. HU dimers required} = \frac{\text{DNA fragment length (bp)}}{\text{desired HU frequency (bp)}} \times 2$$

$$\text{pmoles HU required} = \frac{\text{fmols of 250 ng DNA} \times \text{no. HU dimers required}}{1000}$$

$$\text{ng HU required} = \text{pmoles HU required} \times \text{mw of HU protein}$$

The DNA binding reaction was performed in 30 mM Tris pH 7.5, 100 mM NaCl, 0.02% v/v Tween20, 0.5 mg/ml BSA. Each reaction also contained 250 ng of the DNA fragment and the required amount of HU protein. The total reaction volume was 15 μ L. DNA binding was allowed to occur for 1 h at 37 °C.

Immediately after incubation, 1.5 μ L 10x FastDigest Green buffer was added to each reaction, which was then loaded onto a 0.5% agarose gel. Gels were electrophoresed on ice in TAE buffer at 110 V with constant voltage for 40 min before imaging on a ChemiDoc XRS+ using an XcitaBlue™ conversion screen.

DNA fragments:

A 5514 bp plasmid (pCX-sfGFP(150TAA), cloned by Sanjay Patel) linearised by digestion with HindIII.

pUC18 (ThermoScientific, #SD0051) a 2686 bp plasmid linearised by digestion with HindIII.

PCR fragment. A 1292 bp DNA fragment amplified by polymerase chain reaction. The DNA sequence was chosen arbitrarily, and encodes the maltose binding protein (MBP).

EMSA with short DNA fragments

The oligonucleotides were purchased from Merck. DNA was purified by high pressure liquid chromatography and provided in TE buffer at 100 μ M concentration. Three DNA fragments were used: 30 bp whole duplex, 30 bp with 2-nt gap, 30 bp with nicked phosphate backbone. The sequences are provided in **Figure 3.22**. Annealing of the 30 bp fragments was achieved by heating the DNA to 98 °C for 5 min, then cooling to 4 °C at a rate of 1 °C/min.

Each reaction contained 1 μ M of a 30 bp DNA fragment⁴³⁷ (**Figure 3.22**). The amount of HU varied per reaction and was also calculated as a molar concentration. The DNA binding reaction was performed in 30 mM Tris pH 7.5, 100 mM NaCl, 0.02% v/v Tween20, 0.5 mg/ml BSA. The total reaction volume was 10 μ L. DNA binding was allowed to occur for 10 min at 18 °C.

Immediately after incubation, 2.5 μ L GelPilot DNA loading dye (Qiagen, #239901) was added to each reaction, which was then loaded onto a 10% non-denaturing continuous acrylamide gel. The non-denaturing gels were prepared with 10% acrylamide in 0.1 M Tris-borate pH 8.3, 2 mM EDTA (TBE) and polymerised with a final concentration of 0.2% APS and 0.1% (v/v) TEMED. Gels were electrophoresed on ice in TBE buffer at 100 V with constant voltage for 80 min. Gels were then incubated in PAGE GelRed (Biotium, #41008) diluted 10,000-fold in dH_2O for 30 minutes according to manufacturer's instructions before imaging on a ChemiDoc XRS+ UV transilluminator with an ethidium bromide emission filter.

For analysis of free DNA, ImageLab (BioRad) software was used (**Figure 3.38**). Lanes and bands were manually added to the image. The band corresponding to the control reaction, where all reagents except HU were added, was set as the reference band (intensity = 1.0). The intensity of all other bands were recorded relative to this value.

Each reaction was repeated a minimum of three times. The mean percentage of free DNA remaining and the standard deviation from the mean was calculated for each condition. Statistical significance between groups was analysed using an independent two sample t-test with an alpha level of 0.05.

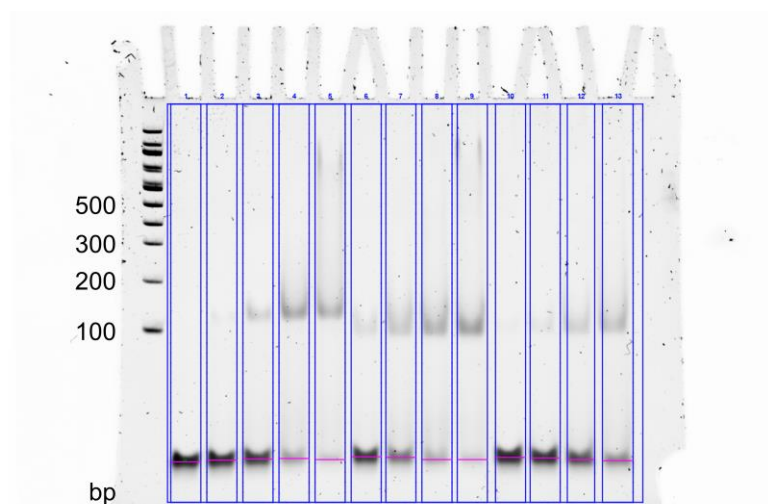


Figure 3.38 Example of the quantification of free DNA remaining in EMSAs. Image Lab software (Bio-Rad) was used to manually add lanes to the gel (blue vertical lines). Bands were manually added in each lane to the DNA band which represents free (unbound) DNA (pink horizontal lines). This was determined by running a 0 μ M HU control condition (lane 1), in which all DNA would be free. Bands with a corresponding migration pattern to the free DNA were analysed in the HU conditions. The band in the 0 μ M HU control was set as a reference band (100% intensity) and all other bands were quantified relative to this.

3.7.9 Circular dichroism

These experiments were performed on an Applied PhotoPhysics Chirascan spectrometer using 5 μ M protein in deoxygenated potassium phosphate buffer (10 mM KPO, pH 7.0, 5% glycerol). Spectra were measured in triplicate between 200 and 300 nm in 1 mm quartz cuvettes under N_2 with a 50 nm/min scan speed, 0.5 nm data pitch, 1 nm bandwidth, and 0.5 second response time. To measure the thermal melting point, spectra were collected every 2 $^{\circ}$ C as temperature increased from 4 to 84 $^{\circ}$ C. The rate of temperature increase was 0.5 $^{\circ}$ C/min with 300 s equilibration time at each temperature.

Chapter 4 - Discussion, conclusions and future work

4.1 Discussion and conclusions

The aim of this thesis was to investigate the role of post-translational modifications in bacterial antimicrobial resistance. To this end, the PTMs of two proteins with roles in antimicrobial resistance were characterised. These were the propionylation of AdeT1, a component of a multidrug efflux pump from *A. baumannii* and acetylation of HU, a DNA-binding protein from *E. coli*. While the PTM of both of these proteins were discovered and reported by others, the molecular and physiological implications of the modifications remained unexplored. Here, unnatural amino acid incorporation through genetic code expansion was used to characterise the effects of these modifications. The work presented in this thesis revealed that both modifications have a role in modulating the function of their respective proteins, indicating possible regulatory consequences for cellular physiology and antimicrobial resistance pathways.

4.1.1 Insights into the role of PTMs in regulating antimicrobial resistance

Chapter 2 reports that when produced in *E. coli*, propionylation of *A. baumannii* AdeT1 increases efflux pump activity, resulting in increased ethidium bromide and erythromycin efflux. This resulted in a 4-fold higher concentration of erythromycin required to inhibit bacterial growth compared to production of wild-type AdeT1. As already mentioned in **2.5 Discussion**, this outcome may be the result of an altered interaction with other efflux pump components or with substrates of the efflux pump. Although produced in *E. coli* in this study, it is feasible that propionylation of AdeT1 has similar effects in *A. baumannii*. As the proteins which AdeT1 interacts with in *E. coli* are compatible enough to form a functioning pump, it is likely that modification of the protein would alter the interactions with its native complex in a comparable manner. As mentioned in **2.2 Introduction**, AdeT1 is not the only efflux pump component to undergo modification.^{255, 268, 359, 363} It is possible that different PTMs have distinct effects on pump activity or function. However, it is also possible that the modifications efflux pumps are subjected to form a universal ‘code’, whereby each modification induces a specific change. Considerably more research is needed before the role of PTM in regulating efflux pump function and activity can be elucidated. As efflux pumps have a well documented role in antimicrobial resistance and are already a target of adjuvant therapies,⁹⁴ I believe this to be a worthy area of future research.

Chapter 3 reports on the effect of acetylation of *E. coli* HU protein at two residues on the DNA-binding interfaces of the protein. Acetylation of the first residue, Lys67, had no significant impact on the DNA-binding activity of the protein while acetylation of the second residue, Lys86, greatly reduced DNA-binding activity. As mentioned in **3.5 Discussion**, an important area of future work is to determine whether this modulation of binding affinity has any impact on gene expression, as has been implicated with other modifications of HU.¹⁰⁴ Only then will the role of this PTM in antimicrobial resistance responses become clearer. With the clear reduction in binding affinity exhibited by HU with Lys86 acetylated, it is very possible that this modification will have effects on gene transcription and represents a promising area of future research. Although the consequences of the modification on gene expression and cellular physiology have not yet been confirmed, as suggested by others, HU may still be a viable target for adjuvant therapy. With more general roles in regulating gene expression, inhibiting HU may weaken cells' survivability and make them more susceptible to antimicrobials. As HU is a highly conserved bacterial protein, any advances furthering our understanding of HU and how it regulates gene expression will be beneficial when developing therapies against a broad range of bacterial species.

An interesting question raised by these investigations is whether the *in vivo* prevalence of the PTM regulating protein function is increased in response to antibiotic treatment. For example, in the original report, AdeT1 was found to be propionylated in both antibiotic susceptible and antibiotic non-susceptible strains of *A. baumannii*.³⁵³ It would therefore be of great interest to determine whether multidrug resistant *A. baumannii* experience increased propionylation when exposed to erythromycin or ethidium bromide. On the other hand, it would be insightful to know whether inhibiting global propionylation has any effect on the minimum inhibitory concentration of antimicrobials. Similarly, there have not yet been any investigations determining whether the amount of acetylation in antimicrobial resistant *E. coli* is altered in response to treatment with antimicrobials. Establishing these links or, perhaps equally importantly, a lack of any link would provide essential insights into the relevance of these modifications in resistance responses in the clinical setting.

4.1.2 Role of PTM crosstalk in regulating antimicrobial resistance

A limitation of both of the studies presented here is that although they characterise the effects of the modification of one protein on the function of that protein, they do not comprehensively investigate the wider effects of modifications in terms of PTM crosstalk. For each protein, only one residue was subjected to modification before characterisation. *In vivo*, proteins may be subjected to multiple modifications simultaneously and in varying combinations. As mentioned in **1.2.3 PTM crosstalk**, there may be a combined effect on protein function resulting from interactions between these modifications.^{129, 236} These effects could be counteractive, complementary, or additive to produce a specific molecular effect and physiological output. For example, the *E. coli* HU protein is a dimer and each monomer may be acetylated on up to 6 lysine residues in any combination. In addition, the protein is also subjected to phosphorylation, methylation, and succinylation.⁴⁵⁸ In this light, characterising only a single lysine residue at a time may be reductive when investigating PTM of this protein.

Further, *in vivo* both of these proteins interact with or form complexes with other proteins and molecules. Although AdeT1 was characterised in a living cell, as already discussed, this was in an *E. coli* host and interactions with native *A. baumannii* proteins were therefore not characterised. *In vivo*, the other components of the efflux pump may also undergo modification and this may too alter the interactions between the proteins in the pump complex and the overall effect of efflux pump function or activity. For HU, the protein was only investigated *in vitro* in interactions with DNA in highly controlled conditions. *In vivo*, many other molecules and proteins are present in the cytoplasm which may interact in with HU and may themselves be subjected to modification. Particularly, as mentioned in **3.2 Introduction**, HU interacts with the Gal repressor proteins⁴⁶² which could also be subjected to modification. Therefore, the interactions that AdeT1 and HU have with other proteins may not only be affected by their own modifications but also of the proteins they interact with, and this was not investigated here.

Finally, any physiological output in a cell is usually the result of pathways involving many proteins and has multiple checkpoints to regulate the final response. As mentioned in PTM crosstalk, the final physiological responses a cell has may be influenced by the combinatorial effects of any modifications of the proteins composing the pathway. Therefore, determining the exact combination of modifications that occur *in vivo* both within a particular protein, the proteins it interacts with, and the proteins downstream in any pathway, and the resulting specific effect of the

combination of modifications is a vast undertaking and was not attempted in this report. As PTMs are affected by numerous factors, including the activity of modifying enzymes and the specific composition of nutrients in the media, it may not ever be possible to reproduce or account for all of these intricacies in the laboratory. However, if an antimicrobial resistance response is regulated by PTMs, PTM crosstalk is likely to be a significant aspect of this. Therefore, it is important to discuss and remember the significance of PTM crosstalk when considering both this report and any future studies.

4.2 Future work and closing remarks

The work presented here provides evidence toward a small but growing body of literature suggesting that PTMs are used as regulatory components in antimicrobial resistance responses. As described in **Chapter 1**, there have been numerous reports of proteins involved in antimicrobial resistance undergoing PTM but fewer works characterising the effects of such modifications. Here, the effects of the modification of two such proteins were characterised and demonstrated to modulate the function of the protein. Primarily, the work presented here suggests that there is much more to uncover about the relationship between PTM and antimicrobial resistance. There are numerous other resistance proteins reported to undergo PTM, and it is likely that even more will be discovered as the PTMs of more proteomes are characterised.

The insights we have on the relationship between PTMs and antimicrobial resistance so far suggests that PTMs may be promising targets for overcoming antimicrobial resistance. This would most likely be through the development of drugs which target a specific PTM, which could be used as adjuvants in combination with existing antimicrobial therapies. For example, efflux pump inhibitors are already being developed as a complementary antimicrobial therapy.⁹⁴ If a drug was developed which targets propionylation, this could reduce efflux pump activity against antimicrobials while also inhibiting any other possible effects of propionylation on other proteins in resistance responses. Once a more comprehensive understanding is built, it may be possible identify crucial PTMs in resistance responses and focus on targeting them. Development of such adjuvants would allow antimicrobials to work much more effectively and restore the use of antimicrobials to which there are currently high levels of resistance.^{14, 73} Such re-introduction of existing antimicrobials would alleviate some of the pressure on new drug development. There is considerably more work to be done before wider conclusions can be drawn and these suggestions can be implemented. However, it is becoming increasingly evident that protein post-translational modifications are an important part of bacterial regulatory processes and require greater appreciation and consideration in future research regarding antimicrobial resistance.

Chapter 5 - General materials and methods

5.1 Bacterial strains

Table 5.1 Bacterial strains used in this thesis.

Strain	Genotype
<i>E. coli</i> BL21 AI	F- <i>ompT hsdS_B</i> (<i>r_B⁻m_B⁻</i>) <i>gal dcm araB::T7RNAP-tetA</i>
<i>E. coli</i> BL21(DE3)	F- <i>ompT hsdS_B</i> (<i>r_B⁻m_B⁻</i>) <i>gal dcm</i> (DE3)
<i>E. coli</i> TG1 KAM32	F' [<i>traD36 proAB lacIqZΔM15</i>] <i>supE thi-1 Δ(lac-proAB) Δ(mcrB-hsdSM)5(r_K⁻m_K⁻) (Δ<i>acrB</i>, Δ<i>ydhE</i>)</i>
<i>E. coli</i> Stbl3	F- <i>mcrB mrrhsdS20</i> (<i>r_B⁻,m_B⁻</i>) <i>recA13 supE44 ara-14 galK2 lacY1 proA2 rpsL20</i> (Str ^R) <i>xyt-5 λ-leumtl-1</i>

5.2 Cloning

5.2.1 PCR Conditions

All PCR reactions were carried out in a Techne TC-512 Thermocycler using PRIMEStar Polymerase (Takara, #R010A). General PCR conditions consisted of a 5 minute initial denaturation at 95 °C; 30 cycles of 10 seconds at 98 °C, 5 seconds at the annealing temperature, and 1 minute per 1 kb at 72 °C; and a 10 minute final extension at 72 °C. The annealing temperature was the melting temperature (T_m) of the primers as determined by SnapGene software (from Insightful Science; available at snapgene.com). For difficult PCR reactions, the annealing temperature was reduced by several degrees or 'ramp up' program was employed, where the annealing temperature begins a few degrees below the T_m , and increases incrementally every 3 cycles, before 30 cycles at the T_m . Where appropriate, PCR reactions were digested with FastDigest *DpnI* (Thermo Fisher, #10819410) as per manufacturer instructions.

5.2.2 Site directed mutagenesis

Site directed mutagenesis was achieved through design of partially overlapping primers (for a list, see **Table 2.3** and **Table 3.5**) and performed using standard PCR conditions (as above) with the entire plasmid amplified. After PCR, the product was digested with FastDigest *DpnI* (Thermo Fisher, #10819410) as per manufacturer instructions. The resulting DNA was analysed by agarose gel electrophoresis and excised. The extracted linear fragment was then directly transformed into *E. coli* Stbl3 cells, where endogenous homologous recombination of the overlapping ends produced the finished product.

5.2.3 Assembly of multiple fragments

For assembly of multiple DNA fragments, NEBuilder (New England Biolabs, #E2621S) was used as per manufacturer instructions. The reaction products were used directly to transform *E. coli* Stbl3 cells.

5.2.4 Restriction enzyme digestion

All restriction enzymes used were FastDigest enzymes (Thermo Fisher) and all reactions were carried out as per manufacturer instructions.

5.2.5 Agarose gels

Agarose gels were prepared by dissolving agarose (Sigma, #A9539) in TAE buffer (0.4 M Tris-acetate, pH 8.3, 10 mM EDTA) to the desired final concentration (0.5-2% agarose) by heating. 10,000x SYBR[™] Safe (Invitrogen, #S33102) was added to the liquid mixture to a final concentration of 1x. The agarose mixture was then poured into a cast, a comb inserted, and allowed to solidify. For most analyses, DNA was mixed with GelPilot DNA loading dye (Qiagen, #239901) and analysed on 1% agarose gel and electrophoresed in TAE buffer at 110 V for 45 minutes. Gels were imaged using a ChemiDoc XRS+ (BioRad) with an XcitaBlue[™] conversion screen.

5.2.6 DNA purification from agarose gels

For gel extraction, DNA bands were excised from the gel and 3x the gel volume of QG buffer (5.5 M guanidine thiocyanate, 20 mM Tris HCl pH 6.6) was added before incubation at 50 °C until the gel was completely dissolved. 1x the gel volume of IPA was then added to the mixture, which was loaded onto a miniprep spin column (Qiagen #27115) and centrifuged at 13,000 *xg* for 1 minute. The supernatant was discarded and the column washed with 700 μ L buffer PB (Qiagen #19066), centrifuged 1 minute at 13000 *xg*, supernatant discarded and washed with 750 μ L buffer PE (Qiagen #19065), centrifuged for 1 minute at 13000 *xg*, supernatant discarded and centrifuged for 1 minute at 13,000 *xg*. DNA fragments were eluted in 30 μ L buffer EB (Qiagen #19086).

5.2.7 Plasmid minipreps

All plasmids were propagated by transformation into *E. coli* OneShot Stbl3 (ThermoFisher, #C737303) cells and extracted using QIAprep Spin Miniprep Kit (Qiagen #27106) as per manufacturer's instructions.

5.2.8 DNA sequencing

All plasmids were sequenced using Sanger sequencing by Eurofins Genomics.

5.3 Protein expression and purification

5.3.1 Antibiotic selection

The following concentrations of antibiotics were used for plasmid selection:

Kanamycin: 50 µg/mL

Ampicillin: 100 µg/mL

Spectinomycin: 100 µg/mL

Unless explicitly stated, these antibiotics were always included in media and agar used to cultivate cells with plasmids containing these resistance genes (for a list, see **Table 2.15** and **Table 3.4**).

5.3.2 Media and buffers

Table 5.2 Media for bacterial protein expression.

Media	Composition
Mueller Hinton Broth (MHB)	2.0 g/L beef infusion solids, 17.5 g/L casein hydrolysate, 1.5 g/L starch
Super Optimal Broth with Catabolite Repression (SOC)	20 g/L tryptone, 5.0 g/L yeast extract, 0.5 g/L NaCl, 0.02 M MgCl ₂ , 0.02 M glucose
Terrific Broth (TB)	24 g/L yeast extract, 20 g/L tryptone, 4% (v/v) glycerol, 0.017 M KH ₂ PO ₄ , 0.072 M K ₂ HPO ₄
Lysogeny Broth (LB)	10 g/L tryptone, 10 g/L NaCl, 5 g/L yeast extract
Lysogeny Broth (LB) agar	10 g/L tryptone, 10 g/L NaCl, 5 g/L yeast extract, 1.5% agar

Table 5.3 Buffers used for protein purification and SDS-PAGE.

Buffer	Composition
PBS	0.05 M NaPi, 0.15 M NaCl pH 7.4
PBST	0.05% (v/v) Tween 20 in PBS
Lysis buffer	0.05 M Tris-HCl pH 8.0, 0.15 M NaCl, 0.01 M imidazole, 1 g/L lysozyme, 100 μ M PMSF
Wash buffer	0.05 M Tris-HCl pH 8.0, 0.15 M NaCl, 0.02 M imidazole
Elution buffer	0.05 M Tris-HCl pH 8.0, 0.15 M NaCl, 0.25 M imidazole
Urea lysis buffer	6 M urea, 0.05 M Tris-HCl pH 8.0, 0.15 M NaCl, 0.01 M imidazole, 1 g/L lysozyme, 100 μ M PMSF
Urea wash buffer	6 M urea, 0.05 M Tris-HCl pH 8.0, 0.15 M NaCl, 0.02 M imidazole
Urea elution buffer	6 M Urea, 0.05 M Tris-HCl pH 8.0, 0.15 M NaCl, 0.25 M imidazole
Phosphate buffer	0.5 M phosphate, 10 % glycerol, pH 7.0
4X SDS loading dye	0.2 M Tris-HCl (pH 6.8); 8% (w/v) sodium dodecyl sulfate; 0.4% (w/v) bromophenol blue; 40% (v/v) glycerol; 0.4 M dithiothreitol
4X SDS resolving buffer	1.5 M Tris-HCl pH 8.8, 0.4% (w/v) SDS
4X SDS stacking buffer	0.5 M Tris-HCl pH 6.8, 0.4% (w/v) SDS
1X TGS running buffer	25 mM Tris pH 8.3, 192 mM glycine, 0.1% (w/v) SDS

5.3.3 Chemical transformation

50 ng of plasmid was added to chemically competent cells on ice and incubated for 30 minutes. Cells underwent heat shock at 42 °C for 45 seconds before being transferred back to ice for 1 minute. 800 μ L of Super Optimal Broth with Catabolite repression (SOC) media containing no antibiotics was added to the cells which were incubated at 37 °C, 1300 rpm for 1 – 1.5 hours in an ThermoMixer® C (Eppendorf) with a 1.5 mL SmartBlock™ (Eppendorf). Cells were then plated on lysogeny broth (LB) agar containing antibiotics for plasmid selection and incubated at 37 °C, overnight. Cell strain used was dependent on expression system and is described in **2.7 Materials and methods** and **3.7 Materials and methods**.

5.4 Protein purification

5.4.1 Nickel affinity purification

Cultures were centrifuged at 5000 xg for 20 minutes at 4 °C. The supernatant was discarded, and pellets resuspended in 10 mL chilled lysis buffer per 1 g cell pellet. Cells were sonicated on ice in bursts of 5 s ON and 15 s OFF using a microtip at 39% amplification until lysed. The lysate was then centrifuged at 18,000 xg , 4 °C, for 20 minutes. The supernatant was collected and filter sterilised through a 0.44 μm syringe filter, then combined with Ni-NTA resin equilibrated in lysis buffer and incubated at 4 °C with gentle agitation for 1-2 hours. The lysate/resin was then poured into a gravity column and the flow through collected. The resin was washed with chilled wash buffer until no protein could be detected in the flow through by a NanoDrop One (ThermoFisher, #ND-ONE-W) measuring protein A_{280} (1 Abs = 1 mg/mL). The protein was then eluted from the column in 1 column volume fractions using chilled elution buffer and analysed by SDS-PAGE.

5.4.2 SDS-PAGE

SDS-PAGE was conducted with a discontinuous buffer system. Gels were hand cast using Mini-PROTEAN® Tetra Cell Casting Module (Bio-Rad, #1658021). For the resolving gel, an acrylamide concentration between 12 to 20% was used, depending on the molecular weight of protein. 30% acrylamide and 4X SDS resolving buffer were diluted with water to the desired final concentrations. For the stacking gel, 7.5% acrylamide was used. 30% acrylamide and 4X SDS stacking buffer were diluted with water to the desired final concentrations. APS and TEMED were used at final concentrations of 0.1% to polymerise both the stacking and resolving gels. Electrophoresis was performed in 1X TGS running buffer in a Mini-PROTEAN Tetra Cell (Bio-Rad, #1658004). Electrophoresis was performed with constant current (35 mA when running 1 gel, 50 mA for 2 gels) at 250 V until the bromophenol blue indicator reached the bottom of the gel (ca. 40-55 min).

5.5 Mass spectrometry

All mass spectrometry analyses were performed by the School of Chemistry Analytical Services at Cardiff University. Protein liquid chromatography-mass spectrometry (LC-MS) were acquired on an Acquity H-Class UPLC system (Waters) coupled to a Synapt G2-Si quadrupole time of flight mass spectrometer (Waters). An Acquity UPLC Protein C4 BEH column 300 Å, 1.7 µm (2.1 x 100 mm) (Waters) was held at 60 °C. The flow rate was 0.2 mL/min and an acetonitrile gradient was employed in the presence of 0.1% formic acid (**Table 5.4**). Mass spectrometry data were collected in positive electrospray ionisation mode and analysed using MassLynx 4.1 (Waters). Deconvoluted mass spectra were generated using MaxEnt 1 software (Waters).

Table 5.4 Protein LC-MS gradient parameters.

Time (min)	A% (H ₂ O with 0.1% formic acid)	B% (acetonitrile with 0.1% formic acid)
0	95	5
3	95	5
50	35	65
52	3	97
54	3	97
56	95	5
60	95	5

5.6 Figures

Any visualisations of crystal structures were rendered in UCSF Chimera, developed by the Resource for Biocomputing, Visualization, and Informatics at the University of California, San Francisco, with support from NIH P41-GM103311.⁴⁹⁰

Any original vectors or drawings used in this thesis were created using Inkscape, a free and open source software.⁴⁹¹

References

1. Wanda, C. R. An overview of the antimicrobial resistance mechanisms of bacteria. *AIMS Microbiology*. **4**, 482-501 (2018).
2. Fleming, A. On the antibacterial action of cultures of a *Penicillium*, with special reference to their use in the isolation of *B. influenzae*. *Br. J. Exp. Pathol.* **10**, 226-236 (1929).
3. Abraham, E. P., *et al.* Further observations on penicillin. *Lancet*. **238**, 177-189 (1941).
4. Abraham, E. P. & Chain, E. An enzyme from bacteria able to destroy penicillin. *Nature*. **146**, 837-837 (1940).
5. Perry, J., Waglechner, N. & Wright, G. The prehistory of antibiotic resistance. *Cold Spring Harb. Perspect. Med.* **6**, (2016).
6. Humeniuk, C., *et al.* β -lactamases of *Kluyvera ascorbata*, probable progenitors of some plasmid-encoded CTX-M types. *Antimicrob. Agents. Chemother.* **46**, 3045-3049 (2002).
7. D'Costa, V. M., *et al.* Antibiotic resistance is ancient. *Nature*. **477**, 457-461 (2011).
8. Sengupta, S., Chattopadhyay, M. & Grossart, H.-P. The multifaceted roles of antibiotics and antibiotic resistance in nature. *Front. Microbiol.* **4**, (2013).
9. Dadgostar, P. Antimicrobial resistance: implications and costs. *Infect Drug Resist.* **12**, 3903-3910 (2019).
10. Christaki, E., Marcou, M. & Tofarides, A. Antimicrobial resistance in bacteria: mechanisms, evolution, and persistence. *J. Mol. Evol.* **88**, 26-40 (2020).
11. O'Neill, J. *Tackling drug-resistant infections globally: final report and recommendations*. The review on antimicrobial resistance. United Kingdom; 2016. Available at: https://amr-review.org/sites/default/files/160525_Final%20paper_with%20cover.pdf. Accessed 30th October 2022.
12. Murray, C. J. L., *et al.* Global burden of bacterial antimicrobial resistance in 2019: a systematic analysis. *Lancet*. **399**, 629-655 (2022).
13. Rice, L. B. Federal funding for the study of antimicrobial resistance in nosocomial pathogens: no ESKAPE. *J. Infect. Dis.* **197**, 1079-1081 (2008).
14. Oliveira, D. M. P. D., *et al.* Antimicrobial resistance in ESKAPE pathogens. *Clin. Microbiol. Rev.* **33**, e00181-00119 (2020).
15. Sader, H. S., *et al.* Antimicrobial susceptibility of *Streptococcus pneumoniae* from North America, Europe, Latin America, and the Asia-Pacific region: results from 20 years of the SENTRY antimicrobial surveillance program (1997–2016). *Open Forum Infect. Dis.* **6**, S14-S23 (2019).
16. Chisholm, S. A., *et al.* Cephalosporin MIC creep among gonococci: time for a pharmacodynamic rethink? *J. Antimicrob. Chemother.* **65**, 2141-2148 (2010).
17. Lee, J.-H. Perspectives towards antibiotic resistance: from molecules to population. *J. Microbiol.* **57**, 181-184 (2019).
18. Sefton, A. M. Mechanisms of antimicrobial resistance. *Drugs*. **62**, 557-566 (2002).
19. Nikaido, H. Multidrug resistance in bacteria. *Annu. Rev. Biochem.* **78**, 119-146 (2009).
20. Ramirez, M. S. & Tolmasky, M. E. Aminoglycoside modifying enzymes. *Drug Resist. Update*. **13**, 151-171 (2010).
21. Borrell, S., *et al.* Epistasis between antibiotic resistance mutations drives the evolution of extensively drug-resistant tuberculosis. *Evol. Med. Public Health*. **2013**, 65-74 (2013).
22. Tipper, D. J. & Strominger, J. L. Mechanism of action of penicillins: a proposal based on their structural similarity to acyl-D-alanyl-D-alanine. *Proc. Natl. Acad. Sci. U.S.A.* **54**, 1133-1141 (1965).

23. Fuda, C. C. S., Fisher, J. F. & Mobashery, S. β -Lactam resistance in *Staphylococcus aureus*: the adaptive resistance of a plastic genome. *Cell. Mol. Life Sci.* **62**, 2617 (2005).
24. Miller, W. R., Munita, J. M. & Arias, C. A. Mechanisms of antibiotic resistance in enterococci. *Expert Rev. Anti Infect. Ther.* **12**, 1221-1236 (2014).
25. Naas, T., *et al.* Beta-lactamase database (BLDB) – structure and function. *J. Enzyme Inhib. Med. Chem.* **32**, 917-919 (2017).
26. Thumanu, K., *et al.* Discrete steps in sensing of beta-lactam antibiotics by the BlaR1 protein of the methicillin-resistant *Staphylococcus aureus* bacterium. *Proc. Natl. Acad. Sci. U.S.A.* **103**, 10630-10635 (2006).
27. Zhang, H. Z., Hackbarth, C. J., Chansky, K. M. & Chambers, H. F. A proteolytic transmembrane signaling pathway and resistance to β -lactams in *Staphylococci*. *Science*. **291**, 1962-1965 (2001).
28. Lewis, R. A., Curnock, S. P. & Dyke, K. G. Proteolytic cleavage of the repressor (Blal) of beta-lactamase synthesis in *Staphylococcus aureus*. *FEMS Microbiol. Lett.* **178**, 271-275 (1999).
29. Clarke, S. R. & Dyke, K. G. H. The signal transducer (BlaRI) and the repressor (Blal) of the *Staphylococcus aureus* β -lactamase operon are inducible. *Microbiology*. **147**, 803-810 (2001).
30. Llarrull, L. I. & Mobashery, S. Dissection of events in the resistance to β -lactam antibiotics mediated by the protein BlaR1 from *Staphylococcus aureus*. *Biochemistry*. **51**, 4642-4649 (2012).
31. Llarrull, L. I., Toth, M., Champion, M. M. & Mobashery, S. Activation of BlaR1 protein of methicillin-resistant *Staphylococcus aureus*, its proteolytic processing, and recovery from induction of resistance. *J. Biol. Chem.* **286**, 38148-38158 (2011).
32. Schwarz, S., Kehrenberg, C., Doublet, B. & Cloeckert, A. Molecular basis of bacterial resistance to chloramphenicol and florfenicol. *FEMS Microbiol. Rev.* **28**, 519-542 (2004).
33. Munita, J. M. & Arias, C. A. Mechanisms of antibiotic resistance. *Microbiol. Spectr.* **4**, 4.2.15 (2016).
34. Floss, H. G. & Yu, T.-W. Rifamycin mode of action, resistance, and biosynthesis. *Chemical Reviews*. **105**, 621-632 (2005).
35. Li, M. C., *et al.* rpoB mutations and effects on rifampin resistance in *Mycobacterium tuberculosis*. *Infect Drug Resist.* **14**, 4119-4128 (2021).
36. Chambers, H. F. Penicillin-binding protein-mediated resistance in pneumococci and staphylococci. *J. Infect. Dis.* **179**, S353-S359 (1999).
37. Hiramatsu, K., *et al.* Genomic basis for methicillin resistance in *Staphylococcus aureus*. *Infect Chemother.* **45**, 117-136 (2013).
38. Arias, C. A. & Murray, B. E. The rise of the Enterococcus: beyond vancomycin resistance. *Nat. Rev. Microbiol.* **10**, 266-278 (2012).
39. McKie, S. J., Neuman, K. C. & Maxwell, A. DNA topoisomerases: Advances in understanding of cellular roles and multi-protein complexes via structure-function analysis. *BioEssays*. **43**, 2000286 (2021).
40. Aldred, K. J., Kerns, R. J. & Osheroff, N. Mechanism of quinolone action and resistance. *Biochemistry*. **53**, 1565-1574 (2014).
41. Ruiz, J. Transferable mechanisms of quinolone resistance from 1998 onward. *Clin. Microbiol. Rev.* **32**, e00007-00019 (2019).
42. Goldstein, B. P. Resistance to rifampicin: a review. *J. Antibiot.* **67**, 625-630 (2014).
43. Nikaido, H. Multidrug efflux pumps of gram-negative bacteria. *J. Bacteriol.* **178**, 5853-5859 (1996).

44. Fernández, L. & Hancock, R. E. W. Adaptive and mutational resistance: role of porins and efflux pumps in drug resistance. *Clin. Microbiol. Rev.* **25**, 661-681 (2012).
45. Muller, C., Plésiat, P. & Jeannot, K. A two-component regulatory system interconnects resistance to polymyxins, aminoglycosides, fluoroquinolones, and β -lactams in *Pseudomonas aeruginosa*. *Antimicrob. Agents. Chemother.* **55**, 1211-1221 (2011).
46. Piddock, L. J. V. Clinically relevant chromosomally encoded multidrug resistance efflux pumps in bacteria. *Clin. Microbiol. Rev.* **19**, 382-402 (2006).
47. Blanco, P., *et al.* Bacterial multidrug efflux pumps: much more than antibiotic resistance determinants. *Microorganisms*. **4**, 14 (2016).
48. Høiby, N., Bjarnsholt, T., Givskov, M., Molin, S. & Ciofu, O. Antibiotic resistance of bacterial biofilms. *Int. J. Antimicrob. Agents.* **35**, 322-332 (2010).
49. Hall, C. W. & Mah, T.-F. Molecular mechanisms of biofilm-based antibiotic resistance and tolerance in pathogenic bacteria. *FEMS Microbiol. Rev.* **41**, 276-301 (2017).
50. Cohen, Nadia R., Lobritz, Michael A. & Collins, James J. Microbial persistence and the road to drug resistance. *Cell Host Microbe*. **13**, 632-642 (2013).
51. Lehar, S. M., *et al.* Novel antibody–antibiotic conjugate eliminates intracellular *S. aureus*. *Nature*. **527**, 323-328 (2015).
52. Magill, S. S., *et al.* Multistate point-prevalence survey of health care–associated infections. *N. Engl. J. Med.* **370**, 1198-1208 (2014).
53. Xie, R., Zhang, X. D., Zhao, Q., Peng, B. & Zheng, J. Analysis of global prevalence of antibiotic resistance in *Acinetobacter baumannii* infections disclosed a faster increase in OECD countries. *Emerg. Microbes Infect.* **7**, 1-10 (2018).
54. Frost, L. S., Leplae, R., Summers, A. O. & Toussaint, A. Mobile genetic elements: the agents of open source evolution. *Nat. Rev. Microbiol.* **3**, 722-732 (2005).
55. Vandecraen, J., Chandler, M., Aertsen, A. & Van Houdt, R. The impact of insertion sequences on bacterial genome plasticity and adaptability. *Crit. Rev. Microbiol.* **43**, 709-730 (2017).
56. Partridge, S. R., Kwong, S. M., Firth, N. & Jensen, S. O. Mobile genetic elements associated with antimicrobial resistance. *Clin. Microbiol. Rev.* **31**, e00088-00017 (2018).
57. Turton, J. F., *et al.* The role of ISAba1 in expression of OXA carbapenemase genes in *Acinetobacter baumannii*. *FEMS Microbiol. Lett.* **258**, 72-77 (2006).
58. Johnson, C. M. & Grossman, A. D. Integrative and conjugative elements (ICEs): What they do and how they work. *Annual Review of Genetics*. **49**, 577-601 (2015).
59. Juhas, M., *et al.* Genomic islands: tools of bacterial horizontal gene transfer and evolution. *FEMS Microbiol. Rev.* **33**, 376-393 (2009).
60. Gal-Mor, O. & Finlay, B. B. Pathogenicity islands: a molecular toolbox for bacterial virulence. *Cell. Microbiol.* **8**, 1707-1719 (2006).
61. Thomas, C. M. & Nielsen, K. M. Mechanisms of, and barriers to, horizontal gene transfer between bacteria. *Nat. Rev. Microbiol.* **3**, 711-721 (2005).
62. Graf, F. E., Palm, M., Warringer, J. & Farewell, A. Inhibiting conjugation as a tool in the fight against antibiotic resistance. *Drug Dev. Res.* **80**, 19-23 (2019).
63. Martinez, J. L. The role of natural environments in the evolution of resistance traits in pathogenic bacteria. *Proc. Royal Soc. B.* **276**, 2521-2530 (2009).
64. European Centre for Disease Prevention and Control. *Antimicrobial resistance surveillance in Europe 2012*. Annual Report of the European

- Antimicrobial Resistance Surveillance Network (EARS-Net). Stockholm: ECDC; 2013.
65. Gillings, M. R., Paulsen, I. T. & Tetu, S. G. Genomics and the evolution of antibiotic resistance. *Ann. N. Y. Acad. Sci.* **1388**, 92-107 (2017).
 66. Blazquez, J., Oliver, A. & Gomez-Gomez, J.-M. Mutation and evolution of antibiotic resistance: antibiotics as promoters of antibiotic resistance? *Curr. Drug Targets.* **3**, 345-349 (2002).
 67. Beaber, J. W., Hochhut, B. & Waldor, M. K. SOS response promotes horizontal dissemination of antibiotic resistance genes. *Nature.* **427**, 72-74 (2004).
 68. Elliott, E., *et al.* In vivo development of ertapenem resistance in a patient with pneumonia caused by *Klebsiella pneumoniae* with an extended-spectrum β -lactamase. *Clin. Infect. Dis.* **42**, e95-e98 (2006).
 69. Fleming-Dutra, K. E., *et al.* Prevalence of inappropriate antibiotic prescriptions among US ambulatory care visits, 2010-2011. *JAMA.* **315**, 1864-1873 (2016).
 70. Browne, A. J., *et al.* Global antibiotic consumption and usage in humans, 2000-18: a spatial modelling study. *Lancet Planet. Health.* **5**, e893-e904 (2021).
 71. Ray, M. J., Tallman, G. B., Bearden, D. T., Elman, M. R. & McGregor, J. C. Antibiotic prescribing without documented indication in ambulatory care clinics: national cross sectional study. *BMJ.* **367**, l6461 (2019).
 72. Korsgaard, H. B., *et al.* *DANMAP 2019 - Use of antimicrobial agents and occurrence of antimicrobial resistance in bacteria from food animals, food and humans in Denmark.* 2020.
 73. Nathan, C. Antibiotics at the crossroads. *Nature.* **431**, 899-902 (2004).
 74. Holmes, A. H., *et al.* Understanding the mechanisms and drivers of antimicrobial resistance. *Lancet.* **387**, 176-187 (2016).
 75. Andersson, D. I. & Hughes, D. Microbiological effects of sublethal levels of antibiotics. *Nat. Rev. Microbiol.* **12**, 465-478 (2014).
 76. Wistrand-Yuen, E., *et al.* Evolution of high-level resistance during low-level antibiotic exposure. *Nat. Commun.* **9**, 1599 (2018).
 77. Seiler, C. & Berendonk, T. Heavy metal driven co-selection of antibiotic resistance in soil and water bodies impacted by agriculture and aquaculture. *Front. Microbiol.* **3**, (2012).
 78. Llor, C. & Bjerrum, L. Antimicrobial resistance: risk associated with antibiotic overuse and initiatives to reduce the problem. *Ther. Adv. Drug Saf.* **5**, 229-241 (2014).
 79. Good Business. Exploring the consumer perspective on antimicrobial resistance. Wellcome Trust (2015).
 80. Edgeworth, J. D., Batra, R., Wulff, J. & Harrison, D. Reductions in methicillin-resistant *Staphylococcus aureus*, *Clostridium difficile* infection and intensive care unit-acquired bloodstream infection across the United Kingdom following implementation of a national infection control campaign. *Clin. Infect. Dis.* **70**, 2530-2540 (2019).
 81. Davies, S. C. *Annual report of the Chief Medical Officer 2011.* London, U.K.; 2011. Available at: <https://www.gov.uk/government/publications/cmo-annual-report-2011-volume-one-on-the-state-of-the-public-s-health>. Accessed 30th October 2022.
 82. The European Parliament and the Council of the European Union. *Regulation (EC) No 1831/2003 of the European Parliament and of the Council of 22 September 2003 on additives for use in animal nutrition.* L 268. Official Journal of the European Union (2003). Available at: <https://eur-lex.europa.eu/LexUriServ/LexUriServ.do?uri=OJ:L:2003:268:0029:0043:EN:PDF>.

83. Årdal, C., *et al.* International cooperation to improve access to and sustain effectiveness of antimicrobials. *Lancet*. **387**, 296-307 (2016).
84. Reygaert, W. Methicillin-resistant *Staphylococcus aureus* (MRSA): molecular aspects of antimicrobial resistance and virulence. *Clin. Lab. Sci.* **22**, 115-119 (2009).
85. Seppälä, H., *et al.* The effect of changes in the consumption of macrolide antibiotics on erythromycin resistance in group A streptococci in finland. *N. Engl. J. Med.* **337**, 441-446 (1997).
86. Marcusson, L. L., Frimodt-Møller, N. & Hughes, D. Interplay in the selection of fluoroquinolone resistance and bacterial fitness. *PLOS Pathog.* **5**, e1000541 (2009).
87. Enne, V. I., Livermore, D. M., Stephens, P. & Hall, L. M. C. Persistence of sulphonamide resistance in *Escherichia coli* in the UK despite national prescribing restriction. *Lancet*. **357**, 1325-1328 (2001).
88. Johnsen, P. J., *et al.* Factors affecting the reversal of antimicrobial-drug resistance. *Lancet Infect. Dis.* **9**, 357-364 (2009).
89. Levin, B. R., Perrot, V. & Walker, N. Compensatory mutations, antibiotic resistance and the population genetics of adaptive evolution in bacteria. *Genetics*. **154**, 985-997 (2000).
90. Carroll, A. C. & Wong, A. Plasmid persistence: costs, benefits, and the plasmid paradox. *Can. J. Microbiol.* **64**, 293-304 (2018).
91. Johnning, A., Kristiansson, E., Fick, J., Weijdegård, B. & Larsson, D. G. J. Resistance mutations in *gyrA* and *parC* are common in *Escherichia* communities of both fluoroquinolone-polluted and uncontaminated aquatic environments. *Front. Microbiol.* **6**, (2015).
92. Andersson, D. I. & Hughes, D. Persistence of antibiotic resistance in bacterial populations. *FEMS Microbiol. Rev.* **35**, 901-911 (2011).
93. Fischbach, M. A. & Walsh, C. T. Antibiotics for emerging pathogens. *Science*. **325**, 1089-1093 (2009).
94. Wang, Y., Venter, H. & Ma, S. Efflux pump inhibitors: a novel approach to combat efflux-mediated drug resistance in bacteria. *Curr. Drug Targets*. **17**, 702-719 (2016).
95. Lu, T. K. & Collins, J. J. Engineered bacteriophage targeting gene networks as adjuvants for antibiotic therapy. *Proc. Natl. Acad. Sci. U.S.A.* **106**, 4629-4634 (2009).
96. Jault, P., *et al.* Efficacy and tolerability of a cocktail of bacteriophages to treat burn wounds infected by *Pseudomonas aeruginosa* (Phagoburn): a randomised, controlled, double-blind phase 1/2 trial. *Lancet Infect. Dis.* **19**, 35-45 (2019).
97. Mazumdar, S. Raxibacumab. *mAbs*. **1**, 531-538 (2009).
98. Greig, S. L. Obiltoximab: First Global Approval. *Drugs*. **76**, 823-830 (2016).
99. Wilcox, M. H., *et al.* Bezlotoxumab for prevention of recurrent *Clostridium difficile* infection. *N. Engl. J. Med.* **376**, 305-317 (2017).
100. Kyaw, M. H., *et al.* Effect of introduction of the pneumococcal conjugate vaccine on drug-resistant *Streptococcus pneumoniae*. *N. Engl. J. Med.* **354**, 1455-1463 (2006).
101. Hwang, I. Y., *et al.* Reprogramming microbes to be pathogen-seeking killers. *ACS Synth. Biol.* **3**, 228-237 (2014).
102. Cain, J. A., Solis, N. & Cordwell, S. J. Beyond gene expression: the impact of protein post-translational modifications in bacteria. *J. Proteomics*. **97**, 265-286 (2014).
103. Kandpal, M., Aggarwal, S., Jamwal, S. & Yadav, A. K. Emergence of drug resistance in *Mycobacterium* and other bacterial pathogens: the

- posttranslational modification perspective. Springer International Publishing (2017).
104. Sakatos, A., *et al.* Posttranslational modification of a histone-like protein regulates phenotypic resistance to isoniazid in mycobacteria. *Sci. Adv.* **4**, eaao1478 (2018).
 105. Tiwari, V. Post-translational modification of ESKAPE pathogens as a potential target in drug discovery. *Drug Discov. Today*. **24**, 814-822 (2019).
 106. Bonne K  hler, J., *et al.* Importance of protein Ser/Thr/Tyr phosphorylation for bacterial pathogenesis. *FEBS Lett.* **594**, 2339-2369 (2020).
 107. Arora, G., Bothra, A., Prosser, G., Arora, K. & Sajid, A. Role of post-translational modifications in the acquisition of drug resistance in *Mycobacterium tuberculosis*. *FEBS J.* **288**, 3375-3393 (2021).
 108. Macek, B., *et al.* Protein post-translational modifications in bacteria. *Nat. Rev. Microbiol.* **17**, 651-664 (2019).
 109. Cobb, M. 60 years ago, Francis Crick changed the logic of biology. *PLOS Biol.* **15**, e2003243 (2017).
 110. Link, H., Kochanowski, K. & Sauer, U. Systematic identification of allosteric protein-metabolite interactions that control enzyme activity in vivo. *Nat. Biotechnol.* **31**, 357-361 (2013).
 111. Yuan, J., Fowler, W. U., Kimball, E., Lu, W. & Rabinowitz, J. D. Kinetic flux profiling of nitrogen assimilation in *Escherichia coli*. *Nat. Chem. Biol.* **2**, 529-530 (2006).
 112. Olsen, J. V. & Mann, M. Status of large-scale analysis of post-translational modifications by mass spectrometry. *Mol. Cell. Proteomics*. **12**, 3444-3452 (2013).
 113. Bastos, P. A. D., da Costa, J. P. & Vitorino, R. A glimpse into the modulation of post-translational modifications of human-colonizing bacteria. *J. Proteomics*. **152**, 254-275 (2017).
 114. Walsh, C. T., Garneau-Tsodikova, S. & Gatto Jr., G. J. Protein posttranslational modifications: the chemistry of proteome diversifications. *Angew. Chem. Int. Ed.* **44**, 7342-7372 (2005).
 115. Deutscher, J. & Saier Jr, M. H. Ser/Thr/Tyr protein phosphorylation in bacteria – for long time neglected, now well established. *J. Mol. Microbiol. Biotechnol.* **9**, 125-131 (2005).
 116. Cozzone, A. J. Protein phosphorylation in prokaryotes. *Annu. Rev. Microbiol.* **42**, 97-125 (1988).
 117. Khoury, G. A., Baliban, R. C. & Floudas, C. A. Proteome-wide post-translational modification statistics: frequency analysis and curation of the swiss-prot database. *Sci. Rep.* **1**, 90 (2011).
 118. Hansen, A.-M., *et al.* The *Escherichia coli* phosphotyrosine proteome relates to core pathways and virulence. *PLOS Pathog.* **9**, e1003403 (2013).
 119. Zhang, J., *et al.* Lysine acetylation is a highly abundant and evolutionarily conserved modification in *Escherichia coli*. *Mol. Cell. Proteomics*. **8**, 215-225 (2009).
 120. Macek, B., *et al.* Phosphoproteome analysis of *E. coli* reveals evolutionary conservation of bacterial Ser/Thr/Tyr phosphorylation. *Mol. Cell. Proteomics*. **7**, 299-307 (2008).
 121. Macek, B., *et al.* The Serine/Threonine/Tyrosine phosphoproteome of the model bacterium *Bacillus subtilis*. *Mol. Cell. Proteomics*. **6**, 697-707 (2007).
 122. Sun, X., *et al.* Phosphoproteomic analysis reveals the multiple roles of phosphorylation in pathogenic bacterium *Streptococcus pneumoniae*. *J. Proteome Res.* **9**, 275-282 (2010).
 123. Prsic, S., *et al.* Extensive phosphorylation with overlapping specificity by *Mycobacterium tuberculosis* serine/threonine protein kinases. *Proc. Natl. Acad. Sci. U.S.A.* **107**, 7521-7526 (2010).

124. Wang, Q., *et al.* Acetylation of metabolic enzymes coordinates carbon source utilization and metabolic flux. *Science*. **327**, 1004-1007 (2010).
125. Zhang, Y., *et al.* Comprehensive profiling of lysine acetylome in *Staphylococcus aureus*. *Sci. China Chem.* **57**, 732-738 (2014).
126. Okanishi, H., Kim, K., Masui, R. & Kuramitsu, S. Lysine propionylation is a prevalent post-translational modification in *Thermus thermophilus*. *Mol. Cell. Proteomics*. **13**, 2382-2398 (2014).
127. Okanishi, H., Kim, K., Masui, R. & Kuramitsu, S. Acetylome with structural mapping reveals the significance of lysine acetylation in *Thermus thermophilus*. *J. Proteome Res.* **12**, 3952-3968 (2013).
128. Takahata, Y., *et al.* Close proximity of phosphorylation sites to ligand in the phosphoproteome of the extreme thermophile *Thermus thermophilus* HB8. *Proteomics*. **12**, 1414-1430 (2012).
129. van Noort, V., *et al.* Cross-talk between phosphorylation and lysine acetylation in a genome-reduced bacterium. *Mol. Syst. Biol.* **8**, 571 (2012).
130. Zhao, Y. & Jensen, O. N. Modification-specific proteomics: Strategies for characterization of post-translational modifications using enrichment techniques. *Proteomics*. **9**, 4632-4641 (2009).
131. Silva, A. M. N., Vitorino, R., Domingues, M. R. M., Spickett, C. M. & Domingues, P. Post-translational modifications and mass spectrometry detection. *Free Radic. Biol. Med.* **65**, 925-941 (2013).
132. Larsen, M. R., Trelle, M. B., Thingholm, T. E. & Jensen, O. N. Analysis of posttranslational modifications of proteins by tandem mass spectrometry. *BioTechniques*. **40**, 790-798 (2006).
133. Yates, J. R. The revolution and evolution of shotgun proteomics for large-scale proteome analysis. *J. Am. Chem. Soc.* **135**, 1629-1640 (2013).
134. Zhou, H., Ning, Z., E. Starr, A., Abu-Farha, M. & Figeys, D. Advancements in top-down proteomics. *Anal. Chem.* **84**, 720-734 (2012).
135. Mann, M. & Jensen, O. N. Proteomic analysis of post-translational modifications. *Nat. Biotechnol.* **21**, 255-261 (2003).
136. Engholm-Keller, K. & Larsen, M. R. Technologies and challenges in large-scale phosphoproteomics. *Proteomics*. **13**, 910-931 (2013).
137. Andersson, L. & Porath, J. Isolation of phosphoproteins by immobilized metal (Fe³⁺) affinity chromatography. *Anal. Biochem.* **154**, 250-254 (1986).
138. Thingholm, T. E. & Larsen, M. R. Phosphopeptide enrichment by immobilized metal affinity chromatography. Springer New York (2016).
139. Choudhary, C., *et al.* Lysine acetylation targets protein complexes and co-regulates major cellular functions. *Science*. **325**, 834-840 (2009).
140. Hebert, Alexander S., *et al.* Calorie restriction and SIRT3 trigger global reprogramming of the mitochondrial protein acetylome. *Mol. Cell.* **49**, 186-199 (2013).
141. Huang, K.-Y., Lee, T.-Y., Kao, H.-J. & al, e. dbPTM in 2019: exploring disease association and cross-talk of post-translational modifications. *Nucleic Acids Res.* **47**, D298-D308 (2018).
142. Ramzy, A., Asadi, A. & Kieffer, T. J. Revisiting proinsulin processing: Evidence that human β -cells process proinsulin with prohormone convertase (PC) 1/3 but not PC2. *Diabetes*. **69**, 1451-1462 (2020).
143. Garcia-Garcia, T., *et al.* Role of protein phosphorylation in the regulation of cell cycle and DNA-related processes in bacteria. *Front. Microbiol.* **7**, (2016).
144. Stock, A. M., Robinson, V. L. & Goudreau, P. N. Two-component signal transduction. *Annu. Rev. Biochem.* **69**, 183-215 (2000).
145. Gao, R. & Stock, A. M. Biological insights from structures of two-component proteins. *Annu. Rev. Microbiol.* **63**, 133-154 (2009).

146. Mijakovic, I., Grangeasse, C. & Turgay, K. Exploring the diversity of protein modifications: special bacterial phosphorylation systems. *FEMS Microbiol. Rev.* **40**, 398-417 (2016).
147. Stancik, I. A., *et al.* Serine/Threonine protein kinases from bacteria, archaea and eukarya share a common evolutionary origin deeply rooted in the tree of life. *J. Mol. Biol.* **430**, 27-32 (2018).
148. Jin, J. & Pawson, T. Modular evolution of phosphorylation-based signalling systems. *Philos. Trans. R. Soc. B Biol. Sci.* **367**, (2012).
149. Hoch, J. A. Two-component and phosphorelay signal transduction. *Curr. Opin. Microbiol.* **3**, 165-170 (2000).
150. Janczarek, M., Vinardell, J.-M., Lipa, P. & Karaś, M. Hanks-Type serine/threonine protein kinases and phosphatases in bacteria: Roles in signaling and adaptation to various environments. *Int. J. Mol. Sci.* **19**, 2872 (2018).
151. Liebeke, M., Meyer, H., Donat, S., Ohlsen, K. & Lalk, M. A metabolomic view of *Staphylococcus aureus* and its Ser/Thr kinase and phosphatase deletion mutants: Involvement in cell wall biosynthesis. *Chem. Biol.* **17**, 820-830 (2010).
152. Truong-Bolduc, Q. C., Ding, Y. & Hooper, D. C. Posttranslational modification influences the effects of MgrA on *norA* expression in *Staphylococcus aureus*. *J. Bacteriol.* **190**, 7375-7381 (2008).
153. Didier, J.-P., Cozzone, A. J. & Duclos, B. Phosphorylation of the virulence regulator SarA modulates its ability to bind DNA in *Staphylococcus aureus*. *FEMS Microbiol. Lett.* **306**, 30-36 (2010).
154. Getz, L. J., Runte, C. S., Rainey, J. K., Thomas, N. A. & Margolin, W. Tyrosine phosphorylation as a widespread regulatory mechanism in prokaryotes. *J. Bacteriol.* **201**, e00205-00219 (2019).
155. Derouiche, A., *et al.* *Bacillus subtilis* SalA is a phosphorylation-dependent transcription regulator that represses *scoC* and activates the production of the exoprotease AprE. *Mol. Microbiol.* **97**, 1195-1208 (2015).
156. Mijakovic, I., *et al.* Bacterial single-stranded DNA-binding proteins are phosphorylated on tyrosine. *Nucleic Acids Res.* **34**, 1588-1596 (2006).
157. Robertson, C. D., *et al.* Phosphotyrosine-mediated regulation of Enterohemorrhagic *Escherichia coli* virulence. *mBio.* **9**, e00097-00018 (2018).
158. Shi, L., Ravikumar, V., Derouiche, A., Macek, B. & Mijakovic, I. Tyrosine 601 of *Bacillus subtilis* DnaK undergoes phosphorylation and is crucial for chaperone activity and heat shock survival. *Front. Microbiol.* **7**, (2016).
159. Nourikyan, J., *et al.* Autophosphorylation of the bacterial tyrosine-kinase CpsD connects capsule synthesis with the cell cycle in *Streptococcus pneumoniae*. *PLOS Genet.* **11**, e1005518 (2015).
160. Bijlsma, J. J. E. & Groisman, E. A. Making informed decisions: regulatory interactions between two-component systems. *Trends Microbiol.* **11**, 359-366 (2003).
161. Zhou, B., *et al.* Arginine dephosphorylation propels spore germination in bacteria. *Proc. Natl. Acad. Sci. U.S.A.* **116**, 14228-14237 (2019).
162. Sun, F., *et al.* Protein cysteine phosphorylation of SarA/MgrA family transcriptional regulators mediates bacterial virulence and antibiotic resistance. *Proc. Natl. Acad. Sci. U.S.A.* **109**, 15461-15466 (2012).
163. Schmidt, A., *et al.* The quantitative and condition-dependent *Escherichia coli* proteome. *Nat. Biotechnol.* **34**, 104-110 (2016).
164. Brown, J. L. & Roberts, W. K. Evidence that approximately eighty per cent of the soluble proteins from Ehrlich ascites cells are Na acetylated. *J. Biol. Chem.* **251**, 1009-1014 (1976).

165. Arnesen, T., *et al.* Proteomics analyses reveal the evolutionary conservation and divergence of N-terminal acetyltransferases from yeast and humans. *Proc. Natl. Acad. Sci. U.S.A.* **106**, 8157-8162 (2009).
166. Ree, R., Varland, S. & Arnesen, T. Spotlight on protein N-terminal acetylation. *Exp. Mol. Med.* **50**, 1-13 (2018).
167. Christensen, D. G., *et al.* Mechanisms, detection, and relevance of protein acetylation in prokaryotes. *mBio.* **10**, e02708-02718 (2019).
168. Birhanu, A. G., *et al.* Nε- and O-acetylation in *Mycobacterium tuberculosis* lineage 7 and lineage 4 strains: Proteins involved in bioenergetics, virulence, and antimicrobial resistance are acetylated. *J. Proteome Res.* **16**, 4045-4059 (2017).
169. VanDrisse, C. M. & Escalante-Semerena, J. C. In *Streptomyces lividans*, acetyl-CoA synthetase activity is controlled by O-serine and Nε-lysine acetylation. *Mol. Microbiol.* **107**, 577-594 (2018).
170. Li, C., *et al.* *Yersinia pestis* acetyltransferase-mediated dual acetylation at the serine and lysine residues enhances the auto-ubiquitination of ubiquitin ligase MARCH8 in human cells. *Cell Cycle.* **16**, 649-659 (2017).
171. Christensen, D. G., *et al.* Post-translational protein acetylation: An elegant mechanism for bacteria to dynamically regulate metabolic functions. *Front. Microbiol.* **10**, (2019).
172. Drazic, A., Myklebust, L. M., Ree, R. & Arnesen, T. The world of protein acetylation. *Biochim. Biophys. Acta. Proteins Proteom.* **1864**, 1372-1401 (2016).
173. VanDrisse, C. M. & Escalante-Semerena, J. C. Protein acetylation in bacteria. *Annu. Rev. Microbiol.* **73**, 111-132 (2019).
174. Vetting, M. W., *et al.* Structure and functions of the GNAT superfamily of acetyltransferases. *Arch. Biochem. Biophys.* **433**, 212-226 (2005).
175. AbouElfetouh, A., *et al.* The *E. coli* sirtuin CobB shows no preference for enzymatic and nonenzymatic lysine acetylation substrate sites. *MicrobiologyOpen.* **4**, 66-83 (2015).
176. Denu, J. M. Linking chromatin function with metabolic networks: Sir2 family of NAD⁺-dependent deacetylases. *Trends Biochem. Sci.* **28**, 41-48 (2003).
177. Kuhn, M. L., *et al.* Structural, kinetic and proteomic characterization of acetyl phosphate-dependent bacterial protein acetylation. *PLOS ONE.* **9**, e94816 (2014).
178. Weinert, Brian T., *et al.* Acetyl-phosphate is a critical determinant of lysine acetylation in *E. coli*. *Mol. Cell.* **51**, 265-272 (2013).
179. Kosono, S., *et al.* Changes in the acetylome and succinylome of *Bacillus subtilis* in response to carbon source. *PLOS ONE.* **10**, e0131169 (2015).
180. Hosp, F., *et al.* Lysine acetylation in mitochondria: From inventory to function. *Mitochondrion.* **33**, 58-71 (2017).
181. Chan, C. H., Garrity, J., Crosby, H. A. & Escalante-Semerena, J. C. In *Salmonella enterica*, the sirtuin-dependent protein acylation/deacylation system (SDPADS) maintains energy homeostasis during growth on low concentrations of acetate. *Mol. Microbiol.* **80**, 168-183 (2011).
182. Hentchel, K. L. & Escalante-Semerena, J. C. Acylation of biomolecules in prokaryotes: a widespread strategy for the control of biological function and metabolic stress. *Microbiol. Mol. Biol. Rev.* **79**, 321-346 (2015).
183. Ouidir, T., Kentache, T. & Hardouin, J. Protein lysine acetylation in bacteria: Current state of the art. *Proteomics.* **16**, 301-309 (2016).
184. Thao, S. & Escalante-Semerena, J. C. Control of protein function by reversible Nε-lysine acetylation in bacteria. *Curr. Opin. Microbiol.* **14**, 200-204 (2011).

185. Zhang, K., Zheng, S., Yang, J. S., Chen, Y. & Cheng, Z. Comprehensive profiling of protein lysine acetylation in *Escherichia coli*. *J. Proteome Res.* **12**, 844-851 (2013).
186. Jones, J. D. & O'Connor, C. D. Protein acetylation in prokaryotes. *Proteomics*. **11**, 3012-3022 (2011).
187. Thao, S., Chen, C.-S., Zhu, H. & Escalante-Semerena, J. C. Nε-lysine acetylation of a bacterial transcription factor inhibits its DNA-binding activity. *PLOS ONE*. **5**, e15123 (2011).
188. Liang, W., Malhotra, A. & Deutscher, Murray P. Acetylation regulates the stability of a bacterial protein: growth stage-dependent modification of RNase R. *Mol. Cell*. **44**, 160-166 (2011).
189. Bi, J., et al. Modulation of central carbon metabolism by acetylation of isocitrate lyase in *Mycobacterium tuberculosis*. *Sci. Rep.* **7**, 44826 (2017).
190. Christensen, D. G., et al. Identification of novel protein lysine acetyltransferases in *Escherichia coli*. *mBio*. **9**, e01905-01918 (2018).
191. Liu, F., et al. Acetylome analysis reveals diverse functions of lysine acetylation in *Mycobacterium tuberculosis*. *Mol. Cell. Proteomics*. **13**, 3352-3366 (2014).
192. Reverdy, A., Chen, Y., Hunter, E., Gozzi, K. & Chai, Y. Protein lysine acetylation plays a regulatory role in *Bacillus subtilis* multicellularity. *PLOS ONE*. **13**, e0204687 (2018).
193. Ma, Q. & Wood, T. K. Protein acetylation in prokaryotes increases stress resistance. *Biochem. Biophys. Res. Commun.* **410**, 846-851 (2011).
194. Weinert, Brian T., et al. Lysine succinylation is a frequently occurring modification in prokaryotes and eukaryotes and extensively overlaps with acetylation. *Cell Rep.* **4**, 842-851 (2013).
195. Colak, G., et al. Identification of lysine succinylation substrates and the succinylation regulatory enzyme CobB in *Escherichia coli*. *Mol. Cell. Proteomics*. **12**, 3509-3520 (2013).
196. Xie, L., et al. First succinyl-proteome profiling of extensively drug-resistant *Mycobacterium tuberculosis* revealed involvement of succinylation in cellular physiology. *J. Proteome Res.* **14**, 107-119 (2015).
197. Pan, J., Chen, R., Li, C., Li, W. & Ye, Z. Global analysis of protein lysine succinylation profiles and their overlap with lysine acetylation in the marine bacterium *Vibrio parahaemolyticus*. *J. Proteome Res.* **14**, 4309-4318 (2015).
198. Sun, M., et al. Characterization of protein lysine propionylation in *Escherichia coli*: global profiling, dynamic change, and enzymatic regulation. *J. Proteome Res.* **15**, 4696-4708 (2016).
199. Yang, M., Huang, H. & Ge, F. Lysine propionylation is a widespread post-translational modification involved in regulation of photosynthesis and metabolism in cyanobacteria. *Int. J. Mol. Sci.* **20**, 4792 (2019).
200. Okanishi, H., Kim, K., Masui, R. & Kuramitsu, S. Proteome-wide identification of lysine propionylation in thermophilic and mesophilic bacteria: *Geobacillus kaustophilus*, *Thermus thermophilus*, *Escherichia coli*, *Bacillus subtilis*, and *Rhodothermus marinus*. *Extremophiles*. **21**, 283-296 (2017).
201. Qian, L., et al. Global profiling of protein lysine malonylation in *Escherichia coli* reveals its role in energy metabolism. *J. Proteome Res.* **15**, 2060-2071 (2016).
202. Ma, Y., et al. Malonylome analysis reveals the involvement of lysine malonylation in metabolism and photosynthesis in cyanobacteria. *J. Proteome Res.* **16**, 2030-2043 (2017).
203. Shi, Y., et al. Malonyl-proteome profiles of *Staphylococcus aureus* reveal lysine malonylation modification in enzymes involved in energy metabolism. *Proteome Science*. **19**, 1 (2021).

204. Chen, Y., *et al.* Lysine propionylation and butyrylation are novel post-translational modifications in histones. *Mol. Cell. Proteomics*. **6**, 812-819 (2007).
205. Garrity, J., Gardner, J. G., Hawse, W., Wolberger, C. & Escalante-Semerena, J. C. *N*-lysine propionylation controls the activity of propionyl-CoA synthetase. *J. Biol. Chem.* **282**, 30239-30245 (2007).
206. Peng, C., *et al.* The first identification of lysine malonylation substrates and its regulatory enzyme. *Mol. Cell. Proteomics*. **10**, (2011).
207. Yang, M.-K., *et al.* Proteogenomic analysis and global discovery of posttranslational modifications in prokaryotes. *Proc. Natl. Acad. Sci. U.S.A.* **111**, E5633-E5642 (2014).
208. Zhang, Z., *et al.* Identification of lysine succinylation as a new post-translational modification. *Nat. Chem. Biol.* **7**, 58-63 (2011).
209. Alleyn, M., Breitzig, M., Lockey, R. & Kolliputi, N. The dawn of succinylation: a posttranslational modification. *Am. J. Physiol., Cell Physiol.* **314**, C228-C232 (2018).
210. Zhang, M., Xu, J.-Y., Hu, H., Ye, B.-C. & Tan, M. Systematic proteomic analysis of protein methylation in prokaryotes and eukaryotes revealed distinct substrate specificity. *Proteomics*. **18**, 1700300 (2018).
211. Plevoda, B. & Sherman, F. Methylation of proteins involved in translation. *Mol. Microbiol.* **65**, 590-606 (2007).
212. Heurgué-Hamard, V., Champ, S., Engström, Å., Ehrenberg, M. & Buckingham, R. H. The hemK gene in *Escherichia coli* encodes the N5-glutamine methyltransferase that modifies peptide release factors. *EMBO J.* **21**, 769-778 (2002).
213. Nakahigashi, K., *et al.* HemK, a class of protein methyl transferase with similarity to DNA methyl transferases, methylates polypeptide chain release factors, and *hemK* knockout induces defects in translational termination. *Proc. Natl. Acad. Sci. U.S.A.* **99**, 1473-1478 (2002).
214. Garbom, S., *et al.* Phenotypic characterization of a virulence-associated protein, VagH, of *Yersinia pseudotuberculosis* reveals a tight link between VagH and the type III secretion system. *Microbiology*. **153**, 1464-1473 (2007).
215. Cao, X.-J., *et al.* High-coverage proteome analysis reveals the first insight of protein modification systems in the pathogenic spirochete *Leptospira interrogans*. *Cell Research*. **20**, 197-210 (2010).
216. Ambler, R. P. & Rees, M. W. ϵ -N-methyl-lysine in bacterial flagellar protein. *Nature*. **184**, 56-57 (1959).
217. Paik, W. K., Paik, D. C. & Kim, S. Historical review: the field of protein methylation. *Trends Biochem. Sci.* **32**, 146-152 (2007).
218. Goy, M. F., Springer, M. S. & Adler, J. Sensory transduction in *Escherichia coli*: Role of a protein methylation reaction in sensory adaptation. *Proc. Natl. Acad. Sci. U.S.A.* **74**, 4964-4968 (1977).
219. Horstmann, J. A., *et al.* Methylation of *Salmonella typhimurium* flagella promotes bacterial adhesion and host cell invasion. *Nat. Commun.* **11**, 2013 (2020).
220. Kisselev, L. L. & Buckingham, R. H. Translational termination comes of age. *Trends Biochem. Sci.* **25**, 561-566 (2000).
221. Dinçbas-Renqvist, V., *et al.* A post-translational modification in the GGQ motif of RF2 from *Escherichia coli* stimulates termination of translation. *EMBO J.* **19**, 6900-6907 (2000).
222. Chen, X., *et al.* Prokaryotic ubiquitin-like protein Pup is intrinsically disordered. *J. Mol. Biol.* **392**, 208-217 (2009).

223. Pearce, M. J., Mintseris, J., Ferreyra, J., Gygi, S. P. & Darwin, K. H. Ubiquitin-like protein involved in the proteasome pathway of *Mycobacterium tuberculosis*. *Science*. **322**, 1104-1107 (2008).
224. Barandun, J., Delley, C. L. & Weber-Ban, E. The pupylation pathway and its role in mycobacteria. *BMC Biology*. **10**, 95 (2012).
225. Liao, S., *et al.* Pup, a prokaryotic ubiquitin-like protein, is an intrinsically disordered protein. *Biochem. J.* **422**, 207-215 (2009).
226. Burns, K. E. & Darwin, K. H. Pupylation versus ubiquitylation: tagging for proteasome-dependent degradation. *Cell. Microbiol.* **12**, 424-431 (2010).
227. Striebel, F., *et al.* Bacterial ubiquitin-like modifier Pup is deamidated and conjugated to substrates by distinct but homologous enzymes. *Nat. Struct. Mol. Biol.* **16**, 647-651 (2009).
228. Cerda-Maira, F. A., *et al.* Molecular analysis of the prokaryotic ubiquitin-like protein (Pup) conjugation pathway in *Mycobacterium tuberculosis*. *Mol. Microbiol.* **77**, 1123-1135 (2010).
229. Iyer, L. M., Burroughs, A. M. & Aravind, L. Unraveling the biochemistry and provenance of pupylation: a prokaryotic analog of ubiquitination. *Biology Direct*. **3**, 45 (2008).
230. Barka, E. A., *et al.* Taxonomy, physiology, and natural products of *Actinobacteria*. *Microbiol. Mol. Biol. Rev.* **80**, 1-43 (2016).
231. Striebel, F., Hunkeler, M., Summer, H. & Weber-Ban, E. The mycobacterial Mpa–proteasome unfolds and degrades pupylated substrates by engaging Pup's N-terminus. *EMBO J.* **29**, 1262-1271 (2010).
232. von Rosen, T., Keller, L. M. & Weber-Ban, E. Survival in hostile conditions: Pupylation and the proteasome in Actinobacterial stress response pathways. *Front. Mol. Biosci.* **8**, (2021).
233. Müller, A. U., Imkamp, F. & Weber-Ban, E. The Mycobacterial LexA/RecA-independent DNA damage response is controlled by PafBC and the Pup-proteasome system. *Cell Rep.* **23**, 3551-3564 (2018).
234. Küberl, A., Polen, T. & Bott, M. The pupylation machinery is involved in iron homeostasis by targeting the iron storage protein ferritin. *Proc. Natl. Acad. Sci. U.S.A.* **113**, 4806-4811 (2016).
235. Csizmok, V. & Forman-Kay, J. D. Complex regulatory mechanisms mediated by the interplay of multiple post-translational modifications. *Curr. Opin. Struct. Biol.* **48**, 58-67 (2018).
236. Soufi, B., Soares, N. C., Ravikumar, V. & Macek, B. Proteomics reveals evidence of cross-talk between protein modifications in bacteria: focus on acetylation and phosphorylation. *Curr. Opin. Microbiol.* **15**, 357-363 (2012).
237. Amin, R., *et al.* Post-translational serine/threonine phosphorylation and lysine acetylation: A novel regulatory aspect of the global nitrogen response regulator GlnR in *S. coelicolor* M145. *Front. Mol. Biosci.* **3**, (2016).
238. Shinar, G., Rabinowitz, J. D. & Alon, U. Robustness in glyoxylate bypass regulation. *PLOS Comput. Biol.* **5**, e1000297 (2009).
239. Cozzzone, A. J. & El-Mansi, M. Control of isocitrate dehydrogenase catalytic activity by protein phosphorylation in *Escherichia coli*. *Microb. Physiol.* **9**, 132-146 (2005).
240. Yu, B. J., Kim, J. A., Moon, J. H., Ryu, S. E. & Pan, J.-G. The diversity of lysine-acetylated proteins in *Escherichia coli*. *J. Microbiol. Biotechnol.* **18**, 1529-1536 (2008).
241. Lee, M. E., *et al.* Mutational analysis of the catalytic residues lysine 230 and tyrosine 160 in the NADP⁺-dependent isocitrate dehydrogenase from *Escherichia coli*. *Biochemistry*. **34**, 378-384 (1995).
242. Stock, J. B., Ninfa, A. J. & Stock, A. M. Protein phosphorylation and regulation of adaptive responses in bacteria. *Microbiol. Rev.* **53**, 450-490 (1989).

243. Wanner, B. L. Is cross regulation by phosphorylation of two-component response regulator proteins important in bacteria? *J. Bacteriol.* **174**, 2053-2058 (1992).
244. Baer, C. E., Iavarone, A. T., Alber, T. & Sassetti, C. M. Biochemical and spatial coincidence in the provisional Ser/Thr protein kinase interaction network of *Mycobacterium tuberculosis*. *J. Biol. Chem.* **289**, 20422-20433 (2014).
245. Shi, L., *et al.* Cross-phosphorylation of bacterial serine/threonine and tyrosine protein kinases on key regulatory residues. *Front. Microbiol.* **5**, (2014).
246. Karmakar, R. State of the art of bacterial chemotaxis. *J. Basic Microbiol.* **61**, 366-379 (2021).
247. Brown, M. T., Delalez, N. J. & Armitage, J. P. Protein dynamics and mechanisms controlling the rotational behaviour of the bacterial flagellar motor. *Curr. Opin. Microbiol.* **14**, 734-740 (2011).
248. Barak, R. & Eisenbach, M. Acetylation of the response regulator, CheY, is involved in bacterial chemotaxis. *Mol. Microbiol.* **40**, 731-743 (2001).
249. Liarzi, O., *et al.* Acetylation represses the binding of CheY to its target proteins. *Mol. Microbiol.* **76**, 932-943 (2010).
250. Anand, G. S., Goudreau, P. N. & Stock, A. M. Activation of methylesterase CheB: evidence of a dual role for the regulatory domain. *Biochemistry.* **37**, 14038-14047 (1998).
251. Anand, G. S. & Stock, A. M. Kinetic basis for the stimulatory effect of phosphorylation on the methylesterase activity of CheB. *Biochemistry.* **41**, 6752-6760 (2002).
252. Lai, S.-J., *et al.* Site-specific His/Asp phosphoproteomic analysis of prokaryotes reveals putative targets for drug resistance. *BMC Microbiol.* **17**, 123 (2017).
253. Choi, U. & Lee, C.-R. Distinct roles of outer membrane porins in antibiotic resistance and membrane integrity in *Escherichia coli*. *Front. Microbiol.* **10**, (2019).
254. Huc, E., *et al.* O-mycoloylated proteins from *Corynebacterium*: an unprecedented post-translational modification in bacteria. *J. Biol. Chem.* **285**, 21908-21912 (2010).
255. Kentache, T., Jouenne, T., Dé, E. & Hardouin, J. Proteomic characterization of N α - and N ϵ -acetylation in *Acinetobacter baumannii*. *J. Proteomics.* **144**, 148-158 (2016).
256. Tsai, C.-H. Acetylome and propionylome of *Acinetobacter baumannii* SK17. National Taiwan University (2015).
257. Xu, W.-X., *et al.* The Wag31 protein interacts with AccA3 and coordinates cell wall lipid permeability and lipophilic drug resistance in *Mycobacterium smegmatis*. *Biochem. Biophys. Res. Commun.* **448**, 255-260 (2014).
258. Lee, J. J., *et al.* Phosphorylation-dependent interaction between a serine/threonine kinase PknA and a putative cell division protein Wag31 in *Mycobacterium tuberculosis*. *New Microbiol.* **37**, 525-533 (2014).
259. Poulsen, C., *et al.* Proteome-wide identification of mycobacterial pupylation targets. *Mol. Syst. Biol.* **6**, 386 (2010).
260. Beckert, P., *et al.* *rplC* T460C identified as a dominant mutation in linezolid-resistant *Mycobacterium tuberculosis* strains. *Antimicrob. Agents. Chemother.* **56**, 2743-2745 (2012).
261. de Vos, M., *et al.* Putative compensatory mutations in the *rpoC* gene of rifampin-resistant *Mycobacterium tuberculosis* are associated with ongoing transmission. *Antimicrob. Agents. Chemother.* **57**, 827-832 (2013).
262. Heym, B., Zhang, Y., Poulet, S., Young, D. & Cole, S. T. Characterization of the *katG* gene encoding a catalase-peroxidase required for the isoniazid

- susceptibility of *Mycobacterium tuberculosis*. *J. Bacteriol.* **175**, 4255-4259 (1993).
263. Cohen, T., Becerra, M. & Murray, M. Isoniazid resistance and the future of drug-resistant tuberculosis. *Microb. Drug Resist.* **10**, 280-285 (2004).
 264. Boudreau, M. A., Fishovitz, J., Llarrull, L. I., Xiao, Q. & Mobashery, S. Phosphorylation of BlaR1 in manifestation of antibiotic resistance in methicillin-resistant *Staphylococcus aureus* and its abrogation by small molecules. *ACS Infect. Dis.* **1**, 454-459 (2015).
 265. Canova, M. J., *et al.* A novel mode of regulation of the *Staphylococcus aureus* vancomycin-resistance-associated response regulator VraR mediated by Stk1 protein phosphorylation. *Biochem. Biophys. Res. Commun.* **447**, 165-171 (2014).
 266. Kaatz, G. W., Thyagarajan, R. V. & Seo, S. M. Effect of promoter region mutations and *mgrA* overexpression on transcription of *norA*, which encodes a *Staphylococcus aureus* multidrug efflux transporter. *Antimicrob. Agents. Chemother.* **49**, 161-169 (2005).
 267. Truong-Bolduc, Q. C. & Hooper, D. C. Phosphorylation of MgrA and its effect on expression of the NorA and NorB efflux pumps of *Staphylococcus aureus*. *J. Bacteriol.* **192**, 2525-2534 (2010).
 268. Abouelhadid, S., *et al.* Characterization of posttranslationally modified multidrug efflux pumps reveals an unexpected link between glycosylation and antimicrobial resistance. *mBio.* **11**, e02604-02620 (2020).
 269. Wipperman, M. F., *et al.* *Mycobacterial* mutagenesis and drug resistance are controlled by phosphorylation- and cardiolipin-mediated inhibition of the RecA coprotease. *Mol. Cell.* **72**, 152-161.e157 (2018).
 270. Sharma, K., *et al.* Transcriptional control of the *Mycobacterial embCAB* operon by PknH through a regulatory protein, EmbR, *in vivo*. *J. Bacteriol.* **188**, 2936-2944 (2006).
 271. Ghosh, S., Padmanabhan, B., Anand, C. & Nagaraja, V. Lysine acetylation of the *Mycobacterium tuberculosis* HU protein modulates its DNA binding and genome organization. *Mol. Microbiol.* **100**, 577-588 (2016).
 272. Gupta, M., *et al.* HupB, a nucleoid-associated protein of *Mycobacterium tuberculosis*, is modified by serine/threonine protein kinases *in vivo*. *J. Bacteriol.* **196**, 2646-2657 (2014).
 273. Hanawa-Suetsugu, K., *et al.* Crystal structure of elongation factor P from *Thermus thermophilus* HB8. *Proc. Natl. Acad. Sci. U.S.A.* **101**, 9595-9600 (2004).
 274. Zou, S. B., Roy, H., Ibba, M. & Navarre, W. W. Elongation factor P mediates a novel post-transcriptional regulatory pathway critical for bacterial virulence. *Virulence.* **2**, 147-151 (2011).
 275. Navarre, W. W., *et al.* PoxA, YjeK, and elongation factor P coordinately modulate virulence and drug resistance in *Salmonella enterica*. *Mol. Cell.* **39**, 209-221 (2010).
 276. Rajkovic, A., *et al.* Cyclic rhamnosylated elongation factor P establishes antibiotic resistance in *Pseudomonas aeruginosa*. *mBio.* **6**, e00823-00815 (2015).
 277. Walburger, A., *et al.* Protein Kinase G from pathogenic *Mycobacteria* promotes survival within macrophages. *Science.* **304**, 1800-1804 (2004).
 278. Wolff, K. A., *et al.* Protein Kinase G is required for intrinsic antibiotic resistance in *Mycobacteria*. *Antimicrob. Agents. Chemother.* **53**, 3515-3519 (2009).
 279. Beltramini, A. M., Mukhopadhyay, C. D. & Pancholi, V. Modulation of cell wall structure and antimicrobial susceptibility by a *Staphylococcus aureus* eukaryote-like serine/threonine kinase and phosphatase. *Infect. Immun.* **77**, 1406-1416 (2009).

280. Huang, Y.-Y., *et al.* Sublethal β -lactam antibiotics induce PhpP phosphatase expression and StkP kinase phosphorylation in PBP-independent β -lactam antibiotic resistance of *Streptococcus pneumoniae*. *Biochem. Biophys. Res. Commun.* **503**, 2000-2008 (2018).
281. Pelletier, M. R., *et al.* Unique structural modifications are present in the lipopolysaccharide from colistin-resistant strains of *Acinetobacter baumannii*. *Antimicrob. Agents. Chemother.* **57**, 4831-4840 (2013).
282. Bartek, I. L., *et al.* The DosR regulon of *M. tuberculosis* and antibacterial tolerance. *Tuberculosis*. **89**, 310-316 (2009).
283. Bi, J., *et al.* Acetylation of lysine 182 inhibits the ability of *Mycobacterium tuberculosis* DosR to bind DNA and regulate gene expression during hypoxia. *Emerg. Microbes Infect.* **7**, 1-12 (2018).
284. Krute, C. N., *et al.* The disruption of prenylation leads to pleiotropic rearrangements in cellular behavior in *Staphylococcus aureus*. *Mol. Microbiol.* **95**, 819-832 (2015).
285. Sucheck, S. J., *et al.* Design of bifunctional antibiotics that target bacterial rRNA and inhibit resistance-causing enzymes. *J. Am. Chem. Soc.* **122**, 5230-5231 (2000).
286. Labby, K. J. & Garneau-Tsodikova, S. Strategies to overcome the action of aminoglycoside-modifying enzymes for treating resistant bacterial infections. *Future Med. Chem.* **5**, 1285-1309 (2013).
287. Mori, M., *et al.* An overview on the potential antimycobacterial agents targeting Serine/Threonine protein kinases from *Mycobacterium tuberculosis*. *Curr. Top. Med. Chem.* **19**, 646-661 (2019).
288. Pensinger, D. A., *et al.* Selective pharmacologic inhibition of a PASTA kinase increases *Listeria monocytogenes* susceptibility to β -lactam antibiotics. *Antimicrob. Agents. Chemother.* **58**, 4486-4494 (2014).
289. Bem, A. E., *et al.* Bacterial histidine kinases as novel antibacterial drug targets. *ACS Chem. Biol.* **10**, 213-224 (2015).
290. Eguchi, Y., Kubo, N., Matsunaga, H., Igarashi, M. & Utsumi, R. Development of an antivirulence drug against *Streptococcus mutans*: repression of biofilm formation, acid tolerance, and competence by a histidine kinase inhibitor, Walkmycin C. *Antimicrob. Agents. Chemother.* **55**, 1475-1484 (2011).
291. Boibessot, T., *et al.* The rational design, synthesis, and antimicrobial properties of thiophene derivatives that inhibit bacterial histidine kinases. *J. Med. Chem.* **59**, 8830-8847 (2016).
292. Chahales, P., Thanassi, D. G. & DiRita, V. J. A more flexible lipoprotein sorting pathway. *J. Bacteriol.* **197**, 1702-1704 (2015).
293. da Silva, R. A. G., *et al.* The role of apolipoprotein N-acyl transferase, Lnt, in the lipidation of factor H binding protein of *Neisseria meningitidis* strain MC58 and its potential as a drug target. *Br. J. Pharmacol.* **174**, 2247-2260 (2017).
294. Conibear, A. C. Deciphering protein post-translational modifications using chemical biology tools. *Nat. Rev. Chem.* **4**, 674-695 (2020).
295. Chen, J. & Tsai, Y.-H. Applications of genetic code expansion in studying protein post-translational modification. *J. Mol. Biol.* **434**, 167424 (2022).
296. Chin, J. W. Expanding and reprogramming the genetic code. *Nature*. **550**, 53-60 (2017).
297. Xie, J. & Schultz, P. G. An expanding genetic code. *Methods*. **36**, 227-238 (2005).
298. Chin, J. W. Expanding and reprogramming the genetic code of cells and animals. *Annu. Rev. Biochem.* **83**, 379-408 (2014).
299. Takimoto, J. K., Deltas, N., Noel, J. P. & Wang, L. Stereochemical basis for engineered pyrrolysyl-tRNA synthetase and the efficient in vivo incorporation

- of structurally divergent non-native amino acids. *ACS Chem. Biol.* **6**, 733-743 (2011).
300. Hao, B., *et al.* A new UAG-encoded residue in the structure of a Methanogen methyltransferase. *Science*. **296**, 1462-1466 (2002).
 301. Mills, E. M., Barlow, V. L., Luk, L. Y. P. & Tsai, Y.-H. Applying switchable Cas9 variants to in vivo gene editing for therapeutic applications. *Cell Biol. Toxicol.* **36**, 17-29 (2020).
 302. Fournier, P. E., Richet, H. & Weinstein, R. A. The epidemiology and control of *Acinetobacter baumannii* in health care facilities. *Clin. Infect. Dis.* **42**, 692-699 (2006).
 303. Harding, C. M., Hennon, S. W. & Feldman, M. F. Uncovering the mechanisms of *Acinetobacter baumannii* virulence. *Nat. Rev. Microbiol.* **16**, 91-102 (2018).
 304. Dijkshoorn, L., Nemec, A. & Seifert, H. An increasing threat in hospitals: multidrug-resistant *Acinetobacter baumannii*. *Nat. Rev. Microbiol.* **5**, 939-951 (2007).
 305. Vincent, J.-L., *et al.* International study of the prevalence and outcomes of infection in intensive care units. *JAMA*. **302**, 2323-2329 (2009).
 306. Wong, D., *et al.* Clinical and pathophysiological overview of *Acinetobacter* infections: a century of challenges. *Clin. Microbiol. Rev.* **30**, 409-447 (2017).
 307. Bergogne-Bérézin, E. & Towner, K. J. *Acinetobacter* spp. as nosocomial pathogens: microbiological, clinical, and epidemiological features. *Clin. Microbiol. Rev.* **9**, 148-165 (1996).
 308. Howard, A., O'Donoghue, M., Feeney, A. & Sleator, R. D. *Acinetobacter baumannii*. *Virulence*. **3**, 243-250 (2012).
 309. Lee, C.-R., *et al.* Biology of *Acinetobacter baumannii*: pathogenesis, antibiotic resistance mechanisms, and prospective treatment options. *Front. Cell. Infect. Microbiol.* **7**, 55 (2017).
 310. Giammanco, A., Calà, C., Fasciana, T., Dowzicky, M. J. & Bradford, P. A. Global assessment of the activity of tigecycline against multidrug-resistant Gram-negative pathogens between 2004 and 2014 as part of the tigecycline evaluation and surveillance trial. *mSphere*. **2**, e00310-00316 (2017).
 311. Lin, M.-F. & Lan, C.-Y. Antimicrobial resistance in *Acinetobacter baumannii*: From bench to bedside. *World J. Clin. Cases*. **2**, 787-814 (2014).
 312. Willyard, C. The drug-resistant bacteria that pose the greatest health threats. *Nature*. **543**, 15 (2017).
 313. Fournier, P.-E., *et al.* Comparative genomics of multidrug resistance in *Acinetobacter baumannii*. *PLOS Genet.* **2**, e7 (2006).
 314. Antunes, L. C. S., Visca, P. & Towner, K. J. *Acinetobacter baumannii*: evolution of a global pathogen. *Pathog. Dis.* **71**, 292-301 (2014).
 315. De Silva, P. M. & Kumar, A. Signal transduction proteins in *Acinetobacter baumannii*: role in antibiotic resistance, virulence, and potential as drug targets. *Front. Microbiol.* **10**, 49 (2019).
 316. Ayoub Moubareck, C. & Hammoudi Halat, D. Insights into *Acinetobacter baumannii*: A review of microbiological, virulence, and resistance traits in a threatening nosocomial pathogen. *Antibiotics*. **9**, 119 (2020).
 317. Lima, W. G., Alves, M. C., Cruz, W. S. & Paiva, M. C. Chromosomally encoded and plasmid-mediated polymyxins resistance in *Acinetobacter baumannii*: a huge public health threat. *Eur. J. Clin. Microbiol. Infect. Dis.* **37**, 1009-1019 (2018).
 318. Mussi, M. A., Limansky, A. S. & Viale, A. M. Acquisition of resistance to carbapenems in multidrug-resistant clinical strains of *Acinetobacter baumannii*: natural insertional inactivation of a gene encoding a member of a novel family of β -barrel outer membrane proteins. *Antimicrob. Agents. Chemother.* **49**, 1432-1440 (2005).

319. Costa, S. F., *et al.* Outer-membrane proteins pattern and detection of beta-lactamases in clinical isolates of imipenem-resistant *Acinetobacter baumannii* from Brazil. *Int. J. Antimicrob. Agents*. **13**, 175-182 (2000).
320. Limansky, A. S., Mussi, M. A. & Viale, A. M. Loss of a 29-kilodalton outer membrane protein in *Acinetobacter baumannii* is associated with imipenem resistance. *J. Clin. Microbiol.* **40**, 4776-4778 (2002).
321. Clark, R. B. Imipenem resistance among *Acinetobacter baumannii*: association with reduced expression of a 33–36 kDa outer membrane protein. *J. Antimicrob. Chemother.* **38**, 245-251 (1996).
322. Tomás, M. d. M., *et al.* Cloning and functional analysis of the gene encoding the 33- to 36-kilodalton outer membrane protein associated with carbapenem resistance in *Acinetobacter baumannii*. *Antimicrob. Agents. Chemother.* **49**, 5172-5175 (2005).
323. Bou, G., Cerveró, G., Domínguez, M. A., Quereda, C. & Martínez-Beltrán, J. Characterization of a nosocomial outbreak caused by a multiresistant *Acinetobacter baumannii* strain with a carbapenem-hydrolyzing enzyme: high-level carbapenem resistance in *A. baumannii* is not due solely to the presence of β -Lactamases. *J. Clin. Microbiol.* **38**, 3299-3305 (2000).
324. Coyne, S., Courvalin, P. & Périchon, B. Efflux-mediated antibiotic resistance in *Acinetobacter* spp. *Antimicrob. Agents. Chemother.* **55**, 947-953 (2011).
325. Martinez, J. L., *et al.* A global view of antibiotic resistance. *FEMS Microbiol. Rev.* **33**, 44-65 (2009).
326. Alvarez-Ortega, C., Olivares, J. & Martinez, J. RND multidrug efflux pumps: what are they good for? *Front. Microbiol.* **4**, 7 (2013).
327. Martinez, J. L., *et al.* Functional role of bacterial multidrug efflux pumps in microbial natural ecosystems. *FEMS Microbiol. Rev.* **33**, 430-449 (2009).
328. Du, D., *et al.* Multidrug efflux pumps: structure, function and regulation. *Nat. Rev. Microbiol.* **16**, 523-539 (2018).
329. Blair, J. M. A. & Piddock, L. J. V. Structure, function and inhibition of RND efflux pumps in Gram-negative bacteria: an update. *Curr. Opin. Microbiol.* **12**, 512-519 (2009).
330. Deng, M., *et al.* Molecular epidemiology and mechanisms of tigecycline resistance in clinical isolates of *Acinetobacter baumannii* from a chinese university hospital. *Antimicrob. Agents. Chemother.* **58**, 297-303 (2014).
331. Vila, J., Martí, S. & Sánchez-Céspedes, J. Porins, efflux pumps and multidrug resistance in *Acinetobacter baumannii*. *J. Antimicrob. Chemother.* **59**, 1210-1215 (2007).
332. Damier-Piolle, L., Magnet, S., Brémont, S., Lambert, T. & Courvalin, P. AdeIJK, a resistance-nodulation-cell division pump effluxing multiple antibiotics in *Acinetobacter baumannii*. *Antimicrob. Agents. Chemother.* **52**, 557-562 (2008).
333. Yoon, E.-J., *et al.* Contribution of resistance-nodulation-cell division efflux systems to antibiotic resistance and biofilm formation in *Acinetobacter baumannii*. *mBio*. **6**, e00309-e00315 (2015).
334. Hernando-Amado, S., *et al.* Multidrug efflux pumps as main players in intrinsic and acquired resistance to antimicrobials. *Drug Resis. Update*. **28**, 13-27 (2016).
335. Alibert, S., *et al.* Multidrug efflux pumps and their role in antibiotic and antiseptic resistance: a pharmacodynamic perspective. *Expert Opin. Drug. Metab. Toxicol.* **13**, 301-309 (2017).
336. Venter, H., Mowla, R., Ohene-Agyei, T. & Ma, S. RND-type drug efflux pumps from Gram-negative bacteria: molecular mechanism and inhibition. *Front. Microbiol.* **6**, 377 (2015).

337. Li, X.-Z., Plésiat, P. & Nikaido, H. The challenge of efflux-mediated antibiotic resistance in Gram-negative bacteria. *Clin. Microbiol. Rev.* **28**, 337-418 (2015).
338. Poole, K. Efflux-mediated multiresistance in Gram-negative bacteria. *Clin. Microbiol. Infect.* **10**, 12-26 (2004).
339. Du, D., *et al.* Structure of the AcrAB–TolC multidrug efflux pump. *Nature*. **509**, 512-515 (2014).
340. Nikaido, H. & Takatsuka, Y. Mechanisms of RND multidrug efflux pumps. *Biochim. Biophys. Acta. Proteins Proteom.* **1794**, 769-781 (2009).
341. Colclough, A. L., *et al.* RND efflux pumps in Gram-negative bacteria; regulation, structure and role in antibiotic resistance. *Future Microbiol.* **15**, 143-157 (2020).
342. Aires, J. R. & Nikaido, H. Aminoglycosides are captured from both periplasm and cytoplasm by the AcrD multidrug efflux transporter of *Escherichia coli*. *J. Bacteriol.* **187**, 1923-1929 (2005).
343. Lee, A., *et al.* Interplay between efflux pumps may provide either additive or multiplicative effects on drug resistance. *J. Bacteriol.* **182**, 3142-3150 (2000).
344. Wieczorek, P., *et al.* Multidrug resistant *Acinetobacter baumannii*-the role of AdeABC (RND family) efflux pump in resistance to antibiotics. *Folia Histochem. Cytobiol.* **46**, 257-267 (2008).
345. Kornelsen, V. & Kumar, A. Update on multidrug resistance efflux pumps in *Acinetobacter* spp. *Antimicrob. Agents. Chemother.* **65**, e00514-00521 (2021).
346. Magnet, S., Courvalin, P. & Lambert, T. Resistance-nodulation-cell division-type efflux pump involved in aminoglycoside resistance in *Acinetobacter baumannii* strain BM4454. *Antimicrob. Agents. Chemother.* **45**, 3375-3380 (2001).
347. Marchand, I., Damier-Piolle, L., Courvalin, P. & Lambert, T. Expression of the RND-Type efflux pump AdeABC in *Acinetobacter baumannii* is regulated by the AdeRS two-component system. *Antimicrob. Agents. Chemother.* **48**, 3298-3304 (2004).
348. Peleg, A. Y., Adams, J. & Paterson, D. L. Tigecycline efflux as a mechanism for nonsusceptibility in *Acinetobacter baumannii*. *Antimicrob. Agents. Chemother.* **51**, 2065-2069 (2007).
349. Lin, M.-F., Lin, Y.-Y. & Lan, C.-Y. The role of the two-component system BaeSR in disposing chemicals through regulating transporter systems in *Acinetobacter baumannii*. *PLOS ONE*. **10**, e0132843 (2015).
350. Coyne, S., Rosenfeld, N., Lambert, T., Courvalin, P. & Périchon, B. Overexpression of resistance-nodulation-cell division pump AdeFGH confers multidrug resistance in *Acinetobacter baumannii*. *Antimicrob. Agents. Chemother.* **54**, 4389-4393 (2010).
351. Nemec, A., Maixnerová, M., van der Reijden, T. J. K., van den Broek, P. J. & Dijkshoorn, L. Relationship between the AdeABC efflux system gene content, netilmicin susceptibility and multidrug resistance in a genotypically diverse collection of *Acinetobacter baumannii* strains. *J. Antimicrob. Chemother.* **60**, 483-489 (2007).
352. Huys, G., Cnockaert, M., Nemec, A. & Swings, J. Sequence-based typing of *adeB* as a potential tool to identify intraspecific groups among clinical strains of multidrug-resistant *Acinetobacter baumannii*. *J. Clin. Microbiol.* **43**, 5327-5331 (2005).
353. Srinivasan, V. B., Gebreyes, W. A., Rajamohan, G., Pancholi, P. & Marcon, M. Molecular cloning and functional characterization of two novel membrane fusion proteins in conferring antimicrobial resistance in *Acinetobacter baumannii*. *J. Antimicrob. Chemother.* **66**, 499-504 (2011).

354. Sugawara, E. & Nikaido, H. Properties of AdeABC and AdeIJK efflux systems of *Acinetobacter baumannii* compared with those of the AcrAB-TolC system of *Escherichia coli*. *Antimicrob. Agents. Chemother.* **58**, 7250-7257 (2014).
355. Forsberg, K. J., *et al.* The shared antibiotic resistome of soil bacteria and human pathogens. *Science*. **337**, 1107-1111 (2012).
356. Card, R. M., *et al.* Application of microarray and functional-based screening methods for the detection of antimicrobial resistance genes in the microbiomes of healthy humans. *PLOS ONE*. **9**, e86428 (2014).
357. Torres-Cortés, G., *et al.* Characterization of novel antibiotic resistance genes identified by functional metagenomics on soil samples. *Environ. Microbiol.* **13**, 1101-1114 (2011).
358. Chen, J., *et al.* VmrA, a member of a novel class of Na⁺-coupled multidrug efflux pumps from *Vibrio parahaemolyticus*. *J. Bacteriol.* **184**, 572-576 (2002).
359. Soares, N. C., *et al.* Ser/Thr/Tyr phosphoproteome characterization of *Acinetobacter baumannii*: comparison between a reference strain and a highly invasive multidrug-resistant clinical isolate. *J. Proteomics*. **102**, 113-124 (2014).
360. Arroyo, L. A., *et al.* The *pmrCAB* operon mediates polymyxin resistance in *Acinetobacter baumannii* ATCC 17978 and clinical isolates through phosphoethanolamine modification of Lipid A. *Antimicrob. Agents. Chemother.* **55**, 3743-3751 (2011).
361. Beceiro, A., *et al.* Phosphoethanolamine modification of lipid A in colistin-resistant variants of *Acinetobacter baumannii* mediated by the *pmrAB* two-component regulatory system. *Antimicrob. Agents. Chemother.* **55**, 3370-3379 (2011).
362. Su, X.-Z., Chen, J., Mizushima, T., Kuroda, T. & Tsuchiya, T. AbeM, an H⁺-coupled *Acinetobacter baumannii* multidrug efflux pump belonging to the MATE family of transporters. *Antimicrob. Agents. Chemother.* **49**, 4362-4364 (2005).
363. Liao, J.-H., *et al.* Acetylome of *Acinetobacter baumannii* SK17 reveals a highly-conserved modification of histone-like protein HU. *Front. Mol. Biosci.* **4**, (2017).
364. Wang, Z., *et al.* An allosteric transport mechanism for the AcrAB-TolC multidrug efflux pump. *eLife*. **6**, e24905 (2017).
365. Murakami, S., Nakashima, R., Yamashita, E. & Yamaguchi, A. Crystal structure of bacterial multidrug efflux transporter AcrB. *Nature*. **419**, 587-593 (2002).
366. Daury, L., *et al.* Tripartite assembly of RND multidrug efflux pumps. *Nat. Commun.* **7**, 10731 (2016).
367. Jeong, H., *et al.* Pseudoatomic structure of the tripartite multidrug efflux pump AcrAB-TolC reveals the intermeshing cogwheel-like interaction between AcrA and TolC. *Structure*. **24**, 272-276 (2016).
368. Mikolosko, J., Bobyk, K., Zgurskaya, H. I. & Ghosh, P. Conformational flexibility in the multidrug efflux system protein AcrA. *Structure*. **14**, 577-587 (2006).
369. Su, C.-C., *et al.* Cryo-electron microscopy structure of an *Acinetobacter baumannii* span multidrug efflux pump. *mBio*. **10**, e01295-e01319 (2019).
370. Barlow, V. L., *et al.* Effect of membrane fusion protein AdeT1 on the antimicrobial resistance of *Escherichia coli*. *Sci. Rep.* **10**, 20464 (2020).
371. Madeira, F., *et al.* The EMBL-EBI search and sequence analysis tools APIs in 2019. *Nucleic Acids Res.* **47**, W636-W641 (2019).

372. Gattner, M. J., Vrabel, M. & Carell, T. Synthesis of ϵ -N-propionyl-, ϵ -N-butyryl-, and ϵ -N-crotonyl-lysine containing histone H3 using the pyrrolysine system. *Chem. Comm.* **49**, 379-381 (2013).
373. Wilkins, B. J., *et al.* Genetically encoding lysine modifications on histone H4. *ACS Chem. Biol.* **10**, 939-944 (2015).
374. Jernaes, M. W. & Steen, H. B. Staining of *Escherichia coli* for flow cytometry: Influx and efflux of ethidium bromide. *Cytometry*. **17**, 302-309 (1994).
375. Paixão, L., *et al.* Fluorometric determination of ethidium bromide efflux kinetics in *Escherichia coli*. *J. Biol. Eng.* **3**, 18 (2009).
376. Blair, J. M. A., Piddock, L. J. V., Wright, G. D. & Collier, R. J. How to measure export via bacterial multidrug resistance efflux pumps. *mBio*. **7**, e00840-00816 (2016).
377. Olmsted, J. & Kearns, D. R. Mechanism of ethidium bromide fluorescence enhancement on binding to nucleic acids. *Biochemistry*. **16**, 3647-3654 (1977).
378. Viveiros, M., *et al.* Demonstration of intrinsic efflux activity of *Escherichia coli* K-12 AG100 by an automated ethidium bromide method. *Int. J. Antimicrob. Agents*. **31**, 458-462 (2008).
379. Wiegand, I., Hilpert, K. & Hancock, R. E. W. Agar and broth dilution methods to determine the minimal inhibitory concentration (MIC) of antimicrobial substances. *Nature Protocols*. **3**, 163-175 (2008).
380. Kowalska-Krochmal, B. & Dudek-Wicher, R. The minimum inhibitory concentration of antibiotics: Methods, interpretation, clinical relevance. *Pathogens*. **10**, 165 (2021).
381. Zhang, D.-f., Jiang, B., Xiang, Z.-m. & Wang, S.-y. Functional characterisation of altered outer membrane proteins for tetracycline resistance in *Escherichia coli*. *Int. J. Antimicrob. Agents*. **32**, 315-319 (2008).
382. Hammerstrom, T. G., Beabout, K., Clements, T. P., Saxer, G. & Shamoo, Y. *Acinetobacter baumannii* repeatedly evolves a hypermutator phenotype in response to tigecycline that effectively surveys evolutionary trajectories to resistance. *PLOS ONE*. **10**, e0140489 (2015).
383. Blattner, F. R., *et al.* The complete genome sequence of *Escherichia coli* K-12. *Science*. **277**, 1453-1462 (1997).
384. Stevenson, K., McVey, A. F., Clark, I. B. N., Swain, P. S. & Pilizota, T. General calibration of microbial growth in microplate readers. *Sci. Rep.* **6**, 38828 (2016).
385. Sauve, A. A., Wolberger, C., Schramm, V. L. & Boeke, J. D. The biochemistry of sirtuins. *Annu. Rev. Biochem.* **75**, 435-465 (2006).
386. Vethanayagam, J. G. G. & Flower, A. M. Decreased gene expression from T7 promoters may be due to impaired production of active T7 RNA polymerase. *Microb. Cell. Fact.* **4**, 3 (2005).
387. Sun, J., Deng, Z. & Yan, A. Bacterial multidrug efflux pumps: Mechanisms, physiology and pharmacological exploitations. *Biochem. Biophys. Res. Commun.* **453**, 254-267 (2014).
388. Alcalde-Rico, M., Olivares-Pacheco, J., Alvarez-Ortega, C., Cámara, M. & Martínez, J. L. Role of the multidrug resistance efflux pump MexCD-OprJ in the *Pseudomonas aeruginosa* quorum sensing response. *Front. Microbiol.* **9**, (2018).
389. Olivares, J., *et al.* Overproduction of the multidrug efflux pump MexEF-OprN does not impair *Pseudomonas aeruginosa* fitness in competition tests, but produces specific changes in bacterial regulatory networks. *Environ. Microbiol.* **14**, 1968-1981 (2012).
390. Cox, G., *et al.* A common platform for antibiotic dereplication and adjuvant discovery. *Cell Chem. Biol.* **24**, 98-109 (2017).

391. Cox, G., *et al.* Plazomicin retains antibiotic activity against most aminoglycoside modifying enzymes. *ACS Infect. Dis.* **4**, 980-987 (2018).
392. Menart, V., Jevševar, S., Vilar, M., Trobiš, A. & Pavko, A. Constitutive versus thermoinducible expression of heterologous proteins in *Escherichia coli* based on strong P_R,P_L promoters from phage lambda. *Biotechnol. Bioeng.* **83**, 181-190 (2003).
393. Munjal, N., Jawed, K., Wajid, S. & Yazdani, S. S. A constitutive expression system for cellulase secretion in *Escherichia coli* and its use in bioethanol production. *PLOS ONE*. **10**, e0119917 (2015).
394. Popov, M., Petrov, S., Nacheva, G., Ivanov, I. & Reichl, U. Effects of a recombinant gene expression on ColE1-like plasmid segregation in *Escherichia coli*. *BMC Biotechnol.* **11**, 18 (2011).
395. Mikiewicz, D., Plucienniczak, A., Bierczynska-Krzysik, A., Skowronek, A. & Wegrzyn, G. Novel expression vectors based on the pIGDM1 plasmid. *Mol. Biotechnol.* **61**, 763-773 (2019).
396. Khlebnikov, A., Datsenko, K. A., Skaug, T., Wanner, B. L. & Keasling, J. D. Homogeneous expression of the P_{BAD} promoter in *Escherichia coli* by constitutive expression of the low-affinity high-capacity AraE transporter. *Microbiology*. **147**, 3241-3247 (2001).
397. Jeong, K. J., *et al.* Constitutive production of human leptin by fed-batch culture of recombinant *rpoS*⁻ *Escherichia coli*. *Protein Express. Purif.* **36**, 150-156 (2004).
398. Leus, I. V., *et al.* Inactivation of AdeABC and AdeIJK efflux pumps elicits specific nonoverlapping transcriptional and phenotypic responses in *Acinetobacter baumannii*. *Mol. Microbiol.* **114**, 1049-1065 (2020).
399. Poole, K. *Pseudomonas aeruginosa* efflux pumps. Caister Academic Press (2013).
400. Dastidar, V., Mao, W., Lomovskaya, O. & Zgurskaya, H. I. Drug-induced conformational changes in multidrug efflux transporter AcrB from *Haemophilus influenzae*. *J. Bacteriol.* **189**, 5550-5558 (2007).
401. Mine, T., Morita, Y., Kataoka, A., Mizushima, T. & Tsuchiya, T. Expression in *Escherichia coli* of a new multidrug efflux pump, MexXY, from *Pseudomonas aeruginosa*. *Antimicrob. Agents. Chemother.* **43**, 415-417 (1999).
402. Kramer, E. B. & Farabaugh, P. J. The frequency of translational misreading errors in *E. coli* is largely determined by tRNA competition. *RNA*. **13**, 87-96 (2007).
403. Foster, P. L. Stress-induced mutagenesis in bacteria. *Crit. Rev. Biochem. Mol. Biol.* **42**, 373-397 (2007).
404. Yu, E. W., Aires, J. R. & Nikaido, H. AcrB multidrug efflux pump of *Escherichia coli*: composite substrate-binding cavity of exceptional flexibility generates its extremely wide substrate specificity. *J. Bacteriol.* **185**, 5657-5664 (2003).
405. Yu, E. W., McDermott, G., Zgurskaya, H. I., Nikaido, H. & Koshland, D. E. Structural basis of multiple drug-binding capacity of the AcrB multidrug efflux pump. *Science*. **300**, 976-980 (2003).
406. Tal, N. & Schuldiner, S. A coordinated network of transporters with overlapping specificities provides a robust survival strategy. *Proc. Natl. Acad. Sci. U.S.A.* **106**, 9051-9056 (2009).
407. Reddington, S. C., Tippmann, E. M. & Jones, D. D. Residue choice defines efficiency and influence of bioorthogonal protein modification via genetically encoded strain promoted Click chemistry. *Chem. Comm.* **48**, 8419-8421 (2012).
408. Kern, W. V., *et al.* Effect of 1-(1-naphthylmethyl)-piperazine, a novel putative efflux pump inhibitor, on antimicrobial drug susceptibility in clinical isolates of *Escherichia coli*. *J. Antimicrob. Chemother.* **57**, 339-343 (2005).

409. Blount, Z. D. The unexhausted potential of *E. coli*. *eLife*. **4**, e05826 (2015).
410. Kaas, R. S., Friis, C., Ussery, D. W. & Aarestrup, F. M. Estimating variation within the genes and inferring the phylogeny of 186 sequenced diverse *Escherichia coli* genomes. *BMC Genom.* **13**, 577 (2012).
411. Ducarmon, Q. R., *et al.* Gut microbiota and colonization resistance against bacterial enteric infection. *Microbiol. Mol. Biol. Rev.* **83**, e00007-00019 (2019).
412. Kaper, J. B., Nataro, J. P. & Mobley, H. L. T. Pathogenic *Escherichia coli*. *Nat. Rev. Microbiol.* **2**, 123-140 (2004).
413. Ramos, S., *et al.* *Escherichia coli* as commensal and pathogenic bacteria among food-producing animals: Health implications of extended spectrum β -lactamase (ESBL) production. *Animals*. **10**, 2239 (2020).
414. Flores-Mireles, A. L., Walker, J. N., Caparon, M. & Hultgren, S. J. Urinary tract infections: epidemiology, mechanisms of infection and treatment options. *Nat. Rev. Microbiol.* **13**, 269-284 (2015).
415. Dawson, K. G., Emerson, J. C. & Burns, J. L. Fifteen years of experience with bacterial meningitis. *Pediatr. Infect. Dis. J.* **18**, 816-822 (1999).
416. Navarro-Garcia, F., Ruiz-Perez, F., Cataldi, Á. & Larzábal, M. Type VI secretion system in pathogenic *Escherichia coli*: structure, role in virulence, and acquisition. *Front. Microbiol.* **10**, (2019).
417. Braz, V. S., Melchior, K. & Moreira, C. G. *Escherichia coli* as a multifaceted pathogenic and versatile bacterium. *Front. Cell. Infect. Microbiol.* **10**, (2020).
418. Johnson, J. R. Virulence factors in *Escherichia coli* urinary tract infection. *Clin. Microbiol. Rev.* **4**, 80-128 (1991).
419. Johnson, J. R. & Stell, A. L. Extended virulence genotypes of *Escherichia coli* strains from patients with urosepsis in relation to phylogeny and host compromise. *J. Infect. Dis.* **181**, 261-272 (2000).
420. Kazemnia, A., Ahmadi, M. & Dilmaghani, M. Antibiotic resistance pattern of different *Escherichia coli* phylogenetic groups isolated from human urinary tract infection and avian colibacillosis. *Iran. Biomed. J.* **18**, 219-224 (2014).
421. Asadi Karam, M. R., Habibi, M. & Bouzari, S. Urinary tract infection: Pathogenicity, antibiotic resistance and development of effective vaccines against Uropathogenic *Escherichia coli*. *Mol. Immunol.* **108**, 56-67 (2019).
422. Gupta, K., Hooton, T. M. & Stamm, W. E. Increasing antimicrobial resistance and the management of uncomplicated community-acquired urinary tract infections. *Ann. Intern. Med.* **135**, 41-50 (2001).
423. Allocati, N., Masulli, M., Alexeyev, M. F. & Di Ilio, C. *Escherichia coli* in Europe: An Overview. *Int. J. Environ. Res. Public Health.* **10**, 6235-6254 (2013).
424. Poirel, L., *et al.* Antimicrobial Resistance in *Escherichia coli*. *Microbiol. Spectr.* **6**, ARBA-0026-2017. (2018).
425. Russo, T. A. & Johnson, J. R. Medical and economic impact of extraintestinal infections due to *Escherichia coli*: focus on an increasingly important endemic problem. *Microbes Infect.* **5**, 449-456 (2003).
426. Bonnefoy, E. & Rouvière-Yaniv, J. HU and IHF, two homologous histone-like proteins of *Escherichia coli*, form different protein-DNA complexes with short DNA fragments. *EMBO J.* **10**, 687-696 (1991).
427. Swinger, K. K., Lemberg, K. M., Zhang, Y. & Rice, P. A. Flexible DNA bending in HU-DNA cocrystal structures. *EMBO J.* **22**, 3749-3760 (2003).
428. Drlica, K. & Rouvière-Yaniv, J. Histone-like proteins of bacteria. *Microbiol. Rev.* **51**, 301-319 (1987).
429. Claret, L. & Rouvière-Yaniv, J. Variation in HU composition during growth of *Escherichia coli*: the heterodimer is required for long term survival. *J. Mol. Biol.* **273**, 93-104 (1997).

430. Ramstein, J., *et al.* Evidence of a thermal unfolding dimeric intermediate for the *Escherichia coli* histone-like HU proteins: thermodynamics and structure. *J. Mol. Biol.* **331**, 101-121 (2003).
431. Kobryn, K., Lavoie, B. D. & Chaconas, G. Supercoiling-dependent site-specific binding of HU to naked Mu DNA. *J. Mol. Biol.* **289**, 777-784 (1999).
432. Kamashev, D. & Rouviere-Yaniv, J. The histone-like protein HU binds specifically to DNA recombination and repair intermediates. *EMBO J.* **19**, 6527-6535 (2000).
433. Swinger, K. K. & Rice, P. A. IHF and HU: flexible architects of bent DNA. *Curr. Opin. Struct. Biol.* **14**, 28-35 (2004).
434. Rice, P. A., Yang, S.-w., Mizuuchi, K. & Nash, H. A. Crystal structure of an IHF-DNA complex: a protein-induced DNA U-turn. *Cell.* **87**, 1295-1306 (1996).
435. Becker, N. A., Kahn, J. D. & James Maher, L. Bacterial repression loops require enhanced DNA flexibility. *J. Mol. Biol.* **349**, 716-730 (2005).
436. Pinson, V., Takahashi, M. & Rouviere-Yaniv, J. Differential binding of the *Escherichia coli* HU, homodimeric forms and heterodimeric form to linear, gapped and cruciform DNA. *J. Mol. Biol.* **287**, 485-497 (1999).
437. Castaing, B., Zelwer, C., Laval, J. & Boiteux, S. HU Protein of *Escherichia coli* binds specifically to DNA that contains single-strand breaks or gaps. *J. Biol. Chem.* **270**, 10291-10296 (1995).
438. Hammel, M., *et al.* HU multimerization shift controls nucleoid compaction. *Sci. Adv.* **2**, e1600650 (2016).
439. Thakur, B., Arora, K., Gupta, A. & Guptasarma, P. The DNA-binding protein HU is a molecular glue that attaches bacteria to extracellular DNA in biofilms. *J. Biol. Chem.* **296**, 100532 (2021).
440. Bhowmick, T., *et al.* Targeting *Mycobacterium tuberculosis* nucleoid-associated protein HU with structure-based inhibitors. *Nat. Commun.* **5**, 4124 (2014).
441. Agapova, Y. K., *et al.* Structure-based inhibitors targeting the alpha-helical domain of the *Spiroplasma melliferum* histone-like HU protein. *Sci. Rep.* **10**, 15128 (2020).
442. Dame, R. T. & Goosen, N. HU: promoting or counteracting DNA compaction? *FEBS Lett.* **529**, 151-156 (2002).
443. Macvanin, M., *et al.* Noncoding RNAs binding to the nucleoid protein HU in *Escherichia coli*. *J. Bacteriol.* **194**, 6046-6055 (2012).
444. Huisman, O., *et al.* Multiple defects in *Escherichia coli* mutants lacking HU protein. *J. Bacteriol.* **171**, 3704-3712 (1989).
445. Kundukad, B., Cong, P., van der Maarel, J. R. C. & Doyle, P. S. Time-dependent bending rigidity and helical twist of DNA by rearrangement of bound HU protein. *Nucleic Acids Res.* **41**, 8280-8288 (2013).
446. van Noort, J., Verbrugge, S., Goosen, N., Dekker, C. & Dame, R. T. Dual architectural roles of HU: Formation of flexible hinges and rigid filaments. *Proc. Natl. Acad. Sci. U.S.A.* **101**, 6969-6974 (2004).
447. Koh, J., Saecker, R. M. & Record, M. T. DNA binding mode transitions of *Escherichia coli* HU $\alpha\beta$: Evidence for formation of a bent DNA — protein complex on intact, linear duplex DNA. *J. Mol. Biol.* **383**, 324-346 (2008).
448. Bettridge, K., Verma, S., Weng, X., Adhya, S. & Xiao, J. Single-molecule tracking reveals that the nucleoid-associated protein HU plays a dual role in maintaining proper nucleoid volume through differential interactions with chromosomal DNA. *Mol. Microbiol.* **115**, 12-27 (2021).
449. Bonnefoy, E., Takahashi, M. & Yaniv, J. R. DNA-binding parameters of the HU protein of *Escherichia coli* to cruciform DNA. *J. Mol. Biol.* **242**, 116-129 (1994).

450. Hashimoto, M., Imhoff, B., Ali, M. M. & Kow, Y. W. HU protein of *Escherichia coli* has a role in the repair of closely opposed lesions in DNA. *J. Biol. Chem.* **278**, 28501-28507 (2003).
451. Boubrik, F. & Rouviere-Yaniv, J. Increased sensitivity to gamma irradiation in bacteria lacking protein HU. *Proc. Natl. Acad. Sci. U.S.A.* **92**, 3958-3962 (1995).
452. Li, S. & Waters, R. *Escherichia coli* strains lacking protein HU are UV sensitive due to a role for HU in homologous recombination. *J. Bacteriol.* **180**, 3750-3756 (1998).
453. Miyabe, Q. M., Zhang, Y., Kano, S. & Yonei, I. Histone-like protein HU is required for recA gene-dependent DNA repair and SOS induction pathways in UV-irradiated *Escherichia coli*. *Int. J. Radiat. Biol.* **76**, 43-49 (2000).
454. Dri, A. M., Rouviere-Yaniv, J. & Moreau, P. L. Inhibition of cell division in hupA hupB mutant bacteria lacking HU protein. *J. Bacteriol.* **173**, 2852-2863 (1991).
455. Fernández, S., Rojo, F. & Alonso, J. C. The *Bacillus subtilis* chromatin-associated protein Hbsu is involved in DNA repair and recombination. *Mol. Microbiol.* **23**, 1169-1179 (1997).
456. Kar, S., Edgar, R. & Adhya, S. Nucleoid remodeling by an altered HU protein: reorganization of the transcription program. *Proc. Natl. Acad. Sci. U.S.A.* **102**, 16397-16402 (2005).
457. Oberto, J., Nabti, S., Jooste, V., Mignot, H. & Rouviere-Yaniv, J. The HU regulon is composed of genes responding to anaerobiosis, acid stress, high osmolarity and SOS induction. *PLOS ONE*. **4**, e4367 (2009).
458. Stojkova, P., Spidlova, P. & Stulik, J. Nucleoid-associated protein HU: a lilliputian in gene regulation of bacterial virulence. *Front. Cell. Infect. Microbiol.* **9**, (2019).
459. Aki, T. & Adhya, S. Repressor induced site-specific binding of HU for transcriptional regulation. *EMBO J.* **16**, 3666-3674 (1997).
460. Aki, T., Choy, H. E. & Adhya, S. Histone-like protein HU as a specific transcriptional regulator: co-factor role in repression of gal transcription by GAL repressor. *Genes Cells.* **1**, 179-188 (1996).
461. Roy, S., *et al.* Gal repressor-operator-HU ternary complex: pathway of repressosome formation. *Biochemistry.* **44**, 5373-5380 (2005).
462. Choy, H. E., *et al.* Repression and activation of transcription by Gal and Lac repressors: involvement of alpha subunit of RNA polymerase. *EMBO J.* **14**, 4523-4529 (1995).
463. Berger, M., *et al.* Genes on a wire: the nucleoid-associated protein HU insulates transcription units in *Escherichia coli*. *Sci. Rep.* **6**, 31512 (2016).
464. Rouvière-Yaniv, J., Yaniv, M. & Germond, J.-E. *E. coli* DNA binding protein HU forms nucleosome-like structure with circular double-stranded DNA. *Cell.* **17**, 265-274 (1979).
465. Remesh, S. G., *et al.* Nucleoid remodeling during environmental adaptation is regulated by HU-dependent DNA bundling. *Nat. Commun.* **11**, 2905 (2020).
466. Kar, S., *et al.* Right-handed DNA supercoiling by an octameric form of histone-like protein HU. *J. Biol. Chem.* **281**, 40144-40153 (2006).
467. Ryan, V. T., Grimwade, J. E., Nievera, C. J. & Leonard, A. C. IHF and HU stimulate assembly of pre-replication complexes at *Escherichia coli* oriC by two different mechanisms. *Mol. Microbiol.* **46**, 113-124 (2002).
468. Kar, S. & Adhya, S. Recruitment of HU by piggyback: a special role of GalR in repressosome assembly. *Genes Dev.* **15**, 2273-2281 (2001).
469. Datta, C., *et al.* Physical and functional interaction between nucleoid-associated proteins HU and Lsr2 of *Mycobacterium tuberculosis*: altered DNA binding and gene regulation. *Mol. Microbiol.* **111**, 981-994 (2019).

470. Sidjabat, H. E., *et al.* The use of SWATH to analyse the dynamic changes of bacterial proteome of carbapenemase-producing *Escherichia coli* under antibiotic pressure. *Sci. Rep.* **8**, 3871 (2018).
471. Tessarz, P. & Kouzarides, T. Histone core modifications regulating nucleosome structure and dynamics. *Nat. Rev. Mol. Cell Biol.* **15**, 703-708 (2014).
472. Kouzarides, T. Chromatin modifications and their function. *Cell.* **128**, 693-705 (2007).
473. Workman, J. L. & Kingston, R. E. Alteration of nucleosome structure as a mechanism of transcriptional regulation. *Annu. Rev. Biochem.* **67**, 545-579 (1998).
474. Dilweg, I. W. & Dame, R. T. Post-translational modification of nucleoid-associated proteins: an extra layer of functional modulation in bacteria? *Biochem. Soc. Trans.* **46**, 1381-1392 (2018).
475. Qin, L., Erkelens, A. M., Ben Bdira, F. & Dame, R. T. The architects of bacterial DNA bridges: a structurally and functionally conserved family of proteins. *Open. Biol.* **9**, 190223 (2019).
476. Alqaseer, K., *et al.* Protein kinase B controls *Mycobacterium tuberculosis* growth via phosphorylation of the transcriptional regulator Lsr2 at threonine 112. *Mol. Microbiol.* **112**, 1847-1862 (2019).
477. Seth, D., Hausladen, A., Wang, Y.-J. & Stamler, J. S. Endogenous protein S-nitrosylation in *E. coli*: Regulation by OxyR. *Science.* **336**, 470-473 (2012).
478. Udo, H., Lam, C. K., Mori, S., Inouye, M. & Inouye, S. Identification of a substrate for Pkn2, a protein Ser/Thr kinase from *Myxococcus xanthus* by a novel method for substrate identification. *J. Mol. Microbiol. Biotechnol.* **2**, 557-563 (2000).
479. Castaño-Cerezo, S., *et al.* Protein acetylation affects acetate metabolism, motility and acid stress response in *Escherichia coli*. *Mol. Syst. Biol.* **10**, 762 (2014).
480. Anand, C., Garg, R., Ghosh, S. & Nagaraja, V. A Sir2 family protein Rv1151c deacetylates HU to alter its DNA binding mode in *Mycobacterium tuberculosis*. *Biochem. Biophys. Res. Commun.* **493**, 1204-1209 (2017).
481. Kamashev, D., *et al.* Comparison of histone-like HU protein DNA-binding properties and HU/IHF protein sequence alignment. *PLOS ONE.* **12**, e0188037 (2017).
482. Grove, A. & Saavedra, T. C. The role of surface-exposed lysines in wrapping DNA about the bacterial histone-like protein HU. *Biochemistry.* **41**, 7597-7603 (2002).
483. Köhler, P. & Marahiel, M. A. Mutational analysis of the nucleoid-associated protein HBSu of *Bacillus subtilis*. *Mol. Gen. Genet.* **260**, 487-491 (1998).
484. Wojtuszewski, K., Hawkins, M. E., Cole, J. L. & Mukerji, I. HU binding to DNA: evidence for multiple complex formation and DNA bending. *Biochemistry.* **40**, 2588-2598 (2001).
485. Koh, J., Shkel, I., Saecker, R. M. & Record, M. T. Nonspecific DNA binding and bending by HU $\alpha\beta$: Interfaces of the three binding modes characterized by salt-dependent thermodynamics. *J. Mol. Biol.* **410**, 241-267 (2011).
486. Lavoie, B. D., Shaw, G. S., Millner, A. & Chaconas, G. Anatomy of a flexer-DNA complex inside a higher-order transposition intermediate. *Cell.* **85**, 761-771 (1996).
487. Kamashev, D., Balandina, A. & Rouviere-Yaniv, J. The binding motif recognized by HU on both nicked and cruciform DNA. *EMBO J.* **18**, 5434-5444 (1999).
488. Wojtuszewski, K. & Mukerji, I. HU binding to bent DNA: a fluorescence resonance energy transfer and anisotropy study. *Biochemistry.* **42**, 3096-3104 (2003).

- 489. Wang, B., Kumar, V., Olson, A. & Ware, D. Reviving the transcriptome studies: an insight into the emergence of single-molecule transcriptome sequencing. *Front. Genet.* **10**, (2019).
- 490. Pettersen, E. F., *et al.* UCSF Chimera—A visualization system for exploratory research and analysis. *Journal of Computational Chemistry.* **25**, 1605-1612 (2004).
- 491. Inkscape, 2022. Available at: <https://inkscape.org/>.

Appendix

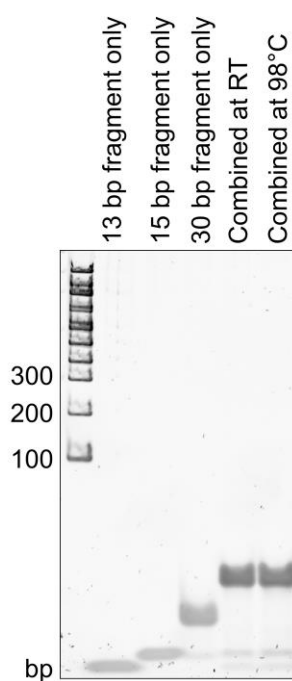


Figure A.1 Confirming 30 bp complex formation by combining smaller DNA fragments for use in EMSAs in **Chapter 3**. The 13, 15 and 30 bp DNA fragments from Chapter 3 were combined in equal molar ratios at room temperature (RT) or by heating to 98 °C before slow cooling to RT as described in **Section 3.7.8 Electrophoretic mobility shift assay**. Samples were taken from each of the oligonucleotides and from the combined conditions, mixed with 5x DNA loading dye and analysed by 10% non-denaturing polyacrylamide gel electrophoresis.

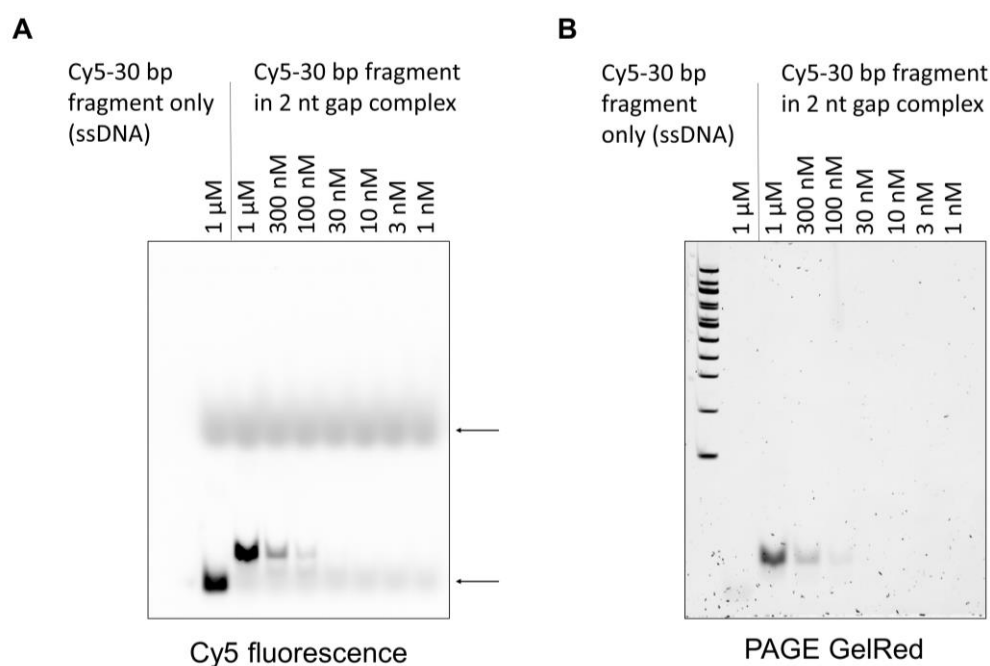


Figure A.2 Investigating the use of fluorescently labelled DNA for use in EMSAs in Chapter 3. An alternative version of the 30 bp oligonucleotide from Chapter 3 labelled with Cy5 (Cy5-30 bp) was ordered as described in **Section 3.7.8 Electrophoretic mobility shift assay**. The Cy5-30 bp fragment was combined with the 13 and 15 bp fragments to create a fluorescently labelled 30 bp DNA fragment with a 2 nt gap. The DNA fragments were combined with 5x DNA loading dye and analysed on a 10% non-denaturing polyacrylamide gel. The gel was visualised with **A** ex 650 nm, em 695 nm to visualise Cy5 and **B** via staining with PAGE GelRed and UV excitation, em 605 nm. Visualising Cy5 fluorescence permitted better visualisation of single stranded DNA (ssDNA), allowing confirmation that when combined, all single stranded DNA forms part of a double stranded DNA complex. However, visualising Cy5 fluorescence did not result in any improved detection of double stranded DNA compared to staining with PAGE GelRed. Further, excitation at 650 nm resulted in the detection of background fluorescence from the tracking dyes included in the 5x DNA loading dye, indicated by arrows.

Table A.1 FASTA sequences of the nucleotides of the primer through to the translated region and stop codon inclusive for all plasmids used in this thesis.

Plasmid	FASTA nucleotide sequence primer, lac operon, translated region, his tag (translated), stop
pAcKST	<p>TAATACGACTCACTATAGGGGAATTGTGAGCGGATAACAATTCCCCTG TAGAAATAATTTTGTTTAACTTTAATAAGGAGATATACCATGGGCAGC AGCCATCACCATCATCACCACAGCCAGGATCCTCGGGTTGTCAGCCTG TCCCCTTATAAGATCATACGCCGTTATACGTTGTTTACGCTTTGAGG AATCCCATATGATGGATAAAAAACCGCTGGATGTGCTGATTAGCGCGA CCGGCCTGTGGATGAGCCGTACCGGCACCCTGCATAAAATCAAACATC ATGAAGTGAGCCGCAGCAAAATCTATATTGAAATGGCGTGCGGCGATC ATCTGGTGGTGAACAACAGCCGTAGCTGCCGTACCGCGCGTGC GTTTC GTCATCATAAATACCGCAAAACCTGCAAACGTTGCCGTGTGAGCGGTG AAGATATCAACAACCTTCTGACCCGTAGCACCAGAAAGCAAAAACAGCG TGAAAGTGCGTGTGGTGAGCGCGCCGAAAGTGAAAAAGCGATGCCGA AAAGCGTGAGCCGTGCGCCGAAACCGCTGGAAAATAGCGTGGGCGCGA AAGCGAGCACCAACACCAGCCGTAGCGTTCCGAGCCCGGCGAAAAGCA CCCCGAACAGCAGCGTTCCGGCGTCTGCGCCGGCACCGAGCCTGACCC GCAGCCAGCTGGATCGTGTGGAAGCGCTGCTGTCTCCGGAAGATAAAA TTAGCCTGAACATGGCGAAACCGTTTCGTGAACTGGAACCGGAACTGG TGACCCGTCGTAAAAACGATTTTCAGCGCCTGTATACCAACGATCGTG AAGATTATCTGGGCAAACTGGAACGTGATATCACCAGATTTTGTGG ATCGCGGCTTTCTGGAATTTAAAGCCCGATTCTGATTCGGGCGGAAT ATGTGGAACGTATGGGCATTAACAACGACACCGAACTGAGCAAAACAAA TTTTCCGCGTGGATAAAAAACCTGTGCCTGCGTCCGATGATGGCTCCGA CCATTTTAACTATGCTCGTAAACTGGATCGTATTCTGCCGGGTCCGA TCAAATTTTGAAGTGGGCCCGTCTATCGCAAAGAAAGCGATGGCA AAGAACACCTGGAAGAATTCACCATGGTTAACTTTTTTCAAATGGGCA GCGGCTGCACCCGTGAAAACCTGGAAGCGCTGATCAAAGAATTCTCTGG ATTATCTGGAATCGACTTCGAAATTGTGGGCGATAGCTGCATGGTGT ATGGCGATACCCTGGATATTATGCATGGCGATCTGGAACCTGAGCAGCG CGGTGGTGGGTCCGGTTAGCCTGGATCGTGAATGGGGCATTGATAAAC CGTGGATTGGCGCGGGTTTGGCCTGGAACGTCTGCTGAAAGTGATGC ATGGCTTCAAAAACATTAAACGTGCGAGCCGTAGCGAAAGCTACTATA ACGGCATTAGCACGAACCTGTAA</p>
pAdeT1	<p>TTTACACTTTATGCTTCCGGCTCGTATGTTGTGTGGAATTGTGAGCGG ATAACAATTTACACAGGAAACAGCTATGACCATGATTACGAATTCGT GTTTGATCCGATTGGTAAAAGCGGTGATGCATTTGCACTGGCAAAAGA TTATGCACTGGAAGCAAAAAATTGGGGCGCAGATCTGAGCCTGAAAGC CTATGTTGATGAACGTGTTGCAGCAGAGGATCTGAAAGTTGGTAAATG TGATGGTGCAATTATTAGCGGTCTGCGTGGTTCGTAGTTTAACAAATA TACGGGTAGCCTGGATGCAGTTGGTGCAGTACCAATATGAAAACCGC AATTAATGCCTATAAACTGCTGAGCAGCCCGATGGCAGCCAAAAATAT GGTTGTTGGTCCGTATGAAATTGCAGGTCTGGGCACCATTTGGTCCGGC ATACCTGTTTGTAAATGATCGTAGCATTAATACCCTGGCCAAAGCAGC AGGCAAAAAAATCGGTGTTTTCAAATATGATGAAGCCAGCCGAAACT GGTTCAGCATGTTGGTGGTCAGGCAGTTAGCGTTGATGTTACCAATGC CGGTGCCAAATTTAACAACCATGAAATTGATATTGTTCCGGCACCAGAT TGTTGCCTTTAAACCGTTTGAACCTGTATAAAGGCCTGGGTGAAAAAGG TGCCATTGTTTCGTTTTCCGCTGACACAGATTAGCGCAGATTTTATCAT TCGCAAAGATCAGTTTCCGGCAGGTTTTGGTCAGAAAAGCCGTACCTG GGTTGCAAGCCAGCTGAATCGTACCTTTGGTATTATTGCCAAATATGA GAGCGATATCCCGAGCAAAATATTGGATGGATATTCCGAAAAATGAACA GCTGAACTATATGAAGATGATGCGTGAAGCACGTATTACGCTGACCAA</p>

Note: AdeT1
gene is
highlighted in
grey and is not
in a translated
region.

	AGCAGGTATTTATGATCCCAAATGATGAACTTCCTGAAGAAAGTGCG CTGCAAAGAAAATCCGAGCAATTTTGAATGTGCCCTGAACGATGAATA A
pAdeT1* Note: AdeT1 gene is highlighted in grey.	TTTACACTTTATGCTTCCGGCTCGTATGTTGTGTGGAATTGTGAGCGG ATAACAATTTACACACAGGAAACAGCTATGACCATGATTACGGTGTTTG ATCCGATTGGTAAAAGCGGTGATGCATTTGCACTGGCAAAGATTATG CACTGGAAGCAAAAAATTGGGGCGCAGATCTGAGCCTGAAAGCCTATG TTGATGAACGTGTTGCAGCAGAGGATCTGAAAGTTGGTAAATGTGATG GTGCAATTATTAGCGGTCTGCGTGGTCGTCAGTTTAACAAATATACGG GTAGCCTGGATGCAGTTGGTGCAGTACCAATATGAAAACCGCAATTA ATGCCTATAAACTGCTGAGCAGCCCGATGGCAGCCAAAAATATGGTTG TTGGTCCGTATGAAATTGCAGGTCTGGGCACCATTGGTCCGGCATACC TGTTTGTTAATGATCGTAGCATTAAATACCCTGGCCAAAGCAGCAGGCA AAAAATCGGTGTTTTCAAATATGATGAAGCCCAGCCGAAACTGGTTC AGCATGTTGGTGGTCAGGCAGTTAGCGTTGATGTTACCAATGCCGGTG CCAAATTTAACAACCATGAAATTGATATTGTTCCGGCACCATTGTTG CCTTTAAACCGTTTGAAGTGTATAAAGGCCTGGGTGAAAAGGTGCCA TTGTTTCGTTTTCCGCTGACACAGATTAGCGCAGATTTTATCATTCGCA AAGATCAGTTTCCGGCAGGTTTTGGTCAGAAAAGCCGTACCTGGGTTG CAAGCCAGCTGAATCGTACCTTTGGTATTATTGCCAAATATGAGAGCG ATATCCCGAGCAAATATTGGATGGATATTCCGAAAAATGAACAGCTGA ACTATATGAAGATGATGCGTGAAGCACGTATTCAGCTGACCAAAGCAG GTATTTATGATCCCAAATGATGAACTTCCTGAAGAAAGTGCGCTGCA AAGAAAATCCGAGCAATTTTGAATGTGCCCTGAACGATGAATGA
pAdeT1-His6 Note: AdeT1 gene is highlighted in grey and is not in a translated region.	TTTACACTTTATGCTTCCGGCTCGTATGTTGTGTGGAATTGTGAGCGG ATAACAATTTACACACAGGAAACAGCTATGACCATGATTACGAATTCGT GTTTGATCCGATTGGTAAAAGCGGTGATGCATTTGCACTGGCAAAGA TTATGCACTGGAAGCAAAAAATTGGGGCGCAGATCTGAGCCTGAAAGC CTATGTTGATGAACGTGTTGCAGCAGAGGATCTGAAAGTTGGTAAATG TGATGGTGCAATTATTAGCGGTCTGCGTGGTCGTCAGTTTAACAAATA TACGGGTAGCCTGGATGCAGTTGGTGCAGTACCAATATGAAAACCGC AATTAATGCCTATAAACTGCTGAGCAGCCCGATGGCAGCCAAAAATAT GGTTGTTGGTCCGTATGAAATTGCAGGTCTGGGCACCATTGGTCCGGC ATACCTGTTTGTAAATGATCGTAGCATTAAATACCCTGGCCAAAGCAGC AGGCAAAAAAATCGGTGTTTTCAAATATGATGAAGCCCAGCCGAAACT GGTTCAGCATGTTGGTGGTCAGGCAGTTAGCGTTGATGTTACCAATGC CGGTGCCAAATTTAACAACCATGAAATTGATATTGTTCCGGCACCATT TGTTGCCTTTAAACCGTTTGAAGTGTATAAAGGCCTGGGTGAAAAGG TGCCATTGTTTCGTTTTCCGCTGACACAGATTAGCGCAGATTTTATCAT TCGCAAAGATCAGTTTCCGGCAGGTTTTGGTCAGAAAAGCCGTACCTG GGTTGCAAGCCAGCTGAATCGTACCTTTGGTATTATTGCCAAATATGA GAGCGATATCCCGAGCAAATATTGGATGGATATTCCGAAAAATGAACA GCTGAACTATATGAAGATGATGCGTGAAGCACGTATTCAGCTGACC AGCAGGTATTTATGATCCCAAATGATGAACTTCCTGAAGAAAGTGCG CTGCAAAGAAAATCCGAGCAATTTTGAATGTGCCCTGAACGATGAACA CCATCATCATCACCATTAA
pAdeT1*-His6 Note: AdeT1 gene is highlighted in grey.	TTTACACTTTATGCTTCCGGCTCGTATGTTGTGTGGAATTGTGAGCGG ATAACAATTTACACACAGGAAACAGCTATGACCATGATTACGGTGTTTG ATCCGATTGGTAAAAGCGGTGATGCATTTGCACTGGCAAAGATTATG CACTGGAAGCAAAAAATTGGGGCGCAGATCTGAGCCTGAAAGCCTATG TTGATGAACGTGTTGCAGCAGAGGATCTGAAAGTTGGTAAATGTGATG GTGCAATTATTAGCGGTCTGCGTGGTCGTCAGTTTAACAAATATACGG GTAGCCTGGATGCAGTTGGTGCAGTACCAATATGAAAACCGCAATTA ATGCCTATAAACTGCTGAGCAGCCCGATGGCAGCCAAAAATATGGTTG TTGGTCCGTATGAAATTGCAGGTCTGGGCACCATTGGTCCGGCATACC

	<p> TGT TTGTTAATGATCGTAGCATTAAATACCCTGGCCAAAGCAGCAGGCA AAAAAATCGGTGTTTTCAAATATGATGAAGCCCAGCCGAAACTGGTTC AGCATGTTGGTGGTCAGGCAGTTAGCGTTGATGTTACCAATGCCGGTG CCAAATTTAACAACCATGAAATTGATATTGTTCCGGCACCATTGTTG CCTTTAAACCGTTTGAAGTGTATAAAGGCCTGGGTGAAAAAGGTGCCA TTGTTTCGTTTTCCGCTGACACAGATTAGCGCAGATTTTATCATTGCGA AAGATCAGTTTCCGGCAGGTTTTGGTCAGAAAAGCCGTACCTGGGTG CAAGCCAGCTGAATCGTACCTTTGGTATTATTGCCAAATATGAGAGCG ATATCCCGAGCAAATATTGGATGGATATTCGAAAAATGAACAGCTGA ACTATATGAAGATGATGCGTGAAGCACGTATTCAGCTGACCAAAGCAG GTATTTATGATCCCAAATGATGAAGTTCCTGAAGAAAGTGCGCTGCA AAGAAAATCCGAGCAATTTTGAATGTGCCCTGAACGATGAACATCATC ATCACCACCACTGA </p>
pAdeT1*(K280 TAG)-His6	<p> TTTACACTTTATGCTTCCGGCTCGTATGTTGTGTGGAATTGTGAGCGG ATAACAATTTCACACAGGAAACAGCTATGACCATGATTACGGTGTGTTG ATCCGATTGGTAAAAGCGGTGATGCATTTGCACTGGCAAAGATTATG CACTGGAAGCAAAAAATTGGGGCGCAGATCTGAGCCTGAAAGCCTATG TTGATGAACGTGTTGCAGCAGAGGATCTGAAAGTTGGTAAATGTGATG GTGCAATTATTAGCGGTCTGCGTGGTTCGTCAGTTTAAACAAATATACGG GTAGCCTGGATGCAGTTGGTGCCTGACCAATATGAAAACCGCAATTA ATGCCTATAAACTGCTGAGCAGCCCGATGGCAGCCAAAAATATGGTTG TTGGTCCGTATGAAATTGCAGGTCTGGGCACCATTGGTCCGGCATAACC TGT TTGTTAATGATCGTAGCATTAAATACCCTGGCCAAAGCAGCAGGCA AAAAAATCGGTGTTTTCAAATATGATGAAGCCCAGCCGAAACTGGTTC AGCATGTTGGTGGTCAGGCAGTTAGCGTTGATGTTACCAATGCCGGTG CCAAATTTAACAACCATGAAATTGATATTGTTCCGGCACCATTGTTG CCTTTAAACCGTTTGAAGTGTATAAAGGCCTGGGTGAAAAAGGTGCCA TTGTTTCGTTTTCCGCTGACACAGATTAGCGCAGATTTTATCATTGCGA AAGATCAGTTTCCGGCAGGTTTTGGTCAGAAAAGCCGTACCTGGGTG CAAGCCAGCTGAATCGTACCTTTGGTATTATTGCCAAATATGAGAGCG ATATCCCGAGCAAATATTGGATGGATATTCGAAAAATGAACAGCTGA ACTATATGAAGATGATGCGTGAAGCACGTATTCAGCTGACCAAAGCAG GTATTTATGATCCCTAGATGATGAAGTTCCTGAAGAAAGTGCGCTGCA AAGAAAATCCGAGCAATTTTGAATGTGCCCTGAACGATGAACATCATC ATCACCACCACTGA </p>
pAmpR-AdeT1-His6	<p> CGCGGAACCCCTATTTGTTTATTTTCTAAATACATTCAAATATGTAT CCGCTCATGAGACAATAACCCTGATAAATGCTTCAATAATATTGAAAA AGGAAGAGTCCATGTTTGATCCGATTGGTAAAAGCGGTGATGCATTTG CACTGGCAAAGATTATGCACTGGAAGCAAAAAATTGGGGCGCAGATC TGAGCCTGAAAGCCTATGTTGATGAACGTGTTGCAGCAGAGGATCTGA AAGTTGGTAAATGTGATGGTGCAATTATTAGCGGTCTGCGTGGTTCGTC AGTTTAAACAAATATACGGGTAGCCTGGATGCAGTTGGTGCCTGACCA ATATGAAAACCGCAATTAATGCCTATAAACTGCTGAGCAGCCCGATGG CAGCCAAAAATATGGTTGTTGGTCCGTATGAAATTGCAGGTCTGGGCA CCATTGGTCCGGCATAACCTGTTTGTAAATGATCGTAGCATTAAATACC TGGCCAAAGCAGCAGGCCAAAAAATCGGTGTTTTCAAATATGATGAAG CCCAGCCGAAACTGGTTCAGCATGTTGGTGGTCAGGCAGTTAGCGTTG ATGTTACCAATGCCGGTGCCAAATTTAACAACCATGAAATTGATATTG TTCCGGCACCGATTGTTGCCTTTAAACCGTTTGAAGTGTATAAAGGCC TGGGTGAAAAAGGTGCCATTGTTTCGTTTTCCGCTGACACAGATTAGCG CAGATTTTATCATTGCAAAGATCAGTTTCCGGCAGGTTTTGGTCAGA AAAGCCGTACCTGGGTGCAAGCCAGCTGAATCGTACCTTTGGTATTA TTGCCAAATATGAGAGCGATATCCCGAGCAAATATTGGATGGATATTC CGAAAAATGAACAGCTGAAGTATATGAAGATGATGCGTGAAGCACGTA TTCAGCTGACCAAAGCAGGTATTTATGATCCCAAATGATGAAGTTC </p>

	TGAAGAAAGTGCCTGCAAAGAAAATCCGAGCAATTTTGAATGTGCCC TGAACGATGAACATCATCATCACCACCCTGA
pAmpR- sfGFP-His6	CGCGGAACCCCTATTTGTTTATTTTCTAAATACATTCAAATATGTAT CCGCTCATGAGACAATAACCCTGATAAATGCTTCAATAATATTGAAAA AGGAAGAGTCCATGGTTAGCAAAGGTGAAGAACTGTTTACCGGCGTTG TGCCGATTCTGGTGGAAGTGGATGGTGATGTGAATGGCCATAAAATTTA GCGTTTCGTGGCGAAGGCGAAGGTGATGCGACCAACGGTAAACTGACCC TGAAATTTATTTGCACCACCGGTAAACTGCCGGTTCCGTGGCCGACCC TGGTGACCACCCTGACCTATGGCGTTCAAGTGCTTTAGCCGCTATCCGG ATCATATGAAACGCCATGATTTCTTTAAAAGCGCGATGCCGGAAGGCT ATGTGCAGGAACGTACCATTAGCTTCAAAGATGATGGCACCTATAAAA CCCGTGCGGAAGTTAAATTTGAAGGCGATACCCTGGTGAACCGCATTG AACTGAAAGGTATTGATTTTAAAGAAGATGGCAACATTCTGGGTCATA AACTGGAATATAATTTCAACAGCCATAATGTGTATATTACCGCCGATA AACAGAAAAATGGCATCAAAGCGAACTTTAAAATCCGTCACAACGTGG AAGATGGTAGCGTGCAGCTGGCGGATCATTATCAGCAGAATACCCCGA TTGGTGATGGCCCGGTGCTGCTGCCGGATAATCATTATCTGAGCACC AGAGCGTTCTGAGCAAAGATCCGAATGAAAAACGTGATCATATGGTG TGCTGGAATTTGTTACCGCCGCGGGCATTACCCACGGTATGGATGAAC TGTATAAAGGCAGCCACCATCATCATCACCATTAA
pBAD hupA- His6	AAGAAACCAATTGTCCATATTGCATCAGACATTGCCGTCACCTGCGTCT TTTACTGGCTCTTCTCGCTAACCAAACCGGTAACCCCGCTTATTAAAA GCATTCTGTAACAAAGCGGGACCAAAGCCATGACAAAAACGCGTAACA AAAGTGTCTATAATCACGGCAGAAAAGTCCACATTGATTATTTGCACG GCGTCACACTTTGCTATGCCATAGCATTTTTATCCATAAGATTAGCGG ATCCTACCTGACGCTTTTTATCGCAACTCTCTACTGTTTCTCCATACC CGTTTTTTGGGCTAACAGGAGGAATTAACATGAACAAGACTCAACTGA TTGATGTAATTGCAGAGAAAGCAGAACTGTCCAAAACCCAGGCTAAAG CTGCTCTGGAGTCCACTCTGGCTGCAATTACTGAGTCTCTGAAAGAAG GCGATGCTGTACAACCTGGTTGGTTTCGGTACCTTCAAAGTGAACCACC GCGCTGAGCGTACTGGCCGCAACCCGCAGACCGGTAAAGAAATCAAAA TTGCCGCAGCTAACGTACCGGCATTTGTTTCTGGCAAGGCACTGAAAG ACGCAGTTAAGCACCACCACCACCACCCTGA
pBAD hupB- His6	AAGAAACCAATTGTCCATATTGCATCAGACATTGCCGTCACCTGCGTCT TTTACTGGCTCTTCTCGCTAACCAAACCGGTAACCCCGCTTATTAAAA GCATTCTGTAACAAAGCGGGACCAAAGCCATGACAAAAACGCGTAACA AAAGTGTCTATAATCACGGCAGAAAAGTCCACATTGATTATTTGCACG GCGTCACACTTTGCTATGCCATAGCATTTTTATCCATAAGATTAGCGG ATCCTACCTGACGCTTTTTATCGCAACTCTCTACTGTTTCTCCATACC CGTTTTTTGGGCTAACAGGAGGAATTAACATGAATAAATCTCAATTGA TCGACAAGATTGCTGCAGGGGCTGATATCTCTAAAGCTGCGGCTGGCC GTGCGTTAGATGCTATTATTGCTTCCGTAAGTGAATCTCTGAAAGAAG GGGATGATGTAGCACTGGTAGGTTTTGGTACTTTTGCCGTTAAAGAGC GTGCTGCCCCTACTGGCCGCAACCCGCAGACCGGTAAAGAGATCACCA TCGCTGCTGCTAAAGTACCGAGCTTCCGTGCAGGTAAAGCACTGAAAG ACGCGGTAAAC CTCGAGCACCACCACCACCACCCTGA
pBAD hupB(K67TAG)His6	AAGAAACCAATTGTCCATATTGCATCAGACATTGCCGTCACCTGCGTCT TTTACTGGCTCTTCTCGCTAACCAAACCGGTAACCCCGCTTATTAAAA GCATTCTGTAACAAAGCGGGACCAAAGCCATGACAAAAACGCGTAACA AAAGTGTCTATAATCACGGCAGAAAAGTCCACATTGATTATTTGCACG GCGTCACACTTTGCTATGCCATAGCATTTTTATCCATAAGATTAGCGG ATCCTACCTGACGCTTTTTATCGCAACTCTCTACTGTTTCTCCATACC CGTTTTTTGGGCTAACAGGAGGAATTAACATGAATAAATCTCAATTGA TCGACAAGATTGCTGCAGGGGCTGATATCTCTAAAGCTGCGGCTGGCC GTGCGTTAGATGCTATTATTGCTTCCGTAAGTGAATCTCTGAAAGAAG GGGATGATGTAGCACTGGTAGGTTTTGGTACTTTTGCCGTTAAAGAGC GTGCTGCCCCTACTGGCCGCAACCCGCAGACCGGTAAAGAGATCACCA TCGCTGCTGCTAAAGTACCGAGCTTCCGTGCAGGTAAAGCACTGAAAG ACGCGGTAAAC CTCGAGCACCACCACCACCACCCTGA

	GGGATGATGTAGCACTGGTAGGTTTTGGTACTTTTGCCGTTAAAGAGC GTGCTGCCCCGTACTGGCCGCAACCCGCAGACCGGT TAG GAGATCACCA TCGCTGCTGCTAAAGTACCGAGCTTCCGTGCAGGTAAAGCACTGAAAG ACGCGGTAAACCTCGAG CACCACCACCACCACC ACTGA
pBAD hupB(K86TAG)His6	AAGAAACCAATTGTCCATATTGCATCAGACATTGCCGTCACTGCGTCT TTTACTGGCTCTTCTCGCTAACCAAACCGGTAACCCCGCTTATTA AAAA GCATTCTGTAACAAAGCGGGACCAAAGCCATGACAAAAACGCGTAACA AAAGTGTCTATAATCACGGCAGAAAAGTCCACATTGATTATTTGCACG GCGTCACACTTTGCTATGCCATAGCATTTTTATCCATAAGATTAGCGG ATCCTACCTGACGCTTTTTATCGCAACTCTCTACTGTTTCTCCAT ACC CGTTTTTTGGGCTAACAGGAGGAATTAACATGAATAAATCTCAATTGA TCGACAAGATTGCTGCAGGGGCTGATATCTCTAAAGCTGCGGCTGGCC GTGCGTTAGATGCTATTATTGCTTCCGTAACCTGAATCTCTGAAAGAAG GGGATGATGTAGCACTGGTAGGTTTTGGTACTTTTGCCGTTAAAGAGC GTGCTGCCCCGTACTGGCCGCAACCCGCAGACCGGTAAAGAGATCACCA TCGCTGCTGCTAAAGTACCGAGCTTCCGTGCAGGTAAAGCACTG TAGG ACGCGGTAAACCTCGAG CACCACCACCACCACC ACTGA
pBAD sfGFP	AAGAAACCAATTGTCCATATTGCATCAGACATTGCCGTCACTGCGTCT TTTACTGGCTCTTCTCGCTAACCAAACCGGTAACCCCGCTTATTA AAAA GCATTCTGTAACAAAGCGGGACCAAAGCCATGACAAAAACGCGTAACA AAAGTGTCTATAATCACGGCAGAAAAGTCCACATTGATTATTTGCACG GCGTCACACTTTGCTATGCCATAGCATTTTTATCCATAAGATTAGCGG ATCCTACCTGACGCTTTTTATCGCAACTCTCTACTGTTTCTCCAT ACC CGTTTTTTGGGCTAACAGGAGGAATTAACATGGTTAGCAAAGGTGAA GAACGTGTTACCGGCGTTGTGCCGATTCTGGTGGAACGGATGGTGAT GTGAATGGCCATAAATTTAGCGTTCGTGGCGAAGGCGAAGGTGATGCG ACCAACGGTAAACTGACCCTGAAATTTATTTGCACCACCGGTAAACTG CCGGTTCGTGGCCGACCCTGGTGACCACCCTGACCTATGGCGTTCAG TGCTTTAGCCGCTATCCGGATCATATGAAACGCCATGATTTCTTTAA AGCGCGATGCCGGAAGGCTATGTGCAGGAACGTACCATTAGCTTCAAA GATGATGGCACCTATAAAACCCGTGCCGAAGTTAAATTTGAAGGCGAT ACCCTGGTGAACCGCATTGAACTGAAAGGTATTGATTTTTAAAGAAGAT GGCAACATTCTGGGTCATAAACTGGAATATAATTTCAACAGCCATAAT GTGTATATTACCGCCGATAAACAGAAAAATGGCATCAAAGCGAACTTT AAAATCCGTCACAACGTGGAAGATGGTAGCGTGCAGCTGGCGGATCAT TATCAGCAGAATAACCCGATTGGTGATGGCCCGGTGCTGCTGCCGGAT AATCATTATCTGAGCACCCAGAGCGTTCTGAGCAAAGATCCGAATGAA AAACGTGATCATATGGTGCTGCTGGAATTTGTTACCGCCGCGGGCATT ACCCACGGTATGGATGAACTGTATAAAGGCAGC CACCATCATCATCAC CATTAA
pET28a AdeT1-His6	TAATACGACTCACTATAGGGGAATTGTGAGCGGATAACAATTCCCTC TAGAAATAATTTTGTTTAACTTTAAGAAGGAGATATACATATGTTTGA TCCGATTGGTAAAAGCGGTGATGCATTTGCACTGGCAAAAGATTATGC ACTGGAAGCAAAAAATTGGGGCGCAGATCTGAGCCTGAAAGCCTATGT TGATGAACGTGTTGCAGCAGAGGATCTGAAAGTTGGTAAATGTGATGG TGCAATTATTAGCGGTCTGCGTGGTTCGTACGTTTAACAAATATACGGG TAGCCTGGATGCAGTTGGTGCCTGACCAATATGAAAACCGCAATTAA TGCCTATAAACTGCTGAGCAGCCCGATGGCAGCCAAAAATATGGTTGT TGGTCCGTATGAAATTGCAGGTCTGGGCACCATTGGTCCGGCATACT GTTTGTTAATGATCGTAGCATTAATACCCTGGCCAAAGCAGCAGGCAA AAAAATCGGTGTTTTCAAATATGATGAAGCCAGCCGAAACTGGTTCA GCATGTTGGTGGTCAGGCAGTTAGCGTTGATGTTACCAATGCCGGTGC CAAATTTAACAACCATGAAATTGATATTGTTCCGGCACCGATTGTTGC CTTTAAACCGTTTGAACGTATAAAGGCCTGGGTGAAAAAGGTGCCAT TGTTTCGTTTTCCGCTGACACAGATTAGCGCAGATTTTATCATTCGCAA

	AGATCAGTTTCCGGCAGGTTTTGGTCAGAAAAGCCGTACCTGGGTTGC AAGCCAGCTGAATCGTACCTTTGGTATTATTGCCAAATATGAGAGCGA TATCCCGAGCAAATATTGGATGGATATTCCGAAAAATGAACAGCTGAA CTATATGAAGATGATGCGTGAAGCACGTATTCAGCTGACCAAAGCAGG TATTTATGATCCCAAAATGATGAACTTCCTGAAGAAAAGTGCCTGCAA AGAAAATCCGAGCAATTTTGAATGTGCCCTGAACGATGAACATCATCA TCACCACCACCTGA
pET28a AdeT1(K280T AG)-His6	TAATACGACTCACTATAGGGGAATTGTGAGCGGATAACAATTCCCTC TAGAAATAATTTTGTTTAACTTTAAGAAGGAGATATACATATGTTTGA TCCGATTGGTAAAAGCGGTGATGCATTTGCACTGGCAAAGATTATGC ACTGGAAGCAAAAATTGGGGCGCAGATCTGAGCCTGAAAGCCTATGT TGATGAACGTGTTGCAGCAGAGGATCTGAAAGTTGGTAAATGTGATGG TGCAATTATTAGCGGTCTGCGTGGTCTGTCAGTTTAACAAATATACGGG TAGCCTGGATGCAGTTGGTGCCTGACCAATATGAAAACCGCAATTAA TGCCTATAAACTGCTGAGCAGCCCGATGGCAGCCAAAAATATGGTTGT TGGTCCGTATGAAATTGCAGGTCTGGGCACCATTGGTCCGGCATACT GTTTGTAAATGATCGTAGCATTAAATACCCTGGCCAAAGCAGCAGGCAA AAAAATCGGTGTTTTCAAATATGATGAAGCCAGCCGAAACTGGTTCA GCATGTTGGTGGTCAGGCAGTTAGCGTTGATGTTACCAATGCCGGTGC CAAATTTAACAACCATGAAATTGATATTGTTCCGGCACCATTGTTGC CTTTAAACCGTTTGAAGTGTATAAAGGCCTGGGTGAAAAAGGTGCCAT TGTTTCGTTTTCCGCTGACACAGATTAGCGCAGATTTTATCATTTCGAA AGATCAGTTTCCGGCAGGTTTTGGTCAGAAAAGCCGTACCTGGGTTGC AAGCCAGCTGAATCGTACCTTTGGTATTATTGCCAAATATGAGAGCGA TATCCCGAGCAAATATTGGATGGATATTCCGAAAAATGAACAGCTGAA CTATATGAAGATGATGCGTGAAGCACGTATTCAGCTGACCAAAGCAGG TATTTATGATCCCTAGATGATGAACTTCCTGAAGAAAAGTGCCTGCAA AGAAAATCCGAGCAATTTTGAATGTGCCCTGAACGATGAACATCATCA TCACCACCACCTGA
pET28a sfGFP-His6	TAATACGACTCACTATAGGGGAATTGTGAGCGGATAACAATTCCCTC TAGAAATAATTTTGTTTAACTTTAAGAAGGAGATATACCATGGTTAGC AAAGGTGAAGAACTGTTTACCGGCGTTGTGCCGATTCTGGTGGAACCTG GATGGTGATGTGAATGGCCATAAATTTAGCGTTTCGTGGCGAAGGCGAA GGTGATGCGACCAACGGTAAACTGACCCTGAAATTTATTTGCACCACC GGTAAACTGCCGGTTCCGTGGCCGACCCTGGTGACCACCCTGACCTAT GGCGTTCAGTGCTTTAGCCGCTATCCGGATCATATGAAACGCCATGAT TTCTTTAAAAGCGCGATGCCGGAAGGCTATGTGCAGGAACGTACCATT AGCTTCAAAGATGATGGCACCTATAAAACCCGTGCGGAAGTTAAATTT GAAGGCGATACCCTGGTGAACCGCATTGAACTGAAAGGTATTGATTTT AAAGAAGATGGCAACATTCTGGGTCATAAACTGGAATATAATTTCAAC AGCCATAATGTGTATATTACCGCCGATAAACAGAAAAATGGCATCAAA GCGAACTTTAAAATCCGTCACAACGTGGAAGATGGTAGCGTGCAGCTG GCGGATCATTATCAGCAGAATACCCCGATTGGTGATGGCCCGGTGCTG CTGCCGGATAATCATTATCTGAGCACCCAGAGCGTTCTGAGCAAAGAT CCGAATGAAAAACGTGATCATATGGTGCTGCTGGAATTTGTTACCGCC GCGGGCATTACCCACGGTATGGATGAACTGTATAAAGGCAGCCACCAT CATCATCACCATTA
pET28a sfGFP(150TA G)	TAATACGACTCACTATAGGGGAATTGTGAGCGGATAACAATTCCCTC TAGAAATAATTTTGTTTAACTTTAAGAAGGAGATATACCATGGTTAGC AAAGGTGAAGAACTGTTTACCGGCGTTGTGCCGATTCTGGTGGAACCTG GATGGTGATGTGAATGGCCATAAATTTAGCGTTTCGTGGCGAAGGCGAA GGTGATGCGACCAACGGTAAACTGACCCTGAAATTTATTTGCACCACC GGTAAACTGCCGGTTCCGTGGCCGACCCTGGTGACCACCCTGACCTAT GGCGTTCAGTGCTTTAGCCGCTATCCGGATCATATGAAACGCCATGAT TTCTTTAAAAGCGCGATGCCGGAAGGCTATGTGCAGGAACGTACCATT

	AGCTTCAAAGATGATGGCACCTATAAAAACCCGTGCGGAAGTTAAATTT GAAGGCGATACCCTGGTGAACCGCATTGAACTGAAAGGTATTGATTTT AAAGAAGATGGCAACATTCTGGGTCATAAACTGGAATATAATTTCAAC AGCCATTAGGTGTATATTACCGCCGATAAACAGAAAAATGGCATCAAA GCGAACTTTAAAATCCGTCACAACGTGGAAGATGGTAGCGTGACAGCTG GCGGATCATTATCAGCAGAATACCCCGATTGGTGATGGCCCGGTGCTG CTGCCGGATAATCATTATCTGAGCACCCAGAGCGTTCTGAGCAAAGAT CCGAATGAAAAACGTGATCATATGGTGCTGCTGGAATTTGTTACCGCC GCGGGCATTACCCACGGTATGGATGAACTGTATAAAGGCAGCCACCAT CATCATCACCATTA
pLacI-AdeT1- His6	GACACCATCGAATGGCGCAAAACCTTTCGCGGTATGGCATGATAGCGC CCGGAAGAGAGTCAATTCAGGGTGGTGAATATGTTTGATCCGATTGGT AAAAGCGGTGATGCATTTGCACTGGCAAAAGATTATGCACTGGAAGCA AAAAATTGGGGCGCAGATCTGAGCCTGAAAGCCTATGTTGATGAACGT GTTGCAGCAGAGGATCTGAAAGTTGGTAAATGTGATGGTGCAATTATT AGCGGTCTGCGTGGTCTGTCAGTTTAAACAAATATACGGGTAGCCTGGAT GCAGTTGGTGCACTGACCAATATGAAAACCGCAATTAATGCCTATAAA CTGCTGAGCAGCCCGATGGCAGCCAAAAATATGGTTGTTGGTCCGTAT GAAATTGCAGGTCTGGGCACCATTTGGTCCGGCATACCTGTTTGTTAAT GATCGTAGCATTAATACCTGGCCAAAGCAGCAGGCCAAAAAATCGGT GTTTTCAAATATGATGAAGCCCAGCCGAAACTGGTTTCAGCATGTTGGT GGTCAGGCAGTTAGCGTTGATGTTACCAATGCCGGTGCCAAATTTAAC AACCATGAAATTGATATTGTTCCGGCACCGATTGTTGCCTTTAAACCG TTTGAAGTGTATAAAGGCCTGGGTGAAAAAGGTGCCATTGTTCTGTTTT CCGCTGACACAGATTAGCGCAGATTTTATCATTTCGCAAAGATCAGTTT CCGGCAGGTTTTGGTCAGAAAAGCCGTACCTGGGTTGCAAGCCAGCTG AATCGTACCTTTGGTATTATTGCCAAATATGAGAGCGATATCCCGAGC AAATATTGGATGGATATTCCGAAAAATGAACAGCTGAACTATATGAAG ATGATGCGTGAAGCACGTATTCAGCTGACCAAAGCAGGTATTTATGAT CCCAAAATGATGAACTTCCTGAAGAAAGTGCGCTGCAAAGAAAATCCG AGCAATTTTGAATGTGCCCTGAACGATGAACATCATCATCACACCAC TAA
pLacI-sfGFP- His6	GACACCATCGAATGGCGCAAAACCTTTCGCGGTATGGCATGATAGCGC CCGGAAGAGAGTCAATTCAGGGTGGTGAATATGGTTAGCAAAGGTGAA GAACTGTTTACCGGCGTTGTGCCGATTCTGGTGGAAGTGGATGGTGAT GTGAATGGCCATAAATTTAGCGTTCTGTGGCGAAGGCGAAGGTGATGCG ACCAACGGTAAACTGACCCTGAAATTTATTTGCACCACCGGTAAACTG CCGGTTCCGTGGCCGACCCTGGTGACCACCCTGACCTATGGCGTTTCA TGCTTTAGCCGCTATCCGGATCATATGAAACGCCATGATTTCTTTAAA AGCGCGATGCCGGAAGGCTATGTGCAGGAACGTACCATTAGCTTCAAA GATGATGGCACCTATAAAAACCCGTGCGGAAGTTAAATTTGAAGGCGAT ACCCTGGTGAACCGCATTGAACTGAAAGGTATTGATTTTAAAGAAGAT GGCAACATTCTGGGTCATAAACTGGAATATAATTTCAACAGCCATAAT GTGTATATTACCGCCGATAAACAGAAAAATGGCATCAAAGCGAACTTT AAAATCCGTCACAACGTGGAAGATGGTAGCGTGACAGCTGGCGGATCAT TATCAGCAGAATACCCCGATTGGTGATGGCCCGGTGCTGCTGCCGGAT AATCATTATCTGAGCACCCAGAGCGTTCTGAGCAAAGATCCGAATGAA AAACGTGATCATATGGTGCTGCTGGAATTTGTTACCGCCGCGGGCATT ACCCACGGTATGGATGAACTGTATAAAGGCAGCCACCATCATCATCAC CATTA
pLac-sfGFP- His6	TTTACACTTTATGCTTCCGGCTCGTATGTTGCCATGGTTAGCAAAGGT GAAGAACTGTTTACCGGCGTTGTGCCGATTCTGGTGGAAGTGGATGGT GATGTGAATGGCCATAAATTTAGCGTTCTGTGGCGAAGGCGAAGGTGAT GCGACCAACGGTAAACTGACCCTGAAATTTATTTGCACCACCGGTAA CTGCCGGTTCCGTGGCCGACCCTGGTGACCACCCTGACCTATGGCGTT

	<p> CAGTGCTTTAGCCGCTATCCGGATCATATGAAACGCCATGATTTCTTT AAAAGCGCGATGCCGGAAGGCTATGTGCAGGAACGTACCATTAGCTTC AAAGATGATGGCACCTATAAAACCCGTGCGGAAGTTAAATTTGAAGGC GATACCCTGGTGAACCGCATTGAACTGAAAGGTATTGATTTTAAAGAA GATGGCAACATTCTGGGTCATAAACTGGAATATAATTTCAACAGCCAT AATGTGTATATTACCGCCGATAAACAGAAAAATGGCATCAAAGCGAAC TTTAAAATCCGTCACAACGTGGAAGATGGTAGCGTGCAGCTGGCGGAT CATTATCAGCAGAATACCCCGATTGGTGATGGCCCGGTGCTGCTGCCG GATAATCATTATCTGAGCACCCAGAGCGTTCTGAGCAAAGATCCGAAT GAAAAACGTGATCATATGGTGCTGCTGGAATTTGTTACCGCCGCGGGC ATTACCCACGGTATGGATGAACTGTATAAAGGCAGCCACCATCATCAT CACCATTAA </p>
pLacUV5- AdeT1-His6	<p> TTTACACTTTATGCTTCCGGCTCGTATAATGTGTGGAAAAGCTTGGAT CCCATGGTTTACACAGGAAACAGCTATGTTTGATCCGATTGGTAAAA GCGGTGATGCATTTGCACTGGCAAAAGATTATGCACTGGAAGCAAAAA ATTGGGGCGCAGATCTGAGCCTGAAAGCCTATGTTGATGAACGTGTTG CAGCAGAGGATCTGAAAGTTGGTAAATGTGATGGTGCAATTATTAGCG GTCTGCGTGCTCGTCAGTTTAAACAAATATACGGGTAGCCTGGATGCAG TTGGTGCACTGACCAATATGAAAACCGCAATTAATGCCTATAAACTGC TGAGCAGCCCGATGGCAGCCAAAAATATGGTTGTTGGTCCGTATGAAA TTGCAGGTCTGGGCACCATTGGTCCGGCATACTGTTTGTTAATGATC GTAGCATTAATACCCTGGCCAAAGCAGCAGGCCAAAAAATCGGTGTTT TCAAATATGATGAAGCCAGCCGAAACTGGTTCAGCATGTTGGTGCTC AGGCAGTTAGCGTTGATGTTACCAATGCCGGTGCCAAATTTAACAACC ATGAAATTGATATTGTTCCGGCACCGATTGTTGCCTTTAAACCGTTTG AACTGTATAAAGGCCTGGGTGAAAAAGGTGCCATTGTTTCGTTTTCCGC TGACACAGATTAGCGCAGATTTTATCATTCGCAAAGATCAGTTTCCGG CAGGTTTTGGTCAGAAAAGCCGTACCTGGGTTGCAAGCCAGCTGAATC GTACCTTTGGTATTATTGCCAAATATGAGAGCGATATCCCAGCAAAT ATTGGATGGATATTCCGAAAAATGAACAGCTGAACTATATGAAGATGA TGCGTGAAGCACGTATTCAGCTGACCAAAGCAGGTATTTATGATCCCA AAATGATGAACTTCCTGAAGAAAGTGCGCTGCAAAGAAAATCCGAGCA ATTTTGAATGTGCCCTGAACGATGAAATCATCATCACCACCACCTAA </p>
pLacUV5- sfGFP-His6	<p> TTTACACTTTATGCTTCCGGCTCGTATAATGTGTGGAAAAGCTTGGAT CCCATGGTTTACACAGGAAACAGCTATGGTTAGCAAAGGTGAAGAAC TGTTTACCGGCGTTGTGCCGATTCTGGTGGAAGTGGATGGTGATGTGA ATGGCCATAAATTTAGCGTTTCGTGGCGAAGGCGAAGGTGATGCGACCA ACGGTAACTGACCCTGAAATTTATTTGCACCACCGGTAACTGCCGG TTCCGTGGCCGACCCTGGTGACCACCCTGACCTATGGCGTTTCAGTGCT TTAGCCGCTATCCGGATCATATGAAACGCCATGATTTCTTTAAAGCG CGATGCCGGAAGGCTATGTGCAGGAACGTACCATTAGCTTCAAAGATG ATGGCACCTATAAAACCCGTGCGGAAGTTAAATTTGAAGGCGATACCC TGGTGAACCGCATTGAACTGAAAGGTATTGATTTTAAAGAAGATGGCA ACATTCTGGGTCATAAACTGGAATATAATTTCAACAGCCATAATGTGT ATATTACCGCCGATAAACAGAAAAATGGCATCAAAGCGAACTTTAAAA TCCGTCACAACGTGGAAGATGGTAGCGTGCAGCTGGCGGATCATTATC AGCAGAATACCCCGATTGGTGATGGCCCGGTGCTGCTGCCGGATAATC ATTATCTGAGCACCCAGAGCGTTCTGAGCAAAGATCCGAATGAAAAAC GTGATCATATGGTGCTGCTGGAATTTGTTACCGCCGCGGGCATTACCC ACGGTATGGATGAACTGTATAAAGGCAGCCACCATCATCATCACCATT AA </p>
pPrKST	<p> TTGTGAGCCTGTCCCGCTTATAAGATCATACGCCGTTATACGTTGTTT ACGCTTTGAGGAATCCCATATGATGGATAAAAAACCGCTGGATGTGCT GATTAGCGCGACCGGCTGTGGATGAGCCGTACCGGCACCCTGCATAA AATCAAACATCATGAAGTGAGCCGCAGCAAAATCTATATTGAAATGGC </p>

	GTGCGGCGATCATCTGGTGGTGAACAACAGCCGTAGCTGCCGTACCGC GCGTGCGTTTCGTCATCATAAATACCGCAAACCTGCAAACGTTGCCG TGTGAGCGATGAAGATATCAACAACCTTCTGACCCGTAGCACCGAAAG CAAAAACAGCGTGAAAGTGCGTGTTGGTGAGCGCGCCGAAAGTGAAAAA AGCGATGCCGAAAAGCGTGAGCCGTGCGCCGAAACCGCTGAAAAATAG CGTGAGCGCGAAAGCGAGCACCAACACCAGCCGTAGCGTTCCGAGCCC GGCGAAAAGCACCCCGAACAGCAGCGTTCCGGCGTCTGCGCCGGCACC GAGCCTGACCCGCAGCCAGCTGGATCGTGTTGGAAGCGCTGCTGTCTCC GGAAGATAAAATTAGCCTGAACATGGCGAAACCGTTTCGTGAACCTGGA ACCGGAACCTGGTGACCCGTCTGTA AAAACGATTTTCAGCGCCTGTATAC CAACGATCGTGAAGATTATCTGGGCAAACCTGGAACGTGATATCACCAA ATTTTTTGTGGATCGCGGCTTTCTGGAAATTAAAAGCCCGATTCTGAT TCCGGCGGAATATGTGGAACGTATGGGCATTAACAACGACACCGAACT GAGCAAACAAATTTTCCGCGTGGATAAAAACCTGTGCCTGCGTCCGAT GCTGGCCCCGACCCTGTTTAACTATCTGCGTAAACTGGATCGTATTCT GCCGGGTCCGATCAAAATTTTTGAAGTGGGCCCGTGCTATCGCAAAGA AAGCGATGGCAAAGAACACCTGGAAGAATTCACCATGGTTAACTTTAC CCAAATGGGCAGCGGCTGCACCCGTGAAAACCTGGAAGCGCTGATCAA AGAATTCCTGGATTATCTGGAATCGACTTCGAAATTGTGGGCGATAG CTGCATGGTGTATGGCGATACCCTGGATATTATGCATGGCGATCTGGA ACTGAGCAGCGCGGTGGTGGGTCCGGTTAGCCTGGATCGTGAATGGGG CATTGATAAACCGTGGATTGGCGCGGGTTTTTGGCCTGGAACGTCTGCT GAAAGTGATGCATGGCTTCAAAAACATTAAACGTGCGAGCCGTAGCGA AAGCTACTATAACGGCATTAGCACGAACCTGTAA
--	--